

RCA Engineer

Vol 18 No 2 Aug Sep 1972



Advanced Technology Laboratories (ATL) is an organization devoted to technology development for RCA's Government and Commercial Systems. ATL is unique in several ways. First, it is healthy and flourishing in a day when many central development laboratories are disappearing from industrial organizations. Second, ATL has unusual technical breadth, extending across many disciplines of science and engineering. Third, ATL embodies the concept of satellite laboratories. Let us examine these three points of uniqueness.

In the past two or three years of declining activity in the electronics industry, the tendency has been to reduce the scope or, indeed, to close development laboratories. Contrary to this trend, ATL has maintained its physical size and has increased its technical contribution to G&CS and the Corporation. In fact, ATL's position is stronger and its future brighter now than it was at the height of the Aerospace era of the 60's.

The unusual technical breadth of ATL is the central theme of this issue. Programs are pursued in ten general technical areas. They are: computers, holography, laser applications, laser recording, LSI and hybrids, microsonics, millimeter waves, pattern recognition, sensors, and thermodynamics. The eighteen technical papers included here represent only a partial coverage of the total ATL activity.

Finally, the Advanced Technology Laboratories is unique because of its organizational structure. ATL performed an intensive review of the requirements for technology transfer in 1968 and determined that a change was required. A satellite laboratory was established at ASD, Burlington in 1969, and another satellite was established at EASD, Van Nuys in 1970. The Central Laboratory in Camden and these two satellites constitute an organization well suited to the requirements for timely transfer of technology to all of the G&CS divisions.

ATL has one other feature which, while not necessarily unique, is certainly essential to its future success—responsiveness. Indeed the importance of ATL's future role will be in direct proportion to its responsiveness to the technological needs of G&CS and RCA.



Paul E. Wright
 Director
 Advanced Technology Laboratories
 Camden, New Jersey

- Editor
- Associate Editor
- Art Editor
- Editorial Secretary
- Subscription
- Subscriptions
- Consulting Editors
- Technical Publications Adm.,
Electronic Components
- Technical Publications Adm.,
Laboratories
- Technical Publications Adm.,
Corporate Engineering Services
- Quality Assurance Board
- Mgr., Quality and Reliability
Assurance, Solid State Div.
- VP, Engineering, NBC
Television Network
- Mgr., Technical Information
Services, RCA Laboratories
- Manager, Consumer Products
Adm., RCA Service Co.
- Chief Engineer,
Record Division
- Chief Technical Advisor,
Consumer Electronics
- Div. VP, Technical Planning
Electronic Components
- Exec. VP, Engineering and
Leased Systems,
Global Communications, Inc.
- Director, Corporate
Engineering Services
- Manager, Engineering
Professional Development
- Division VP,
Government Engineering

Our cover

... a viewpoint of research and development expressed in abstract art. Today's industrial R&D efforts are subject to many external forces. The viewpoint is Dr. Vollmer's (see *The Role of Laboratories*, on p. 5): "A particular project can be thought of as having a trajectory in a multi-dimensional medium in which the axes represent all of the functions of the corporation." **Art credit:** W. J. Vassallo, Advanced Technology Laboratories, Camden, N.J.

P R JANINKA
 FEB 72
 RECEIVED

A technical journal published by
 RCA Corporate Engineering Services 2-8,
 Camden, N.J.

RCA Engineer articles are indexed
 annually in the April-May Issue and
 in the "Index to RCA Technical Papers."

• To disseminate to RCA engineers technical information of professional value • To publish in an appropriate manner important technical developments at RCA, and the role of the engineer • To serve as a medium of interchange of technical information between various groups at RCA • To create a community of engineering interest within the company by stressing the interrelated nature of all technical contributions • To help publicize engineering

achievements in a manner that will promote the interests and reputation of RCA in the engineering field • To provide a convenient means by which the RCA engineer may review his professional work before associates and engineering management • To announce outstanding and unusual achievements of RCA engineers in a manner most likely to enhance their prestige and professional status.

Contents

Editorial Input	ECOS at Intercon '72	W. O. Hadlock	2
Interview	The scientist and social responsibility—an interview with Dr. E. Ramberg		5
Engineer and the Corporation	Role of the Laboratories	J. Vollmer	10
Microsonics	Growing importance of microsonics technology	Dr. D. A. Gandolfo C. L. Grasse G. D. O'Clock, Jr.	12
Laser applications	One gigabit-YAG laser techniques	C. Reno	20
	Precision hover sensor for heavy-lift helicopter	D. G. Herzog	24
	Pulsed GaAs illuminators for night-vision systems	W. W. Barratt	30
Laser recording	Multispectral recording with synthetic gratings	S. L. Corsover	34
Sensors	Visible and infrared sensor arrays for imaging systems	A. Boornard	40
	Wide-angle laser target—designation seeker	G. J. Ammon D. G. Herzog H. C. Sprigings	47
Thermodynamics & mechanics	Novel thermal management techniques	B. Shelpuk P. Joy, Jr.	51
	Refrigeration systems for spacecraft	P. E. Wright	58
Pattern recognition	Automatic speaker identification	J. Richards W. Meeker A. Nelson	64
LSI and hybrid technology	Recent developments in CMOS/SOS	H. W. Kaiser W. F. Gehweiler W. J. Stotz J. I. Pridgen	68
	High speed A to D converters	D. Benima J. R. Barger	73
Computer technology	Simulation—methodology for LSI computer design	A. S. Merriam H. S. Zieper	79
	LSI computer fabrication—SUMC/DV	A. Feller	82
	LSI computer design—SUMC/DV	W. A. Clapp	88
Holography	Holographic digital memories	R. H. Norwalt P. L. Nelson	95
	Holographic storage of multicolor information	G. T. Burton B. R. Clay	99
Millimeter waves	Millimeter wave imaging	Dr. B. J. Levin B. R. Feingold D. J. Miller	106
Division profile	Advanced Technology Laboratories—a profile	M. G. Pietz	112
Engineer and the Corporation	The role of advanced technology marketing	A. T. Hospodor	114
RCA Laboratories	Ion implantation	Dr. C. W. Mueller Dr. E. C. Douglas	116
Engineering and Research Notes	Logic-level-to-pulse converter	M. Lipka	120
	Integrating sphere for use with a spectroradiometer	L. J. Nicastric A. L. Lea	120
Departments	Pen and Podium		122
	Patents Granted		125
	Dates and Deadlines		126
	News and Highlights		127

editorial input

“ECOS” at ; Intercon 72

W. O. Hadlock, Editor

Sociologists, students of psychology, electronic engineers and scientists, and professors from academia; individually and collectively, lunged futilely to grasp a greased pig called *ecology and technology*. But, the great mental exercise expended in giving and receiving the various technical presentations at *IEEE-Intercon 72* was certainly not wasted. On the contrary, it revealed *much* through a forthright interchange of information.

Based on numbers alone, the effort was impressive; fifty or more papers related (directly or indirectly) to ecological problems. Every presentation exhibited a sincere desire and a dedication to achieve a socially favorable milieu. True, the view through the social scientist's glasses was much different from that of the technologists, as you might expect. But we will consider that fact in more detail later.

A global creed

Problems and possible solutions to the ecological dilemma were tackled by engineers and social scientists who mentioned repeatedly the potential roles of government and industry, society, technology, and of individual countries (rich and poor) . . . and by speakers who referred to the implications of adopting a global creed for world ecological systems.

“Technology and the effect on society” is a dramatic topic, subject to analysis by everyone in all walks of life. Diagnosing the ills and prescribing cures are challenging, difficult tasks in an increasingly complex society . . . an ecosystem beset with interdependent physical and social systems.

Certainly, the gloomy prospect of a permanently poisoned ecosystem looms greater than the sum of all its myriad parts such as . . . thermal, air and water pollution; solid wastes and recycling; urban depravation; weaponry

abuses; drug abuses; health, and medicine; population increases and overcrowding; crime detection-and-control needs; power shortage problems; and, the general diminishing of our natural resources.

The true scale of the problem calls for worldwide coordination and implementation of a combination of scientific, demographic, economic, and societal skills. Yet, group-by-group, engineer-by-engineer, community-by-community, every contribution (however minor) will represent a significant forward step in underpinning global goals.

Technology talks

Some ideas on the manifold ways in which engineers and scientists can contribute to the betterment of society were described at *IEEE-Intercon 72*. In this brief editorial only a few selected phases of “society-related” research and engineering can be touched upon.

Generally, there seemed to be an alertness on the part of engineers to address themselves to understanding societal problems, defining such problems, and then considering potential solutions in which they can contribute their talents. The recognition of the need for a mix of technological, social, economic, and institutional forces . . . and the need for prerequisite societal courses of instruction for engineers were some of the most encouraging signs.

Energy crises

National and international needs of supplying 10 kilowatts of power-per-person, for example, were considered in light of the transformation of energy from fossil fuels and nuclear devices. Nuclear reactor engineers and heat-transfer specialists are required to consider attendant pollution, strip mining of coal, and radiation effluents from nuclear plants.

Atop these factors, heat (not electricity) is a larger consideration. Nuclear reactors in or near population centers pose a host of problems; another consideration is that ¼ of *all energy* used in the USA is consumed by the automobile. National studies at Oak Ridge National Laboratory are concentrating on some of these problems.

Privacy and information transfer

Privacy and the relationship to computers was a frequent topic of the panelists. Contrasts between technological advancement and the human desire for privacy were discussed with respect to the role of engineers and their social responsibilities.

Upon introspection, the engineer and scientist observed an apparent underestimation of the shock of technology upon society. As a result, engineers were asked how they plan to transfer their knowledge to those in need. Several independent non-profit groups of engineers were cited as contributing help to underdeveloped countries, to urban communities, and to government agencies.

Transportation, health and medicine

Interesting presentations concerned the role of engineering in health analysis and the application to medicine of the computer and data acquisition, and the use of TV cameras for ophthalmological investigation. Another paper discussed pattern recognition used to determine an airplane's physical characteristics by electromagnetic detection; the same technique can be used to detect the presence of dangerous gases during mine-drilling operations. The use of robots and remote controls as alternatives to transporting people was mentioned. Considering the amount of time people travel to and from work and the resulting frustrations of the rush-hour

traffic, there could be ways in which people could "go to work" without actually commuting. One suggestion was to use a robot located at a factory but remotely controlled from the home of the worker who would have a TV monitor and control facilities.

Pollution monitoring

Computer networks, modeling of systems, and data acquisitions for air and water pollution monitoring were discussed with respect to advances made. Establishment of design criteria for emissions from stationary and mobile sources as well as for ambient air quality were described. These were only a few of the topics highlighting the interests of engineers.

Engineering ethics

Other professional expressions were frequent statements concerning engineering ethics, definitions of "the engineer", and how to definitize societal needs and assign companion priorities.

Societal research presentations

Presentations by societal researchers centered attention on the need for a greater general awareness by industry (and technology) of the ills of society. Emphasis was placed on the responsibility of engineers and scientists in government and industry to engage in research and engineering that contribute to the solution of ecological problems.

Other discussions pointed to the large number of situations where engineers are working on such devices as bombs that are known to be weapons that kill people—or on production of Napalm that will "not be used to cook eggs." But some agreement was reached that deep basic research on some aspects of atomic energy could have applications in both directions depending upon its final uses. "A knife can be used to peel an apple or to stick in someone's belly."

In response, during question-and-answer periods, the many useful returns of space research were cited—such as those in medicine, communications, education, and weather forecasting. Other presentations (dealing with the research concerning offensive weapons) led to panel discussions relating to definitions and need of "offensive and defensive weapons"; the useful and destructive results of research; and the personal responsibility for war, crime, and poverty.

Varying individual viewpoints were cited about the work being done on the "pill." Population control methods and possible abortion techniques were other areas of controversy. The electronic computer and its invasion of privacy in the personal and business life of the individual again came in for much attention by several speakers from academia and industry.

Interesting comments arose about "technical lead time" and "social lag

time" . . . and at least partial agreement that engineers do not receive college instruction and direction from the sociologists—and the societal research courses seldom include anything relating to technology.

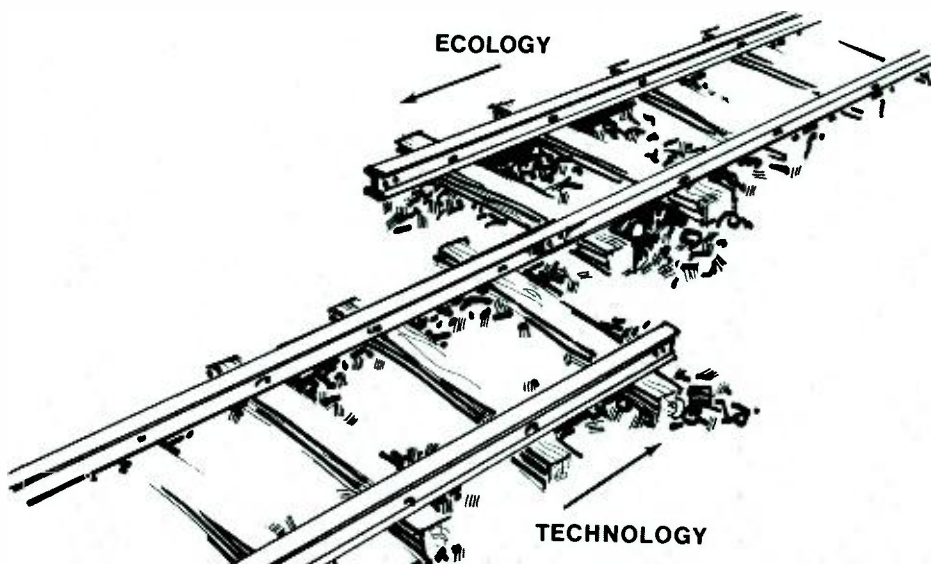
A technical approach

One entire session was devoted to ecology problems and a technical approach to their solution. Speakers and panelists were from engineering, from the government's Environmental Protection Agency, and the United Nations organization.

A broad program for environmental reform (as the government sees it) included some specific ideas for pollution monitoring devices and control systems that are needed. Although air, water, and noise pollution are of great concern, a major problem for the future will be solid-waste disposal.

The United Nation's hopes are many, but the main goal seems to be the fostering of cooperation through a type of "non-aggression" treaty where one nation could be censured for having violated the environment of neighboring nations.

A plan for regionalized non-profit corporations was also proposed to carry out environmental research work. This idea received a great deal of support in the question-and-answer period and could conceivably gain further support from industry and from the Environmental Protection Agency.



The Stockholm conference described at *Intercon 72*

A description of the June conference in Stockholm, Sweden, on world ecological problems was of special interest during one session at *IEEE Intercon 72*. Delegations from all countries of the world are concerned about the "Survival of the Planet." Many countries (including the Soviet Union) have basic problems of cleaning up rivers. Even in developing countries, the lack of clean water, lack of food, and the presence of slums are problems. In 1968, the United Nations devoted a conference to call special attention to World Environmental Problems.

Since the world now knows these facts, the present conference deals more directly with solutions to problems. The new conference involves the best brains available in scientific and societal areas throughout the world. Following is a spectrum covering conference activity:

- 1) Relief of human suffering,
- 2) Management of natural resources and their depletion rates, including diminishing sources of metals, petroleum, lumber, and the despoiling of nature,
- 3) Pollutant identification and the control and preservation of marine environment, avoidance of oil spills, preserving natural environment, and monitoring and control of carbon dioxide content of the atmosphere. Marine pollution was previously largely restricted to inland waters and nationally controlled. Such pollution has now generated to a problem in all waters, including the oceans of the world, and requires international control.
- 4) Study of cultural, societal and educational aspects of environmental issues. Training of ecologists, creation of new environmental ethics, and a change of attitudes on the part of the peoples of the world.
- 5) Economic development and the environment,
- 6) Organizational machinery necessary to implement the decisions reached at Stockholm—
 - a) What United Nations machinery is necessary?
 - b) Is it feasible to deal with the questions?

The agenda for the conference was planned by intergovernmental working groups of 27 countries to lay down the responsibility of governments for their own environmental problems that might affect the environment of their neighbors. This is a breakthrough in international law. For example, upstream countries situated near river systems contribute toxic wastes . . .

and such pollution is carried to downstream countries, affecting them adversely. Such environmental aggression is in a sense severe enough to produce protests and lawsuits.

Many developing countries were hostile toward conference plans at first, feeling that pollution was a disease of rich countries. Now, upon examining their own regional ecological problems, the present level of pollution is realized to be just the "tip of the iceberg."

Lack of potable water is a problem of the entire world. In Algeria, only 20% of the population has access to potable water. This is true of many countries in Africa where cities are developing. Urbanization is highest in the human history in these areas and thus creates very great problems. So, water, sanitation facilities, transportation, housing, and education are universal problems.

Earthwatch stations are being considered to provide a global monitoring system to detect the presence of chemical elements in the atmosphere and water. Data will be channeled to central or regional units from where it is routed to designated observation points which will employ satellites, ocean-going vessels, and station buoys.

An editorial conclusion

Emphatically, the sessions devoted to "technology and the ecology" proved that engineers, scientists, and researchers of societal problems share a sincere mutual concern. Equally apparent was the need for a greater understanding by sociologists of the potential valuable role of technology in solving problems. Just as strongly, the need was highlighted that engineers and scientists must become better acquainted with societal research.

The wide communication gap that exists between the forces of technology and ecology must be closed before any significant progress can be made in defining ecological problems requiring engineering and technical solutions.

But much hope and encouragement looms in the prospect that the many *Transactions* of IEEE as well as the *Proceedings* and *Spectrum* can help provide a communication link.

Moreover, RCA engineers and scientists can make a concerted effort to

close the gap through the publication of papers in the *RCA Engineer*, *RCA Review*, and in external media.

Each published article* will be an indication of hope for the future and will serve to document the progress being made by engineers and scientists in spite of an obvious communication gap.

*For example, see interview with Dr. E. G. Ramberg, this issue.

Future issues

The next issue of the *RCA ENGINEER*, Vol. 18-3, will contain representative papers devoted to "Math and the engineer" Some of the topics to be covered are:

Bayesian statistics

Digital correlator

Computer-assisted design applications

Applications of Walsh functions to solve differential equations

Image enhancement techniques

Preprocessor for pattern recognition

Math in operations research

Math in communications research

Articles on the following themes are planned for future issues.

COS/MOS integrated circuits

Radar and antenna engineering

Transportation

Global communications

Broadband information systems

Crime prevention systems

SelectaVision systems

Command and control

Broadcast and mobile communications systems

Engineering at RCA Ltd.

The scientist and social responsibility—an interview with Dr. E. G. Ramberg

We are often confronted with the image of the scientist puttering away in his ivory tower, concerned only with his technology, indifferent to the pragmatic world. This stereotype has been popularized lately by vitriolic antagonists who question the fruits of scientific effort. Science is accused of dehumanizing society and despoiling the earth. Science stands in apparent opposition to ecology, humanity, and society. The stereotype scientist has thus become a scapegoat. But the scientist is also a member, in good standing, of the earth's community. He, too, has personal convictions of how he fits into the nature of things and what his responsibilities are. It is important that he be heard. For this reason, W. O. Hadlock, Editor, RCA Engineer; C. W. Sall, Technical Publications Administrator, RCA Laboratories; F. J. Strobl, Editor, RCA TREND, conducted an interview with a man who, through an entire career, has always been a humanist and a scientist: Dr. E. G. Ramberg.

DR. EDWARD G. RAMBERG retired on July 1, 1972, after a 37-year career with RCA. His scientific contributions, both theoretical and practical, to the field of physics are well known to his peers. In his efforts, he has always been a team worker. But he is just as highly respected as a humanist. A man of deep religious conviction, Dr. Ramberg has actively sought to relieve some of the suffering in the world. For almost two years, Dr. Ramberg and his wife served as foster parents to a war-injured Vietnamese child. The girl had burns over two-thirds of the surface of her body. During the weeks of healing between the plastic surgery operations, her home was with the Rambergs. For Dr. Ramberg, "it was a very rewarding experience."

In this interview, reviewing Dr. Ramberg's life, we touch upon some of his thoughts on the role of the scientist in society and what advice Dr. Ramberg has for young engineers and scientists.

Dr. Ramberg, why are you a scientist; is it because of family influences, counseling, or just natural curiosity?

It was not a family influence, directly. My father was a humanist—he was interested in philology and archaeology. My mother was an artist. In my case, I think it was just a matter of inclination. At the Gymnasium in Munich, where my brother and I went to school, we were exposed to a broad range of studies. Physics seemed to be a field

in which we felt we could work. My brother is also a physicist. He graduated from Cornell and got the Doctorate in Physics from the Technical University of Munich.

Why did you choose the optics branch of physics?

Actually, I got into optics by chance. I took my junior year at Cornell and then took some time out to improve my financial status. So, I worked for two years as a scientific aid in optical computation with Bausch & Lomb Optical Co. in Rochester, N.Y.

So, like many college students, you needed a job?

Yes, it was essentially because there was an opening. I think I could have worked in other branches of physics as readily. Optics is, of course, to a large extent mathematics. Mathematics was a field which came relatively easily to me. At least an elementary type of mathematics.

I understand you are multilingual in many ways, and not only proficient in the language of mathematics.

I can read in French, German, and Italian and I can get along pretty well speaking in German and Italian and possibly, with a little practice, in French. Other languages are negligible. I have at times spoken a little Russian and Vietnamese.

In what area of optics was your first work at Bausch & Lomb?

They, of course, were interested in lens design and I worked in that area for a while.

Then you joined RCA in 1935 as a junior engineer in the Electronics Research Laboratory in Camden to continue work in optics?

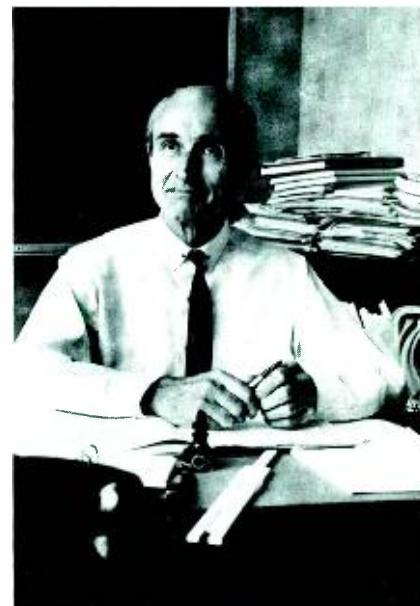
No. When I first came to Camden, I was working especially in the field of secondary emission and, incidentally, trying to understand what was happening in the Iconoscope, along with others in the laboratory.

What work was done on the Iconoscope during that period in Camden from 1935-1942?

When I came there, the tube existed and it was operative. We were really only trying to get rid of the bugs, so the speak—to increase the sensitivity because it was not nearly sensitive enough, and to remove some of its serious faults.

This was an especially interesting period of your career. Many notable individuals were in that group.

Yes, that was Dr. Zworykin's group and some of the people in it were George Morton, Les Flory, Jan Rajchman, Lefty Leverenz, Mannie Piore, Charley Busanovich, Bob Goodrich. We all worked closely together and had good fellowship.



Dr. Ramberg, you have numerous patents. Which one do you consider the most significant to you and the Company?

Well, I am not quite sure, but I suspect that the most basic patent is probably the one on electrostatic multiplier phototubes, although, beyond the first stage, all the further work was done by Rajchman, Snyder, and others. I really just suggested how they might be made. I computed the electric fields and electron paths and indicated that you could make electrostatic multipliers very simply. When the laboratory staff returned from vacation, George Morton built some of the tubes and the idea worked. Afterwards, Rajchman and Snyder did a thorough job and really optimized the design and constructed a workable device that has survived. We still use the original design. My role was concerned with the initial computations.

How do you feel the creative process works? Some say it is 90-percent hard work and 10-percent inspiration; others feel it comes in flashes.

I really think that to be a good inventor, which I do not pretend to be, you have to be saturated in your subject matter and keep your eyes open for other technology, because it is really bringing together different technologies that results in inventions. It can be all in the mind of one person, of course. But, it is always the fruit of cooperative effort. You never start with your own work; it is always somebody else's.

Is there a competitive spirit among scientists which will drive the individual to strive exclusively for his own ends?

People very often cooperate in a group and compete with other groups. So you have cooperation and competition working side-by-side. I don't know whether or not you need the competition, but it is a very common phenomenon. It very easily becomes a game; most of our games are competitive. I think that this is simply habit.

Today we hear much of technical obsolescence—that the half-life of man's technical knowledge is about 7½ years. How do you view this proposition?

While this statement about the "half-life" may be perfectly true, there is a good deal of fundamental information that survives indefinitely. There is a whole lot of classical physics which is as valid now as when it was first con-

ceived. There is a whole lot of mathematics that hasn't changed. You can always add to this basic knowledge and derive satisfaction from doing so. What is obsolescent is only the application to a rather limited field. And, I think there has been a trend for many years in engineering schools to get away from over-specialization and to place more emphasis on fundamentals that will survive longer.

Then you feel that the universities should concentrate on a generalized curriculum rather than producing more and more specialists?

Yes, I think so.

But, doesn't the competition in the business world dictate the need for the specialist?

Yes, that usually comes after you get to the company. I don't think the colleges should teach specialties.

Since specialization does occur when you get to a company, how did it happen in your case?

I had never taken a course in electronics. I had diligently avoided anything in alternating currents or electrical engineering, i.e., until I came here. But, when it was needed I simply tried to learn what I could and what was available.

Why did you avoid it?

Well, you see this is the old story. I avoided it simply because you are presented with a tremendous choice, and you are always up against the question: Now am I really going to understand what I am doing in a relatively narrow field? Or am I going to spread myself very thin? And you have to make some kind of choice. Now, the field in which I concentrated was really theoretical physics before I came here, and alternating currents is way over on one edge of it. In fact, you won't find it taught in most universities in the physics department. Cornell was very much the exception in that respect.

In 1942, you transferred as a research physicist to RCA Laboratories in Princeton. What work were you charged with at the Labs?

Well, at that time I was principally concerned with the electron microscope. Dr. Zworykin had become interested in the device. He recognized its great potential value, noting that encouraging

preliminary results had been obtained at Siemens. He induced first Dr. Marton to come from Brussels and, later on, Dr. Hillier to supervise the building of an electron microscope. Dr. Hillier was an extremely effective, energetic worker and administrator. As I recall, within less than a year he had a practical instrument working, which was installed at the American Cyanamid Company in 1940.

How many electron microscopes did RCA produce?

For a long time there were more RCA electron microscopes in the world than any other make—over 2,000 were produced by RCA. For me, the electron microscope project was a very enjoyable project. I thoroughly enjoyed the group.

In 1949, you interrupted your work to serve as a visiting professor in Munich. When you returned, were you still involved with optics?

Yes, when I came back the color television campaign was started, and I was drawn into it like many other people. I worked in a number of different phases of it; electron optics had much to do with color television.

Who were the others involved in solving some of these problems?

Dr. Goldsmith has one of the oldest and most basic patents. The "mixed highs" is Bedford's contribution. He showed that you could compress the channel for color, owing to the fact that the eye is much less discriminating for chrominance than for luminance and also less discriminating for the blue than for the red-green. Harold Law was primarily responsible for the development of the shadow-mask color viewing tube, which eventually outstripped alternative designs worked on by Paul Weimer, Stan Forgue, Don Bond and others. Ray Kell, Al Schroeder, and Gordon Fredendall all made essential contributions to the development of a practical color television systems. Al Rose and Don North came from Harrison originally. Don North had done particularly important work in the noise area. Al Rose's name is associated more than any other with the development of the image orthicon, which was, in a sense, the final stage in the development of high-sensitivity camera tubes.

Reprint RE-18-2-25



Some of your work in television appeared in print.

Yes; in the period from 1950 on, the Zworykin and Morton book on television needed a new edition and I worked on that—in particular, the added part on color television.

What do your other books deal with?

They are cooperative efforts dealing with electron optics and the electron microscope; photoelectricity and its application; and the utilization of television in science and industry.

Presently, there seems to be a "war on science" or antagonism toward it. College enrollments in scientific fields are down, sociologically everybody seems to be attacking science; it is being viewed as an instrument of war. But many programs that might have been useful to society have gone by the wayside because of this attitude. For example, isn't the curtailment of the space program such a case? Can we not gain much insight from such exploration which will forward our society in the future?

Oh, I think that is certainly true. Yes we can. I must say that the space program, in the past, has been over-emphasized. I think especially the manned space program has become more a spectator's sport and has received tremendous support in part because of that, and in part simply because of nationalist competition that is really not very useful. But I think it will be less so in the future, and I think there is a very important area for space research. I believe it will normalize itself, but I don't think that our priorities have been ideal in that respect in the past.

So it seems our success is almost directly proportional to the emphasis we place on certain areas of research. And the question appears to be "who determines the priorities?"

That is a very complicated business. You can say the mass media have much to do with it, and then you come back to who controls the mass media. In almost all cases, it is a double effect: any group, whether mass media or political figures, in part are led and in part lead. Also, they usually act as amplifiers. I think there is a strong trend in almost any country for political figures to emphasize nationalism, although it is to the detriment of the country itself as well as of the whole world. Nevertheless, it often is an effective way of propelling the individual into a position of prominence, of power which he desires.

If we are to have a national goal to solve our problems, how do you do it within the framework of the economic structure of our free enterprise, profit-making system?

This is a very real problem. I will be very interested in seeing what happens, because ultimately the idea of continuous growth has to stop somewhere. It has to level off. I just do not see how our economic organization is going to adjust to that.

But if we can not solve our problems through the industrial complex, how else could we do it?

I think we are all aware of the fact that we don't have a free economy, and there is continuous competition between a controlled economy and free

economy. Where the free economy fails to be socially productive, the controlled economy will take over. I think that is simply inevitable. And, in fact, in many cases the behavior of the exponents of the so-called free economy is greatly improved by the threat of the controlled economy.

Can religious forces be more effective in dealing with these environmental and social problems?

No, only indirectly. I think it has been said that the ecological movement is a kind of religion, and it is quite possible that this is true. In a sense, religion will certainly play a role because religion is concerned with motivation, and we have to be motivated to do what we do. We won't do things because someone else demonstrates that a certain course is wise unless we also have the will.

Do you think the academic world, accused by some of irrelevancy to daily life, is applying itself properly?

I think the academic world is also searching for what it must do and is, on the whole, deeply concerned with its responsibilities. I suspect, if you examine the whole scene you may find some places where they do a pretty poor job and others where they do a very good job, with a wide spread in between.

Dr. Ramberg, could you tell us of your opinions on what constitutes the right kind of leadership—especially that leadership pertinent to those of college age.

Well, I think, in teaching, the important thing is the teacher and his personal relationship to the student. I mean he must be an example that the student would care to emulate—that is certainly



the basic thing. If he is teaching science he must himself be intensely interested and convey that interest; and at the same time he must have enough appreciation of the other person that he makes an effort to think himself into his position. If he can combine knowledge of the subject and interest in the student he will make a good teacher.

Can inventive thinking be demonstrated and taught to the young student?

Well, I think it can be taught only to inventive and research-minded individuals—simply by example and making it attractive. This is the way it always has been. The great schools have always worked that way.

Do you think that the foreign students are more intense about their learning?

I think the situation varies. It is very hard to generalize. If you take any group of people, the deviation from the mean within that group is tremendously large compared to the difference between the average of the group and that of any other group. Any group reacts to the environment in which it is put, of course, and that may change the average behavior.

The intensiveness of the engineering curriculum leaves little room for liberal arts courses. Because of this, some sociologists claim that they will have to take the leadership in society simply by default. How do you view this possibility?

I think the schools should devote a portion of their program to the social area. Especially in view of the rapid obsolescence of purely technical knowledge, it's pointless to cram in too much highly

specialized material. The fundamentals should be taught instead. That is a big enough task; in addition, I think it is essential to expose the students to their role in society. The decisions will have to be made by them eventually.

But doesn't the sociologist have to turn to the scientist for help in solving present-day crises?

Yes, I think the research scientist is needed. As you indicated, the great problem is how to get these things funded. How do you get, let us say, Congress to provide financial support? There are a good many projects that are important from the point of view of society and yet don't look awfully attractive for commercial exploitation. Medical electronics is one of the classic examples.

Do you feel that the challenge, the opportunity for the new scientist is as great as when you came in?

Oh, I think so, yes. Especially, in the sense of there being no end of problems. We have all experienced the discovery of completely new devices and phenomena. That teaches us that we cannot predict the future. The laser is a concept that was not known at all fifteen years ago. Before 1948, there were such things as solid-state rectifiers, but there was no idea of the flexibility and the range of possible applications of solid-state electronics. There are any number of such examples.

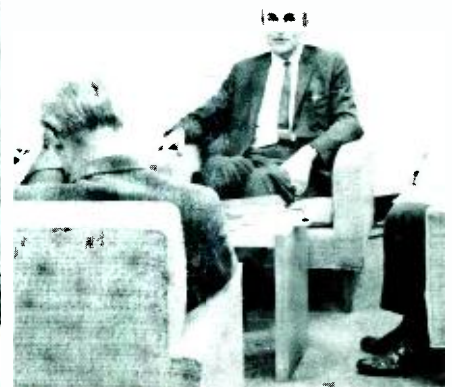
Phrasing the question a little differently, what message would you have for the young people coming into the scientific world today?

Well, that is a very difficult question. I think there are a tremendous number

of problems that have to be worked on, but I don't think that people will be inspired to work on them as long as we don't change the applications of science. I really don't think so. I think that the alienation we experience among young people against science is very real and very understandable too. I don't think the electronic battlefield is going to inspire any young person who isn't already in the midst of it and forgets what it does in the fascination of the technical problems.

What are some of the things that could really inspire young people to work in science?

Paul Goodman wrote an essay called "Can Technology be Humane?" and he answers this question in the affirmative. He points out a number of things that science can and should do. One of them is that scientists and technologists should take a larger view of things, that they should feel a responsibility for the effects of what they do, should look a little bit further than the interest of the problem itself, and also be concerned with the result of its implementation. He feels, that will give the technologist the feeling of being the craftsman who really puts himself into a task because he sees he is creating something beautiful and useful. Another thing he suggests is that science should be a little bit more humble and try to work with nature instead of forcing nature to its will. Of course, this is especially true in agriculture. An extreme antithesis to this is the present use of advanced technology to destroy the very basis of life in Vietnam and in Indochina generally. That is the sort of thing that makes science and technology a threat to survival.



What new devices might be developed to aid humanity in the near future?

Well, I am sure that new tools for increasing our understanding of the world and helping humanity will always be developed; tools like gas chromatography, to mention only one. There is no limit.

Is it possible we may even control powerful forces of nature such as earthquakes?

I don't think so. We deal with tremendously large forces that are very hard to get at, as far as I can see. The thing most likely to be realized is that we will become better and better at predicting earthquakes and their location so that we can avoid great injury and damage by keeping people away from such places.

You have also worked on electronic aids for the blind. What were the specific devices?

That was in 1945. At that time I was working at Haskins Laboratories in New York. They had two major projects: one was to work on reading devices, and the other was to work on guidance devices to enable blind people to avoid obstacles. The principal emphasis was on an ultrasonic guidance device. The reading devices were similar to those on which Les Flory has worked. The guidance device was essentially a sound radar system, utilizing echos.

Did the devices come into fruition?

No. I think they have been used experimentally but have not come into practical use. There are other methods that blind people use that do much the same thing, and they have practiced them for a longer time so that the learning problem isn't such a serious one. Hearing the echo of the foot-fall, using hard-soled heels, or of the tapping of the white cane, is an example.

You have also worked with lasers and holography. Do you see the laser being used in medicine as an operative instrument?

In a limited way, yes, I expect so.

How about the possibility of the laser for brain surgery?

Well, the trouble there is that you want to get into the interior of the brain, and

the scattering and absorption by the tissues for any kind of light or infrared radiation would be too great. Sound is used instead. Sound is focused at the point which is to be destroyed. But, of course, fortunately, chemical methods are beginning to take the place of this process.

In 1970, you made some predictions about holography in an RCA Engineer article. How do you see the future of holography today?

Well, at the time I thought that its future lay more in its auxiliary or instrumental function than in the more obvious uses that people thought of first, such as three-dimensional television or motion pictures. We will see to what extent it will be used to provide very economical video recordings, which would represent the type of function I had in mind.

In research you use certain tools. How do you feel about the computer in scientific research?

I think it is very valuable. But, I think it has its dangers also. The way the computer is used effectively is to use analysis without the computer as far as possible and then to use the computer. The temptation is to start with the computer at the beginning. Then you do not get a general answer—you get only limited answers.

There seems to be a tendency, in some cases, to rely too much on what the computer can help man with.

Yes. The wisdom of the computer is limited by the wisdom of the man who programs it. However, the speed and reliability with which it performs its operations are such that you can do many things with it that you just can't do otherwise.

Dr. Ramberg, you are a member of several professional societies and associations. Do you feel that they are doing their job or should they play a more active role, as some suggest, in lobbying activities?

Well, I do think that it would be very desirable if engineers and scientists would take a greater interest in the purposes for which their work is used; I would welcome lobbying efforts for the proper use of technology. Just lobbying for more funds can't inspire me too much. I expect that of people general-

ly—it is nothing very novel to me. The professional societies may do it. Or, if they don't, there may be separate societies that will do it. How this will work out, I am not quite sure.

You have worked closely with men who are called research scientists, applied scientists or engineers. Do you see any distinction in these labels we apply?

I have never felt that there was very much of a basic difference between these groups. Differences do develop depending on where they happen to work, and what their day-to-day responsibilities are. These may affect their general point of view. But I think a so-called scientist can become an engineer, and an engineer a scientist, depending on where you put him. There are really no basic differences.

Dr. Ramberg, you have earned a great deal of your livelihood within RCA. What are your thoughts about RCA, that is, as a place to work, the people you've seen, the opportunities it offers, etc.?

Well, I think what I've liked about it especially is that as far as I have been able to see, there always has been a great deal of freedom and readiness to have people pursue things they have worked out for themselves, things that interest them and seem hopeful to them. As far as I have seen, there has been little effort to compartmentalize groups very sharply and to keep them to very limited objectives. Of course, there have been cases where there has been tremendous stress on a certain objective, such as color television. But then, the reason for it has been made sufficiently convincing, so that cooperation was obtained spontaneously.

You have had a productive and enjoyable career as you told us. What are your plans for the future?

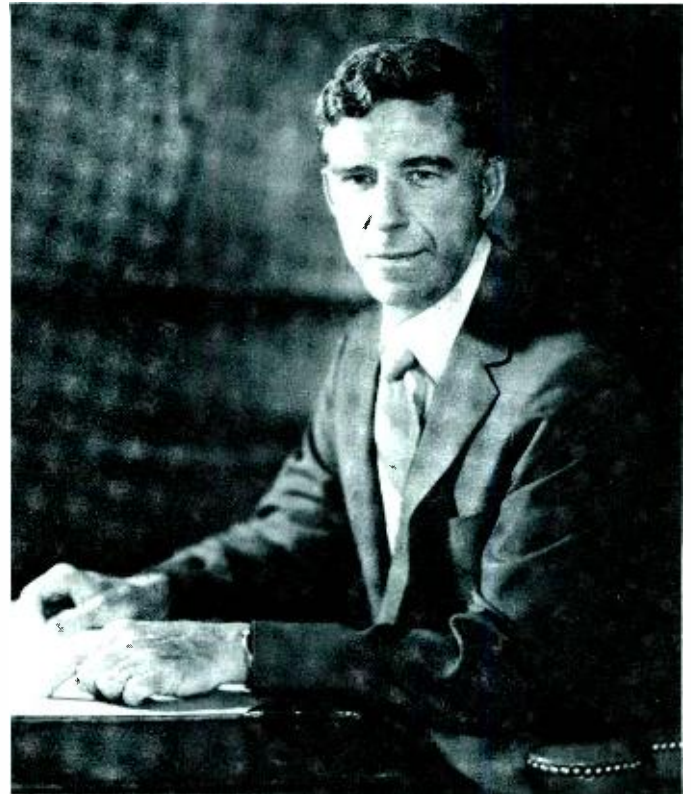
I really haven't made any definite plans. I think I first of all want to rearrange my books and my resources at home, and see what I can best do. I have no special expectation of leaving this area at present. There are always questions like health which may make it desirable to go to a different climate. Climatically I like the Southwest very much, but I don't know whether it would offer me as favorable conditions for activity as I may find here or elsewhere.

The Engineer and the Corporation

The role of laboratories

Dr. J. Vollmer

In an issue devoted to the Advanced Technology Laboratories, it seems appropriate to briefly examine the role of industrial laboratories in today's society. Certainly that role is different today from what it was a decade ago. In fact, the same statement can be made about all of engineering and science. There never has been anything even remotely similar to the techno-scientific enterprise as it exists today. The number of people, the facilities, the money invested, the expectation, the variety, the effect on life—all are on scale without precedent. It should not be surprising if the management, obligations, functions and responsibilities of such an enterprise have been and are being re-defined. This is especially true of that subset of activities which includes new technology, applied research, and advanced development.

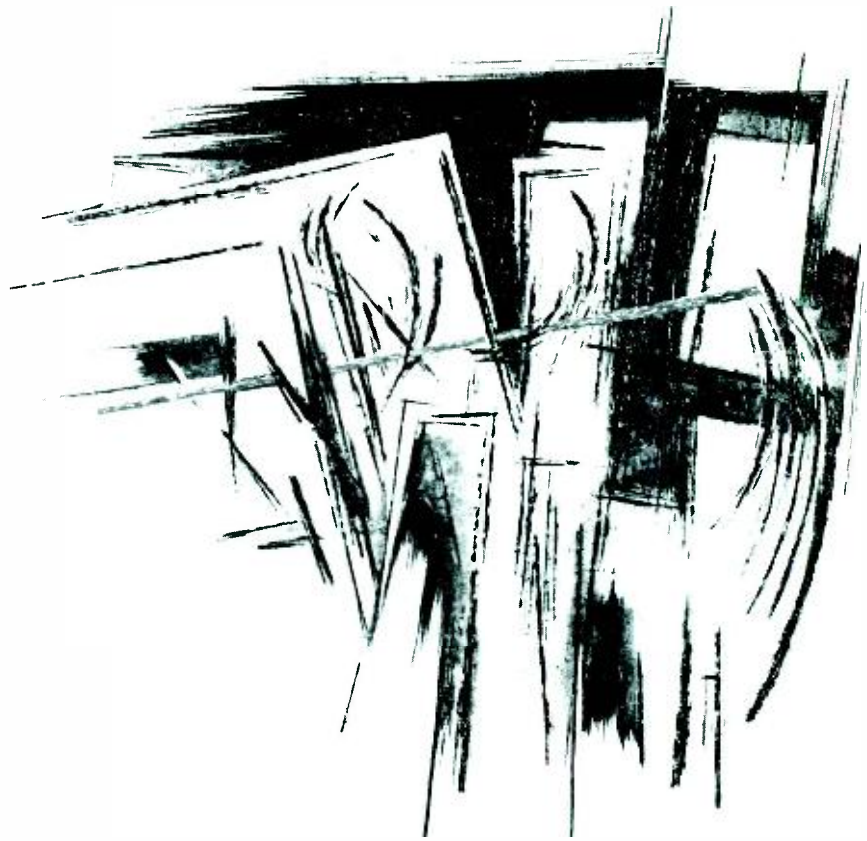


Dr. James Vollmer, General Manager, Palm Beach Division, Palm Beach Gardens, Fla., received the BS in General Science from Union College in 1945, the MA and PhD in Physics from Temple University in 1951 and 1956, respectively. In 1971, Dr. Vollmer graduated from Harvard University's Advanced Management Program. His research interests, publications, and patents cover a wide variety of fields, ranging from infrared properties of materials to plasma physics to quantum electronics. His professional experience includes—in order—five years of teaching at Temple University, eight years of supervising a research group at Honeywell and thirteen years of research supervision at RCA. Before assuming his present position, Dr. Vollmer was Director of the Advanced Technology Laboratories. Dr. Vollmer is a Fellow of the AAAS, a Fellow of the IEEE, and a member of the American Physical Society. His honors include membership in Phi Beta Kappa, Sigma Xi, Sigma Pi Sigma and Eta Kappa Nu. He is currently listed in *American Men of Science*, *Who's Who in the East*, and *Leaders in American Science*.

THERE WAS A TIME when the primary task of R&D groups was to invent new devices, generate new concepts, and solve problems which the groups deemed important. It was assumed that the results would be seized by product-oriented activities and that new markets would be automatically generated. How simplistic that viewpoint was!

Today, new markets rarely, perhaps never, originate in laboratories. Instead corporate goals and policies are established which broadly define the markets in which corporations have chosen to contribute. The role of R&D organizations is then to provide the new inventions and to generate original concepts which the corporations require to achieve their goals. This inversion of leadership role in the establishment of new market thrust is of paramount importance and warrants re-statement. General management has the responsibility for choosing new business areas, and for telling the specialty groups where it wants to go. Research and development groups, in turn, must plan, manage, and implement their programs to assist in the winning of those markets. It is difficult to imagine a pair of tasks which are easier to state or more difficult to accomplish. Unless both are achieved, neither can be achieved. Separately, they have been challenges to man's ingenuity. Coupled, which is the only condition under which they have value, they have baffled and humbled us all. Intellectual isolation, poor definition, bilateral intransigence, communication failure, and mutual disrespect in combination with an incredible complexity of process have made success an infrequent experience.

Perhaps the single most important concept associated with innovation is that technology transfer is not a discontinuous thing; it is a continuum. A particular project can be thought of as having a trajectory in a multi-dimensional medium in which the axes represent all of the functions of the corporation. For every coordinate, there is a threshold value which, if not attained, terminates the path. It is, perhaps, not surprising that successes are rare under such a constrained condition. Nevertheless that's the way it is. The challenge is to control the system in spite of itself.



Nevertheless progress has occurred. Retrospective analyses have provided insights into the elements of successful programs. The dynamics of innovation, a term widely used for the sequence of events from invention to use, has been under broad examination. Studies of the behavior of scientists and engineers in organizations have led to better understanding of motivation and conflict. Thus, the system, the process, and the components have been the objects of intensive study. Out of this research on research have come some insights which have already been incorporated into ATL. The traditional isolation of laboratories has been replaced. In its place are carefully designed communications channels which are highly interactive networks, involving all parts of the RCA organization. Great effort has gone into coupling functions: *marketing, planning, design, research, manufacturing, and finance* are all important terms in the ATL project matrix. Experience indicates that the earlier each activity becomes a part of the innovative process, the higher the probability of its success.

Reprint RE-18-2-1
Final manuscript received June 27, 1972

The articles in the ensuing pages are representative of the ten technologies under development at ATL. All ten were selected in an interactive fashion with the G&CS Divisions served by ATL. A broad-based technology plan exists for each. This is a description of opportunities, strategy, competition, and customers relevant to a technology. Within a technology, several projects exist. These also were chosen, organized, and are being carried on with the participation of diverse, concerned groups. Collectively these groups prepare a technology transfer plan for each project; i.e. they predict a trajectory in that multi-dimensional space of time, people; functions, and events. Implementing the trajectory is the task of all of the members of all of the organizations associated with the program from the recognition of need to a profitable fulfillment. It requires the creativity, the imagination, the technical sophistication, and the dedication of the traditional laboratory—combined with the new insights, the knowledge, the techniques, and the management skills of a directed, collective endeavor.

It is a long way from the idea of building a better mousetrap, but so is the rest of our world.

Growing importance of microsonics technology

Dr. D. A. Gandolfo | C. L. Grasse | G. D. O'Clock Jr.

In recent years, there has been a great surge of interest in acoustic surface waves or microsonics. There is now a great deal of work involving many investigators, covering the spectrum from basic materials research through systems applications. Ongoing work covers 1) development of new acoustic materials (both piezoelectric and non-piezoelectric) and improvements in already known materials, 2) development of heteroepitaxial systems providing desired combination of properties (e.g., piezoelectricity and semiconductor), 3) propagation studies in complex systems (anisotropic or multilayered or both), 4) phonon electron interaction studies, 5) device research on acoustic amplifiers and waveguides, 6) electromechanical transduction studies and 7) applications research on new forms of signal processing. The last aspect, new forms of signal processing, is the driving force behind the current interest. The main theme of this article is to discuss applications and to indicate areas where the surface-wave devices lead to real improvements. In what follows we discuss some of the fundamental aspects of acoustic surface-wave technology, some applications of the technology and the magnitude of the RCA effort.

SURFACE-WAVE TECHNOLOGY has now matured to a degree that permits designers of advanced systems to consider seriously the use of these devices with their attendant advantages in size, cost, and performance. The list of real-world problems being solved by acoustic surface waves, already impressively long for a new technology, is growing rapidly. Here at RCA we are building

- An EW receiver in which a surface-wave dispersive-delay-line frequency discriminator is the key element, and
- A miniature signal processor for an advanced phased-array radar, employing surface-wave correlators.

For a forthcoming space mission—

Reprint RE-18-2-3

Final manuscript received July 10, 1972.

Mariner Venus/Mercury '73—JPL is assembling a receiver using several micro-miniature acoustic surface-wave band-pass filters built by Motorola. Texas Instruments has developed and qualified for field use a surface-wave pulse-compression filter for a small radar. Autonetics has offered FM pulse-compression filters for sale. These examples illustrate the degree to which surface-wave technology has already penetrated electronic systems and reinforce the impression that the systems designer who has not considered

George D. O'Clock, Jr.

Physics Applications
Advanced Technology Laboratories—West
Van Nuys, California

received the BSEE and MSEE from the South Dakota School of Mines and Technology, and has done additional graduate work at UCLA. Mr. O'Clock's present work assignments involve the application of surface-wave acoustic devices to matched filtering and spread-spectrum techniques, along with the development of surface-wave amplifiers, waveguides, and measurement techniques. Before joining RCA, Mr. O'Clock was a member of the technical staff in the Telecommunications Department of TRW Systems. His primary tasks involved the design and development of a microwave front end for the Pioneer F and G (Jupiter Probe) deep space phase-lock command and tracking receiver, the design, fabrication, and miniaturization of microstrip S-Band amplifiers, X-Band stripline mixers, frequency multipliers, and microwave filters; and the conceptual design of acoustic surface-wave matched filters and sequence generators. Prior to joining TRW Systems, Mr. O'Clock served as Assistant Professor of Electrical Engineering at the South Dakota School of Mines and Technology. Mr. O'Clock worked at Hughes Aircraft Company's Infra-Red Laboratories on the gyro stabilization scheme for the TOW Missile Helicopter System. He also served as Officer-in-Charge in the field test phase of the Army's Geodetic SECOR Satellite Tracking Stations. Mr. O'Clock is a member of Sigma Xi, Eta Kappa Nu, and IEEE. He is a Registered Professional Engineer in the State of California, has one patent pending and has authored or co-authored over 12 technical publications.



it may be neglecting a very useful tool.

Some fundamentals

A great body of literature on surface-wave devices now exists, including several comprehensive reviews.^{1,2} Here, some of the basic aspects of the technology requisite for subsequent understanding of the applications will be discussed. In particular, surface-wave propagation and surface-wave transduction are all that need be understood for the applications to be described now. Other aspects of surface waves, such as amplification and waveguidance, are somewhat more remote in terms of the applications they permit, and they are not discussed here.

Propagation

Although numerous propagating modes are possible, the most commonly used is the simplest, the Rayleigh wave. This mode has both transverse and longitudinal components. The transverse component is normal to the surface on which the wave propagates, and the two components are 90° out of phase with each other so that the motion of a particle (i.e., a very small piece of the medium) describes an ellipse. These waves propagate at velocities slightly smaller than those of transverse acoustic vibrations in solids—a convenient approximate figure is 3×10^3 cm/s. Thus, kilometer-long electromagnetic paths shrink to centimeter-long acoustic paths. A device that permits 12.8- μ s processing

Dr. David A. Gandolfo, Ldr.

Physics Applications
Advanced Technology Laboratories—West
Van Nuys, California

received the BS in Physics from Saint Joseph's college and the MA and PhD in Physics at Temple University. Since joining RCA in 1960, he has worked in acoustic surface waves, microwaves, cryogenics, plasma physics, and radiation damage. He has conducted experimental programs in generation, reception, and guidance of surface waves using a variety of transducers and propagation media. He has also studied other microwave delay techniques employing YIG devices and superconductive slow-wave structures. His work in acoustic surface waves covers a broad spectrum, ranging from investigations into mechanisms for generating, detecting, and guiding surface waves to the development of a wide variety of practical devices and the application of these devices to systems problems. His cryogenics experience includes the design and fabrication of superconductive maser magnets and operation of these magnets in liquid helium baths as well as in closed-cycle refrigerators. In the area of plasma physics, Dr. Gandolfo has studied the interaction of electromagnetic waves with rocket exhaust plasma and the effects of this interaction on radar and telemetry systems. He has also experimented with a coaxial-rail gun plasma accelerator. In radiation damage studies, he has measured and analyzed the effects of high-energy proton bombardment on transistors. Dr. Gandolfo is a member of the American Physical Society and a Senior Member of the IEEE. He has authored many technical papers for publication and/or presentation at technical conferences.

time (corresponding to 128 bits at a 10 Mb/s rate) may be embodied in an acoustic crystal less than 3-in. long. On the basis of size alone, it is apparent that surface-wave technology is going to be compatible with modern microelectronic componentry.

Propagation losses, which may place an upper limit on the total processing time that may be envisioned, are approximately only a few tenths of a dB per microsecond for a good crystalline material such as lithium niobate at operating frequencies in the VHF-UHF range. Propagation losses are directly proportional to the square of the frequency and increase to about 1 dB/ μ sec at 1 GHz on lithium niobate. Reduced propagation losses are possible with magnesium aluminum spinel. For polycrystalline materials, such as the piezoceramic PZT (lead zirconate titanate), the propagation loss is considerably greater than in crystalline media, so that such materials are unattractive for frequencies above about 10 MHz.

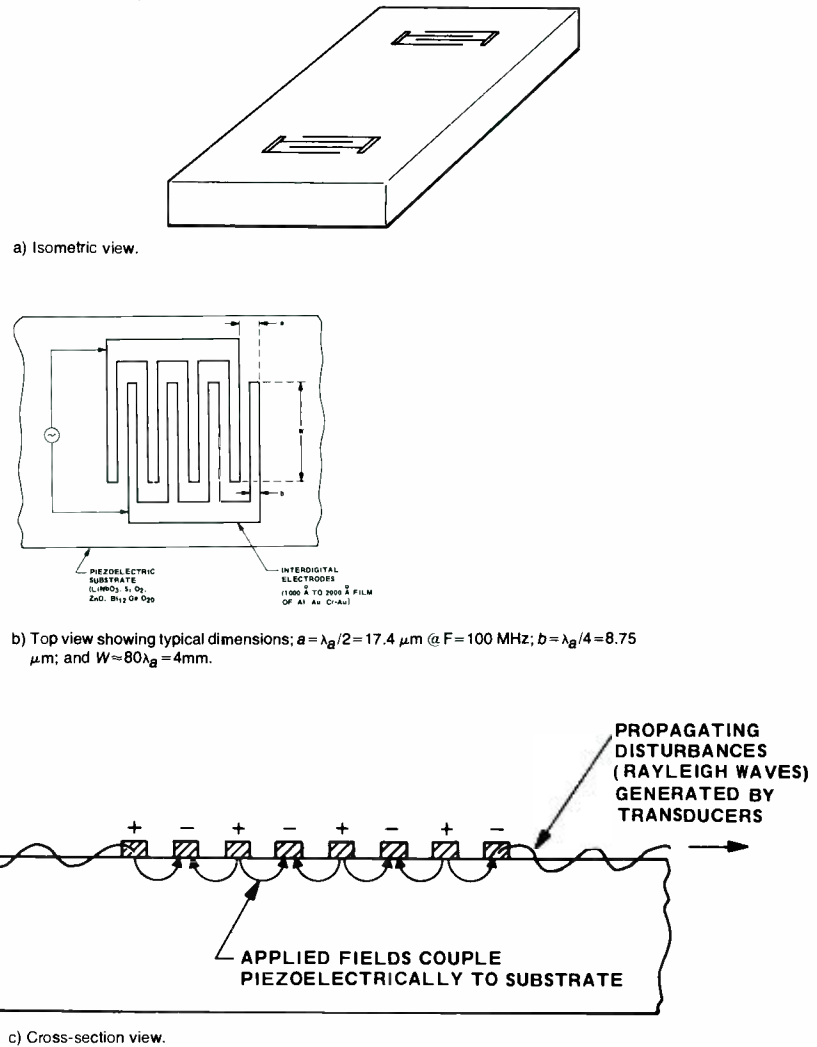
Transduction

From an applications point of view, the most important problem is that of transduction—the efficient conversion of electromagnetic energy into acoustic energy and vice versa. The best way of accomplishing this is the interdigital transducer. This beautifully simple structure not only permits efficient transduction but also makes possible many of the applications described in

Charles L. Grasse
Physics Application
Advanced Technology Laboratories—West
Van Nuys, California

received the BSEE and MSEE from California State University. Mr. Grasse has been with Advanced Technology Laboratories since 1970, where his main responsibility has been in the area of acoustic surface-wave phenomena and their application to microwave signal-processing devices. In his tenure with ATL, Mr. Grasse has been responsible for the design of several microsonic components, including a 400-MHz frequency-dispersive delay device (pulse-compression filter), a 32-bit biphase correlator, a switchable biphase sequence generator and matched filter, a continuously sampled microwave memory device, and a programmable tapped delay line. In addition, Mr. Grasse was responsible for the construction and evaluation of a VHF compressive intercept receiver. Mr. Grasse is currently responsible for the development of an acoustic surface-wave frequency discriminator, as well as a small-signal processor utilizing derivative-phase coded sequence generator and notched filters. His earlier experience has been electronic countermeasures techniques in which he has contributed both theoretical studies and electrical design. Mr. Grasse was also responsible for a signal intercept and analysis technique involving the use of a compressive receiver processor for detection and an advanced signal averaging process for determining signal parameters.

Fig. 1—Delay line employing interdigital transducers. Material is YZ LiNbO_3 , acoustic velocity is 3.48×10^5 cm/s.



this paper. The basic transducer, along with some key features, is described in Fig. 1. These transducers are made by photolithographic techniques identical to those used in LSI processing, and are quite small (as indicated in Fig. 1). For both reasons the acoustic surface-wave signal-processing devices are compatible with microelectronic componentry.

The unique advantage of the surface-wave devices is that the energy is confined to a free surface so that it may be sensed at any point desired along the propagation path. Thus, the interdigital transducer is ideally suited for this technology. By varying the geometry of the transducer, one may synthesize a variety of signal processing functions; the following paragraphs describe these functions along with the systems to which they may be applied.

Applications areas

Some of the many applications of acous-

tic surface-wave technology that have been identified are described in this section. The list is not complete, but the objective here is to treat those applications areas in which surface wave devices are—right now—finding their way into systems. The applications fall into two major areas: those employing dispersive delay lines and those using biphase coded lines. The former include frequency discriminators, linear FM pulse-compression filters and compressive or microscan receivers. The latter includes code generators and matched filters for spread-spectrum communications and for radar pulse compression. A third area is that of bandpass filters which relate to EW and communications systems. (Application of surface wave devices in EW systems is treated in Ref. 3). Each of these is described in some detail below.

Frequency discriminator employing dispersive delay line

The interdigital transducer is a resonant structure; *i.e.*, the separation between adjacent fingers must be equal to one half the acoustic wavelength at the design frequency for efficient transduction. An extended transducer with a gradual change in finger spacing along its length will be sensitive to different frequencies along its length. Thus, signals at different frequencies will be launched (and sensed) at different positions along the transducer. A dispersive delay line using two of these transducers (one input and one output) is illustrated in Fig. 2a. The values of frequency and time delay refer to a device developed at ATL.

By measuring the time delay for a signal traveling through the line, one measures, in effect, the frequency of that signal. Thus, the surface-wave dispersive delay line affords a small, inexpensive technique for realizing a frequency discriminator. The discriminator is a key element in a set-on receiver used in expendable jammers for electronic warfare. The receiver is required to measure the frequency of a hostile radar signal (to an accuracy of ± 2 MHz) and to "set-on" a transmitter which will respond at the same frequency. An accurate frequency measurement is required so that the transmitter may conserve power by concentrating its output directly on the threat frequency. A schematic of a discriminator-receiver is shown in Fig. 2b.

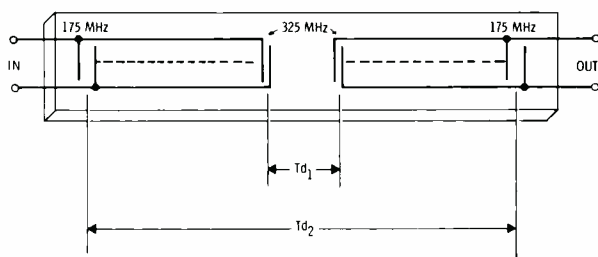
The input signal is down-converted to an IF in the range of 100 to 500 MHz where it is most convenient to fabricate the surface-wave devices. (At this point, we should note that the use of

surface-wave devices will often require frequency conversion; however, the advantages in size, cost, and performance are sufficiently great that one realizes an overall improvement in the system even with the additional complexity of frequency conversion.) The dispersive delay line then provides time delay as a function of the input frequency. The output is detected, amplified, and used as a stop pulse for the frequency counter (which was started by the undelayed received signal). The counter output (stored as a digital word) is thus a function of the input frequency and is used in the acquisition control to start the closed-loop cycle. In this cycle, the vco signal is substituted for the input signal, and is stepped across the band until a match occurs in the comparator between the stored input and vco frequencies. The processing of each vco frequency is identical to that of the received threat signal. The subsequent jamming transmission then occurs (under control of a look-through generator) at this "matched" frequency. The same circuit can also be operated as an open loop with a savings in components and set-on time but with some sacrifice in long-term stability and set-on accuracy.

A dispersive delay line developed at ATL-West (Fig. 3) demonstrates the feasibility of using the surface-wave devices in the frequency discriminator application. This line permits a frequency-measurement accuracy of about 2 MHz over a 150-MHz band.

Linear FM pulse compression filter

Thus, the interdigital transducer lends itself quite naturally to the construction



a) Dispersive delay line. Time delay for highest frequency, $T_{d1} = 2.5 \mu s$; time delay for lowest frequency, $T_{d2} = 12.5 \mu s$.

Fig. 2—Frequency discriminator.

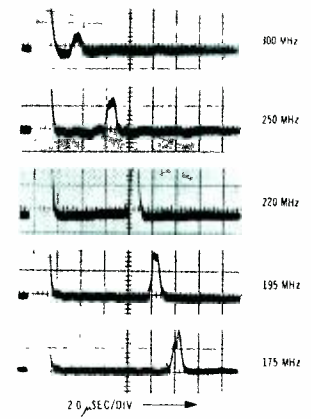
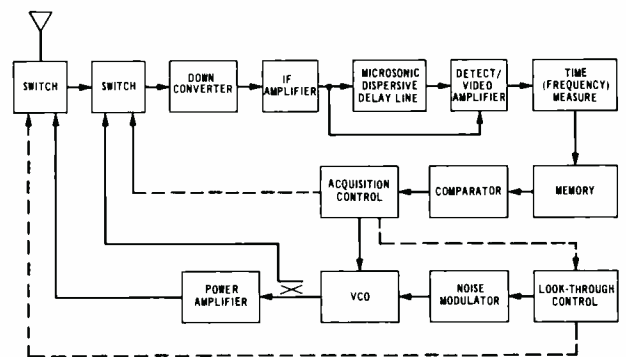
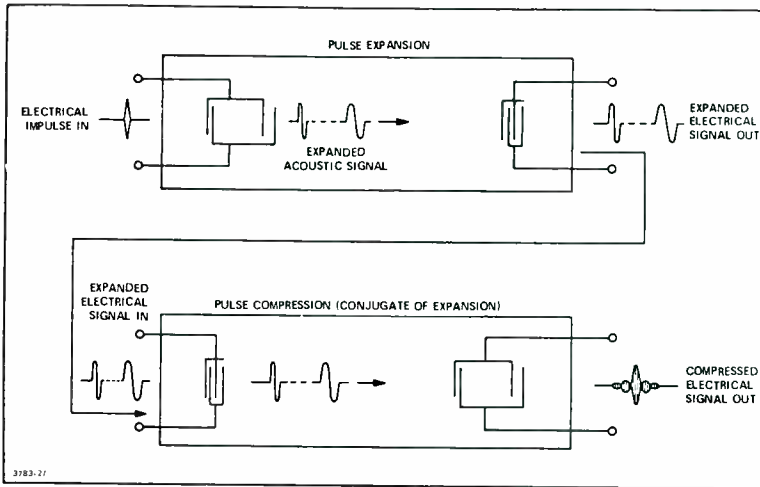


Fig. 3—Time delay vs. frequency for dispersive delay line developed at ATL.

of a dispersive delay line, and this dispersive delay line may form the basis of a frequency discriminator. With the development of such a dispersive transducer, it is now possible to think in terms of an acoustic surface-wave pulse compression radar system. The schematic of Fig. 4a illustrates the operation of such a system. The key element in the system is the dispersive waveform generator (and matched filter). The efficient generation of a linear frequency-modulated waveform may be accomplished by an acoustic surface-wave device employing a dispersive transducer.⁴ The dispersive transducer, as was described previously, is an interdigital device in which the periodicity of the array of fingers is varied linearly such that different regions of the transducer are sensitive to different frequencies. The FM signal is generated (Fig. 4) by applying an electrical impulse to the dispersive transducer. The frequency content of the impulse must be of sufficient energy so that each interdigital finger-pair is able to detect and launch as a surface-wave the frequency for which it was designed. The



b) Expendable ECM device employing frequency-discriminator timing.



(c)

resultant waveform, whose frequency varies linearly throughout its pulse length, is converted to an electrical FM signal by the non-dispersive output transducer. Fig. 4b is a sampling-oscilloscope photograph of the linear FM waveform produced. The pulse is $0.5 \mu\text{s}$ long and varies linearly in frequency from 360 MHz to 440 MHz, for a time-bandwidth product of 80.

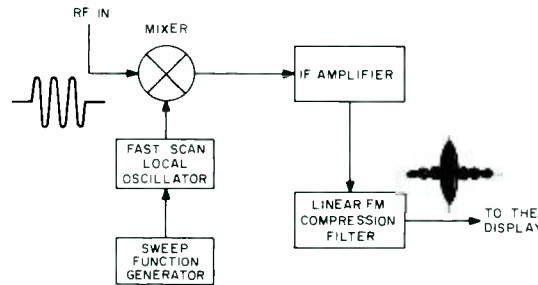
Upon striking a target the signal would be reflected back toward the radar, amplified and presented to the conjugate matched filter (Fig. 4 a). The reflected FM signal is first converted to an acoustic signal by the small input transducer, and then propagated down the substrate beneath the dispersive transducer. When the signal is spatially registered with the dispersive transducer, *i.e.*, when the high-frequency components have propagated to the end of the transducer with small finger spacing and the low frequency components to the end with large finger spacing, all frequency components will interfere constructively. At other times, the signals will interfere destructively (but not completely so) and the output will exhibit the $\sin x/x$ response with one large main lobe and many smaller sidelobes. Fig. 4c illustrates the compressed output pulse from the radar receiver.

VHF/UHF compressive receiver

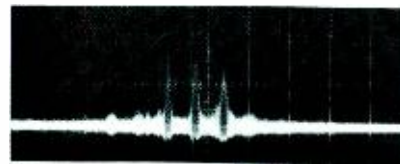
The compressive receiver (Fig. 5a) is an intercept receiver which must be able to monitor the activity of a large number of signal transmissions occurring over a broad range of frequencies, while providing sufficiently high-frequency resolution, sensitivity, and sweep speed

to ensure a high probability of intercepting and identifying specified classes of signals in a dense environment. The increased use of signal space is particularly evident in the VHF and UHF frequency bands where many new and complex broadband communication systems are being developed. Each of these new systems present unique problems that require the advanced signal processing capabilities provided by a compressive receiver intercept technique.

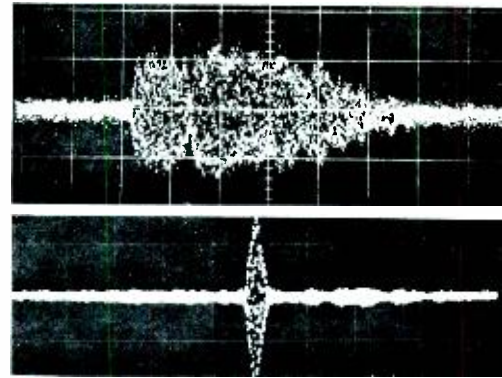
The primary object of the process is to maximize the signal-to-noise ratio and thus enhance the detection process. To accomplish this, the compressive receiver should be matched to the particular RF signal it is desired to receive. In the present application, however, the characteristics of the signal are unknown and such a dedicated receiver is not available. The approach is, there-



a) Compressive receiver.



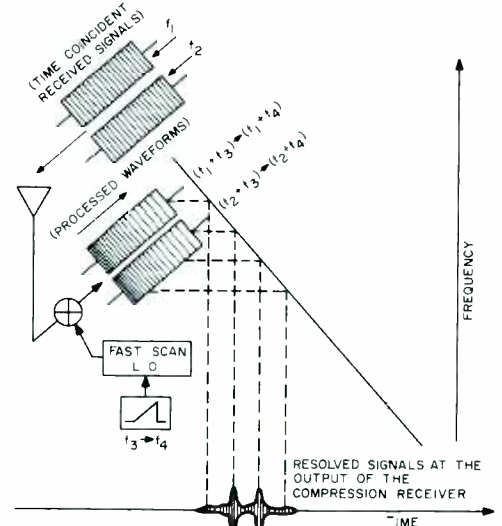
b) Process for separating time-coincident input signals



(b)

Fig. 4—Linear FM pulse compression.
a) Operation of filter showing pulse expansion and compression.
b) Expanded pulse. Horizontal scale is 100 ns/div.
c) Compressed pulse. Horizontal scale is 100ns/div.

fore, to precondition all signals to match the intercept receiver as closely as possible. The received signal is frequency modulated continuously in a process designed to "match" the incoming signal to the compression filter. Since the characteristics of the signal are, for practical purposes, unknown, the compressive receiver is not expected to produce an optimum compressed pulse output. The object is, rather, that the compressive receiver maximize the signal-to-noise ratio for a variety of input signals that are not necessarily matched to the receiver. In theory, therefore, intercept-signal acquisition is limited only by the signal itself. The attainment of the potential compressive receiver performance requires that the following basic conditions be met: 1) the fast-scan local oscillator must have a linear FM characteristic, 2) the scanning must be



c) Experimental separation of two simultaneous pulses.

Fig. 5—Operation of VHF/UHF intercept receiver.

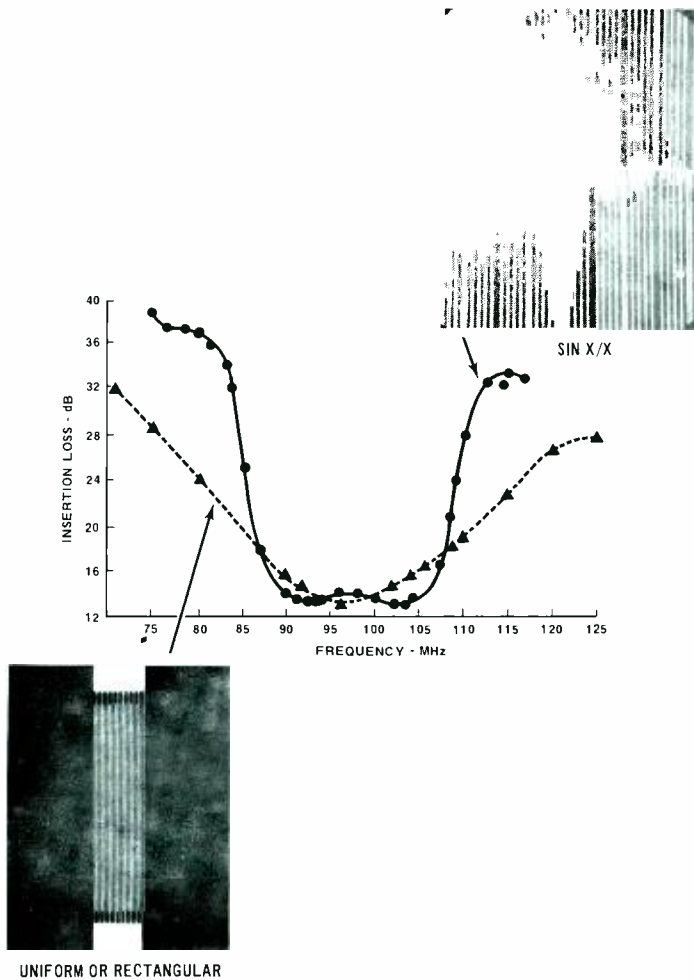


Fig. 6—Shaped passband for two transducer geometries.

accomplished within the duration of the signal it is desired to process, and 3) the compression filter must have a linear FM characteristic matched to the signal produced during the scanning process. When these conditions are satisfied signal acquisition (detectability) is determined only by the available signal energy, and frequency resolution is limited only by the duration of the signal. It is important to note that such a receiver is capable of providing signal processing gain to a wide variety of signals—signals that would normally require their own individual matched filter for detection. Another interesting property of the compressive receiver is its ability to separate virtually time-coincident input signals. The process is illustrated in Fig. 5b. The two signals shown arrive at the input of the receiver at the same time, but with different RF frequencies. Each is processed in the same manner described in the previous paragraph, the result being two linear FM signals, each with a slightly different frequency content. When the two signals are applied

to the dispersive filter, each will be compressed by part of the delay line that is sensitive to its particular frequencies. Because of the time versus frequency characteristic of the filter, the signals

will appear at the output at different times. Fig. 5c illustrates the experimental separation of two simultaneous pulses by the compressive receiver.

At ATL, we have developed a compression filter with a time-bandwidth product of 1500 (10- μ s delay dispersion and 150-MHz bandwidth).⁵ Time-bandwidth products as large as 10^4 appear to be feasible although not yet demonstrated. No technology other than surface waves offers the prospect of such large processing gain in such a small size—and with the added feature of low cost in relatively small volume.

Acoustic surface-wave bandpass filters

This technology permits the implementation of a new class of passive filters.⁶ These inexpensive, microminiature filters offer promise of widespread receiver applications, particularly in cases where incoming signal frequencies are determined by passage through a contiguous filter bank. Once again, the key to the operation of the filters is the interdigital transducer structure which determines the width and shape of the passband through its geometry. The simplest surface-wave filter consists of a pair of closely spaced interdigital transducers on a piezoelectric substrate. For rectangular transducers, *i.e.*, those in which the interdigital overlap is constant along the length of the transducer, a $\sin x/x$ frequency response is produced. On the other hand, if the interdigital overlap of the

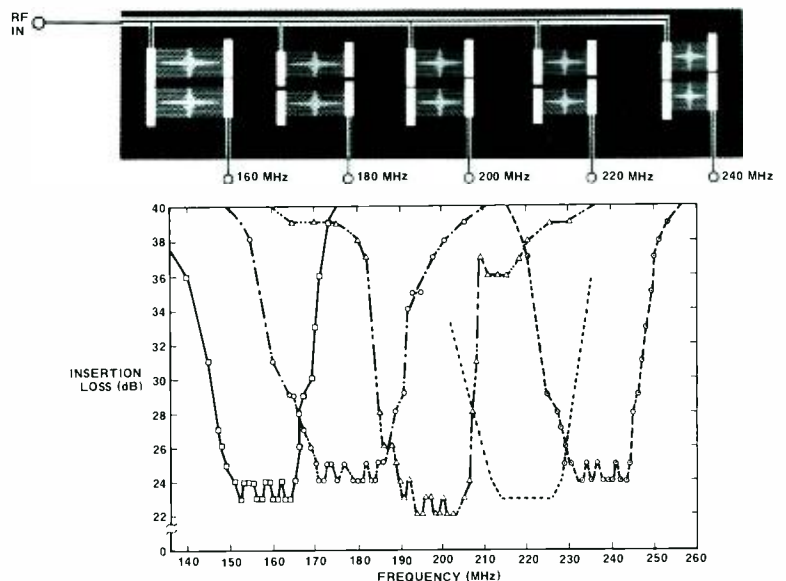


Fig. 7—Acoustic surface-wave contiguous-channel filter bank using five surface-wave filters.

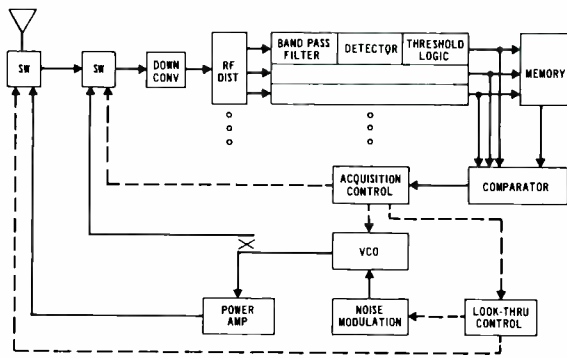


Fig. 8—Expendable ECM employing contiguous filter-bank tuning.

transducer follows a $\sin x/x$ function, then a rectangular passband will be produced. In other words, the shape of the passband is the Fourier transform of the interdigital overlap pattern. Some results are illustrated in Fig. 6 for the two geometries just described. Other geometries and other band shapes are possible.

Perhaps the most significant contribution to be made by surface-wave filters will be in the area of electronic warfare where the need exists for small, inexpensive frequency discriminators in EW receivers. The frequency discriminator will permit the accurate measurement of a threat frequency so that an appropriate response may be made. By appropriate response, we mean one in which power is concentrated at the frequency of the incoming signal rather than dispersed over a broadband. A similar application for the dispersive delay line was described earlier. The advantage of a contiguous-filter-bank discriminator is that it is a parallel process and therefore provides a much quicker acquisition time. A discriminator employing a bank of five surface-wave filters is shown in Fig. 7. Each filter is a pair of $\sin x/x$ weighted transducers. (In a later design the filters consisted of one rectangular and one $\sin x/x$ transducer). The filters operate at center frequencies of 160, 180, 200, 220, and 240 MHz. Each filter has a 20-MHz band, and adjacent bands intersect at the -3 dB points. Insertion loss of 12 dB per channel has been measured. Skirt slopes are between 2 and 5 dB/MHz across the band. The entire bank of filters was easily fabricated on a crystal of lithium niobate measuring only $\frac{1}{2}$ in by 1 in—with a large area remaining.

A block diagram of an ECM receiver employing bandpass filters is shown in

Fig. 8. This illustrates a closed loop automatic tuning receiver similar to that described earlier for the dispersive delay line frequency discriminator. The input signal, after down-conversion, is distributed to the parallel microsonic bandpass filters (which can be either contiguous or individually designed for specific center frequencies and bandwidths). The output of each filter is detected and passed through threshold logic where outputs are compared to establish correct channel identity. The properly identified channel is coded and set in a simple memory. Acquisition control then switches out the signal and

switches in the VCO which is swept across the filter bank until subsequent detection and identification matches the previous input signal. The small size of the surface-wave filters permits about 10 of them to be formed on a crystal whose area is only about 0.5 in. A conventional passive filter bank would be at least one order of magnitude larger. The LSI fabrication technique would permit the surface-wave filters to be produced more cheaply than active filters which might compete in size.

Signal processors employing biphase correlators

The biphase correlator makes use of still another variation of the geometry of the interdigital transducer. It is a tapped delay line in which the taps are spaced from each other by an integral number of wavelengths at the design center frequency. Each tap may be connected to an RF summing bus in one of two senses which are 180° out of phase with each other. A typical biphase coded device is shown in Fig. 9. This simple device may serve as the sequence generator as well as the matched filter for biphase codes. Coded waveform generation is accomplished by impulsing one of the transducers and

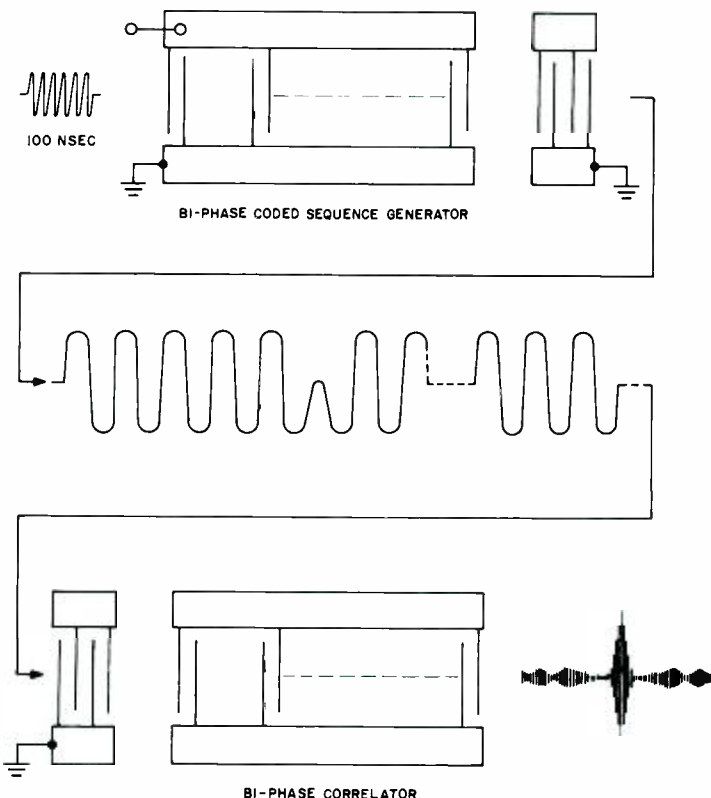
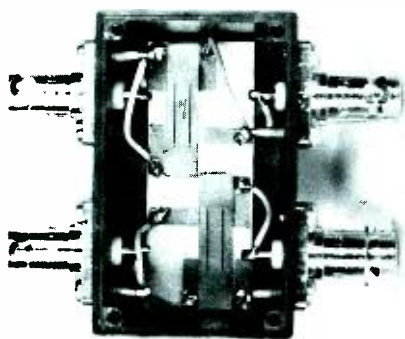


Fig. 9—Typical biphase coded device.

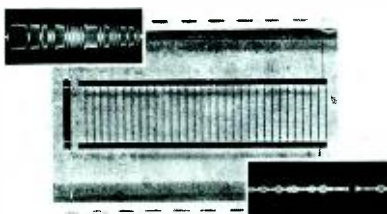
taking the output from the other one. As the signal propagates down the line it will be sensed by each tap in succession. The phase of the signal from each tap will be determined by the way that the tap is connected to the RF summing bus. Matched filtering is accomplished by causing the coded signal to pass along the array of taps in the opposite direction. If the coded signal is applied to the input transducer of device No. 2 (Fig. 9), it will propagate along the line, and the output from the coded transducer will be the autocorrelation function. The large correlation peak will be observed when each bit in the coded signal is spatially registered with a tap of the appropriate phase so that the outputs from all taps interfere constructively. A coded sequence and autocorrelation signal are shown in Fig. 10b for the device pictured in Fig. 10a. The data rate for these devices is determined by the tap spacing. In this case, the spacing is equal to a propagation of $0.1\mu\text{s}$ so the data rate is 10 Mb/s.

The advantages of this simple device are numerous:

- 1) It is completely passive, and, for fixed codes, requires no power (a higher data rate is obtained simply by placing taps closer together);
- 2) It may be batch-fabricated by using the same photoetch techniques developed and perfected for integrated-circuit manufacture; and
- 3) It is very small so that it lends itself quite nicely to the construction of hybrid microwave circuits. (One estimate says that



a) Device photo.



b) Waveforms of the code sequence and correlation.

Fig. 10—Biphase coded sequence generator and correlator.

the use of surface-wave correlators will permit a 4:1 reduction in size from that required for more conventional techniques).

For these reasons, the surface-wave correlators stand an excellent chance of having a major impact on advanced shipboard air defense radar systems such as AEGIS. Because the devices permit linear analog processing of the RF waveforms, the processing gain is improved by about 3 dB. This improvement translates directly into a reduction of the prime power required in the system. The power reduction, combined with the size reduction permitted by the compact form of the surface-wave devices, allows the size of a prototype radar system to be reduced by one entire cabinet. The size and concomitant cost reductions may permit this sophisticated new radar defense system to be extended to more vehicles than hitherto considered realistic.

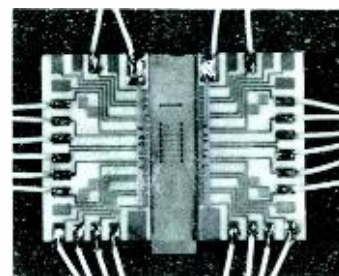
Spread spectrum communications applications

The surface-wave correlators are expected to be useful in another class of applications, *i.e.*, spread-spectrum communications in which digital techniques are employed to achieve security from detection, a high tolerance to jamming, and a degree of noise immunity. The correlators may be used to generate and recognize synchronization signals as well as the data bits of a particular message. Examples of spread-spectrum communications systems are 1) the CNI (communications, navigation, identification) system in which one complex waveform is employed for all the functions in a dense multi-user environment and 2) the RPV (remotely piloted vehicle) system which requires reliable communications among vehicles in a severe jamming environment.

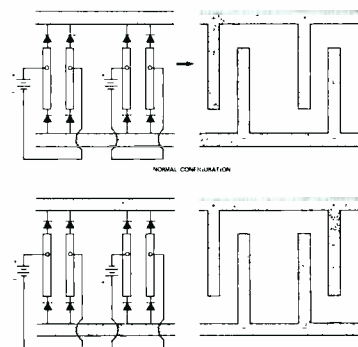
For both of these applications the microsonic correlators require a refine-

ment, code versatility, so that the codes may be changed quickly as the tactical situation requires. Two approaches to the problem of achieving code versatility are being investigated at ATL-West. The desired device is a programmable tapped delay line or "switchable correlator,"^{7,9} and we are implementing it in hybrid and monolithic thin-film forms. Common to both forms is the requirement to connect each tap to the RF summing bus through a control device rather than directly, as in the simple fixed-code devices described earlier. An early hybrid device is shown in Fig. 11a, along with a schematic (Fig. 11b) showing the manner in which the phase of a tap is changed by 180° and the waveforms (Fig. 11c) related to two different tap settings.

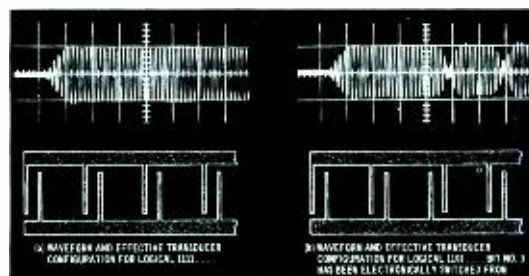
We have considered several kinds of control devices for this application and have actually used commercially avail-



a) Photo of an early hybrid device.



b) Normal and phase-reversed diode configurations.



c) Coded waveforms related to two different tap settings.

Fig. 11—Switchable correlator.

able PIN diodes with beam leads and custom-made silicon-on-sapphire (SOS) diode arrays prepared at RCA Laboratories. Both of these permitted passage of RF in the 100-MHz range and have switching times in the microsecond range. We have designed programmable devices employing switches such as these and control circuitry capable of changing a code of approximately 100-bit length in a time of the order of 1 ms. Fig. 12 shows a bit-programmable line, as well as the sequence generated by it and the auto-correlation output of the conjugate line.

A second monolithic approach uses piezoelectric zinc-oxide films to launch surface waves on a silicon substrate containing arrays of MOS transistors. The gate mobility and therefore drain current in the transistors is weakly sensitive to the strains associated with the acoustic wave, through the mechanism of piezoresistance, and may be used to detect the surface waves. The tap phase may be changed 180° by interchanging the source and drain. It is easy to visualize the control circuitry required to do this, implemented on the same silicon substrate as the tapped delay line. The entire subsystem would be fabricated through LSI methods and should permit inexpensive, large-quantity production.

RCA effort

RCA effort and capability have expanded gradually but impressively in recent years. The authors' own group is performing the familiar advanced technology function of identifying needs in the product divisions and attempting to satisfy those needs with new technology solutions employing the results of current research at RCA Laboratories and other laboratories. The range of microsionics activities at ATL was indicated in the previous section and here we review, briefly, the important contributions being made at other RCA locations.

Basic to success in surface waves is the fabrication technology developed at Micro-Electronic Technology and Solid State Technology Center in Somerville. These groups made the photomasks and carried out the processing for nearly all of the devices described earlier and would provide the basic fabrication know-how required to produce large

numbers of components. ATL continues to work closely with these groups to improve fabrication capability.

We are conducting joint programs with two G&CS divisions: the Electromagnetic and Aviation Systems Division (EASD) and the Missile and Surface Radar Division (M&SRD). With electronic warfare engineers at EASD, we are jointly developing small, inexpensive receivers employing dispersive delay lines and filters for use in expendable jammers. With M&SRD, we are developing portions of a radar signal processor using biphase coded pulse-compression devices. This processor, if used in a shipboard air defense radar, will permit size and power savings which may make it possible to install the system on smaller vehicles.

We are working together with the Laboratories and the Solid State Technology Center (SSTC) to develop the monolithic programmable correlator—a device with tremendously broad spread-spectrum communications applications. RCA Laboratories is developing the quality piezoelectric films needed to generate acoustic waves on nonpiezoelectric substrates like silicon, while SSTC is fabricating the new SOS transistor arrays needed to detect the waves.

A large group at RCA Laboratories in Tokyo is working to develop new acoustic materials, new transducer techniques, and materials that permit

electric-field control of surface-wave velocity. They are also investigating nonlinear propagation.

A group at Princeton is considering filter problems—in particular, the problem of modifying the interdigital transducer geometry to synthesize a complex response such as might be required in a color-TV IF strip. ATL-West is applying the results of this effort to other filters.

We are working closely with yet another group at Princeton in the area of advanced surface-wave materials. This group is developing heteroepitaxial systems such as aluminum nitride, gallium nitride, gallium arsenide, and zinc oxide on refractory and semiconducting substrates. We are evaluating these complex new systems for possible applications in surface-wave amplifiers, waveguides, and integrated subsystems. Informal but close contacts have been made with a group which developed custom arrays of SOS diodes for programmable correlators.

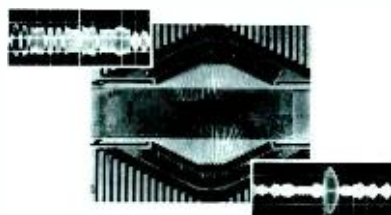
The combined capability of these groups in acoustic surface waves represents an important resource for the development of a wide variety of signal-processing systems.

Acknowledgment

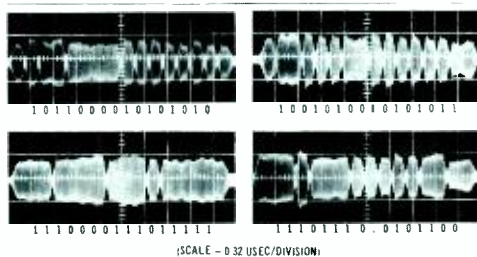
The authors are grateful to the many people who have contributed to the development of the microsionics program at Advanced Technology Laboratories as well as the RCA Laboratories in Princeton and Tokyo, and in the Divisions. Very special thanks are due to R. A. Geshner and J. M. Mitchell who participated in the fabrication of nearly all of the devices described earlier.

References

- White, R. M., "Surface Elastic Waves" *Proc. IEEE*, Vol. 58 (1972) p. 1238.
- Vollmer, J. and Gandolfo, D., "Microsionics" *Science*, Vol. 175 (1972) p. 129.
- Gandolfo, D. A.; Grasse, C. L.; Schmitt, E. J.; "Surface Elastic Waves: New Signal Processing Tools for Electronic Warfare," *Microwaves* (Oct 1971).
- Grasse, C. L. and Gandolfo, D. A., "Acoustic Surface Wave Compressive Receiver", presented at the 1971 IEEE Ultrasonic Symposium, Miami, Florida (Dec 1971).
- ibid*
- Grasse, C. L., Gandolfo, D. A., "Acoustic surface wave filters," 1972 Electronic Components Conference, Washington, D.C.
- Gandolfo, D. A.; O'Clock, G. D.; Grasse, C. L.; "Acoustic surface wave sequence generators and matched filters with adjustable taps," 1971 International Microwave Symposium, Washington, D.C.
- O'Clock, Jr., G. D.; Grasse, C. L.; Gandolfo, D. A.; "Switchable Acoustic Surface Wave Sequence Generator" *Proc. IEEE (letters)*, Vol. 59 (1971) p. 1536.
- op. cit.*, 1971 IEEE Ultrasonics Symposium



a) Photo of sequence generator/correlator along with auto-correlation output.



b) Sequence generated.

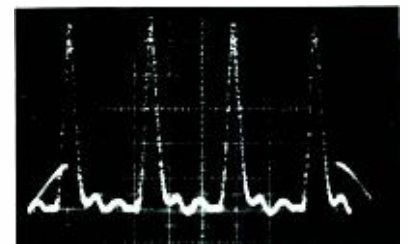
Fig. 12—Programmable 16-bit sequence generator/correlator.

One-gigabit YAG laser techniques

C. W. Reno

Techniques for internally modulating and multiplexing mode-locked Nd^{3+} :YAG lasers have been developed. These techniques are directed toward fulfillment of requirements for 1-gigabit communication systems required specifically for an Air Force spaceborne communications experiment. The advantages of such techniques over more conventional approaches are: 1) 50% more average power out is obtained from the laser by using both polarizations; 2) Modulation with very low modulator drive power is attainable; 3) Selective energy extraction from the cavity, rather than outside loss modulation, provides considerable system efficiency improvement; and 4) The two output beams are naturally multiplexed without loss into one collimated beam.

MODE-LOCKED LASERS have been described in many papers.¹⁻³ In essence, mode locking manifests itself as a series of narrow pulses at a repetition frequency of $f=c/2L$, where c is the velocity of light and L is the distance of separation between the mirrors. The narrowness of the pulse is a function of the fluorescent linewidth and cavity resonance parameters. Although mode locking may occur



Reprint RE-18-2-9
Final manuscript received April 28, 1972

Fig. 1 (top)—Mode-locked laser.

Fig. 2 (bottom)—Mode-locked laser output.

C. W. Reno

Lasers

Advanced Technology Laboratories
Camden, New Jersey

received the BA and MA in Physics from the University of Kansas in 1960 and 1962, respectively. He was a teaching assistant during part of his graduate studies, and he wrote his thesis on paramagnetic resonance in frozen solutions. Since joining Advanced Technology Laboratories, in 1962, Mr. Reno has worked exclusively on laser research. His early experience included work on a 50 p/s Nd^{3+} :CaWO₄ laser radar source. GaAs laser device technology became his major responsibility in 1964; he observed high efficiency room temperature operating GaAs laser diodes. These diodes were then used on a number of programs, including the GaAs laser voice channel, various intrusion alarms, a laser communicator built for ECOM, the communicator-intrusion alarm portion of COIN, and the Surveyor Staff program for NASA. In all of the programs, he had the major responsibility for optics design and optical component specification. In addition to this, he had the major engineering responsibility for the 3-D Laser Surveillance System throughout its evolution. He has been intimately involved in constructing, procuring, and adapting various Nd^{3+} :Cr³⁺:YAG and Nd^{3+} :YAG sources to this program and in IR&D programs aimed at 100-kHz Q-switched lasers. His recent experience includes participating in the system design of a number of illuminator and IR detection systems. He is currently working in the area of laser line scan and intra-cavity laser modulation techniques. He is a member of the Optical Society of America, Sigma Pi Sigma and Sigma Xi and has one patent pending.



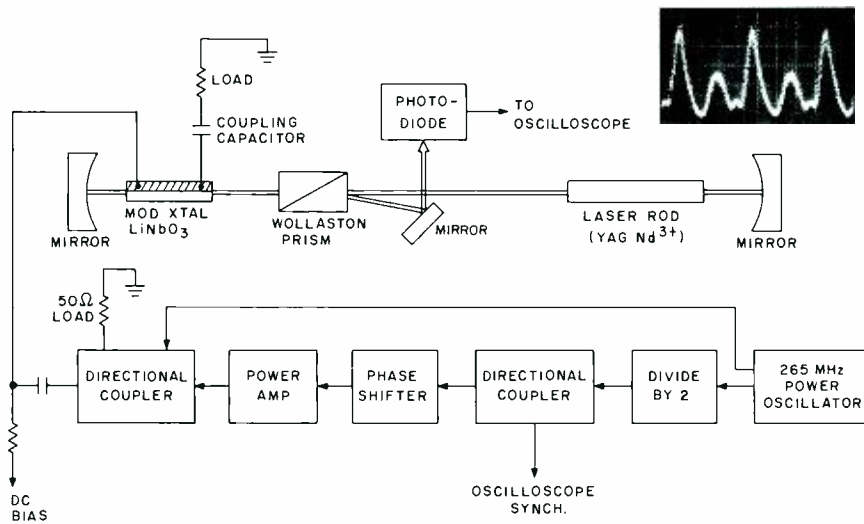


Fig. 7—Half-rate modulation experiment.

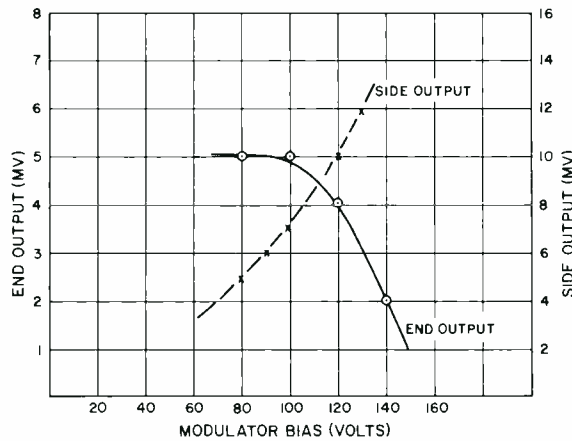


Fig. 8—Output power versus DC bias.

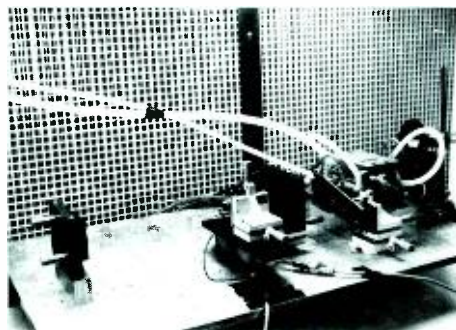
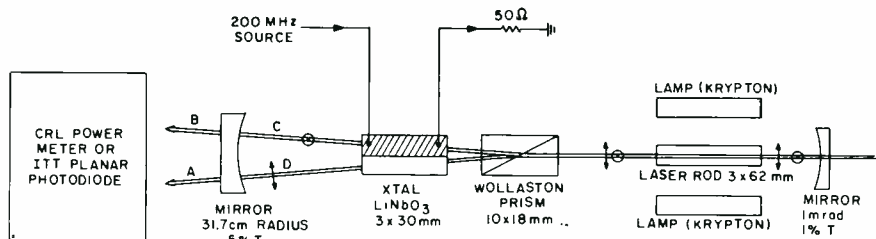


Fig. 9—Orthogonal laser experimental setup.

Derived concepts

Mode-locked partial-cavity-dumped lasers

In the concept of mode-locked partial-cavity-dumped lasers, we combine the features of mode-locked lasers with partial cavity dumping as shown in Fig. 5. The output is a mode-locked-pulse waveform with pulse spacings corresponding to a time $T = N(2L/c)$, where N is an integer. A major advantage that accrues to this scheme is that the output coupling is sampled by the mode-locked pulse. For binary transmissions, this means that good contrast ratios can be maintained with distorted waveforms into the modulator. The value of the electric signal during the short period that the pulse is passing through the electro-optic crystal determines the output coupling.

Mode-locked partial-cavity-dumped orthogonal cavities

In the configuration of mode-locked partial-cavity-dumped orthogonal cavities, shown in Fig. 6, the advantages of all three systems are combined. The laser is operated cw and mode-locked by use of phase modulation in both polarized arms. Outputs from each polarization are coupled by driving the electro-optic modulators independently.

Expected advantages from the use of this technique are:

- 1) Natural multiplexing of two polarized bit streams at optical frequencies which allow use of a common antenna.
- 2) This technique reduces the modulator drive requirements by a factor of 2 in frequency.

Experimental investigation

Partial cavity dumping

In an experiment on partial cavity dumping, shown in Fig. 7, a feedback path is provided for only one polarization in the laser cavity. After the laser is aligned for normal operation, mode locking is accomplished by driving the modulator crystal at the cavity frequency (265 MHz). This results in a 265-MHz output stream of pulses. Fig. 8 shows the variation in output as a function of DC bias coupled by the Wollaston prism.

A half-frequency sinewave was then

BEAM BLOCKAGE

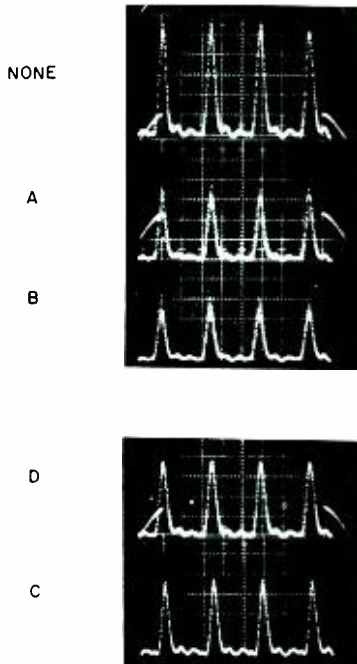


Fig. 10—Dual cavity output waveforms. Mode locked at 200 MHz; diffraction-limited operation. Scale: 2ns/div; total output from 5% mirror is 700 mW.

created by dividing the 265-MHz power oscillator output. This output was amplified and combined with the direct power-oscillator output in a directional coupler. By varying input phase and bias, the output could be varied from equal amplitude for all pulses to dissimilar amplitude for alternate pulses, as shown in Fig. 7. Although the contrast ratios are abominable (i.e., 4:1), this is attributed to a major extent to lack of modulation drive and poor crystal equality.

Orthogonal cavities

The experimental setup used in orthogonal laser experiments is shown in Fig. 9. The laser is operated by placing the point at which the two polarizations are separated in the Wollaston prism at the focus of the 31.7-cm-radius mirror. The laser is then pumped by the two krypton arc lamps. The position (along the lasing axis) of the 31.7-cm-radius mirror is varied to achieve optimum lasing in each cavity in sequence, while the other is blocked without requiring mirror tilts. Then, both polarizations are allowed to oscillate and the mode-lock drive is tuned until optimum mode locking is achieved.

With the mode-lock drive at $f=c/2L$, the results in Fig. 10 were achieved. Note specifically three factors. When one of the cavities is blocked (in Fig. 10d and 10e), the output is greater than half that with both running. Second, the total output power is considerably improved by allowing both oscillations. Finally, as shown in Fig. 10b, c, the amplitudes in the two polarizations are approximately equal.

An additional factor of interest is shown in Fig. 11. These photographs were taken with the laser mode-locked at c/L , which was 400 MHz in this experiment. The results of this experiment are very similar to those at 200 MHz. Note specifically, however, that these results allow extension of the internal cavity techniques to much higher rates because the cavity can be much longer for a given rate. That this harmonic sequence can be extended to higher rates is illustrated in Fig. 12, which exhibits similar results at $3c/2L$, which was 600 MHz in this experiment.

Conclusions

Verification of partial cavity dumping as a means of achieving 1-gigabit communications transmitters at $1.06 \mu\text{m}$ has been approached by transmitting a continuous 10101...datastream. Advantages in drive voltage have been verified. The problems attendant to high-speed information content have not been fully addressed. These problems include pulse-amplitude stability.

BEAM BLOCKAGE

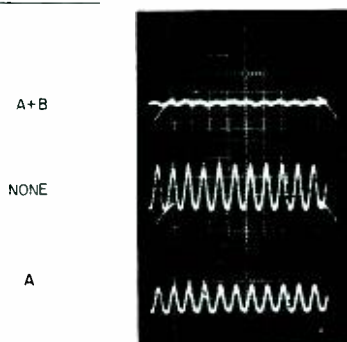


Fig. 12—Orthogonal laser triple-rate experiment. Mode locked at 600 MHz; not diffraction limited. Scale: 2ns/div.

BEAM BLOCKAGE

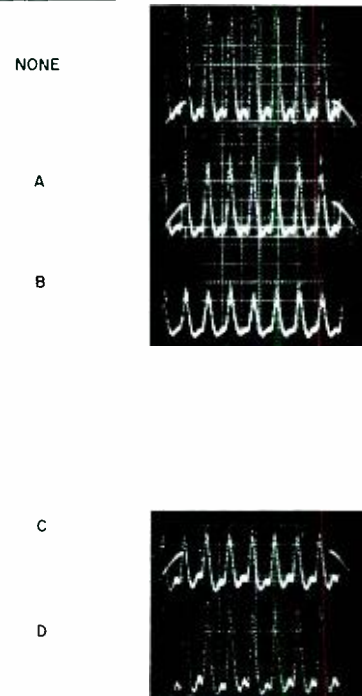


Fig. 11—Orthogonal laser double-rate experiment. Mode locked at 400 MHz; diffraction-limited operation. Scale: 2ns/div; 700-mW output.

The practicability of using a single-gain media (and pump source) to support two laser oscillations has been verified. Advantages in laser efficiency have been seen both in storage of birefringent losses and in coupling only the required output pulses. The advantage in required laser output power is approximately 2:1; the advantage in pump power can approach 3:1 (additional cavity losses modify this number); and the advantage in modulator drive is not just approximately 10:1 in power but is most probably the feasibility of a $1.06\text{-}\mu\text{m}$ system using solid-state state-of-the-art devices.

References

1. Smith, P. W., "The Self-Pulsing Laser Oscillator," *IEEE J. Quan. Elect.* Vol. QE-3 (Nov. 1967) pp. 627-635.
2. Kuizenga, Dirk J. and Siegman, A. E., "FM and AM Mode Locking of the Homogeneous Laser-Part I: Theory," *IEEE J. Quan. Elect.* Vol. QE-6 (Nov. 1970) pp. 694-708.
3. Kuizenga, D. J. and Siegman, A. E., "FM and AM Mode Locking of the Homogeneous Laser-Part II: Experimental Results in a Nd:Y AG Laser With Internal FM Modulation," *IEEE J. Quan. Elect.* Vol. QE-6 (Nov. 1970) pp. 709-715.
4. Ernst, J.; Michon, M.; and Debric, J., "Giant Optical Pulse Shortening: The Pulse Transmission Mode Operation of a Ruby Laser," *Phys. Lett.* Vol. 22 (Aug. 1966) pp. 147-149.
5. Maydan, D., "Micromachining and Image Recording on Thin Films by Laser Beams," *Bell Sys. Tech. J.* Vol. 50 (July-Aug. 1971) pp. 1761-1789.
6. Boyd, G. D. and Kleinman, D. A., "Parametric Interaction of Focused Gaussian Light Beams," *J. Appl. Phys.* Vol. 39 (July 1968) pp. 3597-3639.

Precision hover sensor for heavy-lift helicopter

D. G. Herzog

A helicopter stabilization system under development uses two newly developed sensor techniques—image-correlation tracking and pulsed sine-modulated laser ranging—which are combined with the best all-weather, day-night, pulsed-laser-illuminated gated imaging to measure position offsets and velocities using arbitrary scene references. Positional offsets can be measured in three dimensions to 0.6 in., and velocities as low as 1 in./s at distances of 125 ft. The stabilization system is designed to “freeze” the helicopter in mid-air over a designated cargo handling position even under wind gusts of 45 knots and in dusty environments. A “creep” mode with velocities as low as 1 in./s to 18 in./s can be selected by the pilot. The correlation-tracking device uses the total information of the scene rather than just particular highlights, edges, contrasts or patterns, with no cooperation needed from the ground. The image correlation tube used in the tracking device is a close technological approach to a substitute for the combination of the human eyes, optical nerve, and optical nerve center of the brain. The ranging system is a phase comparison monopulse laser radar that combines the advantages of a cw ranging system (high resolution) and a pulsed ranging system (multiple scene discrimination capability).

RECENTLY, RCA entered into contract with Boeing-Vertol Division for a precision hover sensor to be used on their cargo-handling heavy-lift helicopter. Both sensor and helicopter have some very unique characteristics to provide a unique load handling system. The pilot, upon arrival at the cargo-handling position, presses a “hover” button which causes the helicopter to “freeze” in mid-air. Even with wind gusts as high as 45 knots, the helicopter moves no more than 4 in. To accomplish this, the precision hover sensor uses the ground below the helicopter as its reference, which in turn is the reference for the helicopter flight control system.

As shown in Fig. 1, sensor beams illuminate two areas beneath the helicopter: 1) an outer 20-ft-diameter region, used to measure translation characteristics in the plane parallel to the ground (Δx , Δy , x , y); and 2) an inner (dotted) 6-in.-area, used to measure altitude characteristics (z , Δz , z). A very precise pulse sinewave-modulated laser beam is used to measure z information. Table I summarizes the sensor performance; Fig. 2 is an artist's concept of the sensor.

Upon “hover position initiation”, the scene below is stored electronically to be used as a reference. All future scene information is continuously

Table I—Precision hover sensor performance characteristics.

Hover precision (Δx , Δy , Δz)	± 0.6 in.
z	± 1 in.
Detectable velocity (Δx , Δy , Δz)	± 1 in./s
Data bandwidths (B)	30 Hz
Beep interval (Δx , Δy , Δz)	1 in.
Creep range (Δx , Δy , Δz)	1-18 in./s
Maximum displacement (x , y , z)	± 4 ft.
Altitude	125 ft.
Loss margin	1000
Lock-on time	0.1 s (max)
Re-acquisition time	0.2 s
Hover time (0.6 in.)	2 min
Hover time (1.2 in.)	10 min
Temperature range	-55°C to $+50^{\circ}\text{C}$

compared to the original reference by a special correlation-tracking device using the total information of the scene rather than depending on particular highlights, edges, contrasts, or patterns. Cooperation from the ground using any devices or patterns is highly undesirable because of the



D. G. Herzog, Ldr.
Laser Group
Advanced Technology Laboratories
Camden, N.J.

received the BSEE in 1959 and the MSEE in 1963 from Drexel University. Mr. Herzog joined RCA in 1959 in the Receiver Group of M&SRD where he performed major design work on the BMEWS system, the FPS-16, and MIPIR radar receivers. He also performed many study programs in the radar receiver area. In 1963 Mr. Herzog transferred to ATL, where he worked on high speed electrofax printers, electro-optics, magneto-optics, high-quality kinescope systems and video recorders. Mr. Herzog was promoted to Leader of the Laser Group in 1966. Under his direction, injection laser techniques were developed for advanced intrusion alarms, several full duplex voice communication systems, and a laser tracking ranging system for lunar operation. Current work has demonstrated the capability for a 1-gigabit/second laser communication system using internal modulation for maximum efficiency. All aspects for a space design including thermal control, mechanical stabilization, optics, and pointing and tracking are being considered. A recent achievement in this area is 5-microradian optical tracking using refined conventional techniques. Correlation tracking systems with field of view to accuracy ratios of 10,000 and ranging systems with 0.5-inch accuracies are being developed for helicopter control. Also for helicopter application are very wide field of view 220° low-light-level TV cameras. Mr. Herzog is a member of the IEEE and Eta Kappa Nu; he has published 12 papers in his field.

Reprint RE-18-2-10
Final manuscript received June 27, 1972.

Fig. 1—Precision hover sensor beam patterns from the helicopter.



logistic and communication problems. Advanced all-weather, day-night pulsed-laser-illuminated gated imaging is used to provide quality images to the correlation device even under very dusty environments. This is particularly important with the downwash generated by very large helicopter rotors.

Operation

Operationally the pilot will not always obtain the exact location when he initiates hover. He can then adjust his position without releasing and requiring a new lock-on, by operating his "control stick" in the following way. Initially with the control stick centered, the helicopter is motionless. When the operator momentarily moves the control stick in the direction of desired motion for less than 0.5 s, the helicopter will move 1 in.; this is defined as a "beep". When the control stick is positioned for more than 0.5 s, the system goes into a "creep" mode. Creep velocity is proportional to stick displacement from 1 in./s to 18 in./s.

Both beep and creep will occur up to 4 ft from initial hover position. Beyond this, a new reference location, 4 ft from the initial one, will be taken automatically. In this manner, the helicopter can "walk" along over an extended dis-

tance. Upon return of the stick to center from a creep command, the helicopter will hover at this new position. When the operator pushes the stick beyond the 18-in./s velocity, the system automatically releases from hover control and turns the control over to inertial flight control.

Correlation tracking system

The entire sensor system is roll and pitch stabilized. This maintains the sen-

sor pointing in the vertical and eliminates angular the induced errors that would be generated by roll and pitch of the helicopter. Yaw motion is averaged out in the correlation tracking.

Fig. 3 is a functional diagram of the tracking system. The illuminator consists of an *AlGaAs* laser providing 1-W average power at 50 ns and 20 kp/s with 30-ns risetimes and falltimes. It is kept at room temperature by thermoelectric heating and cooling, within an ambient

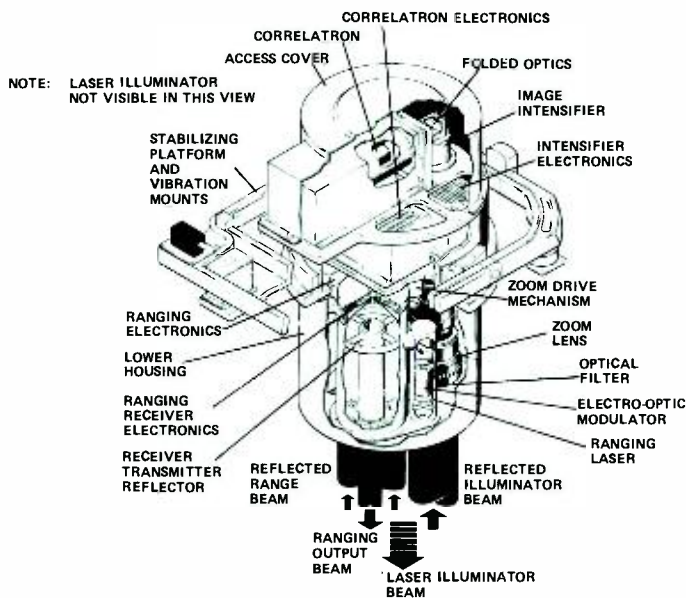


Fig. 2—Artist's concept of precision hover sensor.

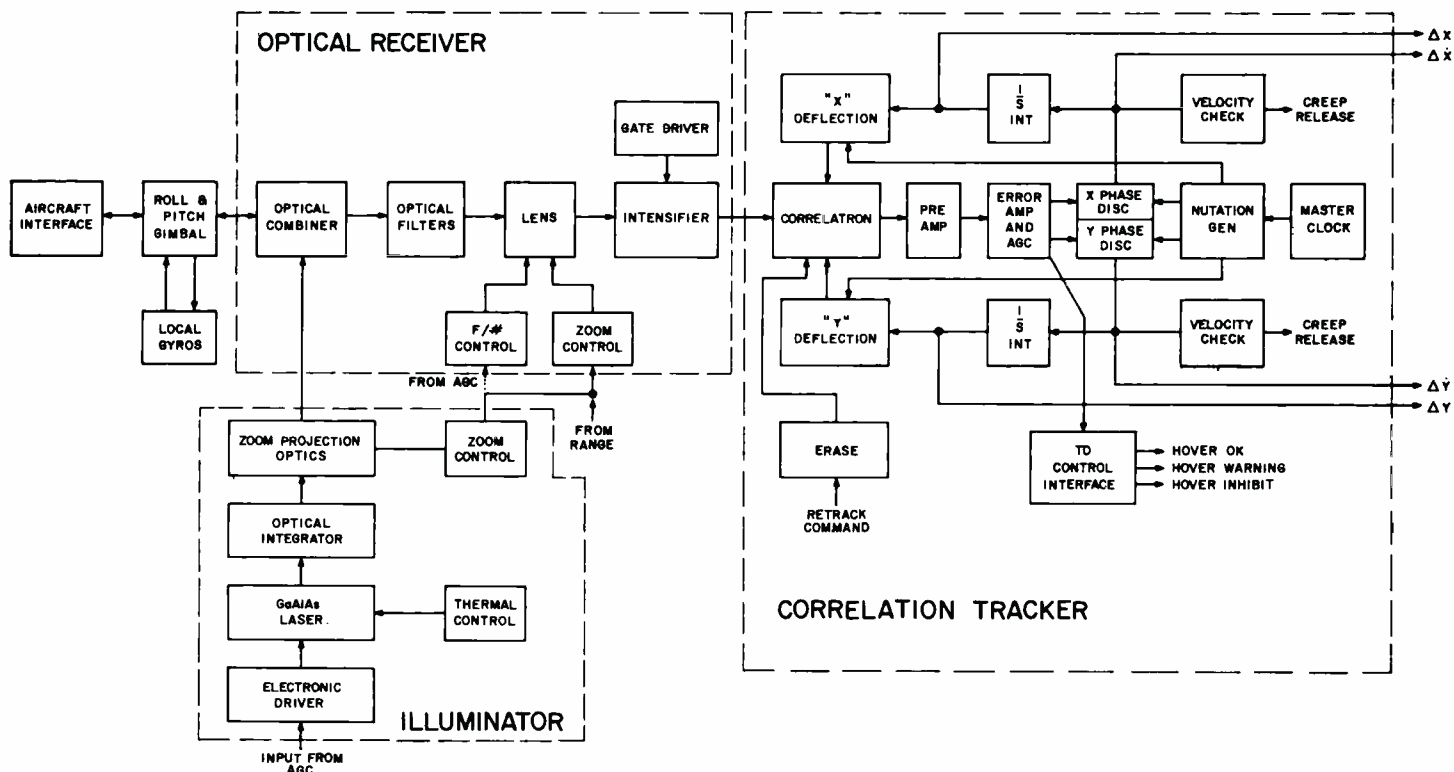


Fig. 3—Tracking functional diagram.

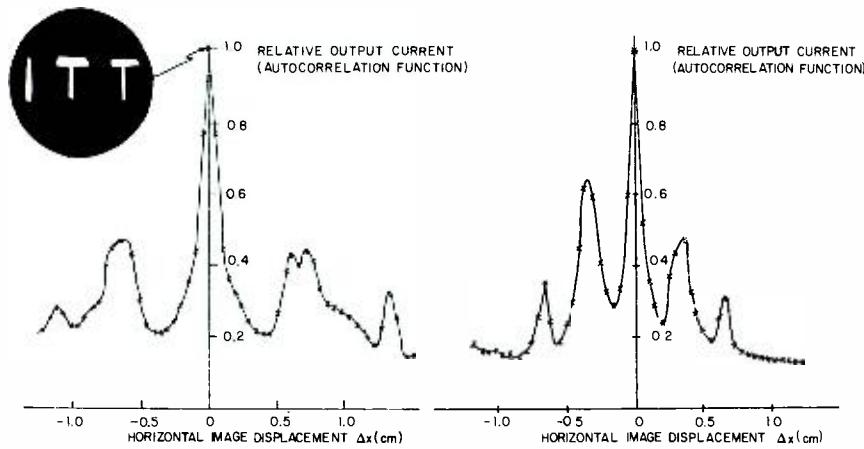


Fig. 4—Autocorrelation function generated by FW231 storage image tube. Insert photograph is a reproduction of the visual output image at the correlation peak. Assymetrics and irregularities of the autocorrelation signal are due to imperfect (hand composed) nature of the optical pattern (shown in the insert). Letter separation: approximately 0.7 cm (left); 0.35 cm (right).

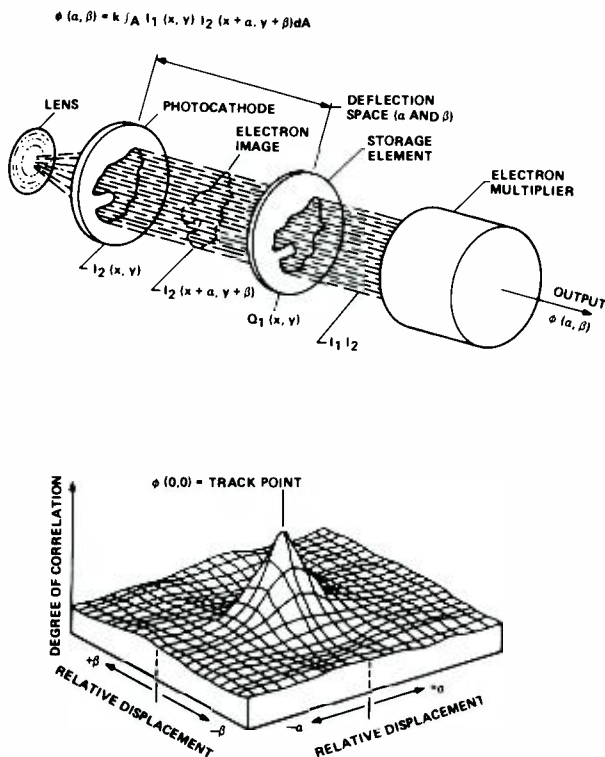


Fig. 5—Simultaneous electron image correlation.

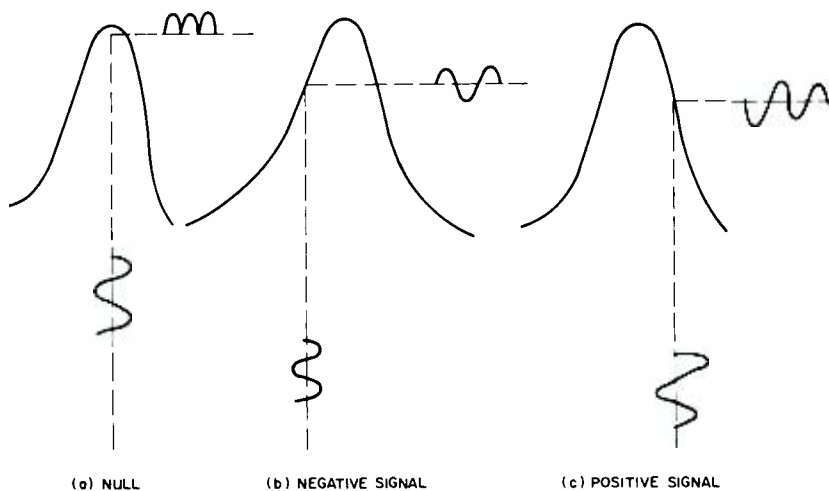


Fig. 6—Tracking concept which allows through-phase detection to maintain location at the peak response.

range of -55° to 50°C . Thus, a constant operating level and wavelength (8500 \AA) are maintained. An optical integrator is used to provide uniform illumination over a 20-ft diameter on the ground. The illumination field is maintained over a 25-ft to 125-ft altitude by a zoom projection lens. The optical receiver has an optical filter (100-\AA wide) which matches the laser and helps considerably in reducing the daylight background energy. The remaining background is suppressed below the illumination level by pulse gating with a duty factor of 0.1%. The receiver field of view is matched to the 20-ft-illumination diameter via zoom lens control. Amplitude variations are suppressed by f -number control of the lens.

The intensifier is gated on with a 25-ns-risetime pulse only when the returning laser light is received. This eliminates backscatter effects by providing a 25-ft window. Light amplification in the intensifier raises the level of the usable light (0.1 fc) for the correlation tracker, developed by Goodyear Aerospace Corporation.

The intensifier signal enters the Correlatron tube, which is the major element of the x - y tracking system. The tube, with appropriate electronics required to generate the correlation function, determines the extent of x and y motions.

With a commercially available image storage tube (ITT FW231), 10^5 to 10^6 individually resolvable picture elements may be stored in the nonviewing condition for hours, sometimes days, without appreciable image degradation. Fig. 4 shows the "static" autocorrelation function generated by an FW231 storage image tube for a simple black-and-white test pattern consisting of the handformed letters *ITT* (see insert in Fig. 4) for changes only in horizontal displacement, (Δx). A maximum magnitude of the output current clearly exists for superposition of the stored and the reading images. The "sidelobes" generated by this particular pattern correspond to the partial image correlation resulting from superposition of the I on the vertical portions of both T 's.

Similar dynamic correlation function signals can be generated by electronically deflecting the reading electron image over the storage mesh, in which case the tube might, more properly, be

called an image-correlation tube. The name *Correlatron* has been applied to the system that is used with the deflection coils and circuitry needed to sweep the real-time image across the storage mesh in a repetitive fashion (in the manner of a TV sweep) for the purpose of evaluating the correlation of the two signals. When operating in a dynamic-correlation mode, the photoelectron image from the photocathode is focused by an axial magnetic field and deflected between the photocathode and the storage element by orthogonal radial deflection fields (see Fig. 5).

In many respects, the image-correlation tube is a close technological approach to a substitute for the combination of the human eyes, optical nerve, and optical nerve center of the brain.

Since the deflection technique varies the entire electron stream, a nutating modulation-tracking technique is used (Fig. 6). When the dynamic incoming image exactly overlays the stored image, a phase-detector output obtained from the waveform of Fig. 6a would provide a null, the waveform of Fig. 6b would provide a negative driving function, and the waveform of Fig. 6c a positive driving function. Closing the loop about the deflection will always deflect the image to maintain alignment. This linearizes the error functions and makes the response independent of the type of scene required to track on.

Using the integrator in the feedback loop allows velocity measurement without the use of differentiation of the position measurement.

Because of the obvious problems in the case of failure during critical load handling (e.g., when a tank is being lifted out of the hull of a ship), all important signals are electronically examined to determine if they are satisfactory for continued operation. If they are marginal, a hover warning is indicated; if they are not satisfactory, a hover inhibit is actuated.

The photos in Fig. 7, 8, and 9 were taken from a helicopter. They show various scenes used as input images to a Correlatron, similar to the one to be used in the precision hover sensor; thus, the autocorrelation of the selected portions of the scenes could be determined. For each of these images, a 1-in.-diameter area of the image was one-to-one imaged onto the photocathode.

Each figure illustrates, in addition to the selected scene, the static and dynamic "match" curve [parts b) and d) of each Fig.], which are the open-loop autocorrelation function and its derivative, respectively. The static match curves for both x and y directions are shown [x and y directions are indicated in a) of each Fig.]. The various scenes illustrate that these two responses differ from each other, and that the amount of information, and hence the maximum inherent autocorrelation possible, differ in the two directions.

The static match curves are obtained by physically moving the glass plate containing the image along the appropriate direction, such that the stored image is compared with its displaced counterpart. The maximum output of the Correlatron, occurring at the peak, indicates the point of maximum autocorrelation. Note that the horizontal node measures displacements of 0.01 inches per division. This indicates the sensitivity of the Correlatron to image displacement.

Tracking loops designed for generating "error" functions proportional to input

image displacement were closed in both the x and y axes. A ± 0.001 -in. displacement in x of the input plate corresponding to a ± 0.24 -in. aircraft motion was then introduced manually. The input to the vertical oscilloscope axis was the output of the x integrator. The thickness of the line is the noise output.

Fig. 9 is a photo taken over water. Although correlation tracking is not possible over dynamic moving images such as water, the Fig. demonstrates the significant capability of the system to track over low-contrast bland images.

Ranging system

The ranging system of the precision hover sensor combines the advantages of both a cw ranging system (high resolution) and a pulsed ranging system (multiple-scene-discrimination capability). This system, a phase-comparison monopulse laser radar, is shown in Fig. 10. The pulsed laser generates 50-ns rectangular pulses with 5-ns risetimes and falltimes. The pulses are generated at a 5-kHz rate determined by the pulse-rate oscillator. The laser pulses are

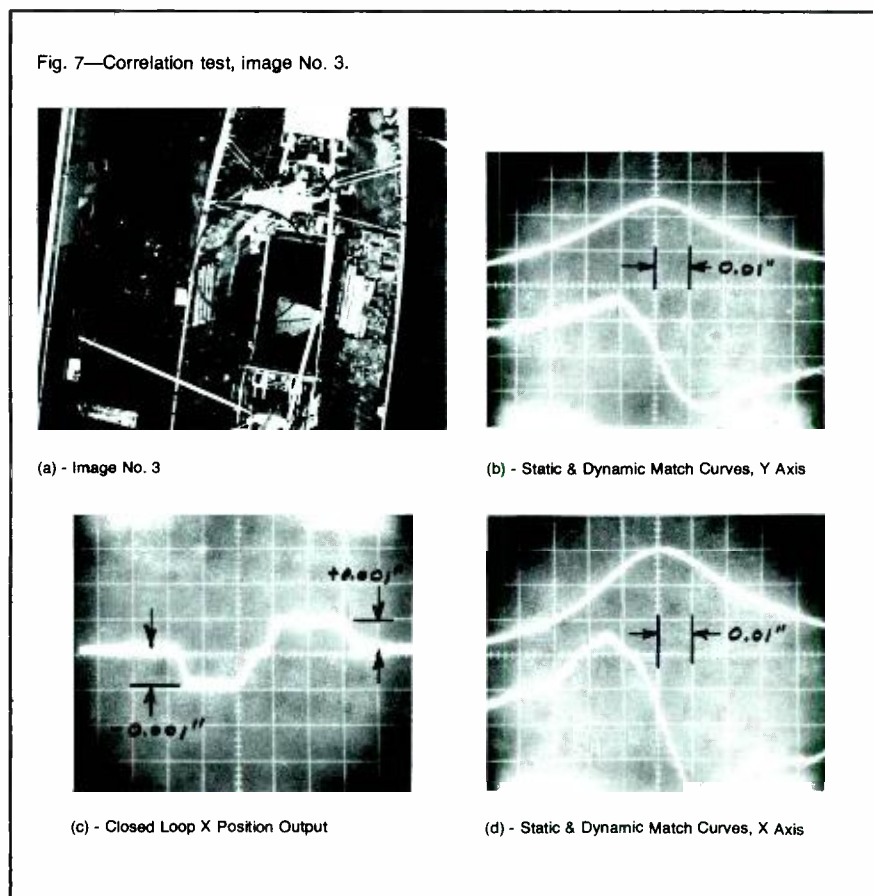


Fig. 8—Correlation test, image No. 1.

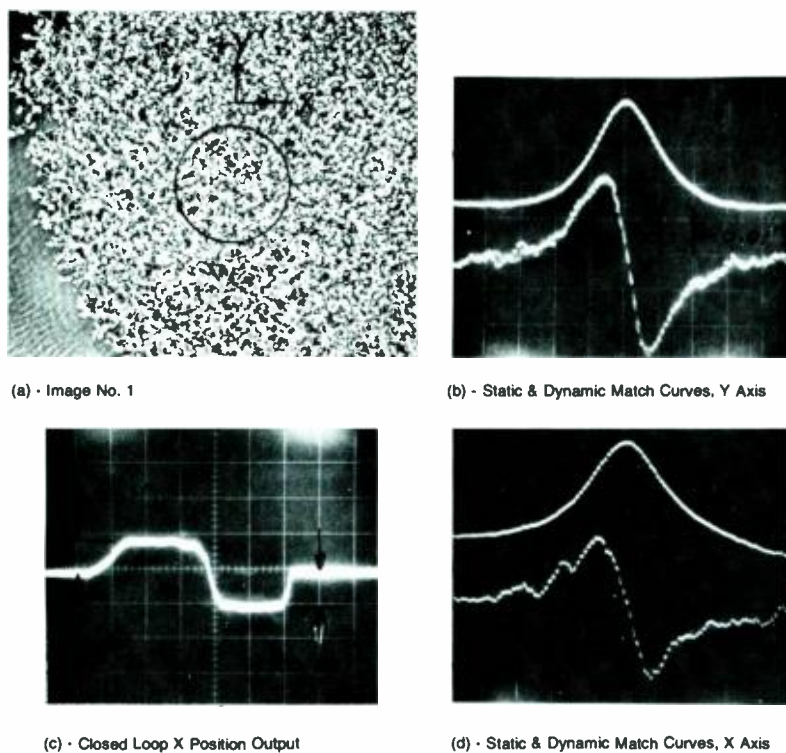
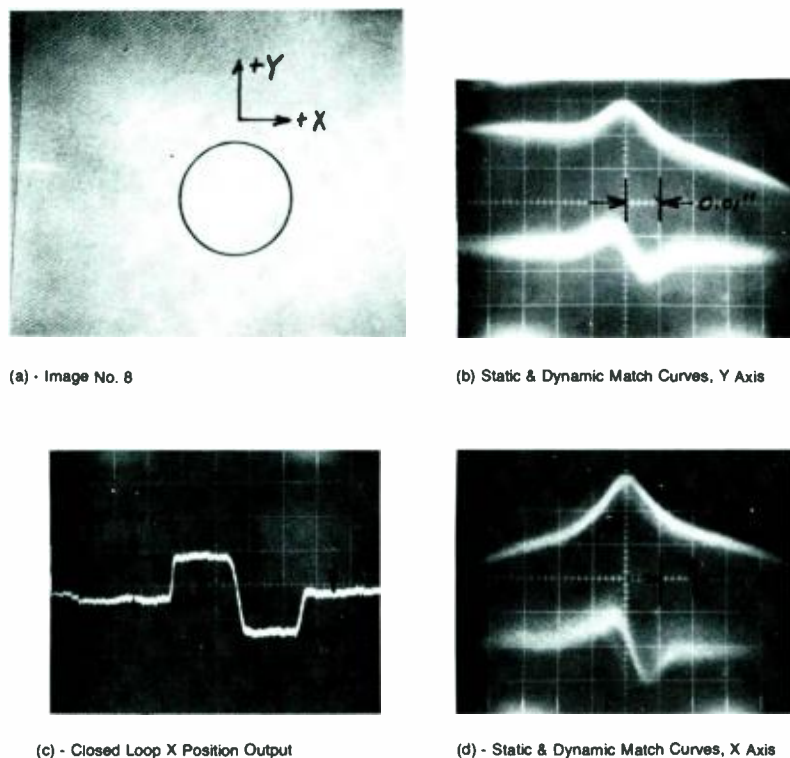


Fig. 9—Correlation test, image No. 8.



passed through an acousto-optic modulator, which impresses 100-MHz sinusoidal modulation on the flat portion of the pulse. The depth of modulation will be 50%. The 100-MHz oscillation frequency is derived from the sum of the local oscillator (99.950 MHz) and master oscillator (0.050 MHz) frequencies. The sinusoidally modulated pulse is directed toward the target through a beam expander. The beam is expanded to provide an eye-safe energy density. For ranging purposes, the laser current will be sampled to detect the pulse leading edge (for coarse ranging) and the modulator drive will be sampled to detect the phase of the transmitted sinusoidal modulation (for fine ranging).

The transmitted beam strikes the scene, and a small portion of the reflected energy is collected by the receiver telescope and focused onto the signal detector and amplifier. The output of the signal detector amplifier and the sampled laser current and modulator drive are processed to obtain the coarse and fine range.

Coarse ranging

The coarse range information is obtained by measuring the time delay between the leading edge of the transmitted pulse and the leading edge of the received signal. The 100-MHz trap is used to remove the high frequency modulation from the received waveform and to provide a clean leading edge to the threshold detector. The outputs from the threshold detectors are digital pulses which are delayed by the same amount of time as the transmitted and received laser signals. This delay is measured in the time-interval counter.

The time-interval counter will range on the last valid return received during a total maximum-range interval of 1000 ft; this allows the system to range through obstacles such as trees. A multiple-scene indication will be generated if more than one valid scene is encountered during the range interval. One hundred range measurements will be summed and averaged in the time-interval counter to produce a coarse range measurement with an accuracy of 5 ft and a resolution of 0.5 ft.

Fine ranging

The fine-range information is obtained

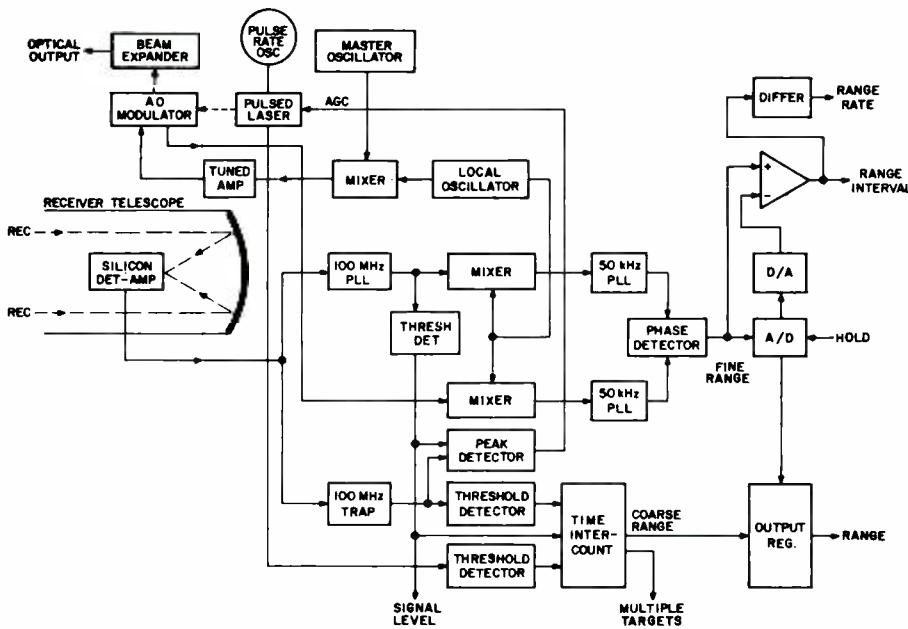


Fig. 10—Phase comparison monopulse laser radar.

by comparing the phase of the transmitted sinusoidal modulation to the phase of the received sinusoidal modulation. The signal-detector amplifier output is first passed through the 100-MHz phase-locked loop to derive a continuous waveform for determining phase. The resultant signals are then mixed with the local-oscillator frequency of 99.950 MHz to produce two 50-kHz IF signals whose phase difference is the same as the phase difference between the transmitted and received 100-MHz signals.

The phase detector provides a DC voltage output which is linearly related to the phase difference, and thus to the fine range. The fine-range information is accurate to 1 in. with a resolution of 0.1 in. over an unambiguous range of 5 ft.

The DC output of the phase detector is fed into an A/D converter to obtain the fine-range information in digital form for combination with coarse-range information. The two measurements are combined in the output register to yield a 1000-ft scale range reading with an accuracy of 1 in. and a resolution of 3/16 in.

A second reason for converting the fine-range information to digital form is to provide an accurate stored reference for deriving the hover-error signals. When the operator wants to put the helicopter into automatic hover, he pushes a button on his control, which generates the hold command. This causes the fine-range information in the A/D converter to be stored in a separate digital register.

This stored fine range is then converted back to analog form in the D/A converter and compared to updated analog fine-range data coming out of the phase detector. The result of this comparison is an analog-error signal corresponding to any small changes in altitude of the helicopter. This signal is then differentiated to yield the rate at which altitude changes are occurring.

Backscatter

Since the received-signal pulse amplitude is held at a constant known value by AGC, the amplitude of the received 100-MHz modulation burst should also be constant at a known value. If the scene being ranged is relatively flat, all of the returned high-frequency modulation will be in phase (coherent) and will be passed through the 100-MHz phase-locked loop. If, however, the return energy is due to backscatter or reflections from tree branches, the energy will not be coherent and the resultant output from the 100-MHz phase-locked loop will be greatly reduced. This property of the ranging system is used to separate the valid scene from undesirable returns. The output from the 100-MHz loop in the signal path will be compared to a preset level and used to "gate" or inhibit the range measurement for that particular return. This "signal level" indicator will also be used to inhibit undesirable pulse returns from entering the AGC loop.

System accuracy

The pulse-comparison monopulse laser radar is somewhat more complex than

either a pulsed or CW system, since it incorporates both detection techniques. However, this combination eliminates the disadvantages of both systems that would otherwise prohibit either from effectively meeting the ranging requirements. Furthermore, the proposed system is not pushing the state-of-the-art in either of its pulse or CW range measurements. The rather loose time-delay-measurement (± 10 ns) and phase-measurement ($\pm 4^\circ$) accuracies will result in an accurate, reliable, noncritical, low-cost system.

As part of the system design, the sources were examined that are capable of introducing errors into the outputs of the position measuring and range measuring systems. These are listed in Table II.

Table II—Error budget for heavy-lift helicopter precision hover sensor.

$\Delta x, \Delta y$ measurement errors [inches (3σ)]		Δz measurement errors* [inches (3σ)]	
Tracking	± 0.4	Ranging	± 0.5
Mechanical	± 0.4	Mechanical	± 0.2
Magnification	± 0.15	Tracking	± 0.2
Atmosphere	± 0.1	Atmosphere	± 0.1
Ranging	± 0.1	Miscellaneous	± 0.15
RSS total	± 0.6	RSS total	± 0.6

* Assumes ground slope of 30°

Conclusions

Under the existing schedules, Boeing expects to demonstrate a flight model of the precision hover sensor during the latter part of 1973. Fabrication and breadboard work completed thus far indicates that all performance criteria will be met.

The several technical innovations applied to the precision hover sensor have opened a wide range of other possible applications. The correlation tracker, for example, might be used for arbitrary-scene trackers, for laser designators, or for other aircraft-landing and hovering aids. Potential applications also exist in pattern recognition, e.g., in mapping and terrain identification.

The range finder, which is the most accurate non-cooperative ranging system yet devised, might be applied to the solution of some unique surveying, short-range navigation, and remote-control problems.

Further, this precision sensor could lead to new concepts in rapid building construction.

Acknowledgment

The author thanks R. Tarzaiski and G. Ammon for their support.

Pulsed GaAs illuminators for night-vision systems

W. W. Barratt

Pulsed GaAs laser diode illuminators for use with gated low-light-level television must produce high intensity, uniform illumination emanating from a minimum source area. Seven such illuminators have been designed and built by Advanced Technology Laboratories in Burlington for use in military applications. The system described in this paper provides a continuously variable optical pulse width (200 ns to 1 μ s) at a repetition rate of 13 kHz and 30 W average power into the field of view of a gated low-light-level TV camera. With continuing developments now underway, such systems should continue to improve in performance, reliability, versatility and cost.

W. W. Barratt
Laser Systems
Advanced Technology Labs
Aerospace Systems Division
Burlington, Massachusetts

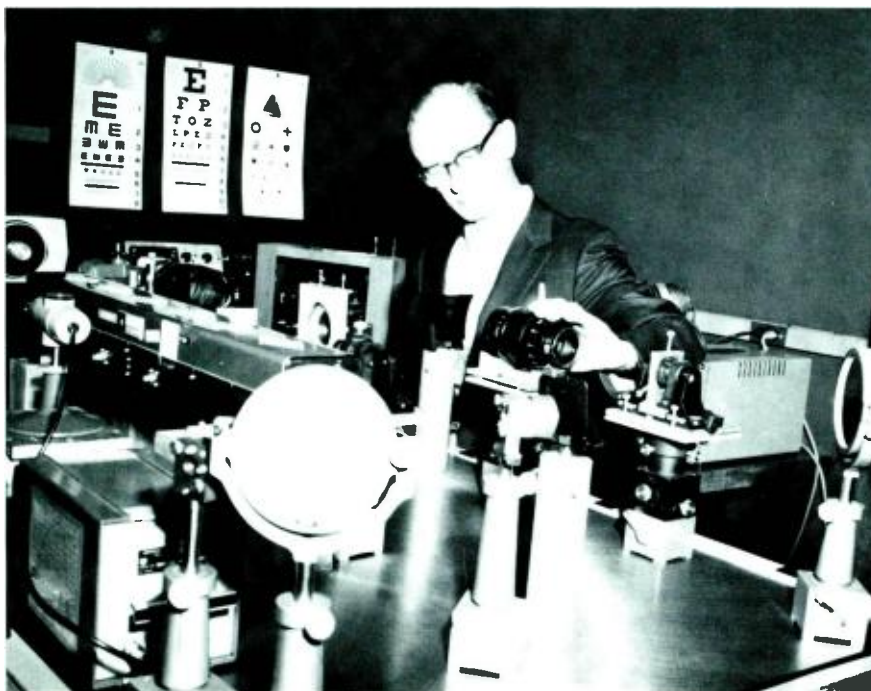
received the IEE Higher National Certification from Coventry College in 1935 and attended graduate program in Physical Optics and Biomedical Engineering at Northeastern University. He joined RCA in 1959 as project engineer on the MULTIMODE Seeker Program. Subsequently, he was responsible for the optical design of the LCSS Automatic Test System and developed the image orthicon camera system for the AN-AFR-2 Satellite Surveillance System. He joined the Advanced Technology Laboratories—Burlington in 1969 as a leader of the Laser Systems Group and was responsible for the development of Pulsed Gallium Arsenide Illuminators. Currently, he is a Senior Engineering Scientist responsible for special projects. He is a member of the American Optical Society and an elected member of RESA.

LOW-LIGHT-LEVEL DEVICES have provided man with the capability to view scenes illuminated only by starlight. The advantages of such systems in military and civilian applications are obvious. However, the resolution of these systems operating under starlight conditions is much lower than that achievable at higher light levels. Further degradation in performance occurs when cloud conditions are present that tend to obscure the starlight, and obviously no device can be made that can see if the illumination is completely cut off. To compensate for these conditions and to improve the resolution of viewing devices where the natural illumination is too low to achieve a high performance, various

means of artificially increasing the scene illumination have been studied and evaluated. The obvious approach of using such devices as spotlights suffers from many disadvantages particularly in military and other applications where the surveillance device must be hidden. For these applications, illumination at infrared wavelengths is necessary.

Although IR illumination systems that emit a continuous radiation, such as IR searchlights, are capable of providing scene illumination, such systems are only effective if the atmosphere between the viewing device and the target is clear. With the presence of mist or fog the image of the target area is obscured by light back-scattered from the mist into the lens of the viewing device. This effect is very familiar to a motorist driving in mist at night; the illumination from his headlights is backscattered into his eyes, completely obscuring his view of the road for any significant distance ahead.

With the advent of "gated" viewing devices in which the imaging system can be turned *on* and *off* rapidly at will, a means of overcoming this backscatter problem is available. With such a system, a short pulse of IR illumination can be emitted with the viewing system gated *off*, and the system only turned *on* when the illumination pulse is returned from the target area. If the illumination pulse is short enough, energy back-scattered from the mist is returned to the viewing device before the returned energy from the target area and while the viewing device is still *off*.



Reprint RE-18-2-13
Final manuscript received April 27, 1972

The backscattered energy from the mist is not, therefore, seen by the viewing device and performance degradation from this effect does not occur. As the viewing device is turned on only for very short period compared to the time between flashes of illumination, a further benefit is accrued in that the scattering of any natural illumination from the mist such as that from the moon is largely rejected, again resulting in considerable improvement in system performance under such conditions.

To achieve this improved system performance, however, considerable demands are placed on the illumination subsystem. The illuminator, therefore, must be capable of providing short pulses of IR illumination of about $1 \mu\text{s}$ duration while still maintaining the same average power as a continuous illuminator and further the rise and fall times of the illuminate pulse must be of the order of 50 to 100 ns to achieve accurate timing and rejection of the backscatter. With the development of efficient Gallium-arsenide (*GaAs*) injection laser diodes by RCA and others, a light source capable of meeting these requirements became available.

Gallium arsenide injection laser diodes

A *GaAs* injection laser diode is constructed, as are other solid state diodes, of an n and a p layer on either side of an active junction. In the *GaAs* diode, however, when current is passed through the junction in a forward direction, IR radiation is emitted from the junction. Under low values of current, the radiation is of relatively low intensity and increases linearly with current until a threshold value of current is reached.

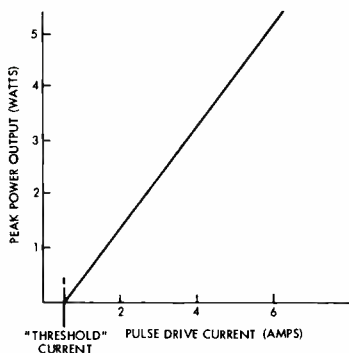


Fig. 1—Typical power output vs. drive current for a 9-mil *GaAs* diode at 77 K.

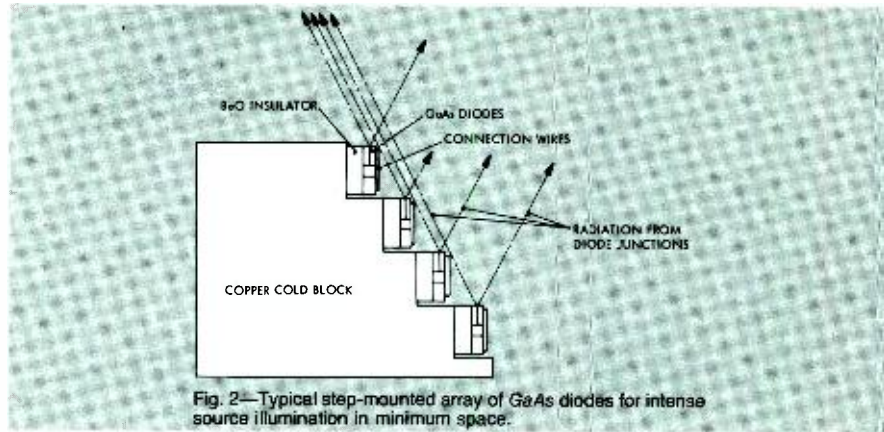


Fig. 2—Typical step-mounted array of *GaAs* diodes for intense source illumination in minimum space.

At this point, the *GaAs* diode begins to operate in a lasing mode; radiation output from this point increases very rapidly with forward current. Fig. 1 illustrates the relative light output from a *GaAs* diode vs. forward pump current. A limit to increase in the drive current is dictated by the temperature rise of the diode. For most efficient operation of *GaAs* diodes the diode operating temperature needs to be reduced to about that of liquid nitrogen, say 77°K. At this temperature, overall power efficiency of the diode can be typically 40% (60% for very good diodes) and the wavelength of emitted energy is 850 nm. For operation at 77°K, the threshold current for standard RCA diodes is about 400 ma for a single diode of 0.009 in. width and 0.014 in. depth; maximum current for a pulse of 1-to-3- μs duration is typically 5 A, at which current the diode will emit a peak power of 4 to 5 W. Forward voltage drop at this current is approximately 2 V.

System requirements and design details

A typical pulsed illuminator using *GaAs* diodes is required to provide 25W of average power into a field of a view of 3 to 4° diagonal with a 3 × 4 format to match a standard gated low-light-level TV system. To design and construct such an illuminator, many technical problems had to be solved such as:

- 1) Mounting a large numbers of individual diodes to present a minimum source area;
- 2) Efficiently cooling the diodes to cryogenic temperatures close to 77°K;
- 3) Driving electronics to provide currents of suitable amplitude with fast rise and fall times;
- 4) Reducing size and weight of a high efficiency optical system to project uniform illumination into the required field of view

independent of the performance of individual diodes.

As a result of investigations conducted by ATL, solutions to these and other problems were resolved.

Diode array assembly

To achieve average output power of the order of 30 W from *GaAs* diodes, which individually provide peak powers of 5 W and which are operating at duty cycles of only 1 or 2%, obviously requires the use of several hundred such diodes. The mounting of such a large number of diodes so that the effective source size is of minimal dimensions while maintaining very efficient thermal packaging presents a difficult problem to a designer. However, maintaining a minimum source size is important: an increase in source-size linear dimensions by a factor of two will result in double the diameter and length of the projection optical system and will increase its weight by almost eight times!

This problem was solved by mounting strips of diodes on steps machined in a copper block in a "staircase" configuration, as shown in Fig. 2. Note that the steps are machined so that radiation

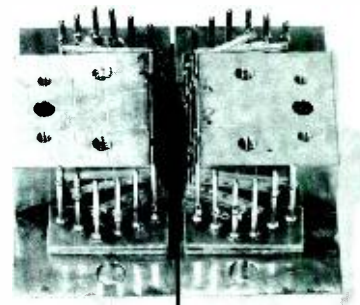


Fig. 3—Complete *GaAs* diode array.

from the diodes in the lower steps just misses the diodes in the higher steps.

Mounting two such modules face to face provides a very compact source of very high irradiance in minimum dimensions. Fig. 3 shows a typical pair of blocks mounted to provide 600 diodes in a source size of only 0.27×0.36 inches.

Diode cooling

The design of a suitable cooling system to maintain the diode array assembly at the required 77°K presents many practical difficulties. Although several methods are currently in use in laboratory systems to achieve low temperatures, only two methods are capable of maintaining the necessary temperature against a heat flux of 60 or more watts input.

Mechanical refrigerators operating on the familiar Stirling cycle using Helium gas are commercially available. Such units can maintain 77°K against considerable heat loads, typical systems for instance are available that are capable of handling input heat loads in excess of 100 W. Although such systems have been used in *GaAs* illuminators, they require very large amounts of input power (2 to 3 KW for a 100-W unit) and contain, as a necessity, high speed reciprocating mechanisms.

The use of liquid nitrogen as the cooling medium has its own peculiar problems, but has many advantages particularly in systems with restricted input power and long, trouble-free continuous operation as a requirement. The liquefaction temperature of nitrogen at ambient pressure is 77°K, making it an ideal fluid for our application. In addition, liquid nitrogen has a relatively high latent heat of evaporation, is cheap, non-toxic, and readily available. For these reasons, most of the RCA *GaAs* illuminators currently manufactured use a liquid nitrogen open-loop cooling system.

Drive Electronics

Current *GaAs* illuminators use up to 600 individual diodes requiring pulse drive currents of about 6 A for a few microseconds with rise and fall times of typically 50 ns. As each diode has a forward voltage drop of about 2 V, driving 600 in a single series string would require drive voltages in excess of 1200 V. Parallel connection would similarly result in impractical values of

drive current.

Transistors capable of proving current pulses of 6 A at rise and fall times of 50 ns are currently available with V_{CEO} values of up to 400 V. The use of such transistors has enabled efficient multiport drive circuits to be developed, each port driving up to 100 diodes in series. Typically, a six-port driver system is used to drive 600 diodes and to provide for variable pulse widths of up to three microseconds at repetition rates of tens of kHz.

Projection optical systems

Radiation from lasing *GaAs* diode arrays differs from that common to rod and gas lasers in several aspects. The most important difference in applications to illuminators is that the radiation is emitted in a wide fan instead of the very "tight" beam familiar to users of rod and gas lasers. The main reason for this wide fan of emission can be found in the very small source size of *GaAs* diodes in which the height of the optical cavity is only 1 or 2 μm .

The presence of this wide fan, however, means that projection optics must be designed with low *f*-numbers if a large percentage of the radiation is to be collected. An optical systems with an *f*-number of 1.25 to 1.5 provides a reasonable balance between collection efficiency and size of optical elements.

However, as the radiation bandwidth is normally only about 50-Å wide, it can be considered as monochromatic. For illuminators having fields of view of a few degrees, therefore, it is only necessary to correct for zonal and third-order spherical aberration in the lens design. This approach leads to lens systems having only three components, all constructed of the same glass type. Such a system, despite its very high speed, can be reproduced in quantity at reasonable cost.

If direct projection of the diode array is used, it can readily be seen that variations in output between individual diodes would result in large undesirable differences in intensity in the illuminated field. To overcome this problem, the radiation from the diode array is "scrambled" before projection by passing it through a parallel-sided quartz prism with the same cross section as the array.

The operation of this integrator can best be understood by reference to Fig. 4, in which a few of the ray paths from a single diode are shown to illustrate the scrambling action. Although the angles of the exit rays are equal to the angles of the entrance rays, the direction and position of the apparent source of the rays are scrambled. Projection of the exit face of the prism, therefore, gives an evenly illuminated field without any "hot spots".

Product design

Advanced Technology Laboratories has, over the last few years, successfully developed the techniques necessary to ensure that efficient, highly reliable, and easily producible pulsed *GaAs* illuminators can be designed as an established RCA product line. To illustrate the degree of sophistication achieved in this area, a typical illuminator system will be described that meets all the MIL specification requirements for such units operating in an airborne environment.

Fig. 5 illustrates the complete illuminator subsystem designed to be used in conjunction with a gated low-light-level TV system. The system, which provides a continuously variable optical pulse width from 200 ns to 1 μs with a repetition rate of 13 kHz, delivers up to 30-W average power into a field of view to match the TV camera.

The illuminator head (1) contains the

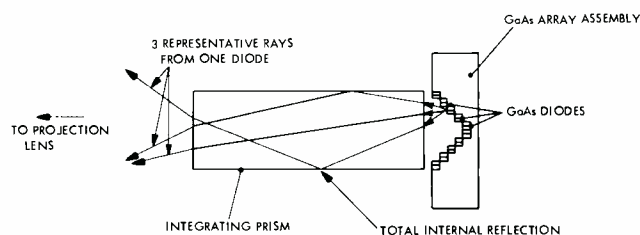


Fig. 4—Operation of prismatic integrator.

GaAs diode array, the liquid nitrogen cold head and an optical prismatic integrator to ensure even illumination in the field of view. Secured to the basic head assembly is an interchangeable projection optical system to provide the required field of view. Changes in the field of view can be easily achieved by interchange of available optical systems of various focal lengths. Despite the stringent requirements for a highly efficient thermal insulation, the design of the illuminator head allows for field disassembly, replacement of the *GaAs* diode array and re-assembly to operational status in less than thirty minutes without requirements for special tools or jigs.

To provide the pulses of current to drive the *GaAs* diodes, a six-port current-drive module (2) is used. This driver module which achieves current rise and fall times of a few tens of nanoseconds, is fabricated using all solid-state components on conventional plug-in printed-board modules to achieve complete interchangeability for field service and maintenance.

Power for the system operation and fail safe protection circuits is provided by a single module termed the illuminator electronics unit (3). This unit accepts the full voltage range of the basic aircraft 28-V supply and provides all the regulated DC voltages and currents required by the system. Full RFI/EMI isolation and protection are also incorporated in this unit. Included are various logic systems to interface with the TV camera and to ensure exact control of the time delay between light pulses and the TV camera gate. Also contained are protection circuits to ensure that no system damage can be caused by incorrect operation procedures and that the *GaAs* array will not be damaged by a system malfunction.

The liquid nitrogen storage dewar (4) is a conventional vacuum-insulated metal-dewar system with a capacity of 25 liters of liquid nitrogen. One filling of this dewar will provide up to 8 hours of continuous operation at full power. An electronic contents system is incorporated to monitor the available liquid nitrogen and the entire dewar is wrapped to provide operator protection in the event of battle damage.

Transport of the liquid nitrogen to the illuminator head is achieved by a flexible vacuum-insulated transfer-line sys-

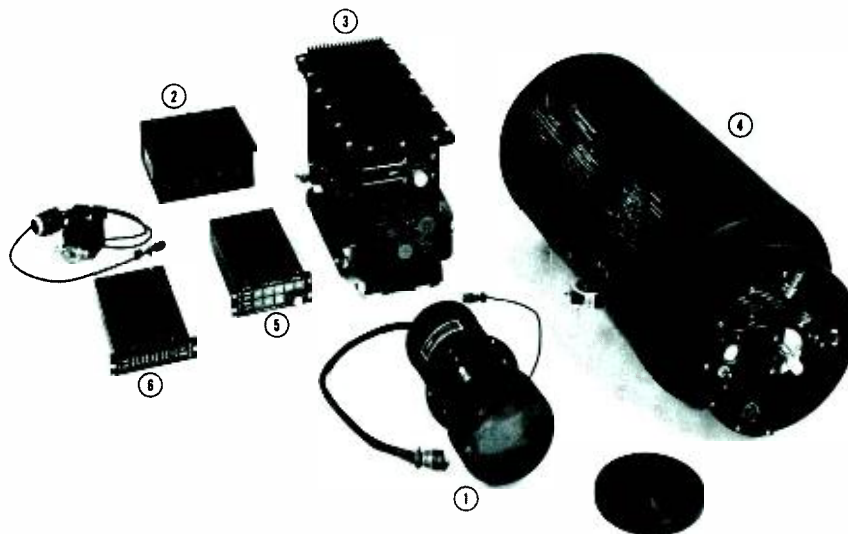


Fig. 5—Complete illuminator subsystem designed for use with a gated low-light-level TV system: 1) illuminator head, 2) driver module, 3) electronics unit, 4) liquid-nitrogen storage dewar, and 5) and 6) control units.

tem equipped with rotary joints as required for the intended application.

Control of the illuminator system is largely automatic in that, in conjunction with a suitable TV camera, target acquisition is achieved by automatic range scanning, and target range follow after acquisition is also automatic. However, two control units (5 and 6) are provided to enable operator participation and manual over-ride if desired. The two operator controls besides allowing for normal ON/OFF and STANDBY/LASE switching functions, provide operator selection of illuminate pulse width and range delay. Also included in one of the operator control panels is a series of illuminated panels to provide complete status indication. Any system malfunction is identified, and by illumination of the appropriate display panel, the operator is alerted as to the particular malfunction present.

Future development

The system described above reveals the considerable progress achieved in converting the *GaAs* diode development by RCA Laboratories and Electronic Components into a new product line for RCA. As with all other products, however, the system presented does not represent the end of development in this area. Considerable effort at both Division and individual level are resulting in continuous improvements in system performance and versatility, coupled with reductions in size and reproducibility costs. Continuing *GaAs* diode de-

velopment, for instance, is resulting in reduced diode array costs while providing increased system power output and efficiency without added system complexity.

Current programs are also underway at ATL to reduce system size and to provide a remote control of variable fields of view by the use of automatic zoom optics.

Considering long-term developments, it is hoped that, with further improvements in the state of the art of *GaAs* diodes, a system can eventually be designed that will achieve present output performance without the use of cryogenic cooling. The advantages of such a system to the user can readily be appreciated.

Acknowledgments

Although the development of pulsed *GaAs* illuminators has been the responsibility of the Advanced Technology Laboratories, the progress achieved would not have been possible without the assistance and willing cooperation of many individuals in several RCA Divisions. Although it is not possible to acknowledge all contributions at this time, particular mention should be made of the outstanding support provided by Dr. H. Kressel and members of the RCA Laboratories as well as Dr. Glicksman and his Staff at Electronic Components, Somerville, without which the success achieved would not have been possible.

Multispectral recording with synthetic gratings

S. L. Corsover

Color-encoded images can be recorded on black-and-white film through the use of synthetically generated diffraction gratings. A recording system based on this principle has been designed and built by Advanced Technology Laboratories. In system tests, good color recognition, 25-line pair/millimeter resolution, and a 25:1 contrast ratio have been achieved.

COLOR IMAGES and other multispectral information can be recorded on black-and-white film through the use of a unique spatial carrier for each spectral band. Recent work in the area of optical signal processing^{1, 2, 3, 5, 6} has demonstrated the feasibility of this technique and its advantages of simplified processing and maintenance of registration.

For example, recordings have been made by successive exposure of an emulsion that was in contact with a rotatable ruling.¹ Each image was photographed with the ruling at a different angle. When the developed transparency was illuminated, the diffraction pattern generated by the desired image was spatially separated from the other diffraction patterns because of the par-

S. L. Corsover, Electro. Optic Laboratory, Advanced Technology Laboratories, Camden, N.J., received the BSEE from Pratt Institute in 1965 and the MSEE from the University of Pennsylvania in 1971. He joined RCA in 1965 as a design and development trainee. Upon completion of this program, he joined the Advanced Technology Laboratories where his responsibilities were in the area of signal-processing electronics for wideband magnetic recorders. Mr. Corsover participated in the development of a 5-MHz bandwidth magnetic recorder that employed direct-recording techniques. On a five-channel 10-MHz recorder study for RADC, his responsibilities included a study of applicable modulation and multiplexing techniques, a study of the feasibility of developing a magnetic headwheel containing 20 heads, and the definition of magnetic and laser-beam recorder specifications and parameters. Mr. Corsover also studied the equalization problems related to a 100-MHz FM laser recorder and developed a wideband 50-ohm linear phase-equalization scheme. Since the beginning of 1969, Mr. Corsover has been the project engineer on a program to record multispectral information on black-and-white film by utilizing synthetically generated diffraction gratings and a display system employing optical signal processing. He has also participated in the investigation of optical spectrum analysis of wideband signals recorded on film and has designed the automation electronics for the production of the holographic memory disks for the ideographic composing machine. Mr. Corsover is a member of Eta Kappa Nu and Tau Beta Pi.



ticular angles used during the recording process. By placing a spatial filter in the focal plane of a two-lens system, only the desired diffraction pattern was passed. The second lens transformed the passed diffraction pattern back into an image.

Previous investigations have been concerned with camera-type systems in which the input information is a two-dimensional image. The object of our work was to demonstrate the feasibility of recording three channels of information on photographic film by using the basic techniques described above in a scanning-laser recording system. The system inputs were electrical signals from a test-pattern generator. These signals were used to modulate the amplitude of three carrier frequencies chosen such that they constructed synthetic gratings at three different angles on the film. The three modulated carriers were then electronically added and used to intensity modulate the laser beam of the laser recorder. Experiments were performed to determine the system performance in the areas of visual appearance, diffraction efficiency, resolution capability, contrast ratio, crosstalk and linearity.

Theoretical background

Diffraction grating as a spatial carrier

The basic concept underlying this work—the diffraction grating as a spatial carrier—has direct analogies in communication theory but is an extension of that theory in the sense that two spatial dimensions are considered rather than the single dimension of time.

The type of diffraction grating considered in this work is the sinusoidal amplitude grating whose amplitude transmittance function, T_G , can be written in the form

$$T_G(x) = \frac{1}{2} + (m/2) \cos(2\pi\beta x)$$

where β is the spatial frequency, in c/mm; m is the peak-to-peak change in amplitude transmittance, or modulation ratio; and x is the distance across the film.

If a transparency having this transmittance function is uniformly illuminated with collimated, coherent light as shown in Fig. 1, and if the resultant field amplitude distribution impinges on a lens, then the Fourier transform (or

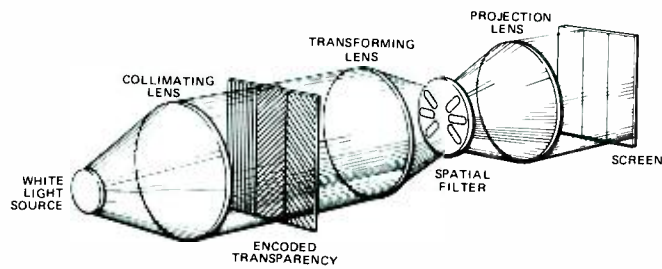


Fig. 1—Technique of displaying color-encoded transparency.

diffraction pattern) of the transmittance function will appear in the focal plane of the lens. The Fourier transform may be operated on in this plane.

To understand the spatial-carrier concept, consider the operation of removing the zero-order, or average-value, term by placing a stop in the system as shown in Figs. 2 and 3. This stop (screen) is referred to as a spatial filter. Lens L_2 effectively performs an inverse Fourier transform on the modified field amplitude distribution existing after the spatial filtering operation.

As a result of the transforming, spatial-filtering, and inverse-transforming operations, the field amplitude existing at the screen of Fig. 2 will have the same form as the amplitude distribution of the original grating, except that the average value term will be missing. Thus the field amplitude distribution, U_s , at the screen will be given by

$$U_s(x) = (m/2) \cos(2\pi\beta x)$$

and the intensity distribution, I_s , on the screen will be given by

$$I_s(x) = U_s^2(x) = (m^2/8) + (m^2/8) \cos(4\pi\beta x)$$

Examination of this intensity function

discloses that the average value of intensity on the screen is a function of the modulation ratio of the original grating. It is also seen that a sinusoidal grating at twice the original frequency is present. In practice, the spatial frequency 2β is unresolvable with the unaided eye. The apparent illumination on the screen is therefore

$$I_A = m^2/8$$

which indicates that by changing the modulation ratio, m , the intensity on the screen is changed.

In the case considered above, m is constant over the entire original grating. If m were made to vary according to the luminance distribution of a real image, $A(x, y)$, the original diffraction grating would have the form

$$T_G(x, y) = \frac{1}{2} + A(x, y) \cos(2\pi\beta x)$$

This form is analogous to an amplitude modulation system where β is the carrier frequency and $A(x, y)$ corresponds to the modulating signal.

It should be noted that when such a grating is optically processed in the system shown in Fig. 2, the intensity distribution on the screen is proportional to $A^2(x, y)$. This is a source of har-

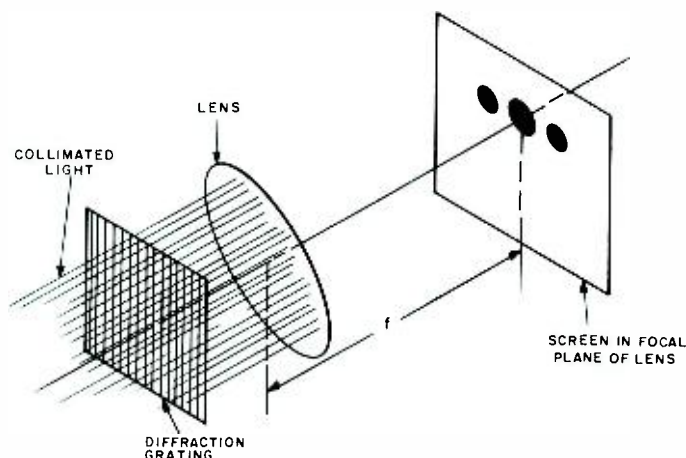


Fig. 2—Fourier-transform property of a lens.

monic distortion and will appear as hue and saturation errors in a color system if left uncorrected.

Spatial encoding and filtering

When the diffraction grating is considered as a carrier, the possibility of multiplexing several images in one area of a transparency can be seen. One possible multiplexing technique is the linear addition of modulated vertical diffraction gratings, each having a different spatial carrier frequency. The radial distance of the diffracted order from the zero order is given by

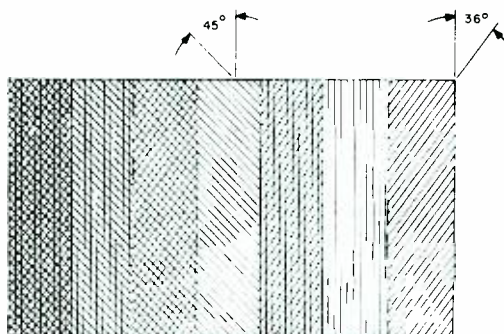
$$d = \beta \lambda Z$$

where β is the spatial frequency of grating (line pairs/mm); λ is the wavelength of light being used; and Z is the focal length of transforming lens.

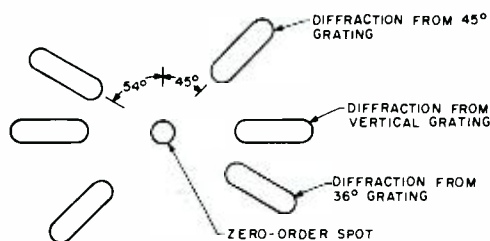
If the carrier frequencies are chosen such that the sidebands of the mod-

WHITE	MAGENTA	CYAN	BLUE	YELLOW	RED	GREEN
RED + BLUE + GREEN	RED + BLUE	BLUE + GREEN	BLUE	RED + GREEN	RED	GREEN

a) Color bar pattern.



b) Encoded transparency.



c) Diffraction pattern.

Fig. 4—Color-encoding process.

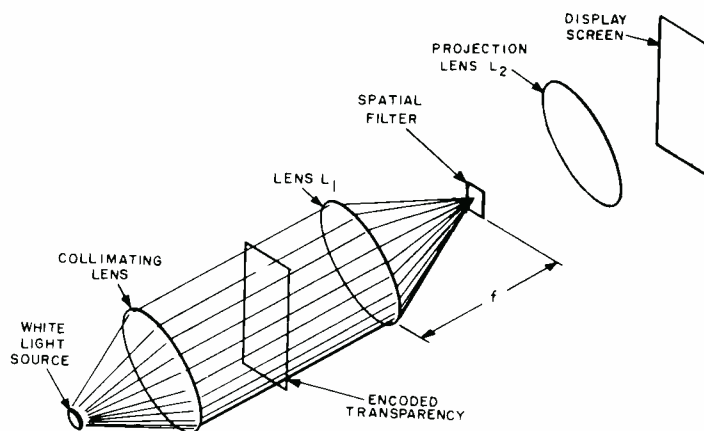


Fig. 3—Display system.

ulated carriers do not overlap, then an individual image can be chosen by passing only its carrier and sidebands with an appropriate spatial filter. While this system is analogous to a frequency-division-multiplexing electronic system, it does not take advantage of the two-dimensional nature of optical systems.

Another possible multiplexing technique is the linear addition of modulated diffraction gratings each having a unique angle. Referring to Fig. 1, it can be seen that the directions of the grating lines and diffraction pattern are 90° apart. Because of this phenomenon, the spectra of angularly separated gratings will be angularly separated in the transform plane. The advantages of the angular separation technique over the frequency multiplexing technique are lower film resolution requirements as well as lower recording and display system modulation transfer function requirements (the modulation transfer function is the sinewave spatial frequency response of a system). For example, all angularly separated gratings could have the same spatial frequency and yet be separable in the transform plane.

The angular separation technique has been used to record color images by assigning unique grating angles to the three primary colors—red, blue and green. Fig. 3 shows a transparency encoded in this manner being displayed. By inserting color filters in the openings of the spatial filter, only the desired color is passed for each grating angle. Although Fig. 3 shows a recording of only primary colors, mixed colors such as magenta, cyan, and yellow can be

recorded by linearly adding two gratings in the same area of the transparency. This process is illustrated in Fig. 4 where a vertical grating is assigned to red, a 45° grating to blue, and a 36° grating to green. If it is desired to record the color-bar pattern shown in Fig. 4a, the proper grating or combination of gratings must be recorded in each of the bars as shown in Fig. 4b (an actual recording would use much higher grating pitches). When placed in the display system of Fig. 3, the encoded transparency will create a diffraction pattern in the transform plane as shown in Fig. 4c. The spatial filter is made by cutting slots corresponding to the diffraction patterns in a piece of opaque material. The zero-order spot is not allowed to pass. Blue filters are placed over the 45° slots, green filters are placed over the 54° slots, and red filters are placed over the horizontal slots in order to add the proper colors to the image which appears on the screen of the display system.

Recording system

Considerations in the choice of electrical carrier frequencies

A schematic representation of the recording system is shown in Fig. 5. The rotating scanning mirror causes the focused spot to scan across the film while the film is transported in a direction perpendicular to the scan direction. At the same time, the intensity of the focused spot is being modulated by the light modulator. The parameters that determine the angles at which gratings are formed are the electrical modulating frequency, the rotational velocity of the scanning mirror, and the transport velocity or scan-to-scan spacing. For

example, if an integral number of cycles per revolution of the scanner are recorded, the intensity peaks of successive scans will line up to form a grating orthogonal to the scan direction. This situation is shown in Fig. 6 for a particular recording geometry. Figs. 7 and 8 illustrate the formation of other grating angles by modulating with different electrical frequencies.

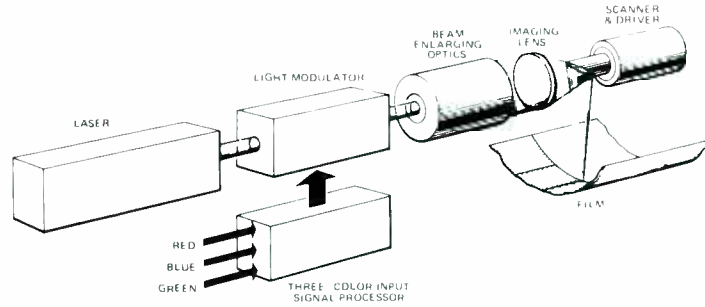


Fig. 5—Recording system.

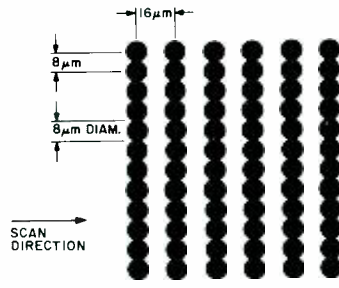


Fig. 6—Vertical synthetic grating.

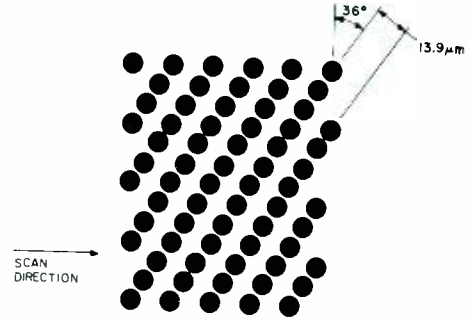


Fig. 7—36° synthetic grating.

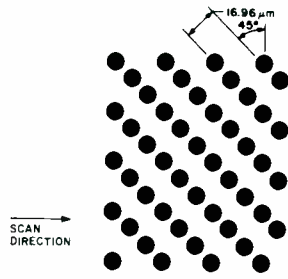
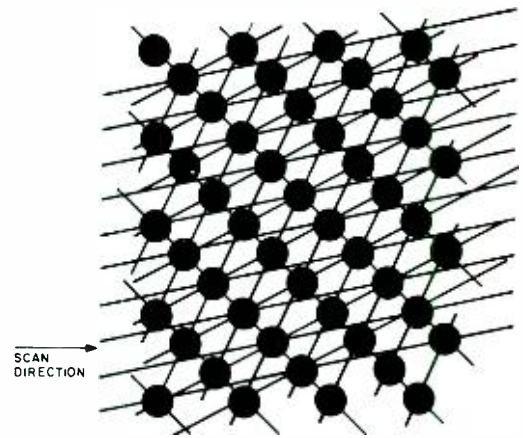
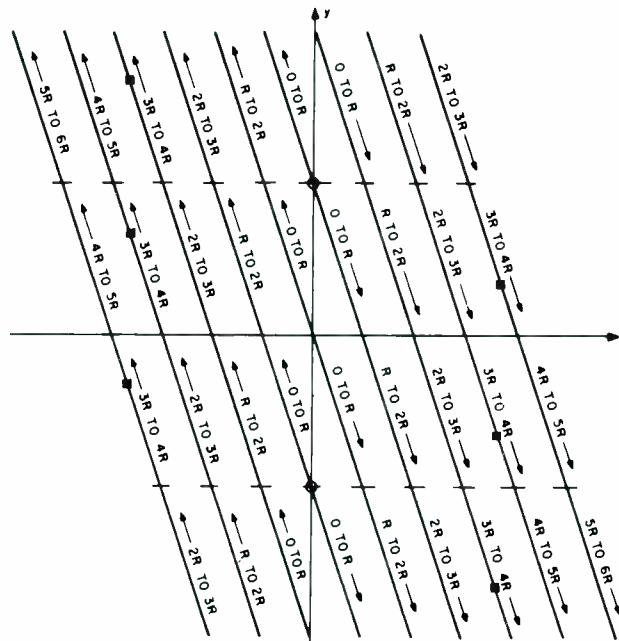


Fig. 8 (above)—45° synthetic grating.
Fig. 9 (right)—45° synthetic grating and spurious gratings.
Fig. 10 (below)—Motion of diffraction patterns through transform plane.



It can be shown that if the scan rate is R scans/s and the scan spacing is known, the loci of the positions of the diffracted spots will be as shown in Fig. 10. Fig. 10 shows only part of the transform plane but indicates how the diffraction patterns move through the transform plane as a function of the recording frequency. For example, if the recording frequency is 3.6 times the scan rate, the diffracted spots will fall in the positions indicated by squares in Fig. 10. If the desired angular location of the diffracted spot and desired grating pitch are chosen, the technique illustrated in Fig. 10 can be used to determine the required electrical carrier frequency.

It is desirable, from system considerations, to have the location of the spots due to the carrier gratings fixed in the transform plane. Movement of the spots could result in inefficient spatial filtering or crosstalk between channels. From the relation between spot location and system parameters, it results that if the electrical carrier frequency $f(t)$, and the scanner rotational velocity R have a fixed relationship, the recorded wavelength will be constant. If the transport velocity has a fixed relationship to the scanner velocity (e.g., 8 micrometers of linear motion per scanner revolution), the entire recording geometry will be independent of the absolute frequencies used.



If fixed relationships are maintained between the electrical carrier frequencies, the scanner rotational velocity, and the transport velocity, constraints are imposed on the choice of recording parameters. In implementing the recording system, it was decided that the film transport, which will be described in greater detail below, could be free running (*i.e.*, not servoed to the scanner). The carrier frequencies and servo reference frequency, however, had to be derived from a common oscillator in order to have the required fixed relationship. This requirement limited the choice of carrier frequencies to those which were rational fraction multiples of the highest carrier frequency. The highest carrier frequency was constrained to be an integer times 10^3 by the servo reference frequency requirements.

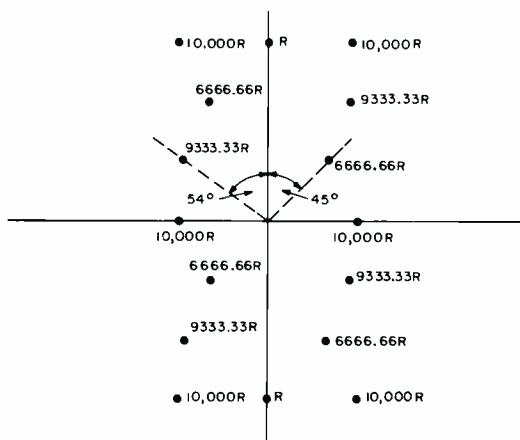


Fig. 11—Predicted location of diffracted spots.

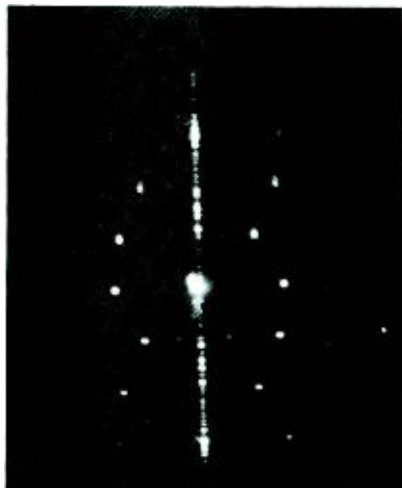


Fig. 12—Diffraction pattern from all three carriers.

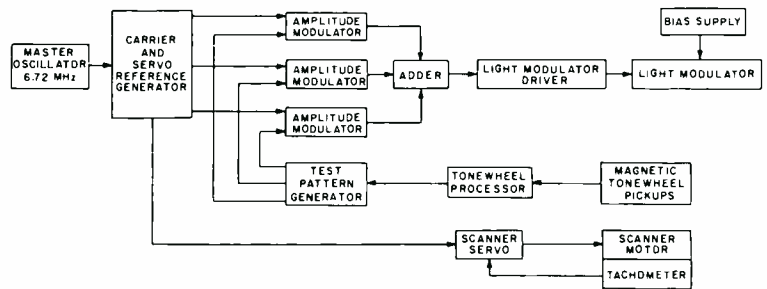


Fig. 13—Electronic system, block diagram.

Film format

In implementing the recording system, a resolution goal of 25 line pairs per millimeter (lp/mm) was established. Sampling theory indicates that this resolution requires a grating pitch of at least 50 lp/mm. A pitch of 60 lp/mm was chosen, which corresponds to a grating spacing of approximately $16 \mu\text{m}$.

To achieve a grating spacing of $16 \mu\text{m}$ in a synthetically generated grating orthogonal to the raster, the recording spot size was chosen to be $8 \mu\text{m}$.

A scan spacing of $8 \mu\text{m}$ was chosen to keep the raster-generated diffraction components low in amplitude and spatially removed from the desired components in the Fourier plane.

The synthetic grating parameters for a scanner rotational velocity of 24 r/s are summarized in Table I. It can be seen that an electrical carrier at 10^4 times the scanner velocity yields a vertical grating. The predicted locations of the diffracted spots are shown in Fig. 11, and a photograph of the diffraction pattern from a region in which all three carriers were recorded is shown in Fig. 12.

Table I—Grating parameters for a scanner rotational velocity of 24 r/s.

Grating angle (degrees)	Grating pitch (lp/mm)	Total cycles (c/r) in scan direction	Electrical carrier frequency (kHz)
Vertical	62.5	10,000	240
45	58.8	6666.66	160
36	71.7	9333.33	224

Electronic system concept

In implementing the synthetic-grating recorder, one objective was to linearly add three modulated carrier frequencies and record them on film. The linear addition possibly could have been accomplished by employing three light modulators and focusing systems and superimposing the resultant spots on

the film. The problems involved in implementing multiple light modulators and focusing optics were avoided, however, by choosing to add the three modulated carriers electronically and using the resulting signal to drive a single electro-optic light modulator. The single modulated beam is expanded and focused as was illustrated in Fig. 5.

A block diagram of the electronic system is shown in Fig. 13. Synchronization between the carrier frequencies and the scanning mirror is achieved by deriving the carrier frequencies and the servo reference frequency from a single master oscillator. Medium-scale integrated circuits were used to divide the master frequency of 6.72 MHz down to the required frequencies. The test pattern generator is a digital system which senses the position of the scanner and counts reference pulses to keep track of elapsed recording time. It uses this information to generate a test pattern. The outputs of the test pattern generator are digital signals and are the modulating inputs to the amplitude modulators. The amplitude modulators are insulated-gate field-effect transistors used in an *on-off* analog switching mode since the input signals were limited to digital signals. The modulated signals are resistively added and amplified and used to drive the light modulator.

Film transport

To achieve a scan-to-scan spacing of $8 \mu\text{m}$ with a scanner velocity of 24 r/s, a transport speed of 7.56×10^{-3} in/s is required. The tolerance goal on this speed was set at $\pm 10\%$.

To achieve these extremely low speed and jitter requirements, the concept of a gravity-driven transport controlled by a fluid dashpot was implemented as shown in Fig. 14.

At the operating speed of 7.56×10^{-3}

in./s. velocity errors due to the difference between static and dynamic friction are possible. Friction was reduced by incorporating air bearings between the film carriage and ways, and by using a fluid seal between the piston shaft and cylinder cap.

The transport speed is regulated with a precision valve that controls the rate at which the fluid can move from the bottom of the cylinder to the top. The clearance between the piston and cylinder walls is small enough that only a negligible amount of fluid can take that path. To provide for the fluid displaced by the piston shaft, a reservoir is connected to the upper half of the fluid line.

Experimental results

Color-bar recordings made on the synthetic-grating recorder resulted in good displayed images. The primary colors were highly saturated and the mixed colors (cyan, magenta, and yellow) were easily recognized. Black regions in the displayed image were generated by turning the carriers off and recording only a bias level of light. Since the film was not opaque in these "black" regions, some light was scattered and the corresponding areas of the displayed image were not as dark as they would have been if the film was opaque.

The diffraction efficiency of the encoded transparency directly influences screen brightness. For a full dynamic range recording, the ratio of first-order diffracted power to zero-order power was 18.5%. The theoretical limit for this ratio is 25%.

Resolution capability was measured using the electronically generated bars in the test pattern. It was found that with color-corrected lenses in the display system, the bars at 25 lp/mm could be resolved but their contrast ratio was very low.

The low-frequency contrast ratio was measured at the output screen of the system shown in Fig. 3. Due to background noise from multiple reflections and scattering, the contrast ratio was limited to 10:1. Using the optical system shown in Fig. 15, the contrast ratio was improved to 24:1. The improvement was due to reducing the background noise by removing the collimating lens and placing the imaging lens directly

against the spatial filter thus reducing the possibilities for stray reflections and scattering.

A qualitative crosstalk test was made in which a recording of a color-bar pattern was displayed using a modified spatial filter. The modified spatial filter passed only the diffraction components from the vertical gratings. Observation of the resultant display indicated no visually discernible difference between the regions corresponding to white (where all three carriers were recorded at one-third dynamic range) and the regions corresponding to red (where only the vertical carrier at one-third dynamic range has been recorded). If crosstalk had existed, the presence of the other carriers would have affected the light diffracted by the vertical grating in the white region.

A linearity test was made to determine how close the system performance was to the theoretically predicted square relation between input signal and diffracted power. A recording of only the vertical carrier was made in which the amplitude of the electrical carrier frequency was increased in steps of 3 dB. The processed transparency was illuminated with a 2-mm-diameter laser beam, and the diffracted and zero-order power corresponding to each recording level was measured using a light meter. The ratio of the first-order power to zero-order power was used as a measure in order to eliminate any effects of film nonuniformities due to bias exposure level variations and banding. The results shown in Table II indicate that the system is relatively close to the theoretical predictions.

Table II—Measured and predicted diffracted power for several recording levels.

Recording level (normalized, dB)	Diffracted power (normalized, dB)	Predicted diffracted power (dB)
0	0	0
+3	4.9	6
+6	10.4	12
+9	17.4	18

Conclusions

The feasibility of color encoding on black-and-white film through the use of synthetically generated diffraction gratings has been demonstrated. Color-bar recordings made with the system resulted in good color recognition, resolution capability of 25 lp/mm, and a contrast ratio of 25:1.

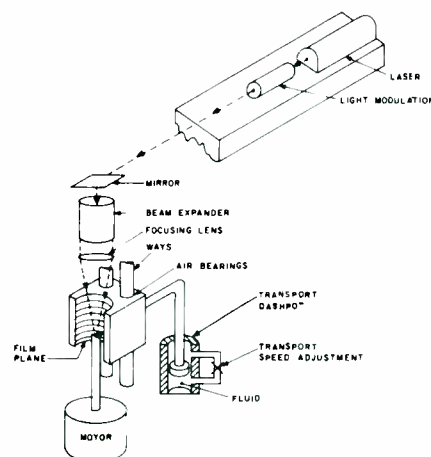


Fig. 14—Synthetic grating optical system and transport.

The applications for color encoding using the synthetic grating technique are in the areas of recording and displaying the outputs of multispectral IR and visible-region line-scan sensors located in aircraft or satellites. Several different system configurations are possible depending on the particular application, with the line-scan video outputs either being recorded directly in an aircraft or transmitted to ground stations for recording and evaluation. The use of phase-type transparencies would allow the rapid and inexpensive replication of encoded imagery for interpretation by multiple users.

Development of the synthetic grating technique will continue toward implementation in state-of-the-art IR sets which contain typically five channels.

References

- Mueller, Peter F., "Linear Multiple Image Storage," *Applied Optics*, Vol. 8, No. 2 (Feb. 1969) pp. 267-273.
- Lamberts, R. L. and Higgins, G. C., "Digital Data Recording Using Superposed Grating Patterns," *Photographic Science and Engineering*, Vol. 10, No. 4 (July-Aug. 1966) pp. 209-221 and Vol. 10, No. 5 (Sept.-Oct. 1966) pp. 263-269.
- Mueller, P. F., "Color Image Retrieval from Monochrome Transparencies," *Applied Optics*, Vol. 8, No. 10 (Oct. 1969) pp. 2051-2057.
- Markevitch, Bob J.V., "Optical Processing of Wideband Signals," Third Annual Wideband Analog Recording Symposium, Rome Air Development Center, Air Force Systems Command, Griffiss Air Force Base, New York, RADC-TR-69-377, Vol. 1 (Oct. 1969) pp. 185-206.
- Hutto, Jr., E., "Low-light-level color photography," RCA Reprint *Optics*, PE-535, p. 10, *RCA Engineer*, Vol. 17, No. 2 (Aug./Sept. 1971) pp. 28-30.
- L. J. Nicastro and E. Hutto, Jr., "Color decoding projector for low-light-level color photography," RCA Reprint *Optics*, PE 535, p. 18, *RCA Engineer*, Vol. 17, No. 2 (Aug./Sept. 1971) pp. 34-37.

Visible and infrared sensor arrays for imaging systems

A. Boornard

Two new solid-state infrared imaging technologies and a new visible light sensor array concept are currently under development at Advanced Technology Laboratories. The infrared sensor arrays are intended for passive imaging over the 8- to 14- μm spectral interval. One type of infrared array consists of mercury cadmium telluride (HgCdTe) quantum detector operating in the photoconductive mode. This array is intended for application in line scan systems and requires an optomechanical scanner and a refrigerator. The other is a two-dimensional array, or mosaic, of pyroelectric sensors composed of thin film triglycine sulfate (TGS) formed on an integrated circuit substrate. The TGS elements are minute thermal detectors. This array would be operated at room temperature in a shuttered mode with each element of the array viewing a single scene element for the entire exposure period. The visible-sensor-array concept is the charge-coupled device (CCD) array which appears to be particularly promising for low-light-level imaging over the 0.4- to 1.1- μm region.

SOLID-STATE IMAGING TECHNIQUES have developed steadily over the past several years, and a large number of imaging approaches have been conceived for operation in the visible and infrared regions of the spectrum. Interest has, in part, been motivated by the usual arguments in favor of solid-state approaches: high reliability, low power consumption, lack of a vacuum envelope, and low-voltage operation. However, in the case of 8- to 14- μm

Reprint RE-18-2-5
Final manuscript received June 27, 1972

infrared imaging, where no camera pick-up tube counterparts exist, development has been spurred by the requirements of modern reconnaissance and surveillance.

The 8- to 14- μm spectral interval is of particular importance for two reasons:

- 1) It corresponds to a transmission window in the Earth's atmosphere, and
- 2) About 38% of the total energy radiated by targets at 300°K is contained within this spectral interval.

The 0.4- to 1.1- μm band corresponds to the response of silicon photosensors.

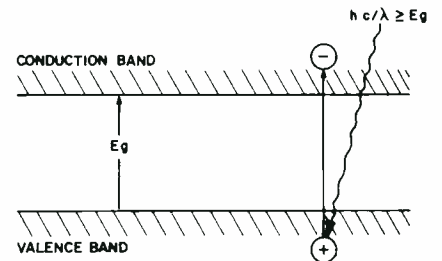


Fig. 1—Representation of intrinsic photoconductivity as typified by HgCdTe .

It encompasses the 0.4- to 0.7- μm visible spectral response of the human eye and peaks at the near infrared wavelength of 0.85 μm . The inherent high sensitivity of silicon photosensors, when combined with well-developed integrated circuit processing technology, offers the promise of large scale, high resolution, multispectral arrays having low light level capabilities.

Line-scan HgCdTe arrays (8- to 14- μm infrared imaging)

Mercury cadmium telluride (HgCdTe) is a ternary alloy formed by chemically combining the semi-metal mercury telluride (Hg, Te) with the semiconductor cadmium telluride (Cd, Te). The resulting mixed crystal is an intrinsic infrared detector; *i.e.*, electrons are excited directly from the valence band into the conduction band by absorbed infrared photons having energy greater than the forbidden gap energy, as illustrated in Fig. 1. Since the energy of a photon is hc/λ , the long wavelength limit of a



A. Boornard, Ldr.
Sensor Development Group
Advanced Technology Laboratories
Camden, New Jersey

received the BS in Physics in 1953 from the College of William and Mary and the MS in Physics from Indiana University in 1955. He served with the U.S. Army from 1955 to 1957. Since joining Advanced Technology Laboratories in 1957, he has been responsible for research and development in a number of diverse areas, including electromagnetic-wave plasma interactions radiation effects in semiconductors, microwave plasma diagnostic techniques, experimental studies of the Cerenkov microwave interaction, microstrip/YIG filters, delay techniques, and applications of bulk negative resistance microwave and millimeter wave devices. Currently, Mr. Boornard's group is working on the development of large scale, high resolution silicon photodiode arrays sensitive over the 0.4- to 1.1- μm spectral band with integrated scan generators and multispectral capability, the development of high sensitivity mercury cadmium-telluride arrays for high resolution cryogenically cooled FLIR systems, and the development of thin-film pyroelectric sensor mosaics for large scale uncooled thermal imaging systems sensitive over the 8- to 14- μm spectral window of the Earth's atmosphere. Mr. Boornard is a member of the American Physical Society.

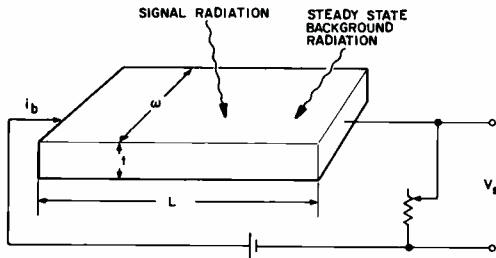


Fig. 2—Basic circuit for a photoconductive infrared detector.

photoconductor's response is

$$\lambda_c = hc/E_g \quad (1)$$

where λ_c is the cut-off wavelength in micrometers; c is the free space velocity of light (2.998×10^{10} cm/sec); h is Planck's constant (6.624×10^{-34} Joule-sec); and E_g is the semiconductor's band gap energy. When E_g is expressed in electron volts, λ_c is $1.24/E_g$.

An important property of $HgCdTe$ is that its band gap can be varied by varying the alloy composition. This permits "tuning" the material to obtain maximum sensitivity over spectral intervals covering a broad range (approximately 3 to 30 μ m). Although the material is most often designated simply as $HgCdTe$, its compositional dependence is usually expressed as $Hg_{1-x}Cd_xTe$, where x represents the mole fraction of $CdTe$. For $x=0.2$ and when cooled to 77°K, the material forms an excellent detector of radiation in the important 8- to 14- μ m spectral band. All other detectors require cooling to much lower temperatures (typically 4.2 to 20°K) to operate over the same band.

Since about 1960, extensive research and development on $HgCdTe$ has been performed, with the result that present day $HgCdTe$ detectors are approaching the limiting detectivity established by the random fluctuations in the energy of the detected photons. Interest in $HgCdTe$ for use in high performance forward-looking infrared systems (FLIR systems) has been widespread because of its excellent detector characteristics when cooled to 77°K, a temperature readily attainable with compact, high-reliability refrigerators.

In photoconductive detectors, the excitation of some excess majority carriers above the thermal equilibrium concentration by the incident signal

photons results in an increase in the conductivity of the detector. The basic circuit for a photoconductive detector is illustrated in Fig. 2. The detector is shown as a thin slab of $HgCdTe$ of thickness t , width W , and length L , through which a constant bias current i_b flows. In the absence of signal radiation, the voltage across the detector is

$$V_o = i_b R = \frac{i_b}{\sigma_0} \frac{L}{Wt} \quad (2)$$

Where σ_0 is the initial conductivity of the detector material. The signal radiation increases the conductivity to a new value $\sigma_1 = \sigma_0 + \Delta\sigma$.

The resulting voltage drop across the sample is the signal voltage, V_s . It can be related to the incident photon flux and to the basic properties of the detector material by the expression

$$V_s = \phi \eta e i_b (\mu_n \tau_n + \mu_p \tau_p) \frac{R^2 W}{L} \quad (3)$$

where ϕ is the photon flux rate (number of photons/cm²/s); e is the electron charge (coulombs); η is the quantum efficiency (number of hole-electron pairs produced per incident photon); R is the resistance of the detector (ohms); μ_n and μ_p are the electron and hole lifetimes, respectively (cm²/V-s); and τ_n and τ_p are the electron and hole lifetimes, respectively (s).

In n-type material, as is the case for $HgCdTe$, $\mu_n \gg \mu_p$ and since $\tau_n \approx \tau_p$, Eq. 3 becomes

$$V_s = \phi \eta e i_b (\mu_n \tau_n R^2 W) / L \quad (4)$$

Eq. 4 shows that large photoconductive signal response requires high quantum efficiency, long carrier lifetime, the highest possible bias current, and the highest possible sample resistance. The last condition is equivalent to obtaining both the thinnest possible sample and the lowest thermal equilibrium carrier concentration.

The usefulness of an infrared detector depends primarily upon its detectivity, which is a measure of the detector's ability to produce an electrical signal that can be detected above the noise level. The specific detectivity D_{λ^*} of a detector is the ratio of the electrical signal-to-noise voltage (V_s/V_n) divided by incident photon signal power (P_{IR}) and normalized with respect to detector area (A) and detector noise bandwidth (Δf); i.e.

$$D_{\lambda^*} = (V_s/V_n)(A\Delta f)^{1/2}/P_{IR} \quad (5)$$

where D_{λ^*} is in cm Hz^{1/2}/watt.

If the detectivity is limited by Johnson noise, i.e. $V_n = V_j = (4kTR\Delta f)^{1/2}$, it can be shown that

$$D_{\lambda^*} = \frac{\eta_{\lambda} e i_b R^{3/2} W^{1/2} \mu_n \tau_n}{2h(c/\lambda) L^{3/2} (kT)^{1/2}} \quad (6)$$

It can be further shown that when random photo-current noise (also called generation-recombination noise) is dominant, D_{λ^*} is given by¹

$$D_{\lambda^*} = \frac{\eta_{\lambda}}{2h(c/\lambda) \eta_b^{1/2} \phi_b^{1/2}} \quad (7)$$

where η_b is the quantum efficiency of the detector for background radiation, and ϕ_b is background photon flux rate.

D_{λ^*} in this case is independent of any photoconductor material parameters, except insofar as the quantum efficiencies may be material-dependent. Photoconductors which follow Eq. 7 are said to be "BLIP" limited detectors, i.e. background limited infrared photoconductor detectors. This theoretical limit is 3.5×10^{10} cm Hz^{1/2}/watt for a photoconductor detector responding to 9.6- μ m radiation when viewing a 295°K background with a 2π steradian field of view. As the field of view is narrowed, the theoretical limit of D_{λ^*} increases, with the limiting value approaching 5.3×10^{10} cm Hz^{1/2}/watt. $HgCdTe$ detectors having detectivities approaching this limit have been made at RCA (see Table I).

Table I—Characteristics of an $HgCdTe$ detector of the RCA 40-element array.

Detector area	5.8×10^{-2} cm ²
Detector bias	1.5 mA
Responsivity	
(500°K, black body)	2000 V/W
Specific detectivity	
(500°K, black body)	6.7×10^8 cm Hz ^{1/2} /W
Peak response	9.6 μ m
Peak responsivity	6300 V/W
Peak specific detectivity	2.9×10^{10} cm Hz ^{1/2} /W
Measurement conditions: 800-Hz chopping rate 7-Hz bandwidth.	

Since $HgCdTe$ represents the best of present day 8- to 14- μ m sensor materials, it is appropriate to examine the potential performance capabilities of a large-scale FLIR system containing a linear array of $HgCdTe$ detectors and forming 5×10^5 resolution elements per picture frame. A simplified block diagram of the arrangement of the system is shown in Fig. 3. The hypothetical

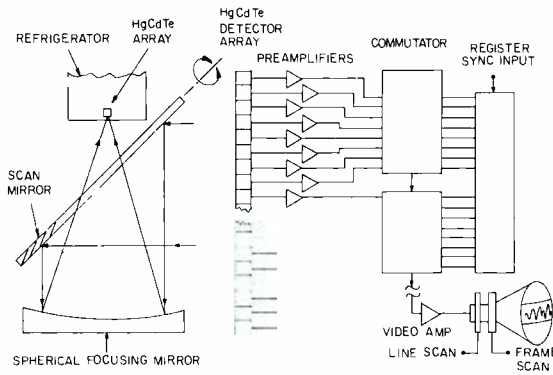


Fig. 3—Simplified arrangement and block diagram of a $HgCdTe$ line-scan IR imaging system.

system specifications are as follows:

- | | |
|--|-----------|
| 1) Instantaneous detector field of view, IFOV | 0.25 mrad |
| 2) Frame rate, F_r | 20/s |
| 3) No. of horizontal resolution elements N_h | 1,000 |
| 4) No. of vertical resolution elements, N_v | 500 |

The IFOV of 0.25 milliradians means that the system should be able to resolve a 10-inch target at a range of one kilometer. The overall field of view scanned by the FLIR would be 7.4° in the elevation plane and 14.8° in the azimuth plane.

It will be further assumed that: 1) $f/2.5$ optics will be used; 2) the scan mirror will be driven with sinusoidal motion with 40% of the cycle being usable for forward scan; 3) $D\lambda^*$ of the average sensor element is 2.8×10^{10} cm Hz^{1/2}/watt; 4) each element is a 3-mil square;

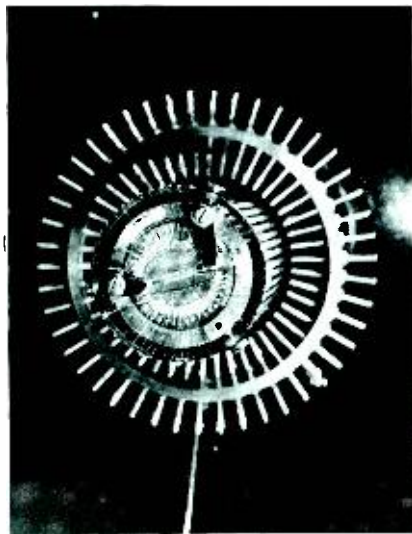


Fig. 4—A 40 element linear array of $HgCdTe$ detectors mounted on the cold finger of a heat-driven Vuilleumier refrigerator, showing the lead-frame and the output signal and bias current pins.

- 5) the average noise figure of the preamplifiers is 2.3 dB (factor of 1.7); and 6) the overall optical degradation factor is 0.4.

It is desired to determine the temperature resolution of the system, *i.e.* the minimum temperature difference between a target and the background which the system can discern. For the type of sinusoidal scan drive assumed, the detector dwell time, τ_d , is

$$\tau_d = 0.4 / (F_r N_h).$$

The detector noise bandwidth, Δf , is given by $\Delta f \approx 0.5 / \tau_d$, which gives a value of $\Delta f = 25$ kHz.

The temperature resolution (in $^\circ K$) of the system ($NE\Delta T$) is given by

$$NE\Delta T = NER_{eff} \left(\frac{dN_\lambda}{dT} \right)_T \quad (8)$$

where NER_{eff} is the effective noise-equivalent radiance (watts/cm²/steradian) and dN_λ/dT is the rate of change of the target radiance. For targets at 300 $^\circ K$, the appropriate value of (dN_λ/dT) is 7.4×10^{-5} W/cm²/steradian/ $^\circ K$ over the 8- to 14- μm spectral band.

The noise equivalent radiance is given by

$$NER = \frac{4F_{NO} \sqrt{\Delta f NF}}{\pi D_c \delta \theta D \lambda^*} \quad (9)$$

where D_c is the diameter of the collector optics, NF is the noise figure of the preamplifier, and δ is the optical degradation. For the parameters selected above, the temperature resolution of the system would be 0.26 $^\circ K$, which would permit high-quality images of a large variety of targets.

Progress at RCA in $HgCdTe$ has included the development of techniques

for preparing high quality $HgCdTe$ in a reproducible manner. The materials growth capability along with detector array fabrication technology has been developed at the RCA Laboratories. Linear arrays containing 40 elements each 3×3 mils have been built and tested with excellent results in a heat-driven VM (Vuilleumier) refrigerator developed at ATL. Integration of such an array into an advanced refrigerator design is the first step in the development of high performance FLIR systems. A photograph of the array mounted on the cold finger of the VM refrigerator is shown in Fig. 4. The integrated array/refrigerator assembly is shown in Fig. 5.

Integrated-circuit pyroelectric imaging arrays

The feasibility of large-scale two-dimensional sensor arrays for thermal imaging over the 8- to 14- μm range is being examined at ATL using thin-film triglycine sulfate (*TGS*) pyroelectric sensors formed on FET integrated-circuit substrates. Pyroelectric sensors are heat-sensitive elements which are capable of detecting minute radiation-induced temperature changes. They have been available as single-crystal point detectors of infrared radiation for several years. Recently, however, a technique was developed at the RCA Laboratories for making thin-film *TGS* in a manner compatible with large-scale integrated-circuit processing methods.

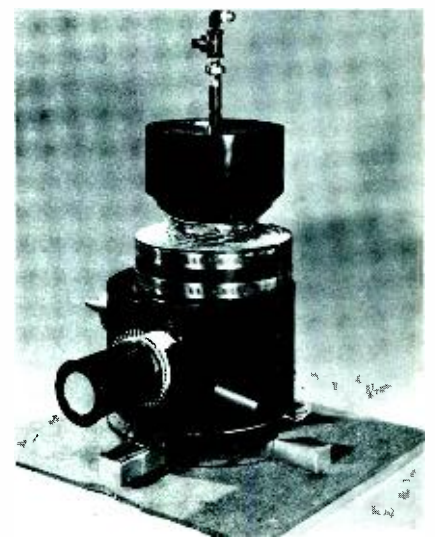


Fig. 5—The Vuilleumier refrigerator used to cool the $HgCdTe$ array of Fig. 4. The refrigerator is capable of maintaining the array at 77 $^\circ K$. The infrared radiation from the scene is focused through an IRTRAN-II window which covers the top of the cold finger vacuum jacket.

Infrared imaging systems employing two-dimensional integrated pyroelectric arrays have two important advantages in that they should require no refrigerator and no optomechanical scanner. The lack of a refrigerator and optomechanical scanner assures large savings in size, weight, and power consumption and would result in highly improved reliability. This greatly simplifies thermal imaging systems and opens the possibility for their use in applications where cryogenically cooled scanned systems are not feasible.

Angular resolution close to 0.25 milliradians should be attainable with moderate f -number optics because the detectors can be made as small as 3 mils on a side. Although detector bandwidth is limited to about 100 Hz or so, operation at video frame rates is possible in a two-dimensional array, since each sensor element views but a single element of the scene for the entire exposure period. At the present time, the sensitivity of pyroelectric detectors is nearly three orders of magnitude less than $HgCdTe$ detectors. However, moderately high system sensitivity should be attainable because of the large detector integration time inherent in two-dimensional array operation. For 8- to 14- μm imaging, systems using pyroelectric sensor arrays should be capable of achieving temperature resolutions of 1 to 3°K.

Pyroelectric effect

Certain materials exhibit a spontaneous electrical polarization, *i.e.*, an alignment of the internal electric dipoles, even in the absence of an applied electric field. The polarization decreases with increasing temperature and vanishes at a specific temperature (the Curie temperature). Because the magnitude of the polarization is temperature dependent, materials exhibiting this property are called pyroelectric. The rate of change of polarization with respect to temperature, dP/dT (known as the pyroelectric coefficient), increases with increasing temperature and is estimated to be 1.4×10^{-8} coulomb/cm²·°K for thin-film TGS at 300°K. Some selected properties of single crystal TGS at 300°K are listed in Table II.

An external electric field is not normally observable in the vicinity of a pyroelectric material, even if it is an insulator, because the polarization field becomes

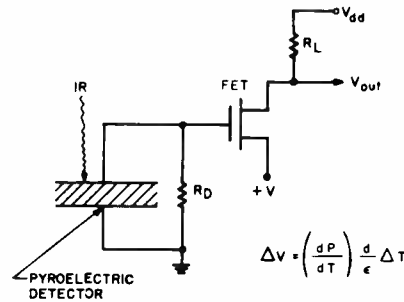


Fig. 6—Basic arrangement of a pyroelectric thermal detector.

Table II—Selected properties of single-crystal triglycine sulfate at 300°K (after Putley, Ref. 2).

Pyroelectric coefficient, dP/dT	2.35×10^{-8} C/cm ² ·°K
Relative dielectric constant, ϵ_r	25–50
Dielectric coefficient, ϵ	$2.1 - 4.42 \times 10^{-12}$ F/cm ⁻¹
Specific heat, C_p	0.97 J/gm ⁻² ·°K
Thermal conductivity, K	6.8×10^{-3} W/cm ⁻² ·°K
Mass density, ρ_m	1.69 gm/cm ³
Thermal diffusivity	0.41×10^{-2} cm ² /s

neutralized by stray charges which are attracted to and bound to the surface. The bound surface charge is unable to respond to rapid changes in the polarization. Thus, a sudden temperature-induced change in the polarization will be accompanied by an observable external electric field while the surface charge is adjusting to the new conditions. It is the measurement of this transient electric field that forms the basis of pyroelectric detectors.

Pyroelectric detectors for thermal imaging

The pyroelectric effect can be utilized to form a sensitive infrared detector by constructing a parallel-plate capacitor with the pyroelectric material as the dielectric. The absorption of infrared radiation results in a temperature-induced change in the polarization which is accompanied by a transient change in the potential across the detector electrodes. A pyroelectric detector with its associated high input resistance and low input capacitance FET amplifier is shown in Fig. 6. The resistance, R_d , which shunts the capacitance, C_d , of the detector is always present by virtue of the leakage resistance of the pyroelectric material. The transient electric field that develops when the detector is subjected to radiation can be measured by the voltage drop across R_d .

For application to infrared imaging systems, the detector RC time constant should be large compared with the frame time to ensure negligible loss of charge during exposure. In this mode

of operation, the detector integrates the infrared scene radiation for the total exposure; and, to a first approximation, the change in detector open-circuit voltage, ΔV , is proportional to the change in temperature, ΔT .

$$\Delta V = \Delta Q / C_d \quad (10)$$

where ΔQ is the temperature-induced change in charge on the detector electrodes in coulombs and C_d is the capacitance of the detector in farads.

$$C_d = \epsilon A_d / d$$

Here, A_d is the area of the capacitor plates in square centimeters, d is the thickness of the pyroelectric material in centimeters, and ϵ is the dielectric coefficient of the pyroelectric material in farads/centimeter.

Since the polarization is equivalent to the charge per unit area,

$$\Delta Q = (dP/dT) A_d \Delta T \quad (11)$$

which leads to

$$\Delta V = (dP/dT)(d/\epsilon) \Delta T \quad (12)$$

The expression for ΔV shows that for thermal imaging arrays, an applicable figure of merit for the pyroelectric material is $(dP/dT)(1/\epsilon)$. Triglycine sulfate was selected for use in integrated-circuit sensor arrays because it has one of the highest known figures of merit.

Pyroelectric detectors in thermal imaging arrays

The development of large-scale two-dimensional arrays of pyroelectric sensors requires the use of thin film pyroelectric materials capable of being deposited on appropriate substrates. Detectors made from thin polycrystalline TGS indicate a required film thickness of between 5 and 15 μm .

A possible pyroelectric detector configuration for thermal imaging arrays is shown in Fig. 7. The pyroelectric elements would be located on the top surface of an integrated-circuit substrate with the active area of each sensor element being defined by the lower electrode of the TGS capacitor. A cross-sectional view of the arrangement of a portion of a sensor cell is shown in Fig. 8. This arrangement is being used in a developmental 16 \times 16 array which has the sensor elements spaced on 10-mil

centers. The lower electrode is attached to the gate of the P-MOS FET, which is used to address the detector and to amplify the pyroelectric signal generated in the detector. The upper electrode is a continuous thin film of semi-transparent conductor such as chromium or an alloy of nickel and chromium.

Referring to the schematic diagram of Fig. 7, it is seen that each sensor cell contains two field-effect transistors formed in close proximity—a signal FET and a reference FET. The FET's are p-channel enhancement units and are normally self-biased in the nonconducting state at zero gate-source voltage. The lower electrode of the pyroelectric sensor is joined to the gate of the signal FET, while the gate of the reference FET is attached to ground. The array would be shuttered with a continuous motion aperture and would be read out one column at a time after exposure to

the scene. Readout is accomplished by switching the drain-to-source voltage of all the FET's in a column, resulting in the simultaneous output of the signals corresponding to each of the sensor cells in that particular column. The signals are amplified and multiplexed to form the video signal.

When a column of elements is addressed, two signals (a reference signal and a sensor signal) are obtained from each sensor cell. In the absence of a radiation-induced signal from the pyroelectric sensor, both signals are pulses whose amplitudes are fixed and are determined by various geometric and semiconductor parameters such as channel width, channel length, gate oxide thickness, effective surface mobility, and the threshold voltage of the particular FET's. These parameters can be expected to vary from one region of the array to the other, principally because of processing-induced varia-

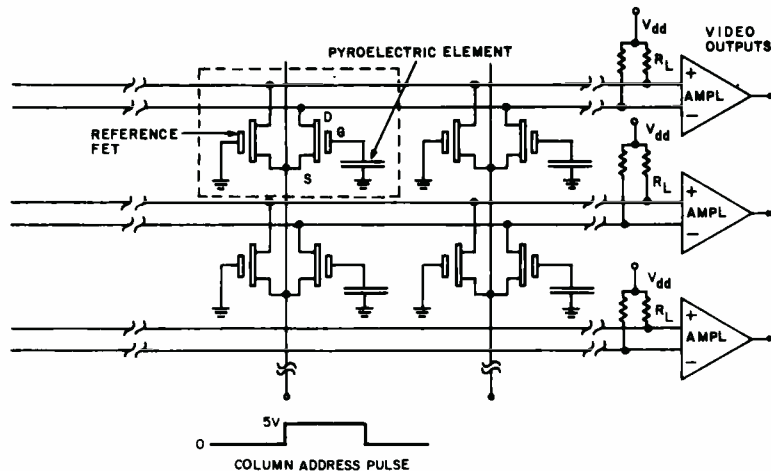


Fig. 7—Schematic of the triglycine sulfate sensor array used in the developmental 16x16 imaging mosaic.

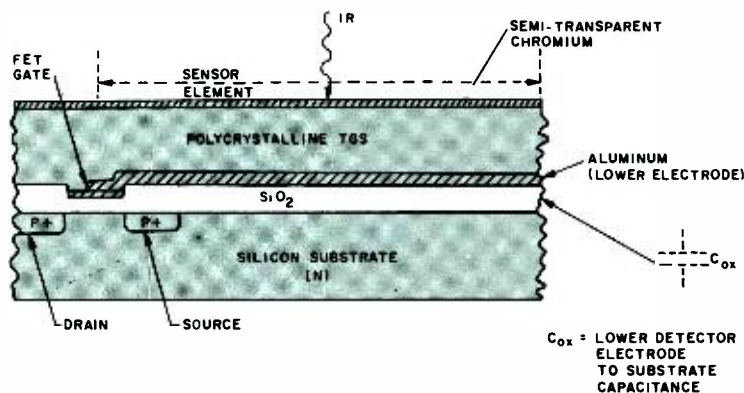


Fig. 8—Cross-sectional view of a thin film pyroelectric sensor element on a bulk P-MOS substrate.

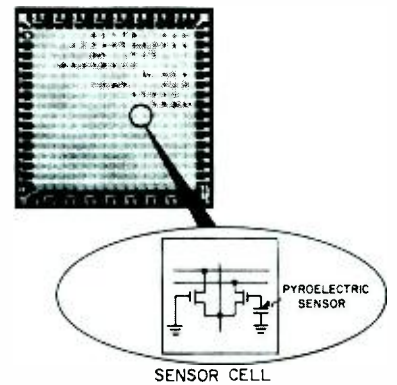


Fig. 9—Photomicrograph of the 16x16-element thin film triglycine sulfate sensor array.

tions. However, when two FET's are formed in close proximity, as is the case within each sensor cell, the variations are virtually nonexistent, and the FET's are nearly identical. Accordingly, when a radiation-induced signal is present on the pyroelectric sensor, it becomes added to the fixed amplitude pulse, and it can be readily amplified by means of an external high-gain difference amplifier. Thus, the use of two FET's formed in close proximity within each sensor cell should accomplish two purposes: 1) it should circumvent fixed pattern noise along the array and 2) it should permit the use of high common mode rejection, high-gain preamplifiers for amplification of low level pyroelectric sensor signals. Additionally, the reference and signal FET arrangement should result in cancellation of FET-induced switching noise since the amplitudes of the switching noise transients should also be virtually identical. Fig. 9 is a photomicrograph of the metallization pattern of a 16x16 array which was processed on a 2-in.-diameter silicon wafer. A larger number of bonding pads is used than is necessary to facilitate measurement and characterization of the array elements.

The layout of an individual sensor cell in the 16x16-element TGS mosaic is illustrated in Fig. 10. Shown are the two FET's per cell, the address line, the signal and reference lines, a ground line, and the lower electrode which defines the active area of the sensor cell. The cross-hatched regions are p+ strips which are diffused into the n-type silicon substrate. The shaded regions are aluminum metallization lines and the small dark rectangles are "crossunder"

openings in the SiO_2 through which the aluminum metallization contacts the p⁺ diffused strips. Each p⁺ diffused ground line is joined to an aluminum line (not shown in the diagram) which extends along two sides of the array to assure attaining ground potential throughout the sensor mosaic.

No serious attempt was made to attain high packing density in this prototype array. The area of the lower electrode is 69 square mils, which corresponds to 69% active detector area per sensor cell. The aluminum metallization lines and the p⁺ diffused strips are 0.5 mil wide, and the spacing between conductors is 0.3 mil. The aluminum gate p-MOS FET's have a channel width of 0.5 mil, a channel length of 0.15 mil and a combined gate-to-source, gate-to-drain and gate-to-substrate capacitance of 0.044 pF. Assuming the TGS and SiO_2 layers to be 10 and 1.5 μm in thickness, respectively, and the dielectric constant of the polycrystalline TGS to be 25, the voltage responsivity would be equal to half that of a comparable sensor element on an insulating substrate.

Progress to date on the 16x16 array has included the fabrication of several wafers of array chips, the standard checkout of selected FET's, the formation of sprayed TGS over the wafers, the deposition of the thin semitransparent upper electrode, and the delineation of the array chips by etching the TGS to access the pads in preparation for wire bonding. The circuitry needed to scan the array and to amplify and multiplex the resulting pyroelectric signals has been designed.

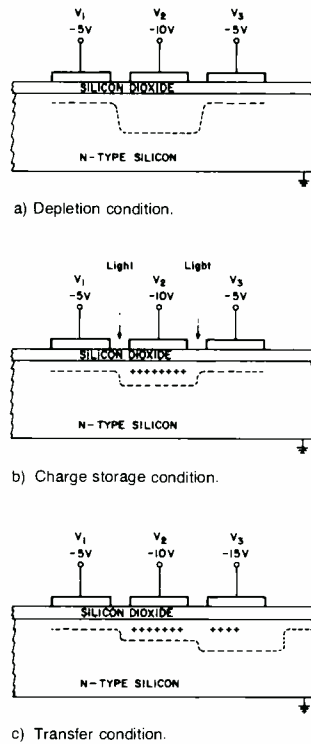


Fig. 11—Cross sectional view of a three-phase charge coupled device. The dashed lines represent both the edges of the depletion regions and the potential wells within the semiconductor. The voltages are typical for n-type silicon devices. When used as an imaging array light enters through the gaps separating the electrodes.

Charge-coupled-device photosensor arrays

The charge-coupled-device (CCD) is a conceptually simple structure which requires a minimum of processing steps and yet offers a wide range of digital and analog applications. It is basically a charge storage and transfer device with charge transfer occurring along a semiconductor-oxide interface. Although their applicability to large scale high resolution visible and near infrared imaging is just beginning to be exploited, the potential of charge coupled devices appears very promising. Two types of CCD arrays will be described; the original three-phase devices and the more recent two-phase CCD arrays developed by Kosonocky and Carnes at the RCA Laboratories.^{3,4}

The CCD array was described by W. S. Boyle and G. E. Smith of the Bell Telephone Laboratories in 1970⁵ and demonstrated shortly thereafter in linear arrays of MOS capacitors formed on n-type silicon substrates.⁶ The key conditions required for proper opera-

tion of a CCD array are that the charge be transferred in a reasonably short time and with small fractional loss of charge in the transfer process. The present silicon art produces material with a sufficiently low density of surface and bulk trapping centers to permit utilization of the CCD concept and transfer efficiencies of close to 99.99% appear attainable. Applications currently being pursued in addition to photosensor arrays include high density serial memories, delay lines, and pulse compression filters.

The simplest form of CCD is a linear array of closely spaced electrodes overlaying an insulator deposited on a uniformly doped semiconductor substrate: the original three-phase single metal level CCD of Boyle and Smith.⁵ Fig. 11a illustrates a section of the device with a negative potential being applied with respect to the substrate on each of the three electrodes. The potential under the center electrode is sufficiently large to deplete the underlying region of electrons and to produce inversion in the region. Depletion of the surface is not a stable condition and in time thermally-generated carriers will accumulate at the surface. However, the surface of high quality SiO_2 -Si interfaces will remain depleted for times on the order of seconds. If minority carriers (holes in the case of n-type silicon) are introduced in the vicinity of the potential well, they will collect and become stored at the surface in the potential minimum defined by the center electrode, as illustrated in Fig. 11b. If the third electrode is now made more negative than the center electrode while the potential of the first electrode remains unchanged, a deeper potential well will be created below the third electrode, and the stored charge will be transported to the region below it (Fig. 11c). The potentials on the electrodes are subsequently readjusted so that the quiescent storage site is located at the third electrode. It is apparent that the purpose of the first electrode is to block flow in the left direction, thus providing unidirectional transport of the stored charge.

The arrangement of a linear array of three-phase CCD's is illustrated in Fig. 12. The electrodes are connected in groups of three and operated with a three-phase voltage supply to give direction to the transfer operation. The

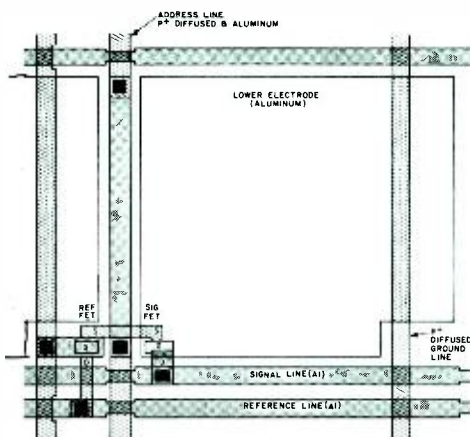


Fig. 10—Layout of an individual sensor cell in the 16x16 element triglycine sulfate array.

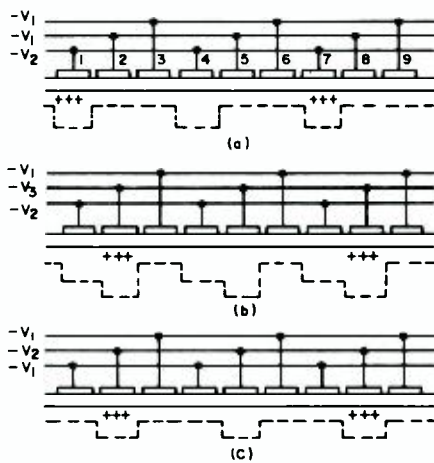


Fig. 12—Schematic of a three-phase charge-coupled-device array.

potentials applied to each electrode are shown in the left column. The applied voltage V_1 is large enough to provide the depletion region. V_2 is larger than V_1 and provides the storage site for the holes injected into the semiconductor. However, V_3 is larger than V_2 , which causes the transfer of holes to the electrodes biased at voltage V_3 . In this manner, charge which represents information is shifted along the entire array. Detection at the output of the array can be accomplished by using a reverse-biased diode. The diode, either a p-n junction or Schottky barrier unit, is biased to a voltage which is more negative than any of the voltages used for transfer. Charge transported to the diode produces a current in an external circuit.

Injection of minority carriers into a non-optical CCD array is usually accomplished by using a diffused p-n junction and an injection gate at the input of the array. In an optical sensor CCD array, the minority carriers are introduced into the potential wells by incident photons having sufficient energy to create hole electron pairs in silicon (photons with energy greater than about 1.1 eV). The holes are stored in the potential minima while the electrons are swept into the substrate. The number of holes collected is proportional to the number of photons arriving from the corresponding scene element. Accordingly, a charge pattern is developed across the array which is an analog of the intensity pattern of the imaged scene.

A linear optical-sensor CCD array would normally require an optomechanical

scanner to produce a two-dimensional image of the scene. However, in certain applications, such as surveillance by aircraft or satellites, the velocity of the vehicle itself provides the necessary scan component.

Both linear and two-dimensional CCD optical sensor arrays are possible, with the latter being essentially formed from a number of linear arrays. A linear CCD imaging array containing 288 electrodes has been built and operated at Bell Laboratories.⁷ The image was scanned across the array and formed 96 resolution elements per scan since each sensor cell contained three electrodes. A similar 3-phase CCD imaging array containing 100 resolution elements has been built and operated at the RCA Laboratories.⁸ Most recently, a 500-element three-phase CCD line-scan array has been built and successfully operated at Bell Labs.⁹ In three phase CCD arrays, light focused on the front side of the array passes through the gaps separating the electrodes and into the silicon substrate. Since the gaps are small compared with the electrodes (2.5 vs. 10 μm) and since there are two gaps per sensor cell, the active area is 14% of the sensor area.

To date, the largest two-dimensional CCD array that has been reported is an experimental 106×64 element structure also composed of three-phase CCD's.⁹ The structure is divided into three functionally different areas: the light-sensitive area, a readout store consisting of 106×64 non-light-sensitive CCD's and a line-readout section consisting of 106×1 array with a readout diode at the input end.

The RCA approach to CCD's as developed at the RCA Laboratories differs in several important respects from the original three-electrode single-level CCD's. Directionality of the charge flow is built into the structure through the use of two thicknesses of channel oxide and two electrodes: a buried polysilicon and an aluminum electrode. A cross-sectional view of the RCA CCD arrange-

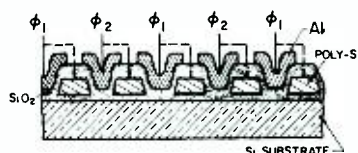


Fig. 13—Cross-sectional view of the RCA two-phase CCD.

ment is shown in Fig. 13. It is operated in a two-phase mode which significantly reduces the complexity of the clocking requirements. Two-phase operation is obtained because the electrodes induce asymmetrical potential wells, with the minority carriers accumulating in the deeper parts of the potential well. In the charge transfer operation of a two-phase CCD array, the potentials on adjacent electrode pairs are switched between $\phi_1 (V_0 - V_1)$, and $\phi_2 (V_0 - V)$. The steps in the oxide thickness produce different potential wells beneath each of the electrodes. The charge transfer operation is similar to that previously described for the three-electrode geometry. The use of polysilicon gates overlapped by aluminum forms a self-aligning electrode structure which should lead to high device yield. This electrode arrangement also offers the possibility of obtaining rather large fringing fields that can aid in the transfer of charge between electrode sections. Although the two-phase CCD requires four electrodes per sensor cell, the use of narrow polysilicon gates should permit a packing density of 1 to 2 square mils per sensor cell.¹⁰ When operated as an imaging array, the incident light must pass through the polysilicon gates if illumination occurs from the front side. The problem of transmission loss through polysilicon gates may not be a serious one if the polysilicon can be made sufficiently thin.

References

1. Long, D. and Schmit, J. L., "Mercury Cadmium Telluride and closely related alloys; in *Semiconductors and Semimetals*, Vol. 5, edited by Willardson, R. K. and Beer, A. C. (Academic Press: New York; 1970) ch. 5.
2. Putley, E. H., "The Pyroelectric Detector," *ibid.* ch. 6.
3. Kosonocky, W. F. and Carnes, J. G., "Charge Coupled Digital Devices," 1971 IEEE International Solid State Circuits Conference, University of Pennsylvania (Feb. 1971).
4. Kosonocky, W. F. and Carnes, J. E., "Two-Phase Charge Coupled Shift Registers," 1972 IEEE International Solid-State Circuits Conference, University of Pennsylvania (Feb. 1972).
5. Boyle, W. S. and Smith, G. E., "Charge-Coupled Semiconductor Devices," *Bell System Technical Journal*, Vol. 49, No. 4 (April 1970) pp. 587-593.
6. Amelio, G. F.; Tompsett, M. F.; and Smith, G. E., "Experimental Verification of the Charge Coupled Concept," *Bell System Technical Journal*, Vol. 49, No. 4 (April 1970) pp. 593-600.
7. Tompsett, M. F.; Amelio, G. F.; et al., "Charge-Coupled Imaging Devices: Experimental Results," *IEEE Trans. on Electron Devices*, Vol. ED-18 (Nov. 1971).
8. Altman, L., "The New Concept for Memory and Imaging: Charge Coupling," *Electronics* (June 1971) pp. 50-59.
9. Bertram, W. J., et al., "Recent Advances in Charge-Coupled Imaging Devices, 1972 IEEE International Convention, New York, paper 5H. 4, March 20-23, 1972.
10. Kosonocky, W. F., and Carnes, J. E. *Private Communication*.



Authors Ammon (left) and Herzog.

G. J. Ammon
Engineer
Applied Physics Lab of
ATL, Camden

received his BSEE from Newark College of Engineering in 1961 and his MSEE from the University of Pennsylvania in 1963. He joined RCA in 1961 and was assigned to the Computer Advanced Development Engineering Department. From 1961 to 1967, Mr. Ammon was involved in the circuit and systems design of tunnel diode, thin film, plated wire and monolithic ferrite memories. He has performed the logic design of several memory exercisers

Wide-angle laser target-designation seeker

G. J. Ammon | D. G. Herzog | H. C. Sprigings

A wide-angle target-designation seeker system was designed to search a wide field of view and discriminate among multiple returns to select targets with the proper signature. It incorporates a sophisticated 12-segment photodetector which provides the steering signals to a servo system to track the laser designated target with exceptional accuracy. A breadboard model of the sensor and processing portion of this system was constructed to determine critical performance characteristics and demonstrate feasibility of the design approach. This breadboard met or exceeded all design goals.

and digital control systems. He was also engaged in the development of a 100-megabit analog-to-digital converter. In 1967, Mr. Ammon joined the Applied Physics group of Advanced Technology Laboratories as Project Engineer on a Laser Tracking and Ranging System developed for NASA. Since then he has been involved in the design of several electro-optic systems such as an optical IFF system, a GaAlAs illuminator system and a receiver seeker for laser designators. Mr. Ammon is presently project engineer for a Precision Hover System for the Heavy Lift Helicopter program. Mr. Ammon is a member of Eta Kappa Nu

Howard C. Sprigings
Manager, Engineering and Development,
Electronic Components,
Electro-Optic Department,
RCA, Ltd.
Montreal

received the BSC degree in 1962 from Sir George Williams University. In 1956 he joined the Northern Electric Company's Materials Inspection Laboratory where he carried out chemical and metallurgical analysis on metals. He was transferred to the Research and Development Laboratories in 1959 and assisted in development work on the NPN planar transistor. Mr. Sprigings joined the Research Laboratories of RCA Limited in April 1960. Initially he was engaged in doing research and development on various types of silicon nuclear particle detectors using oxide passivation techniques. He has been involved in the development of a high power frequency transistor and has been doing research and development of multi-element photodiodes for the detection of 1.06 micron radiation. He has also examined various methods for passivating devices fabricated from ultra-high resistivity silicon. In 1971 he joined the Electro-Optics Department of Electronic Components Division as Manager of Engineering and Development and has since been engaged in directing programmes related to the development of silicon photo-sensors. He is a member of the IEEE and the Canadian Association of Physicists.

ONE OF THE MOST SUCCESSFUL MILITARY APPLICATIONS of the laser has been the target designator. The laser beam is directed at a target by a forward observer and the optical energy reflected by the target is sensed by a bomb with an optical detector. A guidance mechanism within the bomb then uses the detected signals to steer the bomb toward the designated target with exceptional accuracy.

The major disadvantage of existing designator systems is that the aircraft must know approximately where the target is so that the bomb can be released at a point where its sensor can detect the laser energy reflected by the target. Also, if several targets were being designated simultaneously, the bomb would guide itself to the first target it detected and not necessarily the target for which it was intended.

RCA has developed a more sophisticated optical system which overcomes these two disadvantages. This system has a very wide field of view for searching out a designated target. The system also has processing circuitry for sorting out multiple returns and selecting the one with the proper "signature". Because of its increased capability and complexity, this system would normally be incorporated into the aircraft mainframe and used to locate and track a designated target and determine the release point for the less-sophisticated guided bomb. This paper describes a breadboard model of the sensor and the processing portion of this system which was constructed to determine critical performance characteristics and demonstrate feasibility of the design approach.

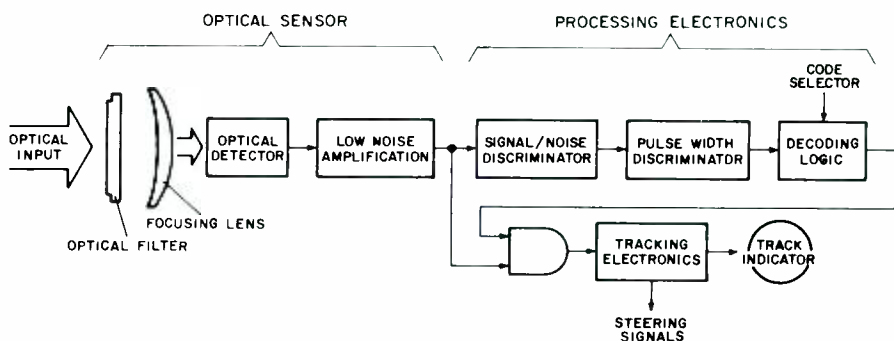


Fig. 1—Wide angle laser target designation seeker.

Reprint RE-18-2-18
Final manuscript received June 27 1972

Signal processing

The wide-angle laser target-designation seeker is shown in block diagram form in Fig. 1. The pulsed optical energy emanating from a designated target is passed through a narrowband optical filter which blocks all signals except those with approximately the same wavelength as the laser designator. The resultant optical signal is collected by a lens and focused onto an optical detector. The position of the focused spot on the photosensitive surface of the detector determines the location of the designated target in the field of view of the seeker system. This "spot" position is determined by examining the minute electrical signals generated by the optical detector.

The weak signals out of the optical detector are first amplified to obtain signals that can be more easily processed. These signals are then fed into the processing electronics where they are tested for identification.

Signal-to-noise test

The processing electronics performs several tests on the amplified optical detector signals to identify the desired designated target. The first test discriminates signal pulses from noise pulses; this is accomplished by establishing a threshold level such that signals with amplitudes above the threshold are passed and signals below the threshold are rejected. The threshold level is set high enough to limit noise-generated false alarms to minimum while maintaining sensitivity to low-level signals.

Pulse-width and coding tests

Signals passing the signal-to-noise test are next examined to see if the received pulse width is narrow enough to be from a laser designator. Finally the incoming

signals are tested to see if their coding corresponds to that of the laser being used to designate the desired target. This test is also used to separate out returns from targets in the sensor's field of view, which are being illuminated by other laser designators. The decoding logic can be set to select signals coming in at one of several slightly different periods. By requiring all designators in the target area to operate at different code settings, the desired returns can be selected by switching the decode logic to a setting corresponding to the proper designator.

Target tracking

Pulsed signals from the optical sensor with the proper amplitude, width, and coding are gated into the tracking electronics which determines the location of the target by comparing the signals from several distinct photosensitive areas on the optical detector. Fig. 2 shows how images from targets in two different portions of the sensor's field of view are focused onto the multielement photodetector.

The photodetector is segmented into 12 isolated photosensitive areas (A through L). The electrical outputs from these areas are processed to generate steering signals which enable a servo system to point the wide-angle laser target-designation seeker at the desired target. If target 1 were the proper target, the signal out of element J of the photodetector (element where image of target 1 is focused) would be gated into the tracking electronics and the servo system would be commanded to steer in the appropriate direction until target 1 is centered on elements A, B, C and D. If target 2 were the proper target, the signals out of elements A, B, C, and D would be gated into the tracking electronics.

Signals out of the quad elements (A,

B, C and D) are processed differently than those out of the remaining elements. The amplitudes of these signals are compared to one another in a linear fashion and steering signals are generated to keep the quad element signals equal in amplitude. This maintains the sensor system pointed at the target with a high degree of accuracy.

The track indicator (Fig. 1) is used to notify an operator that an acceptable signal has been detected and steering signals are available for tracking the source of these signals.

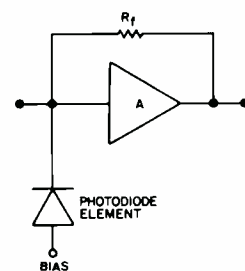


Fig. 3—Preamplifier equivalent circuit.

Preamplifier

The low-capacitance preamplifier is essentially a high-gain inverting amplifier with current feedback from the output to the input. Because of the high open-loop gain, almost all of the photodiode signal current will flow through R_f which then becomes the load resistor in the signal-to-noise equation (Fig. 3). The high gain also keeps the input voltage swing low. This drastically reduces effective capacity thus allowing the use of a very high photodiode load resistance. This is further illustrated as follows. The LaPlace transform equation for the output voltage of this amplifier is given by:

$$V_o(S) = -id(S) \frac{R_f[A/(A+1)]}{1 + R_f\{C_r + [(C_d + C_i)/A]S\}} \quad (1)$$

where $id(S)$ is the transform of the photodiode signal current; R_f is the amplifier feedback resistance; C_r is the capacitance of R_f ; C_d is the photodiode capacitance; C_i is the amplifier input capacitance; and A is the amplifier open-loop gain.

As can be seen from Eq. 1, the effects of the photodiode and input capacity on the overall bandwidth ($BW = 1/(2\pi R_f C_{TOTAL})$) are reduced by the amplifier open-loop gain; thus the amplifier

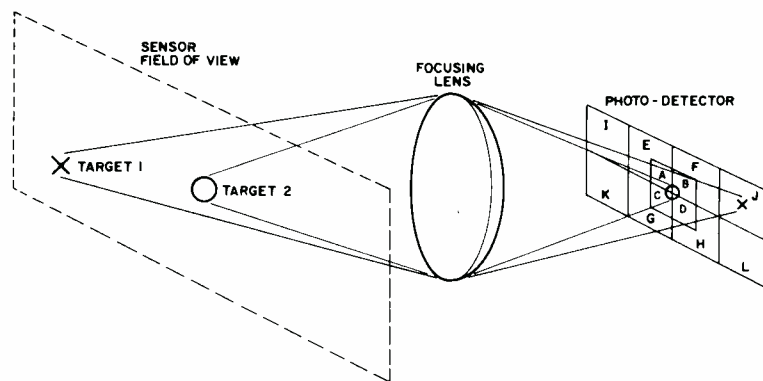


Fig. 2—Locating target with lens and photodetector.

has been designed to yield a high open-loop gain.

The general equation for signal-to-noise ratio for an optical receiver is:

$$S/N = \frac{\rho^2 P_s^2 G^2 R_l}{2eB(\rho P_s + \rho P_b + I_d)G^2 R_l + FkTB} \quad (2)$$

where ρ is photodetector responsivity; P_s is received signal power; R_l is photodetector load resistance; G is photodetector current gain; e is charge on an electron; B is bandwidth of receiver; P_b is background power (due to sunlight); I_d is photodetector dark current; F is receiver amplifier noise figure; k is Boltzmann's constant; and T is receiver temperature.

This equation can be rewritten as:

$$P_s = \frac{2B(S/N)}{\rho^2} \left[\frac{eP_s}{\rho} + \frac{eP_b}{\rho} + \frac{eI_d}{\rho^2} + \frac{2FkT}{\rho^2 G^2 R_l} \right]$$

For a given field of view, pulse width, probability of detection, and false-alarm rate, the B , S/N , and P_b terms will be fixed. The maximum sensitivity (minimum P_s) is then obtained by maximizing ρ , G and R while minimizing I_d and F . The photomultiplier and avalanche photodiode provide high sensitivity by proding gain G . These devices, however, have relatively low values of responsivity ρ . The PIN photodiode has a high responsivity ($\rho=0.65$ at $1.06 \mu\text{m}$) but its gain is only one. This drawback can be overcome by using a low-capacitance circuit and consequently a large load resistance, R_l (for a fixed bandwidth). The low-capacitance circuit can provide a higher sensitivity with a PIN photodiode than either a photomultiplier or an avalanche diode in this system application.

Photodetector

The heart of the wide-angle laser target-designation seeker is the multi-element photodiode detector. This device is shown in Fig. 4. The active area of the sensor is 1.68×0.64 inch and the total package dimensions are 2.25×1.25 inches. Sectoring the detector into 12 isolated photosensitive areas serves two purposes: First, the separate outputs can be compared to generate position information for a signal return. Second, sectoring the detector allows the system to maintain a high degree of sensitivity over a wide field of view.

This is because a major source of noise—background light—is proportional to field of view. By sectoring the detector into many discrete areas, the field of view of each sector is kept small; consequently the background light and thus the resultant noise on each element is small.

The relative sizes of the detector elements are chosen to give the highest sensitivity at the center of the detector. This provides the high signal-to-noise needed for accurate tracking.

The photodetector (Fig. 4) has a substrate material of ultra-high resistivity p-type silicon. Prior to processing, the resistivity of the substrate material is in the 20,000 to 35,000 ohm-cm range. It has been found that the resistivity tends to increase by a factor of two or three during the high temperature processing. In the structure shown, the light enters through the n^+ -junction side of the chip. However, since the depletion layer of this device reaches through to the p^- region at the back of the chip, it is possible to mount the chip such that the light enters through the p^+ side. In applications where narrow transition zone widths are required a v-type groove can be cut into the p^+ surface of the chip through which the light enters, and light will be refracted into one element or the other depending on the position of the light spot in the v-groove. Transition zone widths can be reduced from typically 0.010 inch in a nongrooved device, to less than 0.005 inch in a grooved device for a 0.004-inch light spot.

Some of the key parameters for a photodetector are quantum efficiency, capacitance, dark current, and speed of response. Depending upon the application and specific requirement of the system, tradeoffs between these parameters can be effected, and a device

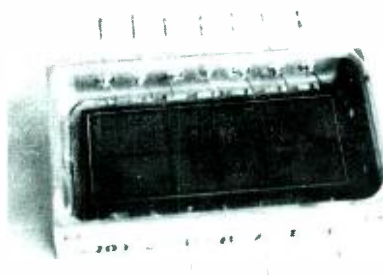


Fig. 4—Sensor array.

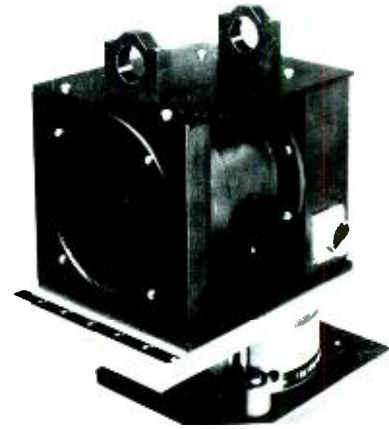


Fig. 5—Optical head.

designed accordingly. To achieve fast response times, the depletion layer must be reduced in thickness, thus causing some loss in quantum efficiency and an increase in capacitance. If the background radiation level is the limiting noise contributor, an increase in quantum efficiency can be realized by operating the detector at a somewhat higher temperature.

The 12-element photodetector exhibited the following typical parameters when a 200-V reverse bias was applied at room temperature:

Parameter	Inner element	Outer element
Dark current	$7 \times 10^{-8} \mu\text{A}$	$4 \times 10^{-7} \mu\text{A}$
Capacitance	3.5 pF	18 pF
Response time	25 ns	25 ns
Quantum efficiency* (1.06 μm)	70%	70%
Transition-zone width	0.008 in.	0.008 in.
Crosstalk	<3%	<3%

*Assuming the particular device under discussion has an antireflective coating and the glass window was coated for maximum transmission at $1.06 \mu\text{m}$.

Since these conditions were not met, the quantum efficiency was 40%.

System packaging

The seeker system was constructed in two packages: the optical sensor and the electronics package. Fig. 5 shows a front-side view of the optical sensor. The optical sensor measures $5.75 \times 5.5 \times 7$ in. and weighs approximately 6 lb. The unit consumes about 5 W of electrical power. The two ring clamps on top of the optical head serve to mount a boresighting telescope used to direct the unit during field testing.

The sensor array is located inside the

rear portion of the optical head. This device is mounted onto a circuit board which contains the preamplifier circuits. The board is positioned to place the detector at the focal plane of the lens system.

Fig. 6 shows a front view of the electronics package. The bottom portion of this package is a 19-inch plug-in rack which holds the eleven $4 \times 4\frac{1}{2}$ inch plug-in boards. Plug-in circuit boards were used for the electronics package of the development model to provide easy access to the circuits for testing purposes. They also provide for easy replacement of a portion of the system with an improved design.

The top portion of the electronics package contains the control and display panel. This part of the unit selects the code that the system will lock on to and the codes that the two simulators will transmit. The lamps indicate the status of the circuitry, the track signal, and which sector contains a signal. The two zero-center panel meters indicate the amplitude of the azimuth and elevation steering signals as they would be transmitted to a servo system.

Two optical-simulator drivers were also designed and constructed to serve as aids in testing and demonstrating the operation of the developmental model. Each unit is a pulsed optical source which emits a $45\text{-}\mu\text{W}$, 60-ns pulse at a wavelength of $1.06\ \mu\text{m}$. The simulator head contains a one-shot circuit, a current driver, a light-emitting diode, a collimating lens, and a narrowband optical filter. The lens limits the output beamwidth to approximately 2° , and the optical filter limits the wavelength spread of the simulator output to $68\ \text{\AA}$ at the half-power point centered within the detection bandwidth of $111\ \text{\AA}$. The simulators are triggered by signals from the electronics package.

Performance

The open-loop-gain vs. frequency characteristics of the preamplifier are shown in Fig. 7. The amplifier has an upper cutoff frequency of about 500 kHz and rolls off at a 6 dB/octave rate. At 4.5 MHz—the measured closed-loop bandwidth—the open-loop gain is about 38 dB. The measured bandwidth with a feedback resistor of 130 kilohms corresponds to an effective total capacitance of 0.25 pF. This large value of

load resistance provides a sensitivity improvement of approximately 8 over conventional preamplifier approaches.

The capacitance of the feedback resistor depends on the type of resistor used. The feedback resistor used in the preamplifier was of the metal-glaze type, which has a capacitance of around 0.05 pF. The measured photodiode capacitance at the bias voltage of 200 was about 4 pF, and the input capacitance of the amplifier (taken from FET specification sheets) should be about 5 pF. For the gain of 70, this corresponds to total load capacitance of about 0.20 pF. The difference between this value and that measured (0.25 pF) is probably due to stray capacity in the circuit layout.

The measured noise out of the preamplifier for the 130-kilohm feedback resistor and 5 MHz bandwidth was 0.23 mV RMS measured with a Hewlett-Packard 3400A RMS Voltmeter. This measurement was made with the photodiode masked to eliminate noise due to background light. This value of noise was used to compute noise figure of the amplifier as 2.3.

The sensitivity of the target-designation seeker was also measured. The optical output from a simulator was measured with a calibrated silicon photodiode detector. The simulator was positioned in front of the optical head so that most of its output was focused on one of the detector equal elements (B, Fig. 2). Calibrated neutral-density filters were then placed in front of the simulator output until the resultant signal was intermittently detected continuously.

This corresponded to a total optical signal on detector element, B, of $0.14\ \mu\text{W}$. The theoretical sensitivity for the same conditions is about $0.10\ \mu\text{W}$.

Matching tests were made on the AGC amplifiers over an 80-dB signal range

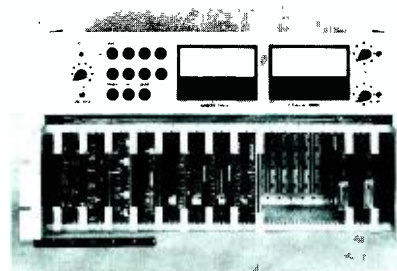


Fig. 6—Electronics package.

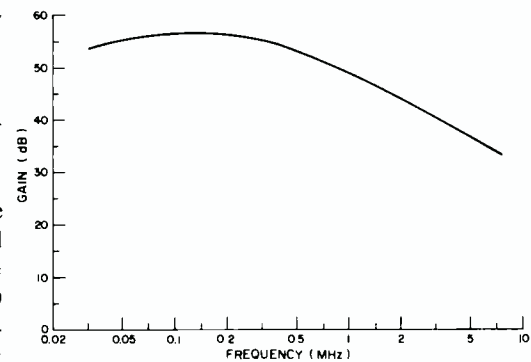


Fig. 7—Open-loop-gain vs. frequency characteristics of preamplifier.

and temperatures of $+55^\circ\text{C}$, $+25^\circ\text{C}$, and -55°C . The dynamic range and S-curve response were also measured. The detector system consisted of a filter, lens, detector, and processing circuitry to provide a sampled-hold azimuth- and elevation-error output. The source was held fixed in position and the detector system azimuth angle was varied. The output of the source was varied using neutral density filters over a dynamic range of 10,000. The results show that the maximum boresight shift over the dynamic range is ± 1.5 minutes or ± 0.44 mrad.

Conclusions

A target designation seeker system was designed which can search out a wide instantaneous field of view and locate a particular target. The heart of this system is the unique 12-element silicon PIN photodiode sensor. The sensor is sectored to maintain high sensitivity over a wide field of view. This 0.68×1.64 -in. monolithic detector represents a difficult but practical manufacturing achievement.

Signals out of the sensor elements are digitized so that they can be processed. Several tests are performed to sort out signals with the proper "signature". These signals are used to generate steering signals that enable a servo system to track the selected target. A breadboard model of the sensor and processing portion of the system demonstrated the critical performance characteristics. Measurements on this breadboard proved the sensitivity, dynamic range, and tracking accuracy to be very close to design goals. The breadboard also demonstrated the system's ability to sort out multiple signal sources and select the one with the proper "signature".

Novel thermal management techniques

B. Shelpuk | P. Joy, Jr.

Nearly all electronic systems must reject heat dissipated within them. Generally, conventional techniques—conduction, convection, radiation—can perform this function. However, new thermal requirements are being imposed on electronic equipment and new techniques—heat pipes, phase-change heat transfer, high-pressure gas convection—are being applied. This paper summarizes these techniques and outlines some of their applications.

EFFICIENT THERMAL CONDUCTION PATHS from heat-dissipating components to the equipment structure or heat sink is the universal first step toward achieving component temperatures consistent with long life and high reliability. For some cases, natural convection provides adequate thermal coupling to the ambient air and thus is a suitable method for maintaining the equipment at safe temperature levels. In other instances, forced-air or forced-liquid cooling systems are required because the heat removal rate is too high for natural convection. When the equipment is operating in a vacuum (*e.g.*, on a spacecraft) or operating at a high temperature, the primary heat-transfer mode is by radiation, and attention must be paid to the principles which govern this phenomenon. These three heat-transfer means—conduction, convection, and radiation

—are the basic tools available to the designer in his task of removing heat from the components in an electronics assembly. There are a number of excellent texts and technical papers which deal with various aspects of these subjects.^{1,2,3}

The thermal management techniques surveyed in this paper have less general application than the basic three just described. These techniques—heat pipes, phase-change heat transfer, and high-pressure gas convection—while not as broadly applicable as the basic three, are extremely effective in certain applications. It is because of this effectiveness that they are being developed.

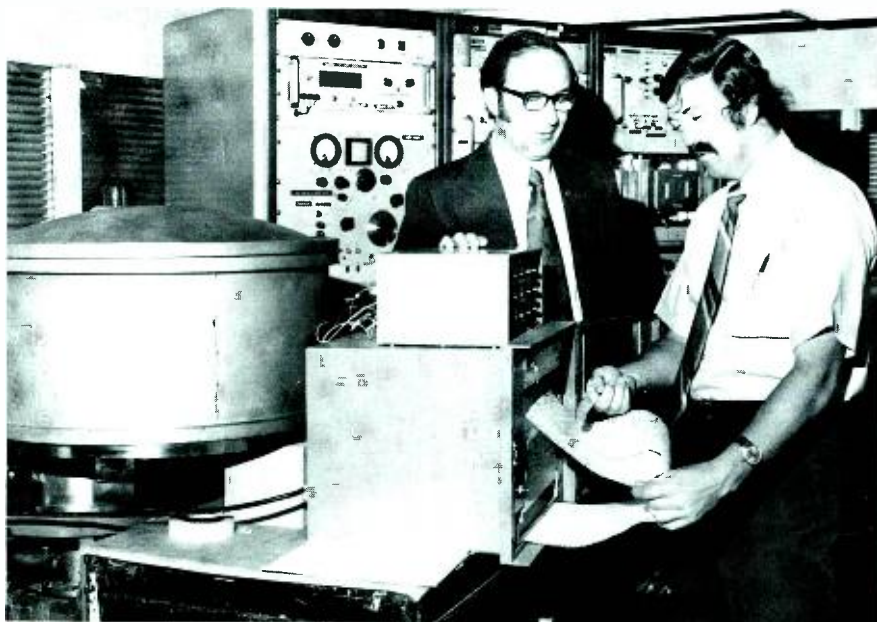
Heat pipes

A heat pipe is a simple self-contained heat-transfer device that exhibits an

Ben Shelpuk, Ldr.
Thermodynamics Group
Advanced Technology Laboratories
Camden, New Jersey

received the BSME and MSME from Drexel Institute of Technology. Following graduation, Mr. Shelpuk joined RCA and became engaged in mechanism design and thermal analysis for combat communications equipment both of conventional design and with micromodule design. Since 1959, Mr. Shelpuk has been a member of Advanced Technology Laboratories. He has been actively involved in much of the thermoelectric cooling activity in RCA, including the design and fabrication of one of the original Navy thermoelectric water chillers, a nine-ton air conditioner, a cascaded Peltier cooler for application to infrared sensitive image tubes, a distillation device for water recovery in space travel, and several energy conversion devices. He was responsible for several thermal analyses of spacecraft systems, and conducted an advanced energy conversion study for a major weapon system. In 1966, Mr. Shelpuk became Engineering Group Leader for the Thermodynamics Group in Advanced Technology Laboratories. As such, he is responsible for Government-funded programs in van air conditioning, cryogenic refrigeration, infrared device refrigeration, heat transfer analysis and design, and heat pipe development. In addition, he has been responsible for company funded work, in Vuilleumier-cycle-refrigeration and low-temperature heat pipes. More recently, Mr. Shelpuk has been responsible for a feasibility study of a spaceborne VM system under NASA contract and the development of a flameless gas heat source for use with a sodium heat pipe at a VM hot cylinder. This was utilized in a VM thermal actuation experiment which showed the feasibility of a low power VM engine under a U.S. Army contract. In addition, he is responsible for the thermal analysis and fusion heat sink development for several electronics systems used in the Apollo program. Mr. Shelpuk is a member of the American Society of Heating, Refrigeration, and Ventilation Engineers, Tau Beta Pi, and Pi Tau Sigma.

Authors Ben Shelpuk (left) and Pat Joy.



Pat Joy
Thermodynamics Group
Advanced Technology Laboratories
Camden, New Jersey

received the BSME and MSME from Drexel University in 1966 and 1969, respectively. Upon joining the Thermodynamics group of Advanced Technology Laboratories in 1966, Mr. Joy participated in the design and development of several low temperature thermoelectric refrigerators for cooling infrared detectors and image tubes. Since 1968, Mr. Joy has been project engineer on ATL's IR&D programs in thermal management. He has developed the bulk of RCA's heat pipe technology in the cryogenic and room temperature range and has designed and built many heat pipe devices including a 1.5W nitrogen heat pipe operating at 77°K, a 55W ammonia heat pipe space radiator, and a 100W integrated heat pipe terminal board for microelectronic circuit cooling. Mr. Joy has developed high pressure gas cooling techniques and recently designed and built a pressurized nitrogen cooling loop for 30 pps Nd:YAG laser target designator. He is currently responsible for analysis, design, and qualification of a frictionless, bimetallic-actuated thermal control louver system for NASA's Atmospheric Explorer satellite.

Reprint RE-18-2-8
Final manuscript received July 20, 1972

effective thermal conductance higher than any known homogeneous material. The classic heat pipe is a closed container with a capillary structure lining the inside walls (Fig. 1). The capillary structure is saturated with a working fluid that absorbs the thermal energy at the evaporator section, transports this energy, and releases it at the condenser.

The mass and energy flow in a heat pipe starts with the absorption of the thermal energy in the evaporator section by the working fluid, which changes phase from liquid to vapor. The large amount of thermal energy absorbed is characterized by the latent heat of vaporization. The thermal energy is transported by mass (vapor) transfer to the condenser end where the vapor pressure is slightly lower due to the temperature of the condenser being less than that of the evaporator. As the vapors condense, the heat stored in the latent heat of vaporization is released, completing the thermal-energy transport cycle. The condensed fluid is next returned to the evaporator to replenish the liquid which is constantly being evaporated. This return is accomplished by capillary forces in the wick; specifically, the difference in the radii of curvature of the liquid-wick-vapor interface between the evaporator and condenser causes a pressure gradient in the liquid. The wick, therefore, may be considered to be a thermally driven fluid pump, and the driving forces in a heat pipe (liquid

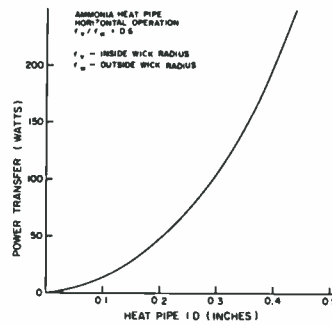


Fig. 2—Heat transfer capacity vs. size of water heat pipes operating horizontally.

and vapor ΔP 's) are caused by the ΔT which is imposed on the pipe.

The versatility of a heat pipe is evidenced by its ability to perform several functions related to heat transfer and temperature control. These functions include:

- 1) *Efficient heat transfer*—The heat pipe can transport thermal energy with a temperature drop several hundred times less than the best solid thermal conductors. This is due to the vapor transport process in which the amount of heat transferred is not directly proportional to the temperature gradient along the pipe as is the case with solid conductors.
- 2) *Flux transformation*—The heat pipe can be used to concentrate or disperse heat by designing the evaporator and condenser areas for the desired ratio of input to output heat flux. Transformation ratios as high as 12:1 have been reported.⁴
- 3) *Temperature integration*—The heat pipe can be used to provide a uniform temperature over a large surface area even when coupled to a time-varying heat source, if no conduction ΔT 's exist in the heat pipe.

Since a change in the input temperature affects only the rate of evaporation and not the temperature level, and since the temperature of condensation is slightly less than the evaporation temperature, the output temperature of the heat pipe will be uniform for a nonuniform heat source temperature.

4) *Separation of source and sink*—The heat pipe can enable a heat sink to be located remotely from the source or sources of heat. In electronic equipment, for example, it is often desirable to pack heat-dissipating elements close together but to have them run as cool as possible. This could previously be achieved only by putting the heat exchanger very close to the source of heat to avoid large conduction temperature drops. The heat pipe can thermally couple a source and a sink which are several feet apart with little thermal degradation.

5) *Variable conductance*—Several heat-pipe techniques can be used to achieve a constant evaporator or condenser temperature regardless of the fluctuations in the input power. These include the vapor-chamber choke with feedback and the moving inert gas volume which can operate with or without feedback.

The performance of heat pipes can be described in terms of two physical parameters. These are the fluid-flow characteristics, which govern the mass transfer and thus the heat transfer capability of the system, and the temperature gradients in the system. The equation which describes the fluid flow for heat pipes with a homogeneous capillary structure is:

$$\frac{2\gamma \cos \theta}{r_c} = \frac{h\eta_l Q (Z + Z_a)}{2\rho_l \pi (r_w^2 - r_v^2) h e r_c^2} + \rho_l g Z \sin \phi + \int \frac{4\eta_v Q (Z + Z_a)}{\pi \rho_v h r_v^4} dz$$

$$\begin{cases} Re_z < 1000 \\ Re_r < 1 \end{cases} \quad (1)$$

where γ is surface tension; θ is surface contact angle; η_l is liquid viscosity; $h e r_c^2$ is the capillary friction factor; ρ_l is liquid density; h is latent heat of vaporization; η_v is vapor viscosity; ρ_v is vapor density; Q is heat transfer rate through the pipe; r_c is capillary pore radius; and Re_z and Re_r are vapor Flow Reynold's numbers with geometry factors as shown in Fig. 1. Various techniques are reported in the literature for optimizing the parameters in Eq. 1 for a set of required performance characteristics. The performance characteristics for electronics cooling applications typically require heat pipes which use ammonia, water, or methanol as a working fluid and are in the 1/8- to 1/2-inch-diameter size range. Fig. 2

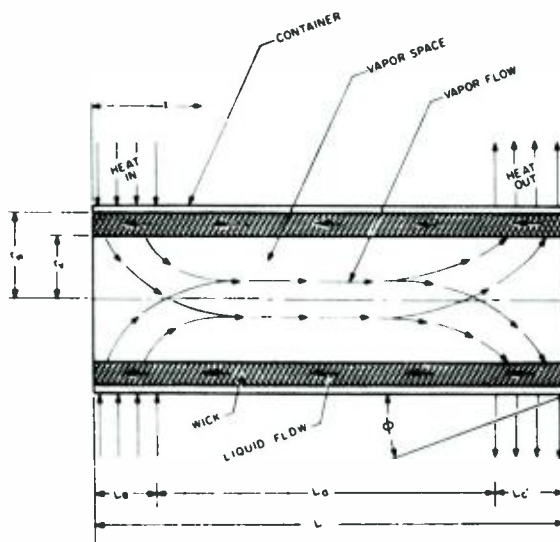


Fig. 1—Heat pipe geometry.

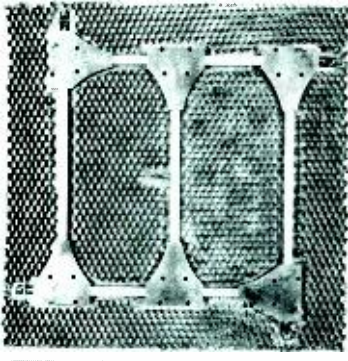


Fig. 3—A 1.5-lb integrated heat pipe honeycomb package for spacecraft heat transfer applications.

shows the capacity vs. size of water heat pipes in this size range operating horizontally.

The typical heat-transfer mode through a heat pipe consists of radial conduction through the capillary structure in both the evaporator and condenser combined with surface evaporation and condensation. Since evaporation and condensation occur with very low thermal resistances, the thermal conductance of a heat pipe is governed by the capillary thermal resistance and can be closely approximated by the following equation:

$$K_{HP} = \pi k / \ln(r_w/r_v) \quad (2)$$

where K_{HP} is heat pipe conductance; and k is capillary-material thermal conductivity.

The tradeoff implied by the relationship of fluid flow and thermal conductance is that a thick, porous capillary that offers minimum resistance to fluid flow also imposes maximum resistance to heat flow. The choices that can be made are shown in Table I.

Table I—Capillary materials and structures.

Capillary type	Relative capacity	Relative temperature gradient	Relative lift capability
Screen	High	High	Moderate
Felt	High	High	High
Sintered powder	Moderate	Low	High
Channel	High	Low	Poor

No single type of capillary structure satisfies all applications. The channel type is restricted to use in a gravity-free environment. The sintered powder type is of prime advantage when made of copper and used with water working fluid.

Heat-pipe applications

Advanced Technology Laboratories has recently built and tested a 1.5-lb integrated heat-pipe-and-honeycomb package for spacecraft heat-transfer applications. The radiator, shown disassembled in Fig. 3, measures $12 \times 12 \times \frac{3}{8}$ in. and contains a network of five discrete ammonia heat pipes integrated with aluminum honeycomb material for high strength and light weight.

The unit was tested in a vacuum with an input heat flux of 13 W/in.^2 , or a total of 52 W on the heat-input side. On the heat-rejection side, the total temperature gradient from the hottest to the coolest point under these conditions was measured to be 12°C , with the average surface temperature at 58°C . To achieve the same results, a solid aluminum radiator of the same area would have to weigh 12 times as much as the heat pipe radiator, or 18 pounds. Although testing was done using single-sided heat rejection, the unit could also be used as a double-sided radiator or as an isothermal equipment mounting platform.

An integrated heat-pipe-and-heat-exchanger package featuring 0.090 -in.-OD ammonia heat pipes was built to answer the growing thermal problem in microelectronics circuits. The heat pipe terminal board, shown in Fig. 4, employs three discrete ammonia heat pipes to remove heat from a 2×1 -in. mounting surface. The unit was tested at heat loads of 100 W total or over 55 W/in.^2 input heat flux with forced air convection over the heat-exchanger fins. Four 1×1 -in. ceramic hybrid resistor circuits served as the thermal load. Test results at 100 W showed the maximum temperature gradient on the surface of the resistor circuits to be 6°C .

ATL has also applied heat pipe techniques to the problem of heat removal from a single high-energy-density source, such as a solid-state microwave diode. As shown in Fig. 5,

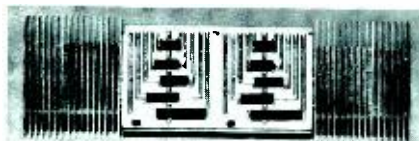


Fig. 4—Heat-pipe terminal board for microelectronic circuit mounting.

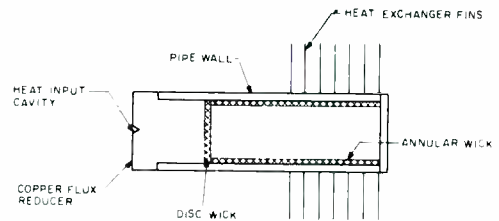


Fig. 5—Diode heat-pipe configuration.

the "diode" heat pipe employs an intermediate copper plug between the heat-pipe evaporator and the heat source. The copper plug serves to reduce the input heat flux from 6200 W/in.^2 at the input cavity to 20 W/in.^2 at the heat pipe evaporator (disc wick). During tests, a laser beam was used to thermally duplicate the heat flux from a solid-state microwave source. Temperature gradients within the copper plug were measured to be over 40°C ; in the heat pipe with forced air cooling, the gradient was 3°C .

Since solid-state devices with much higher heat fluxes are being developed, the use of a better thermal conductor than copper is needed for these applications. The use of type II-A industrial diamond has been studied, since diamond has a thermal conductivity five times that of copper at room temperature. Techniques for bonding diamond to several metals are currently being investigated by RCA Laboratories.

Phase-change techniques

Many applications of electronics equipment call for cyclic operation. A laser designator might operate for five minutes and then be inactive for 20 minutes. Night vision equipment would operate during 8 to 12 hours of night and then be inactive during daylight hours. An aircraft system might have to survive a supersonic dash condition in which the heat sink temperature would exceed acceptable levels for a minute or so. Or finally, a spacecraft system might operate for part of an orbit and then be inactive for the remainder of the orbit. In cases where the weight, size, or power consumption of the heat sink required to satisfy the peak heat-transfer requirements of these systems is prohibitive, the use of a phase-change material is an attractive alternative, as this technique allows for temporal integration of the thermal load.

There are several physical effects that

Table II—Salt hydrates.⁵

Salt hydrate	Melting point (°C)	Latent heat of fusion per unit mass (cal/gm)	Density (gm/cm ³)
Calcium Chloride Hexahydrate (CaCl ₂ ·6H ₂ O)	29.4	40.7	—
Lithium Nitrate Trihydrate (LiNO ₃ ·3H ₂ O)	29.88	70.7	1.55
Sodium Hydrogen Phosphate Dodecahydrate (NaHPO ₄ ·12H ₂ O)	36	66.8	1.52
Ferric Nitrate Enneahydrate (Fe(NO ₃) ₃ ·9H ₂ O)	47.2	—	1.684
Magnesium Sulfate Heptahydrate (MgSO ₄ ·7H ₂ O)	48.4	48.2	—
Sodium Thiosulfate Pentahydrate (Na ₂ S ₂ O ₃ ·5H ₂ O)	49	47.9	1.69
Lithium Acetate Dihydrate (LiC ₂ H ₃ O ₂ ·2H ₂ O)	58	60-90	—
Sodium Hydroxide Monohydrate (NaOH·H ₂ O)	64.3	65	1.72
Barium Hydroxide Octahydrate (Ba(OH) ₂ ·8H ₂ O)	78	72	2.18
Aluminum Potassium Sulfate Dodecahydrate (AlK(SO ₄) ₂ ·12H ₂ O)	91	44	—

Table III—Paraffins.³

Paraffins	Melting point (°C)	Latent heat of fusion per unit mass (cal/gm)	Density (gm/cm ³)
n-Dodecane (C ₁₂ H ₂₆)	-12	—	0.750
n-Tridecane (C ₁₃ H ₂₈)	-6	—	0.756
n-Tetradecane (C ₁₄ H ₃₀)	5.5	54	0.771
n-Pentadecane (C ₁₅ H ₃₂)	10	59	0.768
n-Hexadecane (C ₁₆ H ₃₄)	16.7	56.6	0.774
n-Heptadecane (C ₁₇ H ₃₆)	21.7	41	0.778
n-Octadecane (C ₁₈ H ₃₈)	28.0	58	0.774
n-Nonadecane (C ₁₉ H ₄₀)	32.0	—	—
n-Eicosane (C ₂₀ H ₄₂)	36.7	59	0.778
n-Heneicosane (C ₂₁ H ₄₄)	40.2	48	0.758
n-Docosane (C ₂₂ H ₄₆)	44.0	60	0.763
n-Tricosane (C ₂₃ H ₄₈)	47.5	56	0.764
n-Pentacosane (C ₂₅ H ₅₂)	49.4	—	0.769
n-Tetracosane (C ₂₄ H ₅₀)	50.6	59.5	0.766
Paraffin wax	54.4	35	0.88
n-Hexacosane (C ₂₆ H ₅₄)	56.3	61	0.770
n-Heptacosane (C ₂₇ H ₅₆)	58.8	56.1	0.773
n-Octacosane (C ₂₈ H ₅₈)	61.6	61	0.779
n-Nonacosane (C ₂₉ H ₆₀)	63.4	57	—
n-Triacontane (C ₃₀ H ₆₂)	65.4	60	—
n-Hentriacontane (C ₃₁ H ₆₄)	—	57.8	—
n-Dotriacontane (C ₃₂ H ₆₆)	70	40.7	0.782
n-Tritriacontane (C ₃₃ H ₆₈)	71.0	—	—
n-Tetraatriacontane (C ₃₄ H ₇₀)	72.9	64	—
n-Hexatriacontane (C ₃₆ H ₇₄)	76.1	56.2	—

can be utilized for heat absorption or heat rejection. In terms of application to the problem of cooling in electronics equipment, the use of heat of transition, heat of fusion, or heat of hydration appear to be the most useful effects. There are several salts which undergo hydration at useful temperatures for equipment thermal control. These are summarized in Table II. There are problems of reversibility and package compatibility with these materials which have prohibited broad application, although several proprietary systems are available which appear to use these materials.

Many materials can be made useful for electronic thermal control by exploiting the thermal capacities of their heats of fusion. We have used several members of a family of paraffin waxes; they were chosen for their large heat absorbing capacity and chemical inertness. Some of these materials are listed in Table III. Experimental work with eicosane, docosane, and tetracosane has shown that the published value of heat of fusion can only be achieved with thoroughly refined material. A case in point is paraffin wax listed with a melting point of 54.4°C. This wax is a mixture of several hydrocarbons and other impurities; its heat of fusion is 40% less than other similar members of the family. Similar comparisons can be made between commercial and refined grades of eicosane. To achieve reproducible, high performance results, we have used synthesized, highly refined samples of the materials shown in Table III. However, use of this type of material imposes several constraints on material selection. The materials with an odd number of carbon atoms are very expensive to produce and should not

be used. In addition, since the long chain materials (greater than 20 carbon atoms) are made by combining short chain materials chemically, even number molecules which are odd number multiples of two should be avoided from these same cost considerations. As an example, C₂₆H₅₄ can be bought for \$30/pound, while C₃₄H₇₀ costs \$545/pound.

The third type of phase change considered is a solid-solid transition between crystal structures. This change occurs at temperatures very close to the melting point for the paraffins and is generally lumped into the reported heat of fusion. In general, solid-solid transitions alone are not effective as a heat-absorbing medium.

The second factor beyond material selection bearing on performance is the packaging container. Since the material has low thermal conductivity, large temperature gradients can develop as the hydrocarbon melts. Several techniques to increase conductance into a complete package are feasible. One technique requires the use of metal powder mixed with the hydrocarbon. Another requires the use of a honeycomb structure. A brazed-aluminum plate fin structure, such as that shown in Fig. 6, provides a high-strength lightweight container for the hydrocarbon material and provides effective thermal paths to all parts of the material.

Extensive testing of a system that uses docosane in a plate fin container has shown that the full thermal capacity of such a system can be realized with a maximum temperature gradient of less than 7°F from the electronic chassis to melting thermal material.

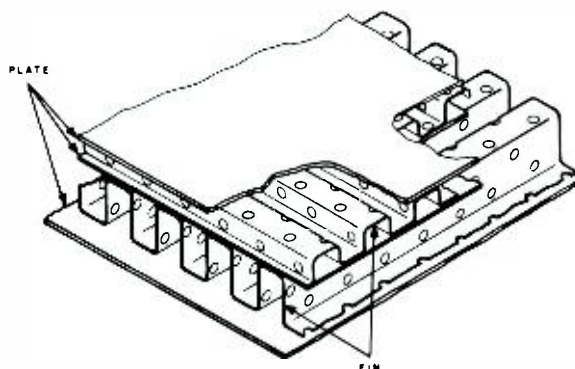


Fig. 6—Brazed-aluminum plate-fin container structure, sectional view.

Phase change applications

Phase-change packages have been used to provide thermal control in two RCA spacecraft systems: the lunar communication relay unit (LCRU) and coherent synthetic aperture radar (CSAR). In both cases, it was impossible to provide enough radiator heat sink area to reject the equipment maximum power dissipation. Since the operating mode for the equipment was 7 hours *on*/15 hours *off* for the LCRU, and 4 hours *on*/4 hours *off* for the CSAR, thermal storage in a phase-change package was selected to supplement the equipment thermal radiator.

A photograph of one of the phase-change packages used, sectioned to show internal construction, is shown in Fig. 7. The container is a very light-weight brazed aluminum structure which is extremely efficient thermally and has excellent structural properties. Table IV shows the weight breakdown between containers and phase-change material for the three units used in the LCRU. Most of the container weight is in the outside mounting surfaces of the packages which must be very flat for good heat transfer; packages with a deep aspect ratio could have been more weight effective. Even with the thin configuration dictated by envelope restrictions, the containers are one-third of the total weight.

The structural aspects of the design of interest result from the maximum local pressure the design must withstand. Pure hydrocarbon waxes melt over a very narrow temperature range with a large volume expansion (15%). Local hot spots in a container could build up very high pressure if they occurred where there was no space for expansion. A cellular honeycomb structure would be one approach to assure that each element of phase-change material has expansion space in close proximity. A better solution is to perforate the fin

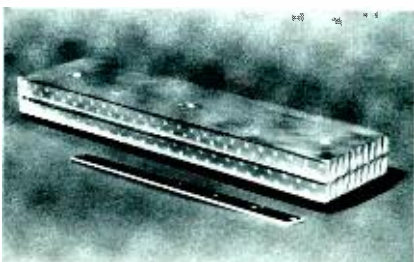


Fig. 7—Internal construction of phase-change package.

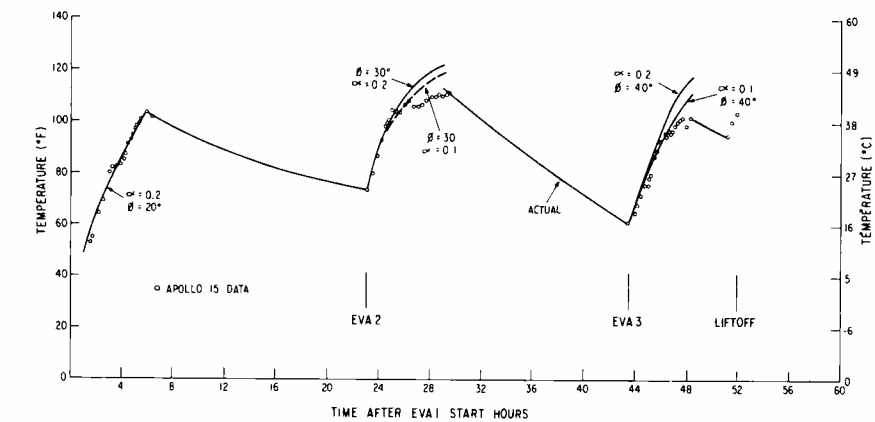


Fig. 8—LCRU temperature prediction and Apollo 15 verification (α =radiator absorptivity, ϕ =sun angle)

structure as shown in Fig. 7 to permit transverse flow, and add 10% by weight of a low-melting-temperature material which makes the material a viscous slurry at temperatures around its melting point. The second factor affecting the structural capability of the container is the ullage (unfilled volume) allowed in the filling procedure. The total expansion that might be experienced over the range of states possible with the phase-change material is 18 to 20%. Thus one would expect the container to be $(1.0/1.2)=83\%$ full with solid material. If the 17% ullage leaked air during storage, liquification of the phase-change material would compress the air to unacceptable pressure levels. Additional ullage must be provided or the container must be leakproof. The design shown in Fig. 7 was limited to a maximum pressure of two atmospheres; this would require 17% of additional ullage. This was an unacceptable volume penalty, so the containers were designed for hermeticity with a forecast pressure buildup of less than 0.1 atmosphere in three years.

The experimental verification of this design was excellent. In extensive thermal-vacuum qualification testing, the packages performed uniformly well after repeated temperature cycles and high and low temperature shocks. Under worst-case test conditions, a maximum gradient of 7°C to the melting wax was experienced. In the mission of Apollo 15, even better performance was observed. Fig. 8 shows LCRU temperatures during the mission. A substantial margin remained in the design even though the Apollo 15 traverse appeared to be hot biased in terms of lunar-dust effects and equipment solar loadings.

The CSAR is a high powered radar which will be used in lunar sounding experiments from the command module during the lunar orbit of Apollo 17. This equipment experiences a sequence of thermal conditions which makes it a classic example of a system benefiting from phase-change thermal control. The equipment is located in the Scientific Instrument Module bay. The protective door for this bay is jettisoned before lunar orbit insertion so that the equipment must survive a hot soak (looking directly into the sun) or a cold soak (view to space). It must also survive two Reaction Control Systems rocket burns which cause a surface heat input of 3 to 7 Btu/s. The equipment must then operate for two orbits at high internal dissipation (120 W) and varying environmental input. After 2 to 4 orbits of non-operating, the equipment will be reactivated. During this entire period, the equipment must be maintained at relatively constant temperature to preserve the stability required by the experiment.

The design of the components required to achieve these goals is very similar to that described for the LCRU. The material used is a tetracosane (melting point 123°F) and it is packaged in a $10 \times 18 \times 1.6$ in. brazed aluminum container.

High pressure gas convection

The thermal problem in crystalline lasers such as ruby and *Nd:YAG* is primarily one of uniformly cooling the laser rod to minimize axial and circumferential temperature gradients while maintaining a safe operating temperature level. Two heat-transfer tech-

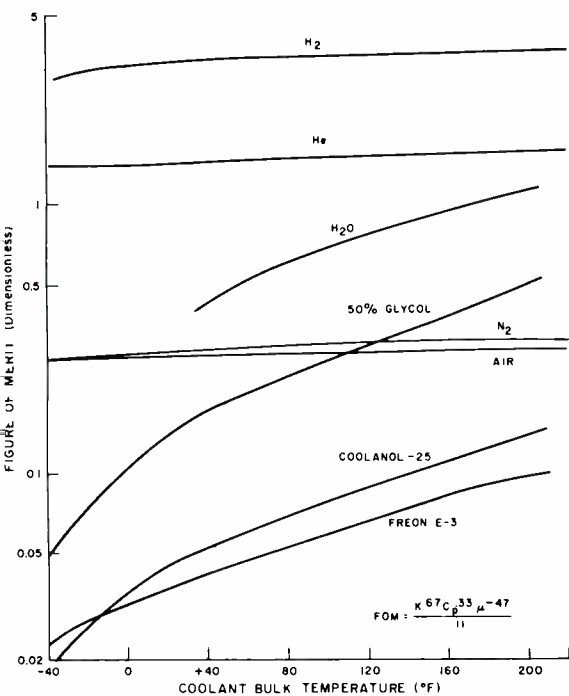


Fig. 9—Coolant figure of merit (for gaseous and liquid coolants) as a function of temperature.

niques that have been widely applied to ruby and *Nd:YAG* lasers are conduction cooling and forced liquid convection. Conduction cooling requires direct contact between part of the surface of the rod and a metallic conductor such as aluminum, with either a brazed or clamped interface. This technique results in minimum axial temperature gradients, but it introduces circumferential temperature gradients and mechanical stresses in the rod which adversely affect optical performance. Forced liquid cooling of the rod results in satisfactory heat transfer while eliminating the mechanical stresses due to clamping; however, the use of a circulating liquid poses serious problems of fluid contamination, nucleate boiling within the optical path, and a lengthy lamp-changing operation requiring fluid evacuation, cleansing, and careful refilling. The use of high pressure gas convection eliminates the majority of these problems and offers several advantages in the areas of maintainability and reliability.

With the use of high pressure gas, the lamp replacement operation can be completed in minutes. The pressurized gas is bled from the system, the laser head cover plate is removed, the lamp is replaced, and the coverplate reinstalled. Any moisture which may have accumulated in the laser head while it was operated is easily removed by

flushing the system with dry nitrogen. The operation is completed by adjusting the internal gas pressure to the desired value and removing the nitrogen supply. The volume of the entire loop is typically 50 in.³. The replacement of a flash lamp, therefore, requires a total system downtime of five minutes, compared to several hours required for liquid-cooled systems.

A major problem that plagues liquid-cooled systems is contamination of the coolant due to a reaction with the containing materials or with the ultraviolet light given off by the flash lamp. These effects result in either a decrease in the fluid transmissivity, a decrease in the wall reflectance, or both. The use of nitrogen gas as a coolant eliminates these problems, since it is relatively inert and is not affected by ultra-violet illumination. In addition, because the coolant is a gas, it is not subject to the localized boiling which impairs the optical coupling in liquid cooled systems.

Liquid-cooled systems are subject to sharp degradations in heat transfer characteristics with decreasing temperature; they are ultimately limited by the freezing-point of the liquid coolant. A comparison of the heat-transfer properties of several gaseous and liquid coolants over the temperature range -40°F to 200°F is shown in Fig. 9. The figure of merit is a dimensionless quantity related to the heat-transfer coefficient for turbulent flow in an annulus, with water at 180°F equivalent to unity. From Fig. 9, it is seen that the candidate gases—helium, hydrogen, nitrogen, air—exhibit constant figures of merit

over the entire temperature range. A 50% water-glycol mixture, which is a common liquid-laser coolant, undergoes a 10:1 reduction in its figure of merit as the temperature is reduced from 200°F to -40°F. This indicates the impossibility of designing a liquid cooled system to operate with constant heat-transfer performance for constant mass flow rate. If the design is based on maintaining a given rod temperature for fluid temperatures in the 160° to 200°F range and the fluid temperature is decreased to -40°, the rod temperature will increase to well above its maximum operating temperature, to about 220°F. On the other hand, if the design is based on achieving proper heat transfer at liquid temperatures of -40°F, then the thermal system will become grossly inefficient at higher liquid temperatures.

Fig. 9 shows that the heat-transfer characteristics of helium and hydrogen are clearly superior to any of the other candidate fluids over the entire temperature range. However, the flammability of hydrogen and the tendency of helium to diffuse into flash lamps preclude their use as laser coolants.

The two important performance parameters in gas cooling are the heat-transfer rate and fluid-flow characteristics. For a given fluid, such as nitrogen, the heat transfer coefficient (*h*) is directly proportional to the gas density and inversely proportional to the annular spacing between the laser rod and cavity wall. [A typical gas flow pattern for a crystalline laser is shown in Fig. 10.] Increasing the gas pressure

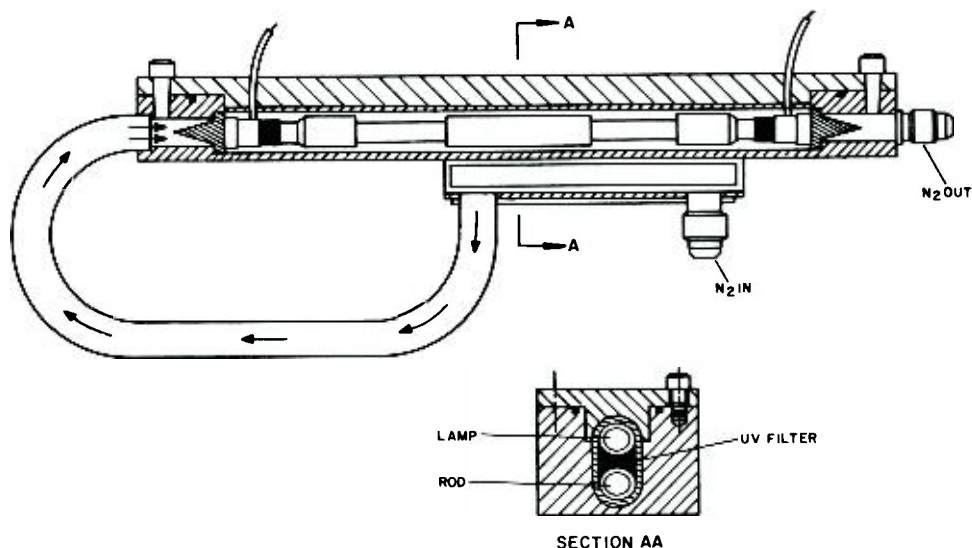


Fig. 10—Gas flow path for *Nd* designator.

Table IV—Container and phase change material weight

Container	Container weight (g)	Phase change material weight (g)	Total weight (g)
Top	802	1543	2345
Internal	136	231	367
External	412	844	1256
	1350	2618	3968

increases its density and results in an increased heat-transfer coefficient for a constant expenditure of fan power. Decreasing the annular rod-to-wall spacing likewise linearly increases h but also increases the flow impedance of the gas. For a constant mass flow rate (M), the gas-flow pressure drop is inversely proportional to density, and the fan-power consumption is inversely proportional to the square of the density; these relationships are summarized in Fig. 11.

The advantages of increasing gas pressures are obvious from the relationships shown in Fig. 11. The disadvantage of increasing pressure is that the weight of the structures which contain the gas must also increase. An optimum thermal design using high pressure gas can only be achieved by trading off the effects of coolant, temperature, pressure, annular spacing, flow-tube area, and mass-flow rate to determine the combination of parameters, which result in the maximum heat transfer performance for a minimum expenditure of coolant-fan or pump power while satisfying constraints of size and weight. A computer program, Laser 1, has been developed by ATL to perform the indicated tradeoffs and facilitate the design of gas-cooled system for a majority of applications.

Gas convection applications

Although the technique of high-pressure gas cooling can be applied to a variety of electronic cooling applications, it is particularly well suited to laser cooling. ATL has built and successfully demonstrated a gas cooled $ND^{3+}:YAG$ laser designator. This designator was operated at repetition rates up to 20 pps and laser output levels of 175 millijoules/pulse. Maximum efficiencies of 1.3%, long pulse,

and 1.1%, Q -switched, have been achieved. The rod is pumped by a 4-mm-bore krypton flash lamp which has an established life of 10^6 shots. Q -switching was achieved with a $LiNbO_3$ crystal. Both laser rod and flash lamp were cooled by forced convection of pressurized nitrogen gas.

Inlet N_2 gas is introduced first to the rod where the gas flows axially down an annular space in the turbulent flow regime. The annular flow path is formed on one side of the rod by the reflective cavity walls and on the lamp side by a curved, ultraviolet filter. After flowing down the rod, the gas is introduced to one end of the krypton flash lamp and flows in similar fashion, axially down the lamp in an annulus in the turbulent flow regime.

At repetition rates of 12 pps and an energy level of 100 millijoules/pulse, the average laser-rod temperature is maintained at 143°F with an inlet nitrogen temperature of 90°F and a nitrogen mass flow rate of 0.7 lbm/min and pressure of 400 lbf/in.² At these conditions, a heat-transfer coefficient of 117 Btu/hr-ft²-°F is achieved at a Reynold's number of 37,100.

Internal circulation of the pressurized gas is achieved by a centrifugal blower capable of moving 0.6 ft³/min at a head of 15-in. H_2O and a pressure of 400 lbf/in.² The external air blower operates at 45 ft³/min against 2-in. head at atmospheric pressure. Heat transfer from the nitrogen gas to the external air is accomplished by an aluminum plate-fin heat exchanger tested at a maximum pressure of 700 lbf/in.².

In laboratory tests of the thermal subsystem, two cylinders of the same geometry as the rod and lamp served as heat sources and permitted initial thermal-evaluation testing. During these tests, helium at 0.7 lbm/min was used as the cooling medium and rod-to-gas temperature gradients were reduced by a factor of 3.5 to 1 when compared to nitrogen at the same mass flow rate.

This Nd-designator system has been operational for nine months and has only required lamp replacement after about 10^6 shots. No problems have been encountered with the internal blower, external blower, or the gas-to-air heat exchanger.

CONSTANT MASS FLOW RATE (\dot{m})

$$\Delta P = k/\rho = \text{PRESSURE DROP}$$

$$P_c = k/\rho^2 = \text{FAN POWER CONSUMPTION}$$

CONSTANT FAN POWER CONSUMPTION (P_c)

$$\dot{m} = k\rho^{2/3}$$

$$h = k\rho^{1/2}$$

WHERE k = PROPORTIONALITY CONSTANT

$$\Delta P = \text{SYSTEM PRESSURE DROP}$$

$$\rho = \text{GAS DENSITY}$$

Fig. 11—System tradeoffs.

For applications such as this, when the laser system must operate continuously for long periods of time, the system heat load must be rejected on a continuous basis.

Many field applications, however, require the system to operate in a cycled mode. For duty cycles of 25% and less, high-pressure gas convection and phase-change-material thermal integration can be integrated to form an effective heat transfer system; both the external air blower and the gas-to-air heat exchanger can be replaced by a finned, phase-change container. Elimination of the external blower results in several benefits, including reduced power consumption, increased reliability, and greatly reduced noise.

Conclusion

The electronics industry is now building systems in which the thermal management requirement is changing from one involving the rejection of large power levels to one in which lower power levels are being dissipated into more localized areas. The laser and semiconductor power sources are examples of components which require new solutions to thermal problems. The techniques described in this paper are in advanced development stages and can be considered for use in equipment design. Work to extend the temperature and power capability of the systems described is continuing; further improvement can be expected in the near future.

References

1. Adams, M. C. William, H., *Heat Transmission* (McGraw Hill Book Co.; New York City; 1954).
2. Eckert, E. R. G., *Introduction to the Transfer of Heat and Mass* (McGraw Hill Book Co.; New York City; 1950).
3. Jacob, M., *Heat Transfer* (John Wiley & Sons; New York City; 1949).
4. Harbaugh, W., *Private Communication*, RCA Lancaster, Pa.
5. Hale, D. V., Hoover, M. J. and O'Neill, M. J., *Phase Change Materials Handbook*, NASA Report CR-61363, NASA Marshall Space Flight Center, Sept. 1971.

Refrigeration systems for spacecraft

P. E. Wright

Cryogenic temperatures are often required in meteorological and communication spacecraft for proper performance of IR radiometers, lasers, and microwave communicators. Based on current projections, cryogenic cooling requirements for spacecraft could reach 7.0 W by 1975. Failure to provide refrigeration systems with high capacity and long life is limiting progress in radiometer and low-noise communications systems. Cryogenic cooling systems appropriate for spacecraft are of three types—two represent developed technology and have been used on space missions: passive coolers and phase-change coolers. However, passive coolers are severely limited in capacity, and phase-change coolers are limited in both capacity and life; neither is adequate for future requirements. The third type—the closed-cycle refrigerator (particularly the Vuilleumier refrigerator)—is still in its development stage, but offers the potential of higher capacity and longer life than the other two types.

METEOROLOGICAL AND COMMUNICATION SPACECRAFT are often required to include a refrigeration capability at cryogenic temperatures (typically 50 to 100°K). Low temperatures are necessary for proper performance of certain components in the IR scanning radiometers, the laser systems, and the microwave communication systems. Cryogenic cooling systems that are appropriate for spacecraft use fall into three general categories.

The first category is the passive cooler; it requires no driving energy. It is a thermal radiator which is shielded from all incoming thermal sources and is physically pointed to deep space. As a result, thermal equilibrium is achieved at a low temperature. Passive coolers with a 100-mW refrigeration capacity at 80°K have been used in spacecraft systems.

Reprint RE-18-2-20
Final manuscript received June 27, 1972.

On the bench in front of author Paul Wright is a thermally actuated Vuilleumier refrigerator.

Paul E. Wright, Director
Advanced Technology Laboratories
Government and Commercial Systems
Camden, N.J.

received the BSME from California Polytechnic State University and the MSME from the University of Pennsylvania. He served in the U.S. Air Force from 1950 to 1954, and was an engineer with the State of California from 1954 to 1958. He joined RCA in 1958. Prior to assuming his present position, Mr. Wright was Manager of the Applied Physics and Mechanics Laboratory at ATL. As Director, Mr. Wright is responsible for over 100 engineers and physicists charged with translating the recent advances of basic research into useful techniques and devices. Typical areas of effort are electro-optics, optics, lasers, millimeterwaves, microwave physics, holography, sensors, microsonics, thermodynamics, pattern recognition, recording techniques, LSI hybrid techniques, and computer technology. Mr. Wright is a Registered Professional Engineer in New Jersey. He is a member of the National Society of Professional Engineers, the New Jersey Society of Professional Engineers, the ASME and the IEEE.



The second category is the phase-change cooler. Several subtypes exist within this category. All, however, are based on the pressure dependency of the temperature of a solid (or liquid) in equilibrium with its vapor. In general, an "ice cube" of a substance (such as methane, argon, or nitrogen) sublimates as it absorbs thermal energy from the component being cooled. These are open-cycle systems, and lifetimes of 6 to 12 months are typical. Phase-change coolers with a 100-mW refrigeration capacity at 80°K have also been used in spacecraft.

The third category is the closed-cycle refrigerator. Substantial investment was made in the 1960's toward the development of these machines for space use because it was realized that the technology of the passive and phase-change coolers could not support the capacity and life requirements of future spacecraft missions. The Reversed-Brayton cycle and the Stirling cycle received most of the attention, but both have severe limitations for space use. About 1965, attention began to focus on the Vuilleumier cycle as the thermodynamic basis for cryogenic refrigerators for use in the space environment. Progress has been encouraging, but flight test has not yet occurred. This type of refrigeration should play an important role in the space programs of the 1970's.

Passive coolers

The high vacuum and the low effective temperature ($\approx 4^\circ\text{K}$) of space provide an environment in which passive radiation can be used to cool spacecraft components to cryogenic temperatures. This type of cooler has the advantages of (1) long life because of no moving parts and no stored coolants, and (2) no requirement for electrical power.

To achieve cryogenic temperatures by means of thermal radiation alone, a radiator must have a high radiation coupling to the 4°K equivalent space heat sink and extremely small couplings, radiative or conductive, to any heat source. There is no surface on the spacecraft that views only cold space. Since the total heat rejection capability by radiation of a black-body surface at 77°K is only 1.29 mW/in^2 , the total amount of heat absorption by the surface from all sources must not exceed this flux value if the 77°K temperature

is to be maintained.

Heat sources

The primary difficulty in achieving a passive cryogenic cooler design is that of achieving maximum thermal isolation of the radiator from sources of heat. Potential radiator input heat sources can be grouped into three general categories:

1) Direct radiant heat flux

- Direct solar energy
- Earth-reflected solar energy (earth albedo)
- Earth-emitted thermal energy (earth IR)
- Moon-reflected solar energy (lunar albedo)
- Moon-emitted thermal energy (lunar IR)
- Spacecraft assembly emitted thermal energy (spacecraft IR)

2) Indirect radiant heat flux

- Direct radiant heat flux reflected to the radiator by the spacecraft assembly
- Direct radiant heat flux reflected to the radiator by the cooler assembly surfaces
- Radiator emitted or reflected heat flux energy reflected back to the radiator by cooler or spacecraft assembly surfaces

3) Conduct and generated heat flux

- Heat flux conducted to the radiator through thermal conduction paths
- Heat flux generated on the radiator surface by electrical resistance losses

This list of potential heat sources highlights the difficulty of limiting the total radiator heat input to less than 1.29 mW/in^2 , especially since the direct solar flux alone has a value of 900 mW/in^2 .

Radiator thermal isolation

The following are the principal techniques for achieving cryogenic radiator thermal isolation:

- 1) Use of shield surfaces to block the radiator field of view from direct or indirect heat sources
- 2) Location of the radiator on the spacecraft to minimize heat input
- 3) Proper selection of system surface finish values (solar absorptance and thermal emittance) and location geometry to maximize heat rejection to space while minimizing thermal reflection and emission inputs to the radiator.
- 4) Achieving high-thermal-resistance radiator mountings
- 5) Providing low-thermal-conductance detector electrical leads
- 6) Limiting the amount of detector heat dissipation

Influence of spacecraft orbit

No single passive cooler design can satisfy all orbital missions; in general,

a different cooler configuration is required for each mission. For instance, consider the following three cases:¹

Case A: Earth-oriented, 200 n. mi., circular orbit in the plane of the ecliptic

Case B: Spin-stabilized, 600 n. mi., sun-synchronous circular orbit with an orbit plane/sun line angle of 45°

Case C: Synchronous, earth-oriented equatorial orbit

Each of these orbital conditions imposes severe design problems for a passive cooler. The case-A orbit has a large earth-view angle which requires relatively large earth shielding to prevent high earth albedo and thermal flux from reaching the detector radiator. In addition, the in-plane sun must be shielded from the detector radiator and probably from the earth shield.

The difficulty in the case-B orbit is due to the spin-stabilization requirement. The earth view and corresponding earth heat flux magnitudes are less than in case A, and the sun is not in the cooler field of view. The spinning condition may require an earth flux shield completely around the detector radiator (such as a conical shield). The increased area of shielding reduces the detector view to space and increases the shield-to-radiator input.

The case-C orbit requires virtually no earth flux shielding, since the view angle is small and the flux magnitudes are low. However, a synchronous equatorial orbit results in the sun rising above and falling below the orbital plane. Therefore, the design problem becomes principally one of providing sun shielding for the detector radiator.

It is clear that a different cooler configuration would be required for each case.

Representative design

An RCA cooler¹ was designed to maintain an IR detector at 80°K with a detector heat dissipation of 5 mW for a TIROS M spacecraft operating at a minimum altitude of 600 n. mi. TIROS M is an earth-oriented, sun-synchronous vehicle which has an angle between the sun and the cooler-mounting-plane normal that is greater than 90° . An engineering test model of the analytical design was built and evaluated in a space simulation chamber. Tests 1, 2 and 3 in Table I were performed with liquid nitrogen heat sinks and test 4 was performed with liquid helium. The test results indicate that actual cooler performance

Table I—Summary of test results on test model of RCA passive cooler.

Test	Shield Temperature (°K)	First stage temperature (°K)	Detector dissipation (mW)	Detector temperature (°K)		
				Measured	Relative to a space sink of 4°K	Relative to a space sink with 5-mW detector dissipation
1	81	167	5	105	81	81
2	81	163	0	94	70	80
3	80	163	5	99	80	80
4	35	163	0	80	71.5	81.5

achieved was within 1°K of the predicted design goal. The entire cooler assembly size was very small, requiring an envelope volume of 8×7×7 in. The approximate cooler assembly weight was 1 lb.

Fig. 1 shows the cooler that was tested. Fig. 2 is a cross-section view, showing the basic design configuration. The cooler consists of three basic components: the cold plate (detector radiator) the radiator/earth-shield assembly, and the thermal shield. The cooler is a two-stage device. The radiator/earth-shield assembly is the first stage and the cold plate is the second stage.

The radiator/earth-shield assembly consists of a radiator, covered with second-surface mirrors to minimize the effects of earth-reflected solar energy, and an earth shield which includes side shields. The cold plate is centered in the shadow of the earth shield. It is mounted to the radiator/earth-shield assembly by means of a spring-loaded, mechanically rugged diaphragm. Suspended between the cold plate and the radiator/earth-shield assembly is a radiation barrier, which is also diaphragm mounted. Two

small radiators are attached to the ends of the radiation barrier to achieve a minimum radiation-barrier temperature. The exposed surface of the cold-plate mounting diaphragm has a high-emissivity finish to dissipate the heat conducted by the diaphragm.

The radiator/earth-shield assembly is mounted inside a thermal shield by means of three fiberglass isolation mounts. All surfaces except the exposed surfaces of the radiator, cold plate, radiation shield radiators, and thermal shield are finished with vapor-deposited gold to minimize all internal radiation couplings. The visible surfaces of the earth shield are finished with vapor-deposited gold to minimize the thermal coupling between the earth shield and cold plate and also to specularly reflect all thermal radiation away from the cold plate.

Multilayer insulation blankets are attached to the inside of the thermal shield and to the radiator/earth-shield assembly, between the assembly and the radiation barrier, to improve the radiation isolation between components.

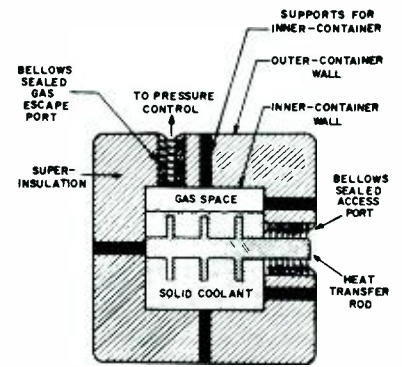


Fig. 3—Phase-change cooler.

Phase-change coolers

Phase-change coolers are generally open-cycle systems in which a substance originally in solid (or liquid) phase absorbs heat and changes to the vapor phase. The vapors of the substance are then vented to space. The major components and their physical arrangement are illustrated in Fig. 3.² Coolers of this type use "ice-cubes" of cryogenics such as methane, argon, or nitrogen. These "ice-cubes" are placed in a well-insulated container and the vapor which results from their sublimation is vented to space. Constant temperature can be maintained within the container by maintaining constant pressure in the vapor space above the cryogen. The pressure-temperature relationship for solid argon in equilibrium with its vapor is shown in Fig. 4. Note that the temperature will remain at 60°K as long as the pressure is held at 10 torr.

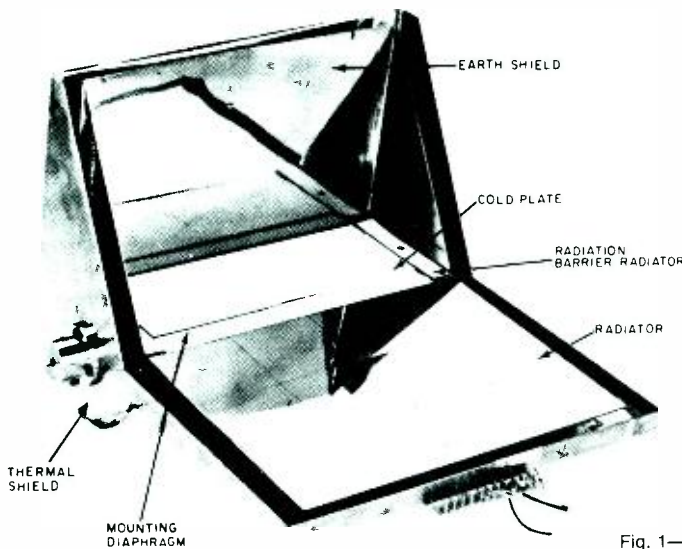


Fig. 1—RCA passive cooler.

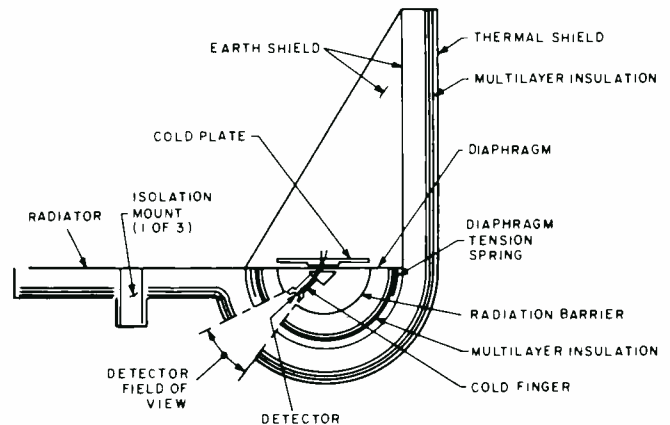


Fig. 2—Cross-section view of cooler.

Two-stage design

Many spacecraft requirements are for a minimum of 1-year life with a capacity of at least 100 mW. This can be achieved, within reasonable weight bounds, only by going to a two-stage design. A combination of cryogenics such as carbon dioxide (see Fig. 5) and argon can be used. The relative position of the components in a two-stage, phase-change-cooler design is illustrated in Fig. 6.

Superinsulation

Since phase-change coolers are generally open-cycle systems, the cryogenics are eventually "used up". Therefore the amount of cryogen required, and thus the cooler weight, depend directly on the length of the mission. Weight is the major design consideration; since it may be excessive for long missions (2 or more years), every means must be taken to reduce the extraneous heat load and to limit heat leaks. Indeed, even for medium and short missions, special attention must be given to the insulation of the container of the cryogenics to limit the extraneous heat leak. Table II lists the properties of two cryogenics. Using the appropriate properties, one can calculate that for every 3 mW of heat load absorbed over a period of 1 year, 1 lb of argon is required. If, for instance, a detector system with a heat load of 100 mW is to be cooled for 1 year and if the extraneous leak through the package is 100 mW, the weight of the required amount of argon alone would be approximately 67 lb. It is clear that reduction of heat leaks is of critical importance in the design of these coolers. It is for this reason that the development of this cooling technique has essentially followed the development of superinsulations.³ Superinsulations are usually blankets of several sheets of thin aluminum foil which act as multiradiation shields with very little heat conduction between and through the sheets.

Table II—Properties of cryogenics.

Cryogen	Temp at P=1 torr	Latent heat of sublimation (cal/cm ³)	Density (g/cm ³)
Argon	55°K	82.6	1.71
Methane	67°K	73.8	0.52

Representative design

The state-of-the-art in phase-change

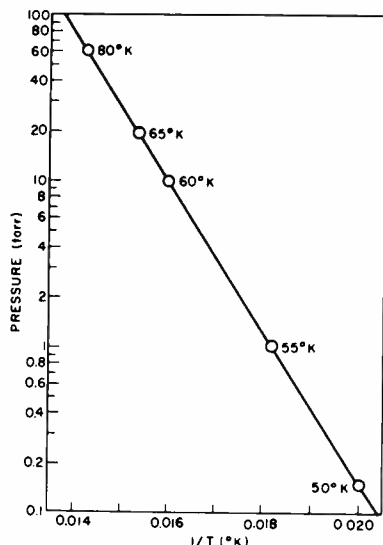


Fig. 4—Argon vapor pressure vs. temperature.

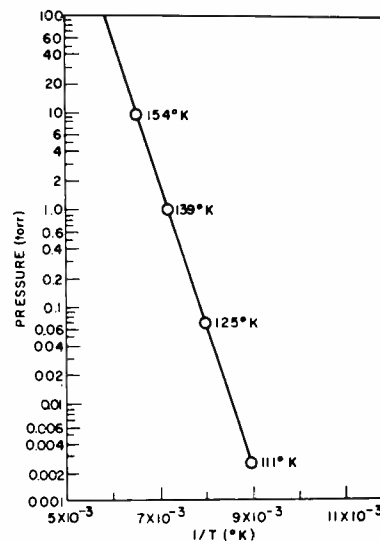


Fig. 5—Carbon dioxide pressure vs. temperature.

coolers is represented by a prototype spacecraft solid cryogen refrigerator

Table III—Measured characteristics of solid cryogen refrigerator.

Characteristic	Measured value
Detector operating temperature	52°K
Argon lifetime	1 year
Allowable detector heat load	17.6 mW
Carbon dioxide temperature	129°K
Carbon dioxide lifetime	1 year
Heat leak to argon	28.6 mW
Heat leak to carbon dioxide	74 mW
Refrigerator weight including cryogenics	34.1 lb

developed to provide cooling at a temperature of 50°K for an IR detector.⁴ The refrigerator is a two-stage system using carbon dioxide and argon as the cryogenics. It was sized to operate for 1 year with an outside skin temperature of 300°K. Table III shows the measured characteristics of the refrigerator.

Closed-cycle refrigerators

Future spacecraft missions will have an increasing requirement for cryogenic

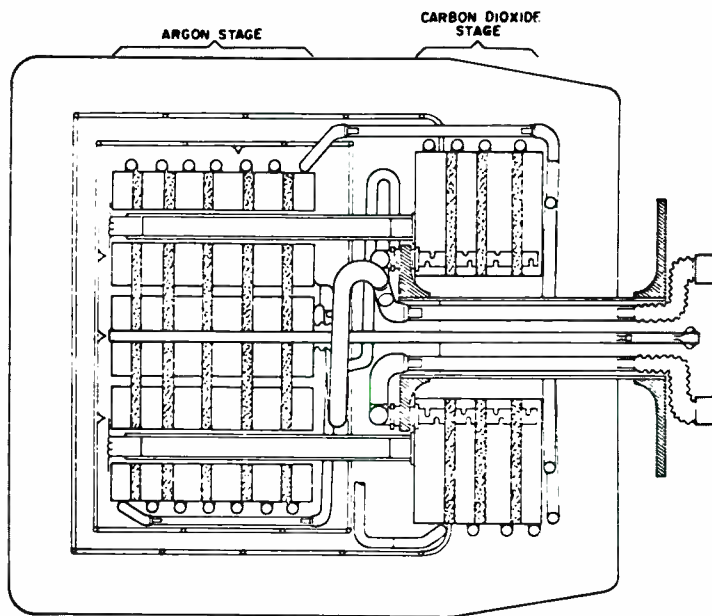


Fig. 6—Schematic of solid argon—solid carbon dioxide open-cycle refrigerator.

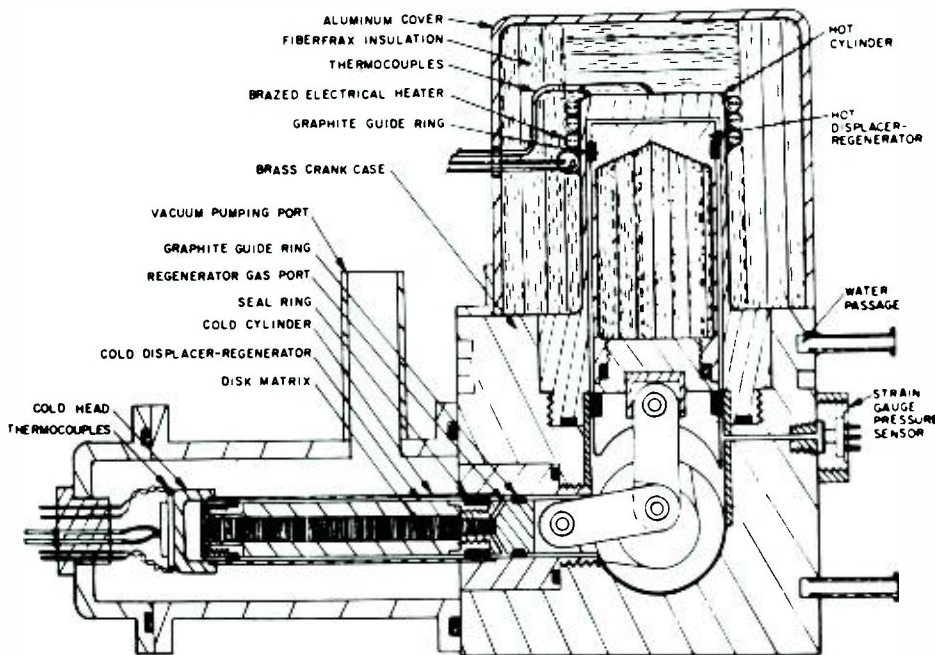


Fig. 7—RCA Vuilleumier refrigerator, cross-section.

refrigeration. Contributing to this requirement will be radiometric and communications systems. Infrared detector operation in radiometers requires temperatures in the range of 90° to 100°K, depending on detected wavelength. In interspacecraft communications, varactor diodes used in parametric amplifiers should be cooled to as low a temperature as possible (cooling reduces transmitter power requirements by reducing the signal needed for accurate information transmission); 70°K offers a good compromise between performance and system complexity.

The refrigeration capacity represented by an IR detector consists of 1) active power dissipated; 2) heat leaks through leads, mounting platform, cold finger and thermal link; and 3) extraneous radiant heat leak from the optical system. The capacity to meet these requirements will be in the range of 0.30 to 1.00 W, with 0.50 W a good design value.

The thermal capacity required by a cooled parametric amplifier is more difficult to specify accurately since its major component is the heat leak down the coaxial connections. The requirements on the coax for high electrical and thermal performance conflict, but a design which leads to a total thermal

load of 0.75 W appears to offer a good tradeoff.

The progress in radiometer and low noise communications systems is limited by the lack of high capacity, long-life refrigeration systems which are insensitive to orientation and orbit parameters. In addition, a projection of future spacecraft missions indicates that the cryogenic cooling requirements will be in the 3.0 to 5.5 W range, possibly reaching 7.0 W. It is clear that neither the passive cooler nor the phase-change cooler can meet these needs. It was for that reason that investigation of closed-cycle (mechanical) refrigerators for spacecraft use was begun in the early 1960's. The majority of this research has been sponsored by the Air Force. More recently, NASA has established a research and development program for a closed-cycle spacecraft refrigeration system.

Reversed-Brayton cycle

Several programs have been sponsored by the Air Force to develop refrigerators for space use which operate on the Reversed-Brayton cycle. There are two versions: the turbo-refrigerator and the rotary-stroking refrigerator. These development programs^{5 6} have met with only limited success, with long life capability (2 to 5 years) the most

elusive goal.

Stirling cycle

The Stirling cycle is the thermodynamic basis^{7, 8} widely used for refrigeration loads of 1 to 10 W at 75°K or lower for terrestrial applications. These machines have a rather short life (usually less than 2000 hours between maintenance periods). They also suffer from vibration of the cold head which adversely affects detector performance. These two characteristics severely limit the usefulness of Stirling refrigerators for space environments.

Vuilleumier cycle

Rudolph Vuilleumier patented (U.S. Patent 1,275,507) a unique heat-driven refrigerator in 1918. Similar concepts were later patented by Vannevar Bush in 1938 (U.S. Patent 2,127,286), and K. W. Taconis in 1951 (U.S. Patent 2,567,474). These patents all describe different physical apparatus to achieve refrigeration, but are all thermodynamically similar. Refrigeration is produced due to gas compression and expansion brought about by a high-temperature heat source and an ambient-temperature heat sink. The idealized cycle has perfect mechanisms, perfect heat transfer, and no gas friction, and thus operates without mechanical energy input. The history of Vuilleumier (VM) refrigeration is described in references 9 through 14. The implementation of the VM cycle can produce a refrigeration machine uniquely suited to the space environment. Since the pressure pulses are produced by the joint action of displacer-regenerators and heat transfer from a high temperature heat source, the need for a compressor driven by an electric motor is eliminated. Thus, the 100- to 1000-W demand on the spacecraft's electrical power system made by other types of mechanical refrigeration is replaced by a small radioisotope or a solar collector. In addition, long life is potentially available with the VM refrigerator because of the inherent slow speed and light bearing loading in these machines.

RCA VM refrigerator

RCA has built several experimental models of VM refrigerators. Fig. 7 is a cross-sectional view of an early model. All significant components of the VM cycle are identified. One of the latest refrigerators, which features complete

thermal actuation, is shown in the author's photograph. This machine achieves 1.6 watts refrigeration capacity at 77°K which is in close agreement with the performance predicted by RCA's computer model¹⁷ of the VM cycle. This agreement indicates that the thermodynamic characteristics of the VM cycle are well understood and that the design rules can be accurately implemented in hardware.

The state-of-the-art in VM refrigeration has not reached maturity with respect to life, however. To date, periods of operation without maintenance have been reported at less than 1000 hours from all investigators. Substantial work in this area remains to be done. In fact, it may be necessary to depart from the conventional mechanization of the displacer-regenerator motion to achieve the full potential of the VM cycle for long life. A refrigerator is now being designed which features a novel mechanical configuration. This should provide both low production cost and long life.

ICicle

An interesting concept for the deployment of a central refrigeration system in spacecraft has been studied by RCA under contract to the Goddard Space Flight Center at NASA. It is known as Integrated Cryogenic Isotope Cooling Engine System (ICICLE). An artist's concept of the system is shown in Fig. 8. A centrally located VM refrigerator is connected to the heat source, a small radioisotope, by a sodium heat pipe. The cold head of the refrigerator is connected to the cryogenic heat loads by nitrogen heat pipes. The connection between the refrigerator and the radiator heat sink is accomplished with a constant temperature ammonia heat pipe. The conclusion of the study was that the system is feasible for long life space missions (2 to 5 years) and can probably be implemented by 1975.^{15, 16}

Conclusions

Passive coolers offer the advantages of long life and no requirement for electrical power. The technology development has been completed, and they have been used in several space missions. They are limited, however, to small refrigeration loads ($\ll 1$ W) and must be "tailored" to the orbit—a process which is often difficult. The passive cooler will continue to be used

in limited applications where refrigeration load size and orbit allow.

Phase-change coolers offer reliability and freedom from orbital constraints. The technology development has been completed, and they also have been used in several space missions. They are restricted, however, to small refrigeration load (< 1 W) and short life (< 2 year) missions.

Closed-cycle coolers, particularly the VM refrigerators, will be used during the 1970's. ICICLE-type systems will be used on spacecraft with requirements for large refrigeration loads (> 1 W) and long mission times (> 2 years).

References

1. Private communications, R. Scott and R. Williams of AED, RCA Corporation.
2. Wolfe, W. L. (Editor), *Handbook of Military Infrared Technology* (Office of Naval Research; Dept. of Navy; Washington, D.C.; 1965).
3. Glaser, P. E., et al., "Multilayer Insulation," *Mechanical Engineering*, (Aug. 1965).
4. Caren, R. P., and Coston, R. M., *Design and Construction of an Engineering Model Solid Cryogen Refrigerator for Infrared Detector Cooling at 50°K*, NASA Contract NAS5-9549 (1968).

5. Wapato, P. G., *Design and Development of a Miniature Non-Reciprocating Closed Cycle Cryogenic Cooler*, Air Force Contract Report AFFDL-TR-67-9 (1967).
6. Fowle, A., et al., *Reciprocating Cooling Techniques for Space Based Infrared Sensors*, Air Force Contract Report AFFDL-TR-65-14.
7. Finkelstein, T., "Generalized Thermodynamic Analysis of Stirling Engines," SAE Annual Meeting (1960).
8. Du Pre, F., and Daniels, A., "Miniature Refrigerator Opens New Possibilities for Cryog-electronics," *Signal Magazine* (Sept. 1965).
9. Yendall, E. F., "A Novel Refrigerating Machine," *Advances in Cryogenic Engineering*, vol. 2, pp. 188-196 (1960).
10. Chellis, E. F., and Hogan, W. H., "A Liquid-Nitrogen-Operated Refrigerator for Temperatures Below 77°K," *Advances in Cryogenic Engineering*, vol. 9, (1964) pp. 545-551.
11. Private communications, R. White and W. J. Uhl, Jr., Air Force Dynamics Laboratory.
12. Turner, F. T., and Hogan, W. H., "Small Cryopump with Integral Refrigerator," *The Journal of Vacuum Science and Technology*, vol. 3, No. 5, pp. 525-527.
13. Magee, F. N., and Doering, R. D., "Vuilleumier Cycle Cryogenic Refrigerator Development," Air Force Technical Report AFFDL-TR-68-67 (Aug. 1968).
14. Rule, T. T., and Quale, F. B., "Steady State Operation of the Idealized Vuilleumier Refrigerator," 1968 Cryogenic Engineering Conference, Case Western Reserve University, Paper J-2 (Aug. 1968).
15. Wright, P. E., et al., *ICICLE Feasibility Study*, NASA Contract NAS5-21039, (1970).
16. Shelpuk, B., Crouthamel, M. S., and Cygnarowicz, T., "ICICLE," Space Technology and Heat Transfer Conference, ASME, Los Angeles, California (June 1970).
17. Crouthamel, M. S., and Shelpuk, B., "A Combustion Heated, Thermally Actuated Vuilleumier Refrigerator," International Cryogenic Conference, Boulder, Colorado (Aug. 1972).

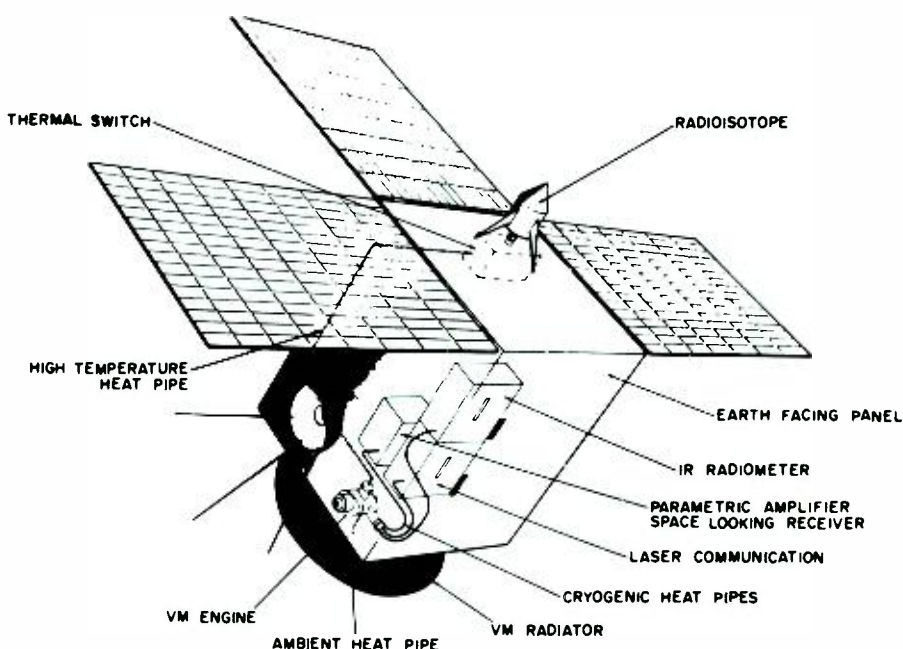


Fig. 8—Artist's Concept of an ICICLE system as it would integrate into a post-1973 spacecraft. Use of a Vuilleumier engine permits cryogenic refrigeration of a multiplicity of experiment, with maximum reliability and minimum weight.

Automatic speaker identification

J. R. Richards | W. F. Meeker | A. L. Nelson

J. R. Richards, Ldr.

Signal Processing and Signature Analysis
Advanced Technology Laboratories
Camden, N.J.

received the BSEE from Drexel University in 1959 and the MSEE from the University of Pennsylvania in 1966. Excerpts of his Master's thesis—"Experimental Comparison of Statistical Techniques for the Classification of Complex Patterns in Photographic Data"—were presented at the International Conference on Pattern Recognition in Los Angeles in 1967. Mr. Richards is continuing his graduate studies toward the PhD at the University of Pennsylvania. Prior to joining ATL in 1970, Mr. Richards was with the Philco-Ford Corporation where he developed a technique for utilizing speech recognition for the automatic measurement of intelligibility in a voice communications channel. He also developed and computer-simulated a highly-successful word-recognition technique for the Mitre Corporation. Mr. Richards has authored several papers on the subject of speech recognition, he has two patents pending, one for a computer-controlled photographic display system and one on a speech privacy system. He is a member of the IEEE.

W. F. Meeker

Signal Processing and Signature Analysis
Advanced Technology Laboratories
Camden, N.J.

received the BSEE in 1939 from Ohio University and the MSEE in 1958 from the University of Pennsylvania. During the past 25 years Mr. Meeker has conducted extensive research into the development and design of acoustical devices and communications systems. He has been in charge of noise surveys and the design of inter-communication systems for use in submarines and armored vehicles. He has served as a project engineer on many contracts, including a study and investigation of specialized electroacoustic transducers for voice communications in aircraft active ear defender systems, and a study of communications in high ambient noise for the US Army Signal Corps. He has served as audio and acoustical consultant for many development and design contracts. Mr. Meeker's work at ATL has concentrated on automatic speaker authentication and automatic language identification. He is a contributing author to *Communications Systems Engineering Handbook*. He holds singly or jointly eleven patents on audio devices. He is a licensed Professional Engineer in New York State and is listed in the Eighth Edition of *American Men of Science*. He is a member of the IEEE and a fellow of the Acoustical Society of America.

A. L. Nelson

Signal Processing and Signature Analysis
Advanced Technology Laboratories
Camden, N.J.

received the BEE from the University of Minnesota in 1958 and the MSE from the University of Pennsylvania in 1967. In 1959, he joined the Surface Communications Division of RCA and participated in vocoder evaluation and speaker recognition studies. He also contributed to a study of automatic speech recognition, both in evaluation of computer-processed speech data and in the preparation of computer programs for speech recognition. Since joining ATL, he has been participating in studies of the application of feature abstraction techniques to problems in speech recognition and speaker authentication, and in studies of speech synthesis. He has been responsible for obtaining the tape recordings which were the data bases for most of ATL's studies in speech processing and recognition and speaker identification and authentication. He has also given programming support to studies of magnetic anomaly detection and seismic signal processing. He is presently assisting with the development of computer programs for automatic language identification and with the collection of the tape recordings for this study.

The Speech Processing Group of the Advanced Technology Laboratories is presently directing effort toward solving the problem of automatic speaker recognition and has achieved encouraging results with a limited number of speakers. This paper describes an approach which does not require a cooperative speaker; that is, the speaker is not required to say a predetermined message. The approach, however, is equally applicable to a cooperative speaker situation where a person is willing to speak a set of words or phrases to have his identity established. The uncooperative situation is clearly the more challenging of the two and provides the broader opportunity in both military and commercial application.

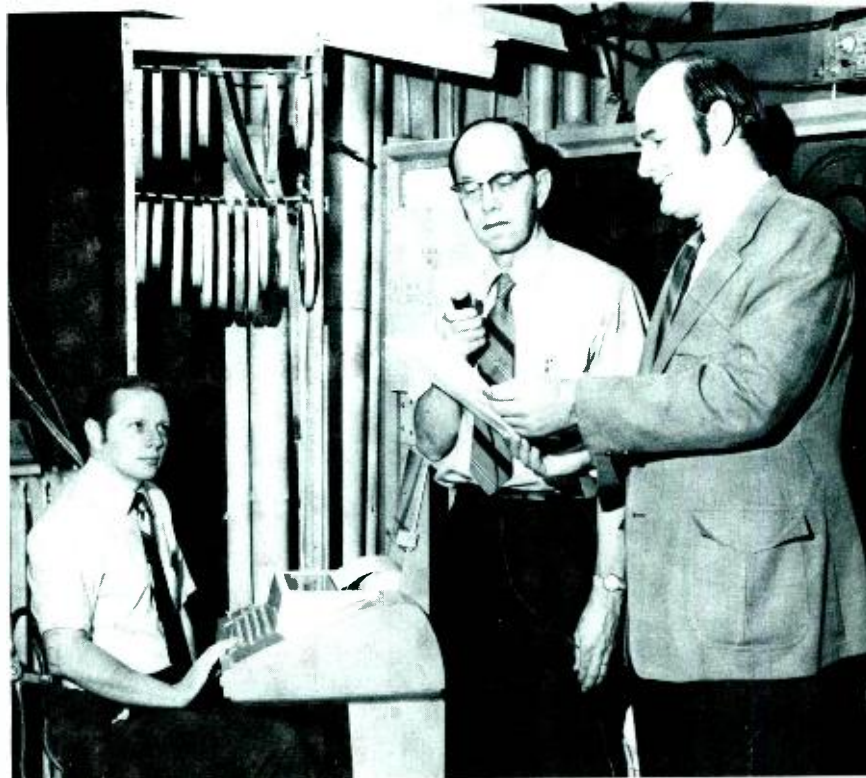
RECOGNITION OF THE VOICE of an acquaintance is a common experience. The nature of the human's speech-producing mechanism is such that characteristics are imparted to speech which reflect the dimensions of the individual's vocal tract as well as learned patterns of speech production. A question still exists as to whether

speech characteristics are sufficiently unique and stable for identification of an individual on the basis of his voice with accuracy comparable to that of fingerprinting. If highly accurate and automatic identification of voice is achievable, there are a large number of potential applications in the fields of law enforcement, credit authorization, and military and industrial security. Some attempts at legal applications have

Reprint RE-18-2-4

Final manuscript received July 10, 1972

Authors (left to right) Richards, Meeker, and Nelson.



already been made; their limitations have been pointed out by a panel of scientists concerned with the question of validation of such approaches for legal application.¹

Background

Speech sounds are primarily of two types—voiced and unvoiced. For voiced sounds, such as the vowels, the vocal cords vibrate, producing a line spectrum with the fundamental generally in the range of 70 to 180 Hz for males, with harmonics extending to 8000 Hz and higher. Unvoiced sounds, such as *s* and *sh*, are those produced by turbulence of the air stream. A few speech sounds, such as *z*, combine the two types. The spectrum of each type is shaped by the vocal tract to produce various sounds. Speech information is carried by the type of sound, the shape of the spectrum and its temporal variations, including brief interruptions for sounds such as *p* and *t*. Phoneticians, analyzing speech sounds on the basis of production and linguistic use, conclude that there are about 40 basic speech sounds, called phonemes, in English. [*Phoneme* is the smallest unit of speech that serves to distinguish one utterance from another in a language, as the *p* in pin or the *f* in fin.] The correspondence between phonemes and the shape of the sound spectrum is exceedingly complex in speech and a one-to-one correspondence cannot yet be established with high accuracy. Nevertheless, automatic phoneme recognition can be accomplished with sufficient accuracy for use in speaker recognition and is used in the system to be described.

Before describing the automatic method used in voice recognition, it is important to define some terminology used by researchers. In general, speaker identification/recognition refers to the problem of relating the voice signal with the person who spoke it. In this paper, the terms *detection* and *classification* are used. *Detection* is the task of determining whether an unknown voice sample belongs to any person in a limited group of known speakers, and *classification* is the task to determine which speaker in the group produced the voice sample.

Speaker identification system using phoneme recognition

The following paragraphs will describe

a system for fully automatic speaker identification from continuous uncontrolled speech. The system employs automatic speech-recognition circuitry to recognize and extract speech elements (usually vowels) so that the statistics of each can be accumulated separately. While identification on the basis of a single type of speech element provides only moderate accuracy, the results for a number of elements are combined for improved accuracy.

The automatic speech-recognition circuitry was developed at RCA in the course of work on the automatic recognition of words from continuous speech. For speaker identification, the characteristics of each phoneme class from each speaker are analyzed and separately tabulated. Consequently, the characteristic manner in which individual phonemes are pronounced by different speakers is used to identify or differentiate between speakers. Although the characteristics of a particular sound may not be unique for a given speaker, it is unlikely that all of the sound characteristics in even a limited set of sounds will be identical with those of another speaker.

The speaker identification system consists of the automatic phoneme-recognition circuitry, computer interface circuitry for organizing and quantizing the data, and a digital computer programmed for the accumulation, storage, and processing of the speech characteristics. The Lockheed MAC-16 computer shown in Fig. 1 is a basic laboratory tool in the speech processing group and is utilized for computer simulation of a multitude of speech processing techniques from speech recognition to speech bandwidth compression. The computer has 8192 words of core storage (16-bit words), a drum memory of 128,000 words, and two IBM-compatible tape units. The speaker identification system utilizes only a small portion of the total capability of the MAC-16 computing system.

The RCA automatic real-time speech analysis equipment used to recognize and segment phoneme-like elements has been described in detail.^{2,3} Basically, the recognition equipment performs a spectral analysis of the speech and recognizes sound elements on the basis of their spectral and temporal properties. The equipment makes use

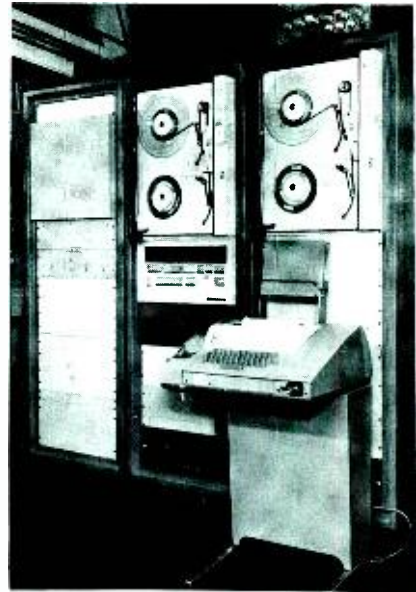


Fig. 1—Computer facility centered around Lockheed Electronics MAC-16 computer.

of analog-threshold logic, operating on the rectified output of a 19-channel filter bank covering the range from 200 Hz to 8000 Hz to provide such features as spectral energy, spectrum slopes, local maxima, local minima, transitions, sequences, and simultaneous occurrences. For automatic speech recognition, a hierarchical organization of feature-abstraction networks is utilized to detect automatically the occurrences of particular sound elements. For the speaker-recognition experiments, the automatic speech-recognition equipment is used to recognize a set of phoneme-like elements from conversational speech. Table I lists some of the phoneme categories the equipment recognizes along with a key word to define the type of sound represented by the category. Fig. 2 shows the hardware required to extract the phonemes used to perform speaker identification.

During the occurrence of each such phoneme category, the slope of the logarithmized spectrum is employed to measure speaker characteristics. The definition of the spectrum slopes (dE/df) can be seen from Fig. 3. In practice, the spectrum slope is derived as 19 analog signals that are integrated over the duration of the selected phoneme, then quantized to three levels corresponding to positive, negative, or zero values.

A block diagram of the speaker identification system is shown in Fig. 4. It con-

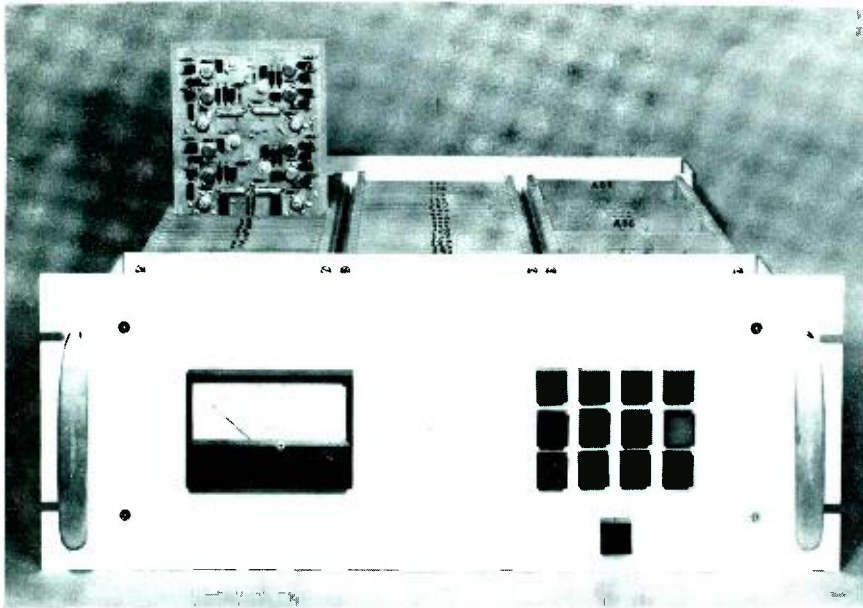


Fig. 2—Equipment to extract and recognize phonemes.

sists of a preprocessor subassembly, recognition circuitry, interfacing circuitry, and the MAC-16 computer.

The preprocessor subsystem performs the basic spectral analysis and spectrum slope derivation used both for speech recognition and speaker identification. The feature- and phoneme-recognition circuitry performs automatic recognition of the speech elements and indicates the presence of a recognized phoneme and its identification to the interface. The interface circuits multiplex the 19 spectrum slopes to a pulse amplitude modulated (PAM) stream, quantizes each slope to 10-bit precision, and submultiplexes the binary decisions from the phoneme recognition circuitry into a single digital bit stream and transmits the data to the computer. When

one or more of the phonemes are present, signified by a "one" from the phoneme recognition circuitry, the software integrates the 19 spectral slope signals over the duration of the recognized phoneme. When the phoneme terminates, each of the integrated spectrum slope values is quantized to one of three levels, corresponding to a positive, negative, or zero slope. The zero-slope range is established at $\pm 4\%$ of the full-scale value. Logic in the software package rejects phonemes of less than 40 ms in duration. The 19 quantized spectrum slopes for each of the recognized phonemes and the number of occurrences of the phonemes are the speech characteristics which are utilized to identify speakers.

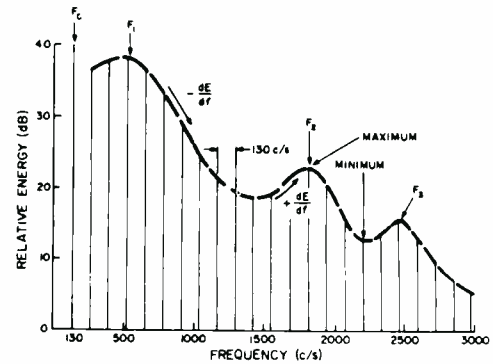


Fig. 3—Graphical illustration of spectral slopes.

The first requirement in designing a speaker identification system is to gather a set of speaker statistics over the population of speakers who are to be identified. This gathering of statistics is referred to as the design phase. Once all the speaker statistics have been collected and cataloged, the second phase of operation can begin—the identification phase. The speech statistics of an unknown speaker are obtained and compared to the library. If the speech characteristics of the unknown speaker match those of a known speaker with the required degree of accuracy, the unknown speaker is identified.

Design phase

The basic steps in the design phase, in which a library of speaker characteristics is obtained, are performed for each speaker in sequence, as follows:

- 1) The number of occurrences of each slope value for each channel for each feature is counted, forming the array. [Feature refers generally to a phoneme.]

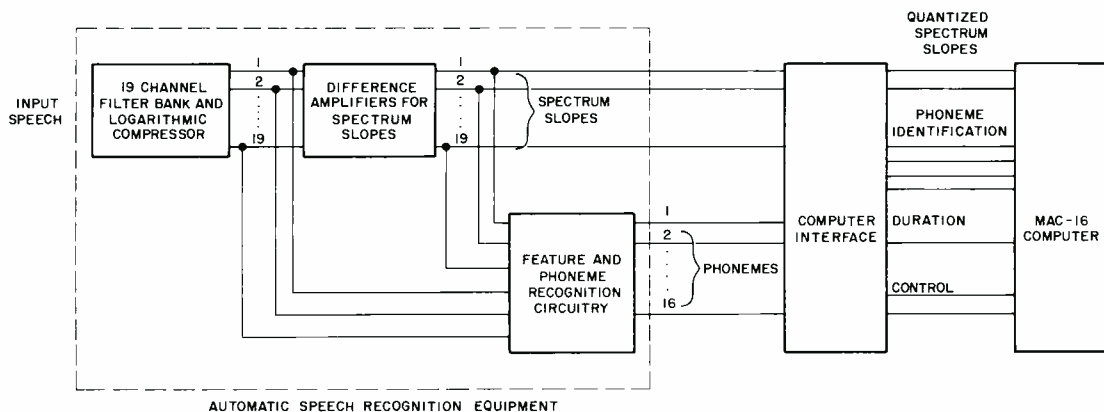


Fig. 4—Block diagram of equipment for speaker authentication experiments.

$$N(i, j, f, s)$$

where i is the slope value $1 \leq i \leq 3$
 j is the channel number $1 \leq j \leq 19$
 f is the feature number $1 \leq f \leq m$
 s is the speaker number $1 \leq s \leq 30$

- The number of occurrences of each feature is counted, forming $RNEF(f, s)$
- Relative frequency-of-occurrence tables are formed.

$$RRFO(i, j, f, s) = N(i, j, f, s) / RNEF(f, s)$$

- For each group of three occurrences for each feature, the summed, squared deviations are computed as

$$SDVSQ_3(k, f, s) = \sum_{j=1}^{19} \sum_{i=1}^3 [(RRFO(i, j, f, s) - SRFO_3(i, j, f, s))]^2$$

where k represents the k^{th} group of three, and $SRFO_3(i, j, f, s)$ is the relative frequency of occurrence table for three occurrences of a feature.

- The means and standard deviations of $SDVSQ_3(k, f, s)$ are computed for each feature; these are designated $M(f, s)$ and $S(f, s)$.

Steps 4) and 5) provide a basis for setting an acceptance threshold for detection. The total number of occurrences of each feature, the relative frequency of occurrence tables, the means, and the standard deviations are written to tape and constitute the library reference data for each speaker.

Identification phase

The basic steps in the identification phase are carried out as follows for each voice sample to be identified:

- The number of occurrences of each slope value for each channel for each feature in the sample of speech to be identified (test sample) is counted, forming the array

$$N(i, j, f)$$

where i is the slope value $1 \leq i \leq 3$
 j is the channel number $1 \leq j \leq 19$
 f is the feature number $1 \leq f \leq m$

- The total number of occurrences of each feature in the test sample is counted as

$$TNEF(f)$$

- Relative frequency-of-occurrence tables are formed for the test sample, as

$$TRFO(i, j, f) = N(i, j, f) / TNEF(f)$$

- Summed squared deviations

$$SDVSQ(f, s) = \sum_{j=1}^{19} \sum_{i=1}^3 [(TRFO(i, j, f, s) - TRFO(i, j, f))]^2$$

An acceptance threshold is utilized to determine the acceptance or rejection of each feature in the test sample based on the summed-squared deviations. If

Category No.	Phoneme	Key Word	Category No.	Phoneme	Key Word
1	i	Feet	9	v	Live
2	l	Fit	10	u	Book
3	e	Let	11	z	Zebra
4	ae	Bat	12	8	Sat
5	o	Bird	13	f	fat
6	A	But	14	n	now
7	o	Law	15	w	was
8	U	hood			

Table I—Phoneme categories used in deriving phoneme sequences.

any feature has been rejected, the speech sample is rejected; that is, it is considered not to have been uttered by the speaker S . If no features have been rejected or, optionally, if no more than one feature has been rejected (provided at least one feature has the required number of reference and test feature occurrences), the speech sample is considered to have been uttered by speaker S , and thus is detected as belonging to a member of the group. If this occurs for only one speaker's library tables, the sample is classified as belonging to that speaker. If detection results with more than one speaker's tables, the sample is classified as belonging to the speaker whose tables produced the minimum weighted sum $[w(s)]$. Thus

$$w(s) = \min \sum_{f=1}^8 SDVSQ_A(f, s)$$

where $SDVSQ_A(f, s)$ represents the accepted summed squared deviations.

The software provides options in the identification procedure so that the frequency range, number of phonemes and acceptance threshold may be varied.

Results

The results of 30 speaker detection and classification experiments are shown in Table II. A classification only experiment using four vowel features— i , I , E , and u —learning on 60 seconds and testing 15-second samples yielded a correct recognition rate of 85%; the recognition rate increased to 93.4% as the learning time was increased to 90 seconds. In the detection and classification experiment, a maximum acceptable value was set for the weighted sum; if the winning speaker's weighted sum exceeded the present value, no decision was rendered. Results of this experiment using the first 8 features in Table

I, learning on 90 seconds, and testing 15-second samples, yielded a recognition rate of 96% with no decision being made on 17% of the test samples.

The results stated in this paper are from preliminary tests using high quality English speech. However, other experiments have been conducted with limited bandwidth and reduced signal-to-noise ratios. System performance degraded moderately with restricted bandwidths and noise. Experiments are continuing to evaluate the effects of various factors, such as the number of speakers, selection of features and number of occurrences of each feature required.

While the results of the experiments utilizing the system described indicate that accurate automatic speaker identification can be achieved under limited conditions, questions remain concerning the effects on system performance of such factors as noise, bandwidth truncation, spectral distortion, and time. Although the ultimate automatic speaker identification system has not yet been developed, the accuracy of the system described is such that it presently can be used profitably in many practical applications.

References

- Bolt, Cooper, David, Denes, Pickett, and Stevens, "Speaker Identification by Speech Spectrograms; A Scientists' View of its Reliability for Legal Purposes", *Journal of Acoustical Society of America*, Vol. 47 (1970) pp. 597-612.
- Martin, T. B., Zadell, H. J., Cox, R. B., and Nelson, A. L., "Recognition of Continuous Speech by Feature Abstraction", AF Systems Command, AFAL-TR-66-139, (May 1966).
- Scott, P. B., Nelson, A. L., and Barger, J. R., "Signal Processing for Multiple Access", AF Systems Command, AFAL-TR-69-45 (March 1969).

Table II—Automatic speaker identification results showing the effects of learning time and number of features.

No. of features	Learn data (seconds)	Recognition data (seconds)	Correct recog %	Error %	Reject %
4	60	15	85	15	0
4	90	15	93.4	6.6	0
8	90	15	96	4	17

Recent developments in CMOS/SOS

H. W. Kaiser | W. F. Gehweiler | W. J. Stotz | J. I. Pridgen

W. F. Gehweiler

Signal Processing Laboratory
Advanced Technology Laboratories
Camden, N.J.

received the BSEE with honors from the Milwaukee School of Engineering in 1959. After completing RCA's Engineering Training program in 1960, he was assigned to the Missile and Surface Radar Division, where he worked on the BMEWS (Tracking Radar Data Take Off) project in a design and development capacity. In 1961, he joined Advanced Technology Laboratories, where he was active in optical correlation techniques. In 1965, he began work in secure communications, including environmental testing, specifications for testing and acceptance tests, and digital system design and analysis. Mr. Gehweiler participated in a code storage IR&D project in 1967. This experience covered MOS devices, domain tip propagation logic, the Ovonic memory device, and magnetic memories. In 1968, he was responsible for an IR&D project on electronic correlators, and in 1969, he designed, built, and tested a CMOS/SOS correlator array. He worked on digital filters, which included real-time, analog equivalent filters and matched filters using FFT and correlation techniques in 1970. Both radar and communication systems were included in the study. In 1970-71, he designed four SOS arrays; all of these arrays were successfully fabricated and tested.

W. J. Stotz

Signal Processing Laboratory
Advanced Technology Laboratories
Camden, N.J.

received the Diploma in Electrical Engineering from Drexel University in 1959 and the BSEE from Drexel in 1968. He is also a graduate of the Naval Materiel School in Washington, D.C. Mr. Stotz joined the RCA Missile and Surface Radar Division in 1953 as a laboratory technician. He became a member of the engineering staff in 1959 and transferred to EASD in Van Nuys where he contributed to the design of the Display Information Processor for the NORAD System, and designed the BMEWS DATA Simulator for the SAC data link. He has contributed extensively to the design and testing of a variety of secure communications equipments in both EASD and ATL. He participated in the design and development of the numeric speech translating system and was responsible for the field tests of that equipment. Mr. Stotz has also been active in the high-speed digital logic field. He also has done work on high-speed digital arithmetic circuitry using ECL circuit techniques. For the past year he has been actively engaged in the layout and design of artwork for CMOS-type integrated circuits for both bulk silicon and sapphire substrates.

Junius I. Pridgen

Signal Processing Laboratory
Advanced Technology Laboratories
Camden, N.J.

received the BEE from the University of Virginia in 1964 and the MSEE from Georgia Institute of Technology in 1971. He also did graduate work at the University of Virginia (1964-1967) and was employed by Lockheed-Georgia Company as a Training Specialist in Advanced Technology Training from 1967 to 1970. Mr. Pridgen joined RCA in 1971 on the Graduate Rotational Program and was permanently assigned to Advanced Technology Laboratories in February 1972. Since joining RCA, he has been involved in the design and testing of CMOS/SOS arrays. Mr. Pridgen is a member of Tau Beta Pi and Eta Kappa Nu.

Much has been written^{1 2 3} over the past several years concerning the complementary metal oxide semiconductor/silicon-on-sapphire (CMOS/SOS) technology and its potential to satisfy an ever growing requirement for a high-speed low-power LSI technology. Significant progress has been made during the past year to bring the technology from its laboratory development stage to a viable pilot-production-line process. Aluminum-gate CMOS/SOS has been in pilot production since October 1971. It has been followed by silicon-gate CMOS/SOS, in pilot production since February 1972. Higher speed operation in the 100- to 200-Mb/s range will be obtained ultimately by the marriage of silicon-gate-technology and the deep-depletion CMOS/SOS process.

Authors (clockwise from upper left) Gehweiler, Kaiser, Stotz, and Pridgen.



H. W. Kaiser, Ldr.

Signal Processing Laboratory
Advanced Technology Laboratories
Camden, N.J.

received the BSEE from Lehigh University in 1956, at which time he joined the RCA Specialized Training Program. He has completed all course requirements for the MSEE at University of Pennsylvania. At the completion of the training program, Mr. Kaiser was assigned to the Communications Systems Division where he was a design engineer and, later, project engineer for the Air Force and Navy Data Link programs. From 1963 through 1966, Mr. Kaiser was responsible for the design of secure communication equipment. On this program, he was promoted to Leader, Design and Development. Since 1967 he has been respon-

sible for IR&D programs in signal processing pertaining to communication and radar equipment. In this capacity he is responsible for advanced circuits and designs using MOS technology and LSI packaging techniques. Major current group effort has been directed toward characterization studies and system designs using the CMOS/SOS technology. Applications to digital filters, FFT's, and communication and radar signal processing systems have been developed with a significant number of CMOS/SOS arrays designed. Mr. Kaiser's group is also involved in the design of special purpose memory systems using custom designed LSI bulk silicon CMOS arrays. Associative processor and push-down-list memory systems have been designed and built.

ALUMINUM-GATE CMOS/SOS PROCESSES have taken several years to reach their present pilot-line production status. The present process is referred to as the co-aligned, aluminum-gate, double-epitaxial (epi), CMOS/SOS process and is a slight modification of the process previously described.¹ The important modification made to the previously described double-epi process was the use of a single mask step to define the gate areas of both the n- and p-type devices. The cross-sectional view of the device structure is shown in Fig. 1. A description of each mask layer follows:

- Level 1: Defines p-type material islands used for the n-MOS transistors.
- Level 2: Defines n-type material islands used for the p-MOS transistors.
- Level 3: Defines channel oxide of both n-MOS and p-MOS devices.
- Level 4: Defines the diffusion area of the n-MOS transistors.
- Level 5: Defines area of contact holes for array interconnections.
- Level 6: Defines metallization.
- Level 7: Defines area of contact holes for array input/output access pads.

Several developmental arrays have been designed, processed and successfully tested using this process and are described later in this paper.

During 1971, the use of polycrystalline silicon as a gate electrode was successfully demonstrated with CMOS/SOS, and preliminary rules were established for the design of circuits using this technique.

Silicon gates offer the same advantages to CMOS/SOS as they do to all other MOS technologies: shorter gate lengths, lower V_T , higher speeds, additional interconnection level, slightly higher packing densities (especially true for lower frequencies since smaller devices are used), and lower gate and crossover capacitance.

Fig. 2 shows the silicon-gate structure and some of the steps in the process. Both the structure and the processing are similar to the aluminum-gate case. Masks 1 and 2 perform the same function as before and define the p and n islands, respectively. A 1200-Å oxide is then grown on the silicon islands and a layer of polysilicon is deposited on the wafer. Mask 3 defines the silicon-gates and ultimately the channels for

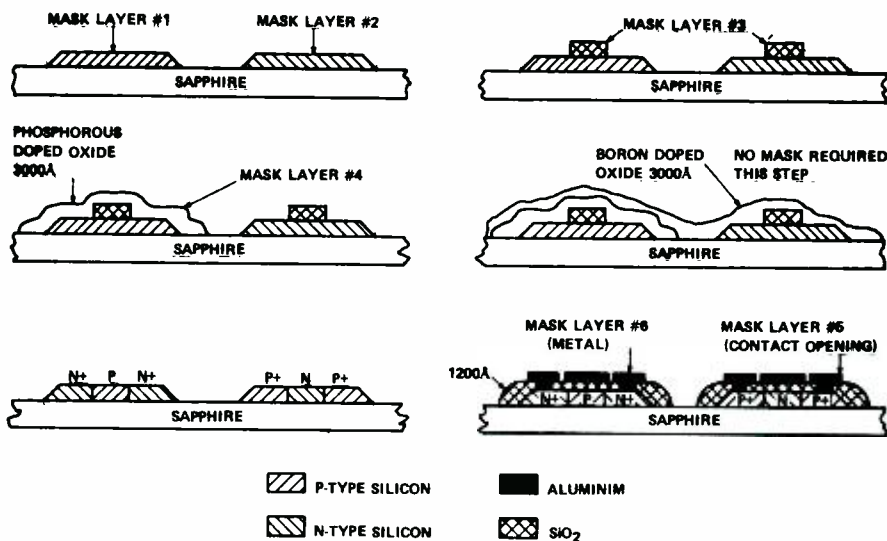


Fig. 1—Illustrated use of mask levels.

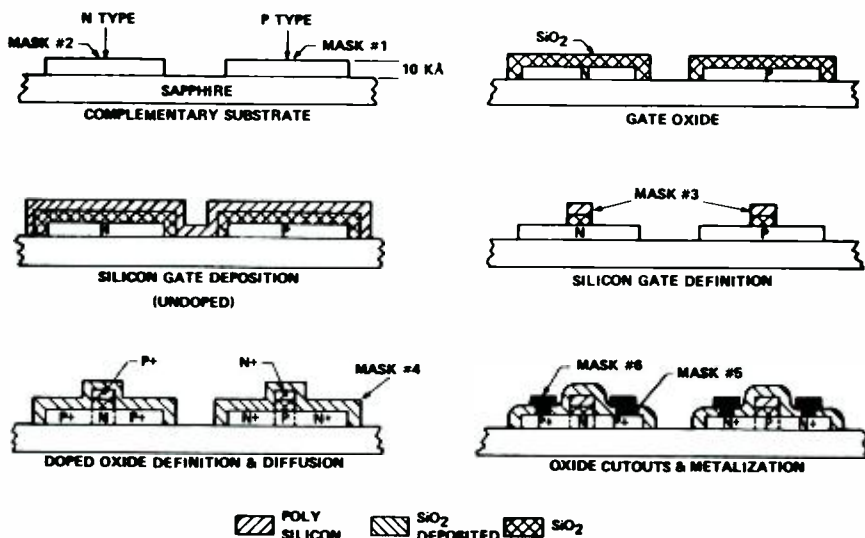


Fig. 2—Silicon-gate, double-epi CMOS/SOS structure.

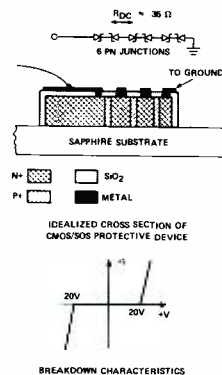
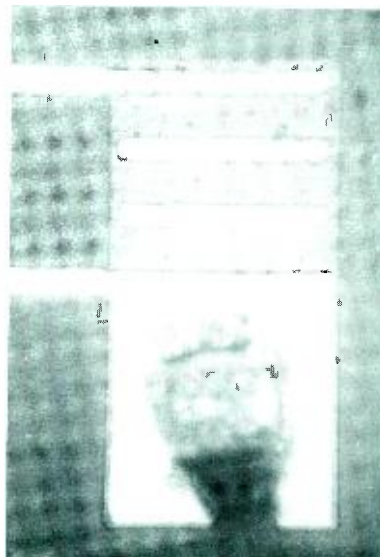


Fig. 3—Gate protection device.

Reprint RE-18-2-16
Final manuscript received June 28, 1972.

both type devices. The devices are doped in the same manner as the aluminum-gate process using mask 4. The doped oxides are stripped off and a 5000-Å oxide deposited over the entire wafer. The contacts and metal interconnections are again formed using masks 5 and 6.

In addition to the concentrated effort to fully mature the sos process, several important peripheral developments have taken place during the past year to greatly increase process yield. New alignment keys and layout rules have been developed, mask formats delineated, and protective devices designed for high electrostatic voltage-transient protection.

Fig. 3 shows the protection device similar to the one currently being used. The only difference is in the number of p-n junctions. Current units have four junction pairs resulting in a slightly higher breakdown voltage. The current device structure being used consists of a series of alternate heavily doped n+ and p+ diffusions which schematically can be represented by a series of reverse-biased Zener diodes and alternate forward-biased diodes.

The aluminum-gate CMOS/sos process has been transferred from the RCA Laboratories in Princeton to the Solid State Technology Center at Somerville, and a pilot line has been in operation since October 1971. Several array designs have served as test vehicles for the line during this time. The major vehicle has been the ATL-designed TA6140 seven-stage binary ripple counter. This array is functionally and pin compatible with the RCA commercial CMOS CD 4024A. Several thousand of these arrays have been processed.⁴ Further details on performance are included in later paragraphs of this paper.

Significant accomplishments of the pilot line are:

- 92% of the sapphire wafers started complete the processing cycle.
- Yields at wafer probe are comparable to the yields obtained on the monolithic CMOS production lines.

The silicon-gate process has also been used to process an equivalent of the aluminum-gate seven-stage counter with the predictable results of higher speed operation. However, finalized design rules for this process have not

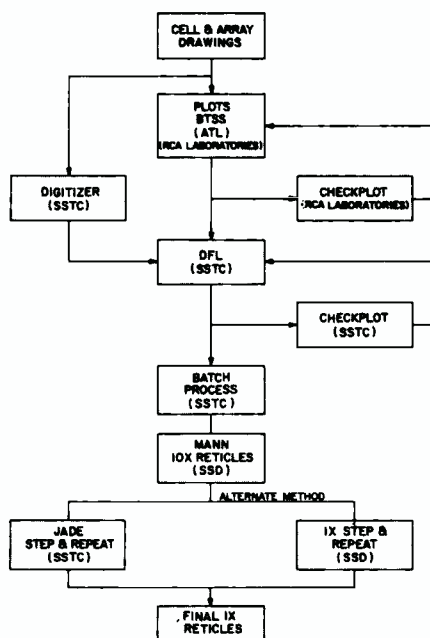


Fig. 4—Artwork and mask generation, flow diagram.

been established, and the ultimate performance of the silicon gate approach may be masked by the understandably conservative design rules used on early arrays.

Silicon-gate technology will ultimately supplant the metal gate structure in CMOS/sos as well as other MOS forms. Future processing trends in sos, however, will tend toward higher speed operation in the 100- to 200-Mb/s range by coupling silicon-gate technology to the deep depletion process for making devices. This marriage eliminates the problems associated with the metal-gate deep-depletion process previously described¹ and, because of lowered threshold voltages, promises the higher speed. This approach is certainly experimental at this time and will require a certain incubation period before it can be considered a viable process.

To summarize the processing state-of-the-art in sos, the coaligned aluminum-gate, double-epi process is now in pilot production, with silicon gate a short step behind. Silicon-gate deep depletion is on the horizon.

Artwork and mask generation

The artwork generation programs for CMOS/sos arrays utilize the latest procedures available at the RCA

Laboratories, Princeton; SSTC, Somerville; SSTC, Camden; and ATL, Camden. Two methods can be used to provide artwork information in design-file language (DFL) for use in driving the D. W. Mann artwork generator and/or the Gerber Plotter. The selection of either artwork generator need not be made at the time of circuit digitization and can be easily made prior to creation of the final artwork tape.

The first and most direct method of creating a DFL tape is by use of a modified Calcomp, model 502, plotter. This unit is used as a drawing digitizer and furnishes an output tape containing the digitized polygons of the array in DFL. This procedure is performed by the SSTC Design Automation Activity in Somerville.

When the geometric designs of a CMOS cell are completed, layer drawings are made. The information pertaining to line location, length, width, direction, and usage are machine interpreted into a DFL and placed on magnetic tape. This method of putting drawing information into a computer program language for machine processing is often referred to as digitizing.

A Calcomp, model 502, flatbed plotter has been modified by SSTC⁵ for use in conjunction with a PDP-8 computer as a digitizing system. A locator is used on the plotter stylus in place of the pen. Its position over a point of interest and an electrical command from the operator causes the x- and y-coordinate position of the stylus to be detected and transmitted to the PDP-8 computer for interpretation. When the digitizing process is complete, the procedure is reversed and the stored program is fed back to the plotter and a hard copy plot is made of each layer.

The second procedure that can be used is the computer-aided artwork generation system using the PLOTS (plotting language on time sharing) program. This procedure can be followed wherever access can be made to a BTSS (basic time sharing system) terminal. This system is used to generate artwork, plot it on a visual display storage scope and/or Calcomp plotter for verification, and then convert it into the DFL format.

Using the PLOTS program, it is possible to work from crude sketches and

to progress rapidly and accurately to the physical 10X reticles.

The sketches of the cell and array layouts are made on gridline paper at a scale factor of 500X or 1000X for the cell drawings and 100X for the array layout. From these sketches, descriptions of the individual layers are written in PLOTS. The prepared description (artwork statements) is entered into an allotted file space in the Spectra 70/45 at Princeton via a Teletypewriter transmitter/receiver. The Spectra 70/45 at Princeton is part of the BTSS and the file created in the PLOTS program is accessible to the three RCA activities (Camden, Somerville, and Princeton) which participate in the artwork-generation cycle.

The flow diagram of Fig. 4 illustrates the parallel paths taken in the two aforementioned procedures. Also shown is the use of the D. W. Mann artwork generator and the Jade step-and-repeat equipment in obtaining the 10X and 1X reticles, respectively. An alternate source for the 1X step-and-repeat cycle is also shown.

Developmental arrays

The following represent some of the most recent CMOS/SOS arrays designed by ATL Camden:

- Seven-stage binary counter (Al-gate), Fig. 5
 - 90x100 mils
 - 162 devices
 - 35 MHz @ 15 V
 - 14-lead DIP
- Seven-stage binary counter (Si-gate), Fig. 6
 - 90x100 mils
 - 162 devices
 - 43 MHz @ 15 V
 - 14-lead DIP
- Sequence generator test chip (Al-gate), Fig. 7
 - 106x110 mils
 - 252 devices
 - 40 MHz @ 15 V
 - 24-lead DIP
- Sequence-generator test chip (Si-gate), Fig. 8
 - 106x110 mils
 - 252 devices
 - 50 MHz @ 15 V, 35 MHz @ 10 V.
 - 24-lead DIP
- Multipurpose arithmetic building block, Fig. 9
 - 95x130 mils
 - 280 devices
 - 20 MHz @ 15 V
 - 24-lead DIP

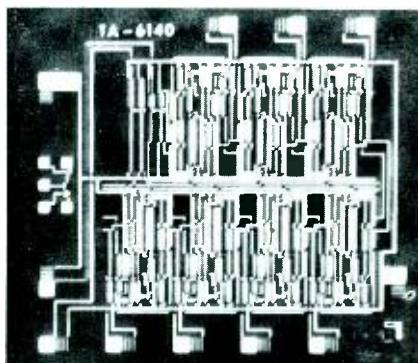


Fig. 5—Seven-stage binary counter (Al-gate).

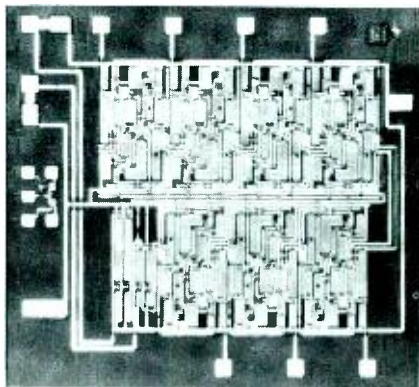


Fig. 6—Seven-stage binary counter (Si-gate).

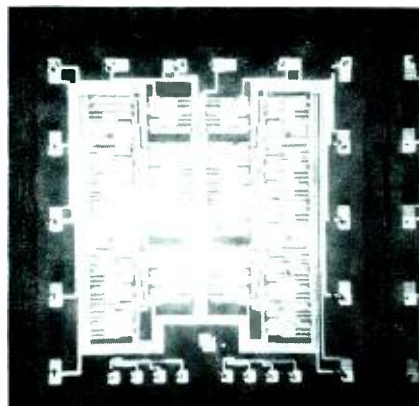


Fig. 7—Sequence generator test chip (Al-gate).

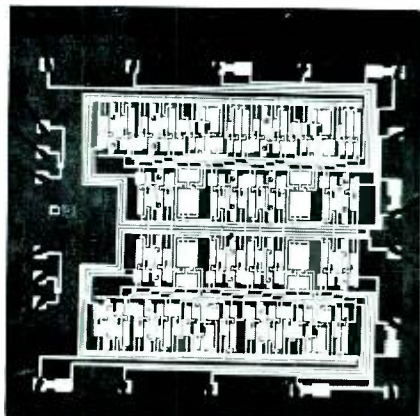


Fig. 8—Sequence generator test chip (Si-gate).

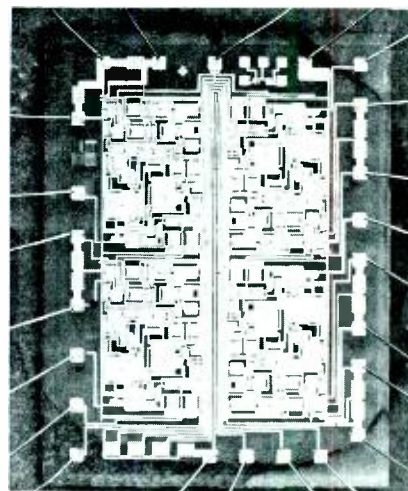


Fig. 9—Multipurpose arithmetic building block.

Array performance

The most thoroughly tested CMOS/SOS array to date is the TA6140 aluminum-gate seven-stage counter. The following information, although pertaining directly to the counter, is representative of what may be generally achieved using conventional loading and production design rules for a general class of arrays.

The counter array power dissipation as a function of frequency and supply voltage is shown in Fig. 10. The value at DC is the average static leakage power of the array. This is an average value since the leakage power is dependent on the states of the seven stages. Minimum leakage power occurs when the array is in the reset condition. The average DC power is 39 μ W, 200 μ W, and 500 μ W for supply voltages of 5, 10, and 15 V, respectively. In the static-reset condition, the previously mentioned power values are reduced by a factor of two.

At the lower frequencies, the power curves are linear since the dynamic power ($P_{dyn} = CV^2f$) for CMOS logic circuits is proportional to frequency.⁴ The

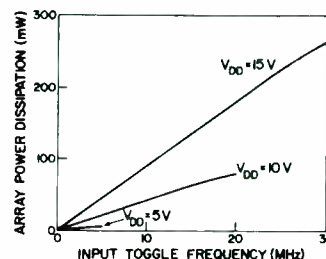


Fig. 10—Al-gate counter; array power dissipation vs. frequency and supply voltage.

slopes of the three power curves are 0.812, 3.37, and 8.42 mW per MHz. Each of the seven outputs was loaded with 15 pF. The dynamic power can be reflected as an equivalent stage capacitance of 16.25 pF, 16.85 pF, and 18.7 pF for 5 V, 10 V, and 15 V, respectively. The predicted capacitance based on 1200-Å thickness is 15.32 pF. The trend, as fabrication progresses, has been toward a lower equivalent capacitance. The difference between predicted and test results could therefore be closer than the existing 10 to 20%. However, the 10 to 20% difference must presently be attributed to the transient power.

The curves depart slightly from the linear condition when the toggle frequency approaches the maximum value. This is not apparent on all the curves as the difference is slight and the scale is necessarily large. This departure is a result of the first-stage operation of the counter. Normally, the logic signals swing between the supply voltage and ground; but at the higher frequencies, the signals never reach these values. The voltage swing, V , in the dynamic power equation is therefore reduced, causing the power to become sublinear.

The total power did not change appreciably over the temperature range 25°C to 125°C; however, power measurements below 500 kHz were not taken. The maximum toggle frequency did change; the results are shown in Fig. 11. Mobility as a function of temperature is also shown; this is the major factor that affects the frequency response of the CMOS circuits. The current characteristics of an MOS device are linear functions of mobility.⁶

A summary of the array electrical characteristics is given in Table I. Measured and predicted values are shown for comparison. The measured

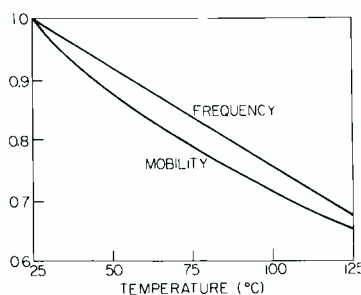


Fig. 11—Normalized toggle frequency and mobility vs. temperature.

Table I—Seven-stage counter SOS array electrical characteristics.

Characteristics	V_{DD} (volts)	Measured typical values	Predicted* values
Maximum toggle frequency (MHz)	5	6.8	—
	10	22.4	—
	15	32.5	37.5
Propagation delay (ns) (input clock to 1st output)	10	46	—
	15	32	27.5
Propagation delay (ns) (n output to n+1 output)	10	21	—
	15	15	15
Propagation delay (ns) (reset to any output)	10	48	—
	15	33	30
Output rise time (ns)	10	34	—
	15	23	20
Output falltime (ns)	10	37	—
	15	27	23.8

$T_A = 25^\circ\text{C}$, 15-pF load on each output, and input pulse risetime and falltime=5 ns

*Predicted values based on effective channel length of 0.31 mil and oxide thickness of 1200 Å.

values were generally within 20% of the typical values. The highest frequency measured at 15 V was 44 MHz.

Preliminary performance results have been obtained with the silicon-gate version of the counter. These data are also presented for general information.

Table II contains the dynamic electrical characteristics. The maximum toggle rates have all increased about 10 MHz over the aluminum-gate version and the propagation delays have decreased about 15%. The static characteristics and temperature effects are expected to be the same as for the aluminum-gate case. Fig. 12 shows the power as a function of supply voltage and frequency. The power slopes are: 0.6 mW/MHz @ 5 V; 3.2 mW/MHz @ 10 V; and 9.2 mW/MHz @ 15 V. The performance in Table II is expected to be improved by another 10 to 20% when an alternate silicon-gate mask with smaller channel lengths is used.

Table II—Seven-stage counter Si-gate/SOS array electrical characteristics.

Characteristics	V_{DD} (volts)	Typical values
Maximum toggle frequency (MHz)	5	16.6
	10	35.8
	15	43.1
Propagation delay (ns) (input clock to 1st output)	10	38.6
	15	30.5
Propagation delay (ns) (n output to n+1 output)	10	13.9
	15	11.1
Propagation delay (ns) (reset to any output)	10	41.2
	15	31.0
Output risetime (ns)	10	28.8
	15	24.1
Output falltime (ns)	10	37
	15	27

$T_A = 25^\circ\text{C}$, 15-pF load on each output, and input pulse risetime and falltime=5 ns.

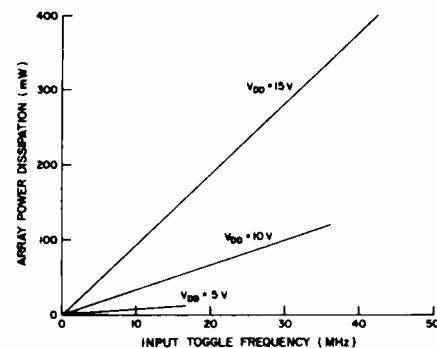


Fig. 12—Si-gate counter array power vs. input toggle frequency and supply voltage.

Conclusions

The aluminum-gate CMOS/SOS process has reached a high level of maturity and has been operating in a pilot production line by SSTC personnel since October 1971. It can now be considered a viable LSI technology based on the results of this operation. Design automation programs and computer simulation models simplify the design of these arrays.

The silicon-gate CMOS/SOS pilot line has been operating since February 1972 with equally fine results. This process will ultimately replace the metal gate process and all new designs should therefore be considered in silicon-gate versions.

Acknowledgments

The progress of CMOS/SOS herein reported could not have been possible without the dedicated work of the RCA Laboratories personnel in J. Scott's activity. J. Meyer, E. Boleky, D. Flatley, W. Schneider, J. Sarace, S. Policastro and N. Kudrjashev are but a few of the individuals who have contributed significantly to this effort.

References

- Boleky, E. J.; Crossley, P. A.; Meyer, J. E.; Policastro, S. G.; Schneider, W. C.; "Silicon-on-sapphire, the ultimate MOS technology". RCA Reprint, *Solid-State Technology*, PE-552, RC-4 Engineer, Vol. 17, No. 3 (Oct/Nov 1971) pp. 46-49.
- Burns, J. R. and Scott, J. H., "Silicon-on-Sapphire Complementary MOS Circuits for High-Speed Associative Memory". *AFIPS-Conference Proceedings*, Vol. 35, (1969) p. 469.
- Meyer, J. E.; Burns, J. R.; Scott, Jr., J. H., "High-Speed Silicon-on-Sapphire 50-Stage Shift Register". *1970 IEEE ISSCC Digest of Technical Papers*, p. 200.
- Gehweiler, W. F., "Characteristics of a Silicon-on-Sapphire CMOS 7-Stage Binary Counter". *IEEE ISSCC*, 16-18 Feb. 1972, Philadelphia, Pa. *1972 IEEE ISSCC Digest of Technical Papers*, p. 96-97.
- Helpert, E. P.; Miller, J. C.; Reessler, D. G.; "Design automation—promise and practice". RCA Reprint, *Solid-State Technology*, PE-552, RC-4 Engineer, Vol. 17, No. 3 (Oct/Nov 1971) pp. 6-9.
- Meyer, J. E., "MOS Models and Circuit Simulation". *RC-4 Review*, Vol. 32, No. 1 (March 1971).

High speed A to D converters

D. Benima | J. R. Barger

High speed, high resolution analog to digital conversion forms the bridge—or perhaps one should say the mountain pass—between the analog world of sensor data, video and audio communications, and radar signals and the fast, powerful world of the digital computer. The computer can now apply a measure of sophistication and flexibility to the processing of analog information far beyond what can be achieved with analog tools alone. Advanced Technology Laboratories, in studying the possibilities and limitations of the wideband, high-resolution analog-to-digital conversion process, has evolved several unique, advanced concepts. Two of these will be discussed: the VAROM concept and the related innovation of *sampling on the fly*.

IN CONVENTIONAL CONVERTER SYSTEMS, the analog voltage is measured, and the measurement result is used to generate a digital output; while in the VAROM (voltage-addressable read-only memory), all the possible digital outputs are already present and stored in a read-only memory. The conversion process then consists of using the analog voltage to select the address that contains the proper digital output word.

Sampling on the fly refers to the measurement of an electrical signal while it is changing, in contrast to the

conventional method of first converting the signal to be digitized to DC and then performing the measurement on the latter.

Conventional conversion techniques

A closer look at some aspects of the conventional A/D conversion process is necessary to appreciate the significance of these two new concepts. Fig. 1 is a simple flow chart of the elementary conversion process. Few systems are quite this simple. Usually, the conversion takes place in two or more steps, as shown in Fig. 2. Step conversion involves the added complication of a conversion back to analog followed by

D. Benima

Signal Processing Laboratory
Advanced Technology Laboratories
Camden, N. J.

received the BEE from the Delft Institute of Technology, Netherlands in 1954. From 1954 through 1956, he worked at the University of Toronto Computing Center. In 1956 he joined Remington Rand Univac where he assumed responsibility for assignments involving the basic logic switch, backplane wiring, connector design, and factory liaison for the LARC Computer. Mr. Benima joined RCA Information Systems Division in 1959. In this capacity, he worked on high speed memory drive and sensing circuits for the 601, Spectra 45 and 55 computers, analysis of large core memories, design of fail safe power supplies, and various other assignments involving logic and memory design. In 1970, Mr. Benima joined the Signal Processing Laboratory of ATL, where he is assigned to high speed logic and memory technique developments with his main activity in the area of high speed analog-to-digital conversion.

J. R. Barger

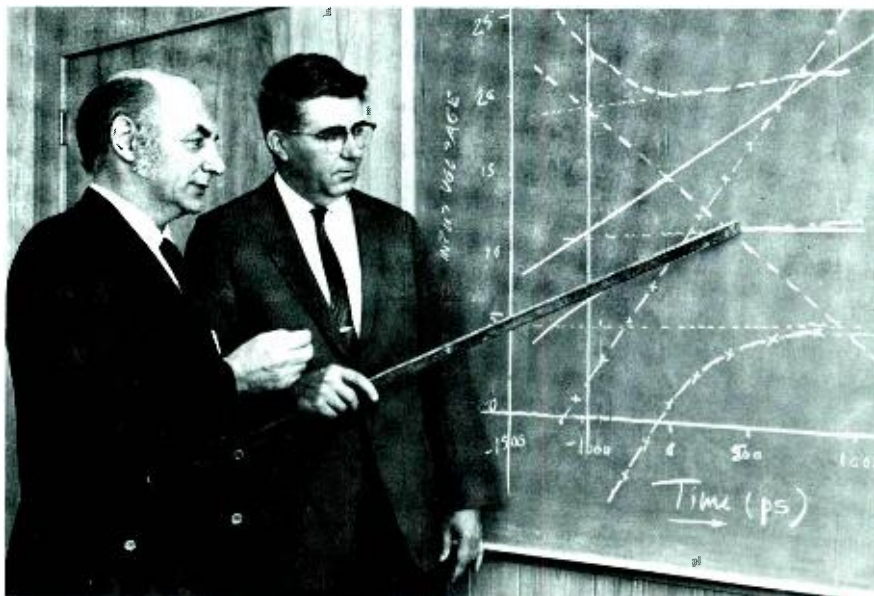
Signal Processing Laboratory
Advanced Technology Laboratories
Camden, N. J.

received the BEE from Ohio State University in 1952. Since joining RCA in 1952, he has contributed circuit designs for LORAN, fire-control radar, automatic checkout equipment, and various digital logic systems. In 1966, he joined the Signal Processing Laboratory of ATL. He has contributed to circuit designs for signal processing equipments for speech recognition system and an automatic Magnetic Anomaly Detection (MAD) unit. Mr. Barger is a member of IEEE; he has been awarded two patents.

Reprint RE-18-2-19

Final manuscript received June 26, 1972

Authors Benima (left) and Barger.



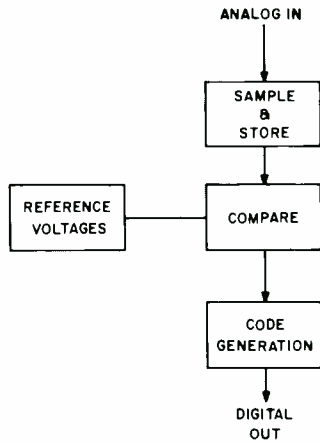


Fig. 1—A/D conversion flow chart.

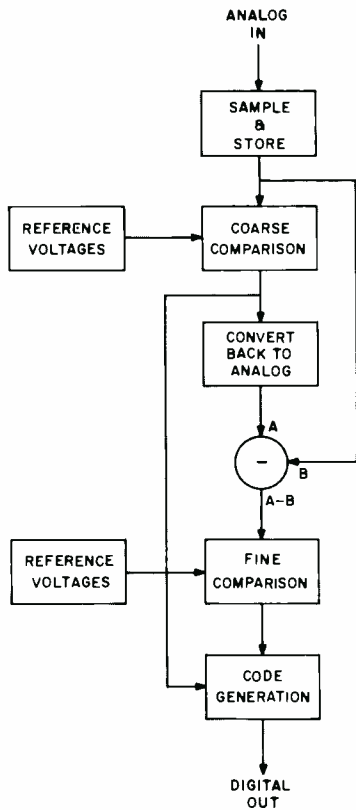


Fig. 2—Flow chart of a two-step conversion process.

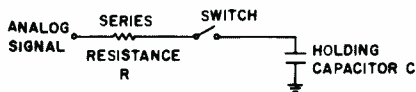


Fig. 4—Model of a sample and hold.

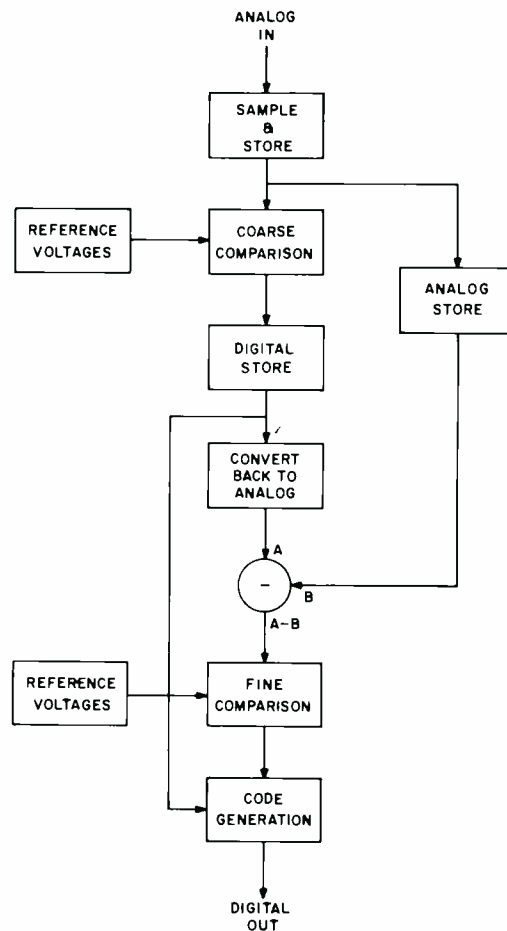


Fig. 3—Two-step conversion with overlapping operations.

a subtraction. However the additional complication is generally more than offset by a reduction in the converter hardware.

At substantially higher conversion speeds, the difference between one-step and multistep systems becomes significant: when the conversion rate increases, the time available for each conversion shrinks and it becomes impossible to carry out the entire multistep conversion in one conversion period (the time between two successive samplings). In that case, consecutive conversions must be overlapping. A flow chart for a conversion process with overlapping conversion is shown in Fig. 3. All two-step conversion systems with conversion rates of 20 MS/s (20 megasamples per second) and up are of the general type shown in Fig. 3.

Limitations of conventional techniques

By referring to this flow chart, one can easily identify the weaknesses of the two-step conversion process when high

conversion rates (required for the handling of high frequency signals) are encountered. The digital-to-analog conversion and the second analog store are sources of considerable error, especially at high speeds. However, the largest source of error is the very first operation of sample and hold. In fact, any sample-and-hold operation is subject to a so-called "tracking" error which is due to fundamental electrical laws and which cannot be eliminated by improved design. This error becomes prohibitively large at higher speeds. The exact magnitude of the error depends on the signal history. For a 50-MHz sinewave, for example, the error will vary between $\pm 11\%$.

Fig. 4 shows the general model for a sample-and-hold circuit. Waveforms associated with the operation of such a circuit are shown in Fig. 5. Note that the switch periodically opens and closes. When the switch is closed, the holding capacitor charges toward the analog input signal and follows or "tracks" the signal. When the switch

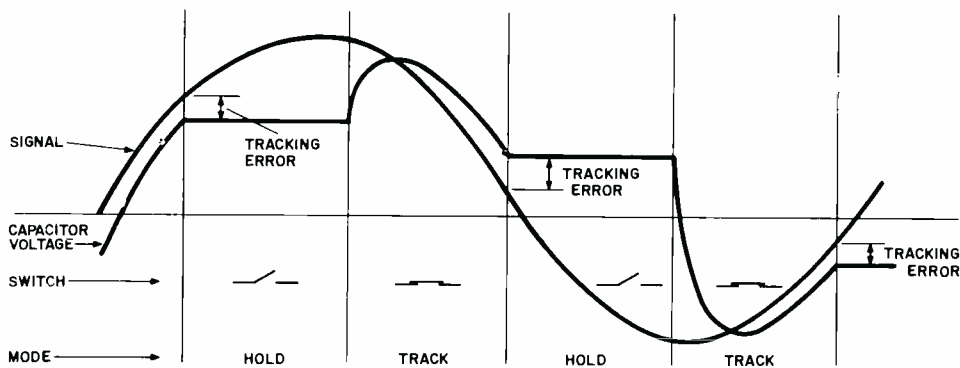


Fig. 5—Tracking error resulting from time lag in holding-capacitor response.

opens, the capacitor retains the voltage as it was at that instant. It is this unchanging voltage that is measured in the conversion process. The unavoidable series resistance R in any realizable switch, in conjunction with the holding capacitor, creates a time constant, RC , which slows the tracking of the signal by the capacitor and results in a lag which is of the order of $RC (dV/dt)$, where RC is typically 1 ns, and the result is a large tracking error when dV/dt is large, as is the case for wideband signals.

VAROM concept

The tracking error can only be eliminated by removing C —that is, by not immobilizing the signal, but rather by measuring the signal while it is changing. This technique rules out the use of any two-step process and poses

the problem of measuring accurately a signal while it is changing at an exceedingly fast rate. Fig. 6 illustrates how this can be accomplished using strobed comparators in a VAROM configuration. The operation is remarkably straightforward. Each of the $2n$ sub-ranges which together make up the total signal range is served by a comparator. Fig. 6 shows three comparators of a column which contains $2n$ comparators. The output of each comparator can be frozen in its instantaneous state by means of a strobe. If, at the time of strobing, the signal value is between reference level n and reference level $n+1$, the comparator outputs will be such that only gate n has a high output. This high output selects word n from the read-only memory (ROM), and this word represents the proper output code for a voltage with a value between reference n and $n+1$.

Sampling-on-the-fly concept

Simple as it is, the combination of the VAROM concept and the sampling-on-the-fly approach affords, in principle, a much higher speed and a much higher resolution conversion than any of the conventional multistep sample-and-hold systems.

While avoiding many of the problems inherent in previous systems, the new approach is not a cure-all, but rather has its own peculiar difficulties. However, these new difficulties are expected to yield to technical improvements, while the tracking error along with other faults in conventional systems are of a fundamental nature and are irreducible beyond a certain limit.

The most serious problem of the sampling-on-the-fly concept is the spread in strobing times of the comparators (of which there are $2n$ for an n -bit converter). This spread gives rise to a so-called "aperture" error, which is a fluctuation in the time of sampling. Such a fluctuation detracts from the resolution of the converter and the effect is more severe as higher frequencies are being processed. It can be shown that beyond certain levels of resolution and speed, special alignment procedures are needed to ensure that strobing times fall within a sufficiently narrow range. The refinement of these procedures is one area of continuing effort at the Advanced Technology Laboratories.

The VAROM tends to compare unfavorably with conventional systems in power consumption and number of components. However, the basic simplicity of its structure allows packaging economies which can offset its higher component count.

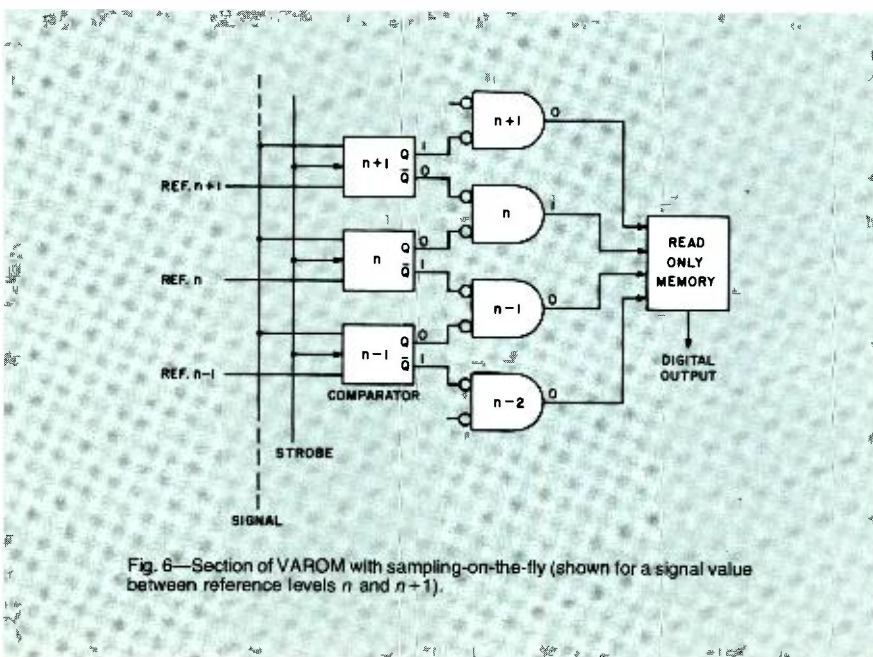


Fig. 6—Section of VAROM with sampling-on-the-fly (shown for a signal value between reference levels n and $n+1$).

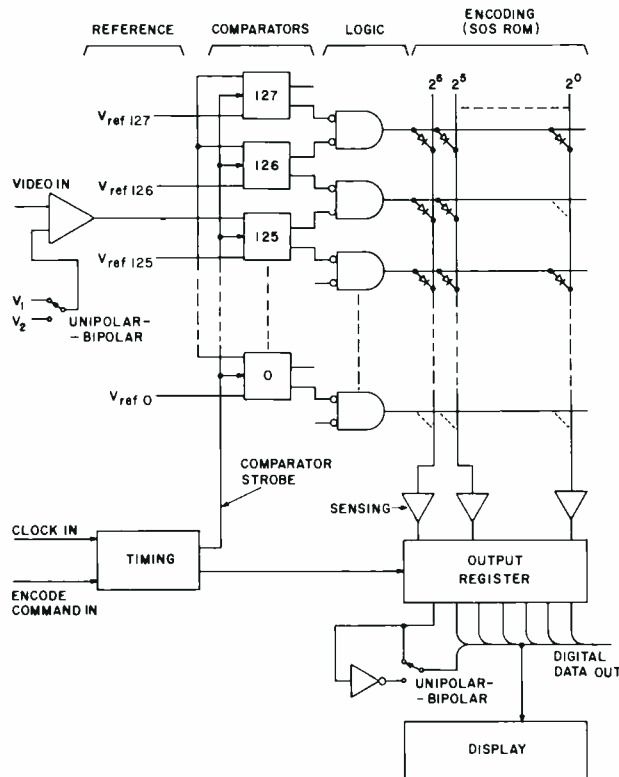


Fig. 7—Block diagram of ATL 30-MS/s, 7-b/S, A/D converter.

Packaging

The VAROM and sampling-on-the-fly principles discussed are embodied in the 30 MS/s, 7b/S (30 megasamples per second, 7 bits per sample) A/D converter built at ATL. The block diagram of this converter is shown in Fig. 7. A practical way had to be found for interconnecting

the 128-word ROM and the comparator logic. Fig. 8 shows the elegant solution of this problem, an sos ROM¹ measuring 55×58 mils and containing only 8-word lines which are coded with a fixed pattern. This chip is mounted on a thick-film substrate which also contains 8

comparators (4 Motorola MC 1650 chips) and 8 logic gates (2 Motorola MC 1663 chips). The substrate² is mounted in a 30-lead 0.8×1-inch beryllium-oxide package. This package constitutes almost a complete 3-bit A/D converter. Eight of these packages are mounted on a printed-circuit board, and two of these boards comprise the bulk of the 7-bit converter.

It is interesting to note that all the packages are completely identical, including the sos ROM's. The 128 different output codes are derived from the one fixed code produced within the 3-bit packages by discretionary wiring, which consists of drilling out a total of 28 via holes on the printed boards.

Future expansion

This highly modular packaging concept is well suited for expansion. In fact, the 3-bit modules used in the present converter and the printed-circuit boards on which they mount, contain redundant elements which allow them to be used without any modification for a 512-comparator, 9-bit converter. Future designs are aimed at increasing the sampling rate to 100 MS/s, the resolution to 8 to 10 bits, while reducing the dissipation and size. The future for very-high-speed, high-resolution A/D conversion looks bright, and ATL is building the skills necessary for securing RCA's position in this field.

References

1. Produced by the RCA Laboratories, Princeton.
2. Made by MET, Somerville.

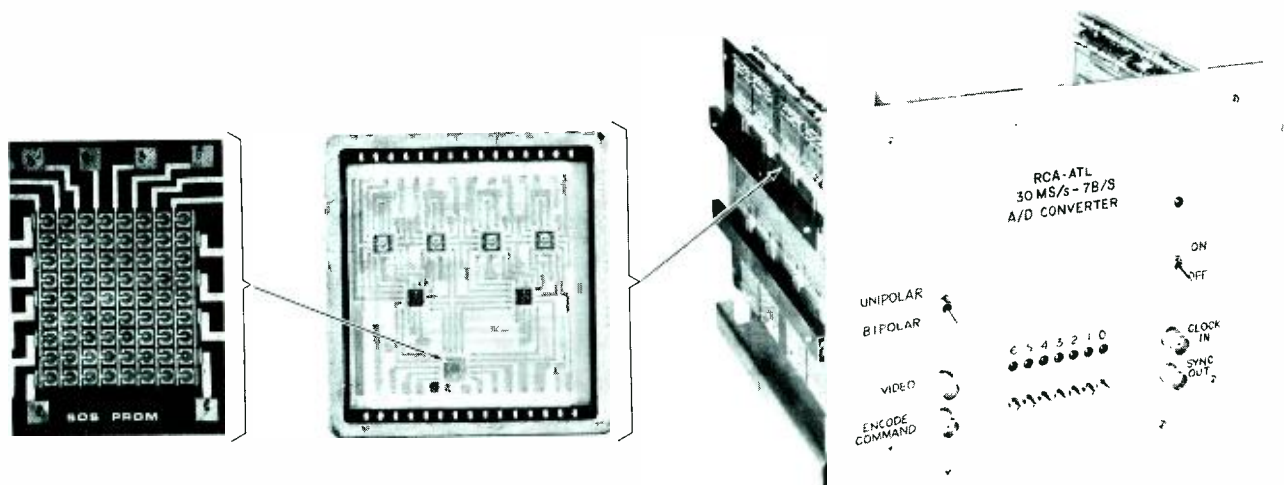


Fig. 8—The A/D converter, approximately 8×9×7 inches, dissipating 50 W., shown with the 3-bit hybrid (3.5×) and the SOS read-only memory (36×).

Simulation—methodology for LSI computer design

A. S. Merriam | H. S. Zieper

The development of LSI technology (arrays of greater than 100 gates of non-regularized logic) requires the availability and use of a variety of design aids to assure competitive cost, schedule, and implementation cycles. Such a system of design aids has been developed by the Applied Computer Systems group of the Advanced Technology Laboratories and was the basis for the successful construction of the first LSI processor using custom C-MOS arrays—the SUMC/DV. A measure of the success of the design approach described in this article is that the demonstration LSI processor, from concept to power-on, took less than one year and was checked out in less than four weeks.

H. S. Zieper, Mgr

Applied Computer Systems Laboratory
Advanced Technology Laboratories
Camden, N.J.

received the BSEE in 1955 and the MSEE in 1959 from Worcester Polytechnic Institute where his graduate-level experience included an assignment as a graduate assistant on the staff of the Electrical Engineering Department. In 1956, Mr. Zieper joined the faculty of Worcester Junior College, where his responsibilities included development and extension of the entire course of electronics study. Mr. Zieper joined RCA in 1959, being initially assigned to the BMEWS project to develop a digital check-out system for the display information processor. Subsequent assignments involved system and preliminary logic design for a number of general-purpose processors. He was a key member of the group which conceived and developed the RCA 4100-series of central processors, this work included the specification, design, and checkout of software operating systems for the RCA 400-series of equipment, and consulting work during the system design of the RCA 3301 family. Mr. Zieper assumed the position of Manager, Computer Systems Research and Applications in 1970. This group has a wide range of activity, covering the design of LSI microprocessors using C-MOS technology through software studies, including a variety of digital-system and logic-simulation efforts. As Manager of the Applied Computer Systems Laboratory, he was responsible for the enhancement of the CMOS D/A system, development of hybrid techniques, and the implementation of the SUMC-DV hardware.

Ann S. Merriam, Ldr.

Applied Computer Systems Laboratory
Advanced Technology Laboratories
Camden, N.J.

received the BA in Mathematics from Goucher College in 1945 and the MA in Physics from Bryn Mawr College in 1959. She has taught mathematics at the school and college level, and, in 1956, held a General Electric Fellowship for Mathematics Teachers. She has completed courses in electrical engineering and computer and automata theory of the Moore School of the University of Pennsylvania. Miss Merriam came to RCA as an engineer in 1959. Since then she has worked on threshold logic, systems use of content-addressed memories, logic design of an experimental test machine, logic design of an exerciser for testing high-speed carry circuits, automata theory applied to design of control in digital computer, systems descriptions in Iverson language, and system simulation in Fortran, Simscript, and GPSS. She has contributed to the logic and systems design of the demonstration vehicle for the Space Ultrareliable Modular Computer (SUMC). This year she has served as project engineer on a SUMC multiprocessor system design study recently completed for NASA's Astrionics Laboratory at Marshall Space Flight Center. Miss Merriam is a member of IEEE and an associate member of Sigma Xi.

COMPUTER SIMULATION has many advantages, at many levels, and for many purposes. Advanced Technology Laboratories has long recognized these advantages and has fostered continued development of a variety of simulation programs, both models and language. The evolutionary aspect of these efforts is an asset because a simulation which grows with a design not only earns its way but remains with potential for still further usefulness.

Simulation hierarchy

In the early stages of system planning, system simulation has proved useful in forcing system architects to make definite, though tentative, identification of critical parameters and to hypothesize solutions. The simulation itself will work out implications of these early postulations, thus freeing the architect to correct, to experiment, and to postulate further. Areas of tradeoff become apparent when a proposed

Authors Merriam (left) and Zieper.

model is studied in its dynamic form. Of all simulations, the system simulation continues most useful throughout the life of a project and after its completion because, when modified to follow the developing design, its predictive capabilities make it a correspondingly developing tool for design guidance. In its final form it will forecast final system behavior in a variety of environments.

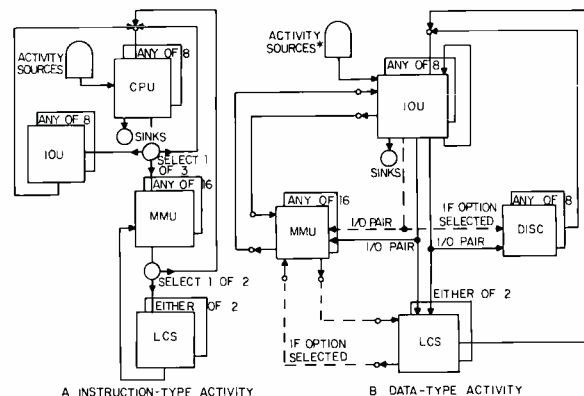
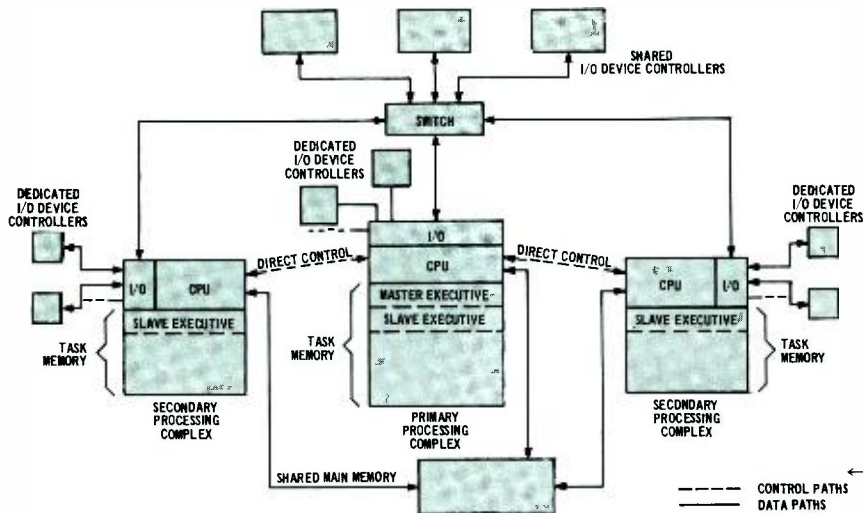
After major units and capabilities of a system have been specified, simulations in greater detail are appropriate for the study of register-to-register data paths and their control. Such detail would overburden a total system simulation; but, once details have been studied in a separate simulation, they may be summarized and fitted into the larger system simulation to increase the fidelity and sensitivity of the overall model.

At another level, still further detail can be attained by simulating the combinatorial nets and sequential logic required for data paths and control. This level supplies considerable insight into logic techniques for fault detection as well as the necessary check upon logic design.

From the comparative study of several candidate models, a promising system can eventually be built either from off-the-shelf logic modules or from relatively new components which are more fundamentally characterized. Since the second situation is the one familiar to ATL, simulations at the circuit-device level are commonly used. Parameters of such simulations typically include the physical characteristics of the semiconductors involved.

One of the inescapable facts of LSI





*INSTRUCTION-TYPE ACTIVITY MAY TRIGGER DATA-TYPE ACTIVITY
BOTH TYPES MAY GO ON MULTIPLY AND SIMULTANEOUSLY

Fig. 1—System level modular simulation—typical model.

Fig. 3—System-level modular simulation—Multimod.

technology is that electrical components, and even logic nets, are no longer individual but inseparable parts of a much larger aggregate. When the physical component or logic net cannot be probed and tested for correctness, its simulated image can. The technique can be extended from cell to chip and ultimately to the test vehicle itself which, if built in final hardware, is expensive and offers only limited variation for design experimentation. The cost of several alternatives is prohibitive. Simulation brings the study of dynamic characteristics of several candidate systems within reasonable cost.

The principles of simulation modeling can be summarized as follows:

- 1) Any detail can be simulated at an appropriate level.
- 2) Simulation of any detail can be parameterized and applied as a "black box" to a higher order simulation.
- 3) The exercise of principles 1) and 2) can be used in succession until an economical model with desired summary of results is achieved.

The fact that very good simulations have been constructed at each level of modeling tempts the imagination that a single simulation of this hierarchy could be extended vertically. In particular, the most detailed simulation could, by extended construction, include the entire system and yield the most information, yet be undesirable. Size and complexity would make the detailed simulation too costly to run and perhaps impossible to debug. Extensive summarizing would be required for comprehension of results, a process threatening to negate the investment in detail.

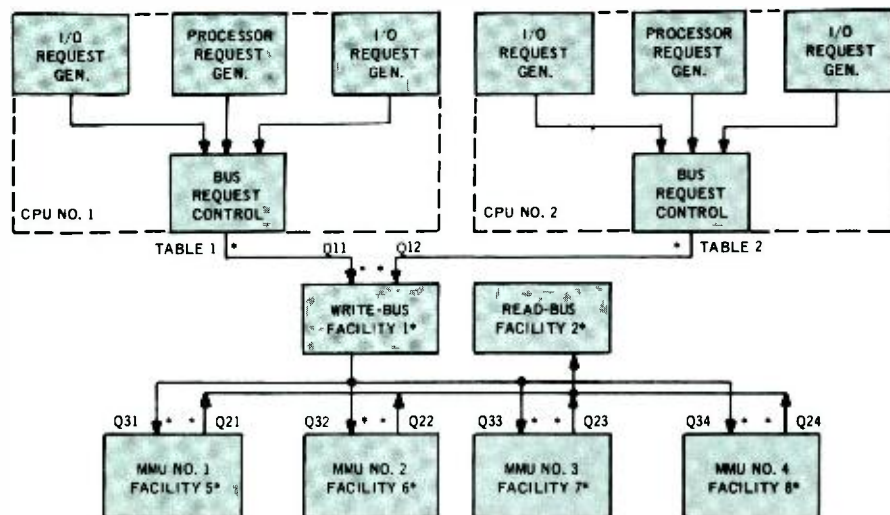
Another temptation is the desire to automate the above principles and to make the output of one simulation the input to the next. Experience indicates that, aside from the cost of really good interfacing of simulations, there is a major drawback involving automatic transition. For this, the analyst-designer must either review simulation

results and characterize the "black box" module for the next higher (less detailed) simulation or must select the relevant parameters for the next lower (more detailed) simulation. These are not routine tasks. They call on the designer's experience and judgment, and such exercise in turn builds the designer's experience and judgment. Discontinuities in the simulation hierarchy are opportunities for flexibility and innovation in the simulation schedule, which would be made rigid under automatic transition.

Modularity

Modularity has always been a common-sense feature of ATL system models and simulations. The reasons are that modularity makes for ease in model construction, program writing, program debugging, addition and deletions, and substitutions for comparisons. The last three capabilities are of particular value in making tradeoff studies. Fig. 1 shows a typical model for a multiprocessor system. Modules have been differentiated according to gross function and then according to more specific function. Although this model is strongly hardware oriented, it shows sub-modules of an executive, or conventionally software, nature. It is characteristic of a system simulation that interest is on function and feasibility rather than on implementation.

Techniques of modularity are exemplified in two "families" of system simulations developed in ATL—the Multibus and the Multimod simulations. Although these are primarily hardware models, the same modeling principles may be extended to software systems or even to firmware combinations.



*POINTS OF COLLECTION OF STATISTICS

Fig. 2—System-level modular simulation—Multibus.

The Multibus, as shown in Fig. 2, models a configuration of independently functioning central processing units, sharing the use of main memory units and independently using a common two-way bus structure. Intuition suggests that the processing power of the system increases at a decreasing rate with the addition of more central processors and more main memories because of interference on the common bus. Even a semiquantitative evaluation of this situation involves the assessment of too many factors for much further intuition.

The rate at which any central processor unit (CPU) requests use of the bus has been recognized as no simple random distribution. The present Multibus models create distributions with a mixture of modified random rate fetches and stores, and constant rate generators representing requests of I/O (input/output) devices. The simulation program is set up so that controlled bursts of I/O activity can be supplied for each CPU as the simulation run progresses. All generators are characterized by an average rate of request production which may be varied. Typically, the I/O request generators average from one-tenth to one-sixth the average rate of the CPU request generators.

Modularity not only of functional unit but of functional type is exhibited by the Multimod family of models; Fig. 3 indicates the types and multiplicity of available modules. The outstanding feature of this family is that two processing activities are recognized as distinct and almost independent:

- 1) *Instruction-type activity*, which simulates the fetching, storing, and processing of data and control information from a progression of local stores (main memory units and large core storage), and
- 2) *Data-type activity*, which simulates the simultaneous transfer of blocks of data between local stores and I/O devices (generically termed "discs" in the multimods).

Where the instruction and data activities impinge is well defined so that their interaction can be controlled and studied. Strings of I/O transfers can start and end only when triggered by occasional instructions from a central processor. Since data activity transfers will use the same memory units and backing stores accessed by a central processor (instruction type) activity, the two activities can interfere by contending

Table I—Simulation hierarchy

Application area	Simulation program	Languages
System simulation	Multibus Multimod	GPSS GPSS
Algorithm simulation	Alsim	Assembly
Logic simulation	Logsim 3, 4 Worstsim Logsim rom	Fortran/Assembly Fortran Fortran
Circuit simulation	Fetsim Ecap	Fortran/Assembly

for common facilities.

Both the Multibus and Multimod families of system simulations have proved adaptable and easily controlled.

Design package

Characteristics of the ATL approach to design based on simulation are:

- A series of programs tailored to specific level of application, and
- Each program requiring human technical interaction at points of program transition for control, adaptation and checking.

Implementation of a comprehensive variety of computer design aids has resulted in a succession of simulation programs which are integrated into a basic array implementation design automation capability. The simulation spectrum ranges from system to process level. Programs are written in a variety of languages, with each being appropriate to the particular level of the design being simulated with a specific program.

For ATL, the hierarchy of simulations is illustrated by Table I. The results of any simulation in a group tabulated here are useful (raw or summarized) to a simulation in the group directly above

until the system simulation group is reached. To select the correct simulation program, the user must establish carefully the area of application. Attempts to use a program, or language, out of its area of intent can be successful but is always inefficient. Attempts to increase the efficiency of simulation programming have fostered a multiplicity of specialized languages. At the circuit level alone, a variety are offered. In Table II, ten programming languages are characterized as to intent and features.

A set of simulation programs permits the user accurately to execute and repeat experiments on a modeled system. The use of simulation, however, does not indicate automatically that a design is valid or that errors may exist. The results of a simulation interpreted by a knowledgeable user tell a lot. For example, a logic-network simulation may indicate a potential race condition (one in which the fortuitous arrival of inputs subverts the intent of output), but it is up to the user to decide whether it will prevent him from attaining design goals. In general, a simulation is useless unless a trained user evaluates the results critically. To the new user, this fact may tend to diminish the appeal of a simulation program. On the contrary, a simulation program permits an imaginative user to make precise studies on critical areas in order to estimate the attention due any single problem area.

An arithmetic unit provides an illustration of the joint use of different simulation programs. When an adder is evaluated, and the timing, especially of

Table II—Circuit-level simulation languages.

Program Language	Features	Uses																
		DC analysis					Linear AC frequency response analysis			Transient analysis								
		Linear	Nonlinear	Sensitivity	Worst case	Stored models	User Fortran statements	Nominal	Sensitivity	Worst case	Stored models	User Fortran statements	Linear	Nonlinear	Stored models	User Fortran statements	Automatic initial condition	Equilibrium
Ecap	X																	
Asap	X	X	X	X									X	X				X
Panc	X	X	X	X														
Lisa	X		X															
Cornap	X																	
Nasap	X		X															
Sceptre	X	X			X	X							X	X	X	X	X	X
Net-ir	X	X			X								X	X	X	X	X	X
Circus	X	X											X	X	X	X	X	X
Trac	X	X			X	X							X	X	X	X	X	X

the carry, is of interest, primary factors considered include:

- Size of gate devices,
- Impact of system capacitance in at least three levels of detail,
- Logic loading, and
- Functional logic structure.

Both gate-logic and circuit simulations are used to evaluate the design. Inspection of logic tentatively identifies the critical paths. Circuit simulation establishes the switching-time ranges used within the path. Finally, gate-logic simulation verifies that the logic net will operate as intended within the switching ranges of the devices and that the path tentatively identified as critical is actually critical.

Circuit models

Over the years, ATL has been developing an integrated set of digital simulation programs at several levels of design—from the microcircuit to the total system. Each program remains usefulness to the overall design capability by supplying parameters for, or accepting parameters from, other programs in the set.

Fetsim is a sophisticated MOS-circuit-analysis program language which performs DC and transient analysis of P-MOS, N-MOS and C-MOS integrated circuits. All transistor currents and voltages are computed directly in terms of such processing parameters as oxide thickness, threshold voltage, carrier mobility, effective mask geometry, and substrate doping level. The flexibility provided by using these processing parameters permits response to an MOS technology change by ad-

justing the appropriate input parameter. By explicitly accounting for the substrate doping levels of both-N-MOS and P-MOS transistors, accurate predictions are made as to saturation currents, saturation voltages and corresponding gating effects.

Circuit-analysis programs generally employ numerical integration methods that have their step size limited when the circuit time constants are widely separated in magnitude. Since MOS circuits, in general, are of this type, the smallest time constant (which may be 0.5×10^{-9} second or less) will determine the interval of integration and so require excessively long running time. A new numerical integration program developed at RCA has been incorporated into Fetsim. The principal considerations in the new numerical integration routine involve the Jacobian matrix, which minimizes the effect of many small circuit time constants and permits larger intervals of integration. This, in turn, has produced up to 10:1 reductions in computer execution time. Further improvements in program running time can be expected when subroutines employing sparse matrix techniques are included in Fetsim.

Fetsim is supplemented by such programs as Ecap and Trac to provide a total capability in circuit simulation over a range of technologies while aimed at particular analysis needs. Table II suggests the diversity of simulations and uses possible.

Gate models

The logic element simulation languages, of which Logsim IV is a member, deal with the logic element as a Boolean transfer device with time parameters.

AND and NOR gates and J-K flip-flops are typical elements accepted by the program. Inputs to such a program are: logic-type identifiers, logic element connectivity, logic element timing data, input exercising sequences and user report controls.

Essentially, the simulator program is a test jig within which the logic network, described by the input parameters, is exercised by the logic designer. The results are then displayed in some printed form. Worstsim is a version of this basic simulation which has been especially configured to allow evaluation of pulse degradation as a function of delay tolerances associated with individual circuits. Another version is Failsim, which permits the user to evaluate logic network performance as specific elements "fail" according to statistically described modes.

Logsim IV presently heads a series of computer programs developed during the past years to simulate the logic operation dynamically at the element level. It is a binary-valued, nominal-case logic simulator in which the output levels of all elements are normally either high or low, and element output levels are switched according to delay information provided by the user. Logsim IV contains all the features of three earlier versions and adds new capabilities and features.

Written in assembly language, rather than the Fortran of earlier versions, Logsim IV accepts card formats established so that each card type can be easily recognized and interpreted by the user without any special programming knowledge. It has an easily modified structure so that new options can be added as required. Tables can be

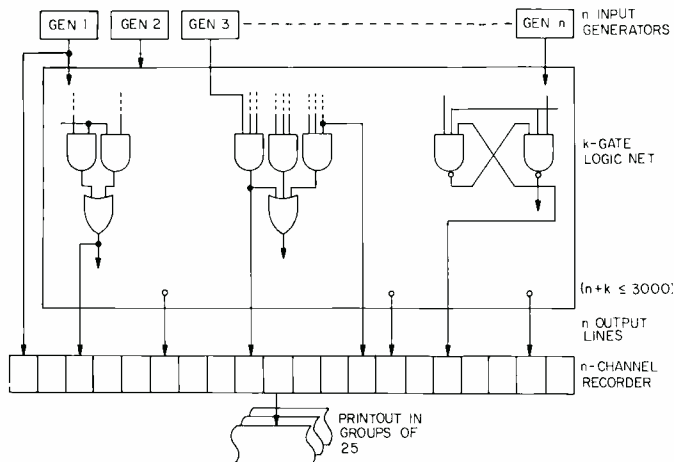


Fig. 4—Logsim simulation structure.

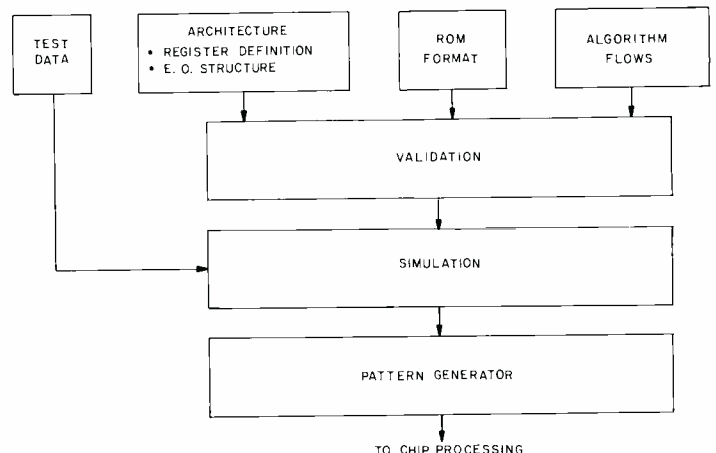


Fig. 5—Algorithm simulation structure.

expanded to accommodate new card and gate types, and most routines are written independently of other routines.

Logsim IV preprocesses the input data to find errors such as duplicated or misspelled gate names, missing input data, and inconsistent parameter specifications which would give incorrect results. Input data to Logsim IV are in the form of punched cards and data file tapes which describe the logic net and how it is to be exercised, specify operating parameters, and indicate the outputs desired. The basic output is a timing diagram listing binary output levels ("H" or "L", or "0" or "1") of selected gates during the intervals requested by the user. Diagnostic messages are printed whenever errors in input or unusual operating conditions have been encountered. Logsim IV can simulate models of a combination of up to 3000 gates and generators, and contains an internal library of 18 gate types. Provisions are included which allow the user to specify the logic structure of a gate or function not in the internal library.

The relationship of functional parts of a logic simulation are shown in Fig. 4. The generators drive the model with scheduled inputs of binary levels which are "worked through" the logic nets. The states of the outputs from these nets are recorded at timed intervals and printed in a standard report form.

Algorithm models

Alsim demonstrates use of a computer model for checking micro-operations. The purpose of the program language is to provide expression of a model of detailed architecture of a computer to be evaluated at the functional algorithm level of block diagram analysis. Fig. 5 shows the algorithm simulation components. Key initializing data describe a computer model as to:

- Block diagram details,
- Control memory format,
- Algorithm flows.

The exercising routine is a test program incorporating experimental inputs and independently calculated results. The simulation run passes the inputs through algorithmic processing as suggested by the block diagram. In this way, the simulation seeks to prove that proposed algorithms will implement the correct data transformations. This simulation is important for checking

```

LOAD REG ZFR0,0
LOAD REG ONE,1
LOAD REG TWO,2
LOAD REG THREE,3
LOAD REG FOUR,4
LOAD REG FIVE,5
LOAD REG SIX,6
LOAD REG SEVEN,7
LOAD REG MAXPDSND,1FFFF
LOAD REG INTDPDR,2
LOAD REG MULTIVDR,11
LOAD REG IDAR,00
LOAD REG X2,00060
LOAD REG X3,060
LOAD REG X4,060
LOAD REG B,20000
LOAD REG ILS,2FF
LOAD MEM MEM,100,140
LOAD MEM MEM,140,20180
LOAD MEM MEM,160,20000
LOAD MEM MEM,180,30000
LOAD MEM MEM,300,00000
TERMS E38
TRACE A E2,E38
BEGIN E1 T=10 F=50 P=20

```

Fig. 6—An Alsim program listing.

peculiar end effects which are difficult to predict.

Load cards are used to initialize register values in memory. These values and the data path are coded in hexadecimal notation for the simulator. In the sample listing of Fig. 6, registers are loaded with test controls, operand addresses, a direct operand and the address of the input device. The ILS register is loaded with an instruction address, which when incremented is the address of the next instruction in memory, and then the memory itself is loaded: TERMS E38 stops the simulation at E38, and TRACE prints out the register and bus values of each EO from E1 to E38. The BEGIN card starts the simulation at E1 and limits the run time to 10 minutes, 50 EO's simulated, or 20 pages of output—whichever is reached first.

System models

System simulation program models—Multimod, Multibus and others—are characterized by two kinds of features: those that ATL has found convenient to its general use, and those of the programming language. Because these programs are processed in a batched environment, it has been convenient to build not only a model but a "device" to control the model, both in the same package. The user then supplies parameters to the control device, which initializes, runs, reinitializes, and reruns until a series of experiments has been executed non-stop. Within any run, the control device regulates bursts of activity demanded of the model; i.e., it simulates for the model the changing requirements of a dynamic environment. After each of the runs, the control device will elicit a selection of reportable statistics for the

user. Refinement of the program control module is a feature that has accrued with experience in systems simulation.

The program models have been written in GPSS (general purpose simulation system). This is a mature and well-maintained language, written to make simulation and the results of simulation available to engineers. It is easy for the nonprogrammer to learn, and once learned, results can be quickly produced.

A GPSS program consists of a fixed framework which represents the potentiality of all activity in the model, a set of reference constants which must be initialized before a run, and some activities called "transactions" which are present for a prescribed time, and which, during that time, drive the simulation.

The background program is similar to a conventional stored program—a succession of instructions and necessary declarations. Reference constants are stored in, and accessed from, one- and two-dimensional arrays. The transactions, however, traverse the background program, temporarily activating it to simulate busy equipment or software in use. Transactions are assigned certain characteristics called "transaction parameters" by which their activities can be controlled and modified.

Collection of queue statistics, an indication of bottlenecking in the system, and establishment of frequency tables—particularly of interval times—have been made easy for the user in GPSS. Consequently, reporting of results can be rich.

Conclusion

Use of the described programs, languages, and models—and maintenance of engineering expertise in the use of them—have contributed largely to ATL's present position in the LSI-computer-design field. Because of the new economics of chip fabrication, system configurations (particularly multiprocessing conglomerates) are being postulated as never before; and because of their complexity, they must be dynamically analyzed. Time and expense preclude building pilot models. Resources have been saved and confidence gained through system simulation.

LSI computer fabrication— SUMC/DV

A. Feller

The SUMC/DV (Space Ultrareliable Modular Computer Demonstration Vehicle), which required the design and fabrication of ten different array types, was designed, partitioned, assembled, tested, and made completely operational in less than one year. The importance of the ATL simulation and design automation programs in achieving these results is discussed in Ref. 1. This paper describes the assembly, the physical and electrical characteristics, and the basic electrical testing procedures used on SUMC/DV. The paper includes a description of the packaging concepts, the physical assembly, the fabrication and testing of the various components including the LSI CMOS arrays, the hierarchy of the memory complement, the clock generation and distribution scheme, additional system testing techniques, and the procedure employed in the electrical checkout of the system. A companion paper,² describes the basic system design, logic design and array partition, program debug, system testing procedures, performance, and throughput capability of the system.

THE STANDARD-CELL APPROACH for designing CMOS LSI arrays was developed in December 1969 by Advanced Technology Laboratories, Government and Commercial Systems, with NASA support. To measure the effectiveness of this approach in designing and fabricating a series of custom LSI arrays and assembling them into a complex system within a short time, ATL received an additional contract in January, 1971 to design and fabricate

a CMOS LSI computer: the SUMC/DV.

Packaging approach

Because NASA's initial principal objective in awarding the SUMC/DV program was to demonstrate the system feasibility of designing and applying the standard cell CMOS LSI array design techniques, the project goals required

that the system and through-put requirements be achievable by low-cost commercially available, standard packaging techniques.

The SUMC/DV is contained within 10- \times 12- \times 9-in. (0.63 ft³) aluminum frame housing. Contained in this assembly is the main CPU, comprising more than 18,000 transistors (implementing more than 6800 gate functions), a 2048 \times 16-bit main memory, a 32- \times 16-bit CMOS scratchpad memory, a 256- \times 70-bit electrically programmable ROM, a CMOS clock generator and distribution system, and other circuits that perform such functions as I/O interface to the teletype, CMOS-TTI interface, lamp drivers, bipolar sense amplifiers, and voltage overload protection. The total weight is approximately 17 lbs. The power supply unit is housed in a separate, self-contained unit. A photograph of the SUMC/DV assembly is shown in Fig. 1.

Because of its flexibility and universality, the pluggable ceramic dual in-line package is used throughout the system.

A. Feller, Ldr.

Advanced Circuit Technology
Advanced Technology Laboratories
Camden, N.J.

received the BSEE and MSEE from the University of Pennsylvania in 1951 and 1957, respectively. He has also pursued graduate studies toward PhD in EE. From 1951 to 1958, he worked as a design and development engineer in the Broadcast Television activity of RCA. In 1958, Mr. Feller transferred to the Computer Advanced Development Activity. In this capacity he developed high speed circuits and interconnection techniques for proposed new computers. Since 1964, he has been active in applying computer-aided techniques to circuit design. In the bipolar area he worked on the development of a universal array that used fixed metallization patterns stored in the computer to implement complex functions. In the area of MOS circuits, Mr. Feller wrote a computer program that implemented static and transient analysis of p.n. and complementary MOS integrated circuits. This work led to the standard-cell PMOS family of circuits that are in extensive use throughout the industry. Mr. Feller was promoted to his present position in 1968. In this capacity he directed the development of applying design automation techniques for automatic generation of the mask artwork for complementary MOS circuits. In the past year, Mr. Feller directed the design and fabrication of an advanced LSI ultrareliable computer using arrays generated by a design automation technology developed under his responsibility. Mr. Feller has been awarded three patents in high speed switching circuits.

Reprint RE-18-2-12
Final manuscript received July 10, 1972.



Nine of the ten LSI arrays are housed in a 40-pin dual in-line package (DIP). The system also uses 14-, 16- and 24-pin DIP's. However, because of the high capacitance associated with this package, a substantial improvement in system performance could be achieved by repackaging using a low capacitance, multilevel, ceramic substrate hybrid approach.

SUMC/DV plug-in cards

Excluding the main memory, the SUMC/DV is contained on seven plug-gable 122-pin cards, each 7×7 in. square. One of the seven cards, the multiplexer register, shown in the lower right-hand portion of Fig. 2, which shows the inside of the SUMC/DV plus the component and wiring side of two of the cards. It contains fifteen LSI arrays, twelve 40-pin packages, and three 24-pin packages. Contained within these arrays are almost 5000 transistors performing 1700 gate functions. In addition, the card contains five standard CMOS-TTL inverter level shifters.

To provide the capability to monitor more than 90% of the various internal hardware registers with only negligible effects on the system performance, a pluggable monitoring system was designed and fabricated. This system uses 16-pin plugs attached to flexible flat ribbon cables that are permanently connected to a test set as shown in Fig. 3. The multiplexer register board con-

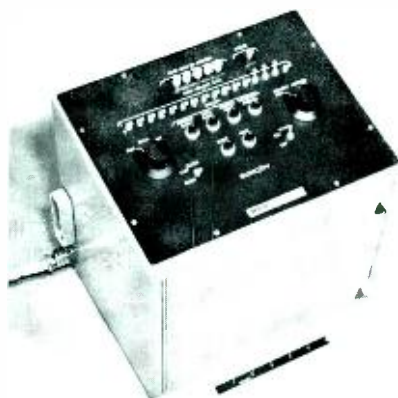


Fig. 1—SUMC/DV computer.

tains three locations that can accept the 16-pin connectors. When such connections are made, it is then possible to view directly on the test set the contents of the three 16-bit registers. The test set and its operation during the debug sequence are described in Ref. 2.

During the time the connectors and long flat ribbon cables are connected, they present a heavy capacitive load to the SUMC/DV, preventing the computer from working at its maximum rate during the debug or maintenance phase. To ensure proper program operation during this phase, the timing of the internal clock generator can be set from the SUMC/DV front panel to two nominal rates—a fast and slow mode. When the register monitor plugs are connected, the clock generator is set in its slow

mode. After the monitoring plugs have been removed, the clock is reset to the fast mode, permitting the SUMC/DV to operate at its maximum capability. The use of the test set and the ability to monitor most of the SUMC/DV circuit registers without permanently loading the system have proved to be very valuable tools in quickly debugging the computer.

Interconnection and wiring

The wiring philosophy of the SUMC/DV was based on minimizing the total interconnection capacitance, avoiding heavy wire buildup, and depending heavily on computer programming for wire list generation, wire list checking, and checking for missing and wrong connections. Therefore the wiring scheme is essentially a loosely coupled, point-to-point wiring approach. This description applies not only to the printed-card wiring as shown in Fig. 3 but also to the backplane wiring. Ground planes and power strips were not used because of the increased interconnection capacitance that would have resulted. Because of the high ratio of transition time to propagation delay, plus the high intrinsic noise immunity of CMOS circuitry, inductive crosstalk posed no serious problem.

Partitioned logic

The principal objective in partitioning the logic was to optimize the system performance. Minimizing the number of

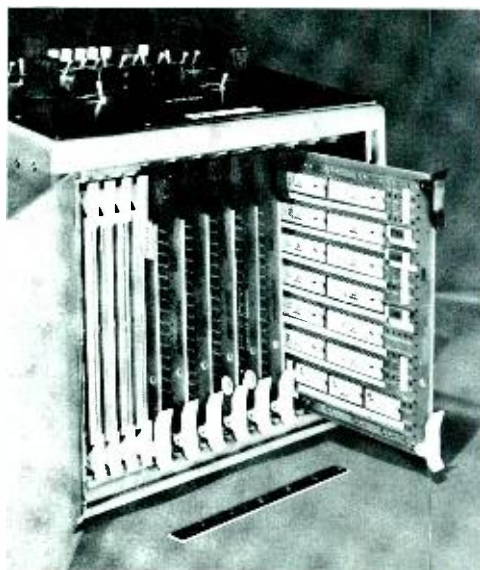


Fig. 2—SUMC/DV interior and plug-in cards.



Fig. 3—SUMC/DV with test set.

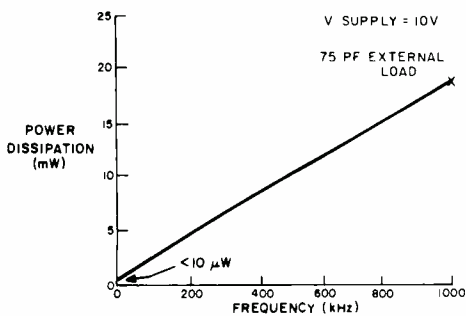


Fig. 4—PRR (001A) average power dissipation vs. clock frequency.

array types was of only secondary importance to system optimization since the principal aim of the entire SUMC/DV program was to demonstrate that the design automation programs and simulation techniques could produce a large number of LSI chip types in a short time and that the assembled and integrated chips would result in an operational system. A description of the partitioning concept from the system viewpoint is described in Ref. 2.

Basic technology

The SUMC/DV program has produced an operational computer which demonstrates the effectiveness of three technological approaches:

- 1) The use of custom LSI arrays in producing a powerful complex system with increased performance, capability, and flexibility—while simultaneously making dramatic reductions in cost, design time, weight, power, assembly and test time.

- 2) The economies, efficiencies, capabilities, and quick turn-around features of the standard-cell design automation approach for generating a large number of complex LSI arrays for a specially partitioned system.
- 3) The features and advantages of using complementary MOS circuitry in new system and equipment design. Although the outstanding features of the CMOS technology have been previously described and reported in various publications, some of the special features of this circuitry from a system viewpoint bear repeating and further interpretation.

Some of the important system features of CMOS circuitry are:

- Symmetrical high noise immunity—from system and equipment viewpoints the high symmetrical noise immunity (40 to 45% of supply voltage) of CMOS circuits is one of their most desirable features.
- Reliable operation over a wide range of temperature, process variations, circuit parameters, and voltage.
- Extremely low dissipation—reduced power-supply requirements, simplification of power distribution, simplification of package design because of virtual elimination of cooling requirements, and realization of LSI arrays.
- LSI circuits—provide dramatic reduction in weight and volume of equipment, in total number of parts (and subsequently smaller required inventory), higher performance, low cost documentation, simplification of system debugging and testing.
- Single power supply.
- Two firm single swing levels equal to supply voltage and ground.
- Extremely high speed/power ratio.
- Excellent interface capability.
- Conducive to circuit and system innovation.

Static and dynamic testing of LSI arrays

The procedure followed by ATL in testing each of the SUMC/DV arrays is described below. The testing consisted of several phases:

- *Logic simulation*—In this phase, the logic designer verifies that the logic contained on the chip implements the desired logic function. To perform this function ATL developed a series of logic simulation programs.¹

- *Automatic generation of array tests*—To test all of the gate functions on the LSI arrays, the Agat and Fltsim programs were used.¹ These programs, developed by H. I. Hellman of Communication Systems Division, automatically generate all required test sequences for combinatorial logic and provide an efficient tool for sequential logic.

It is important to note that the automatic test generation program complements the tests used in the logic simulation phase, not substitutes for them. The important distinction is that the automatic programs will provide tests that will check that the chip functions in accordance with how it is mechanized and interconnected, not as to whether it performs the logic function for which it was originally intended.

Although nine of the ten SUMC/DV chips contain sequential logic, including the hard-to-test, hidden, independent, control storage elements, it was not necessary to utilize the sequential test program. The combinatorial test generation program, Agat, was the only one required. This simplicity of testing was accomplished during the design and partition of the chip. In several cases, gates were added and/or pins dedicated to facilitating testing of the chips by combinatorial procedures only. It was a highly successful approach and

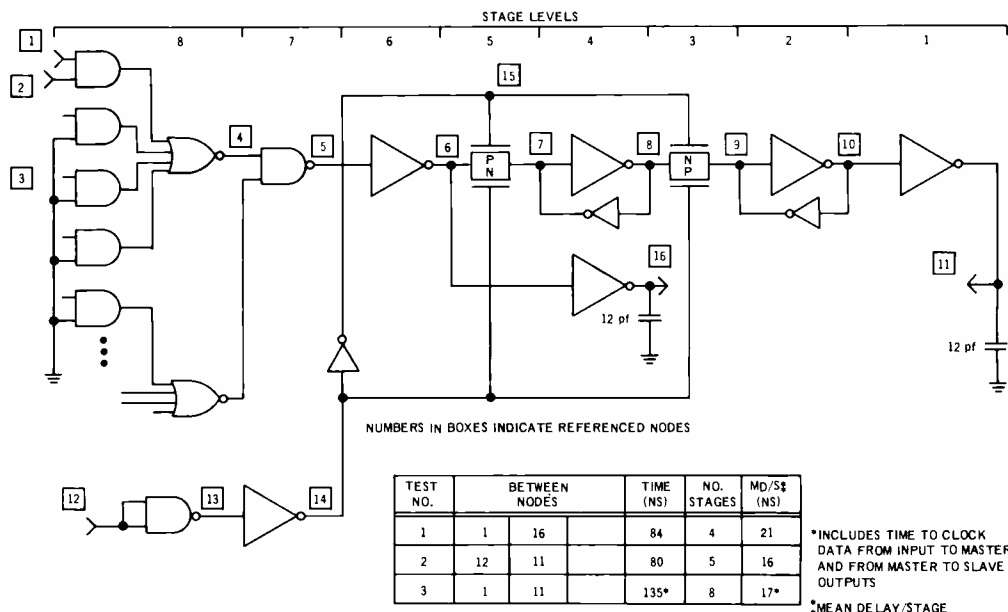


Fig. 5—Dynamic testing of PRR multiplexer register chip (type 001).

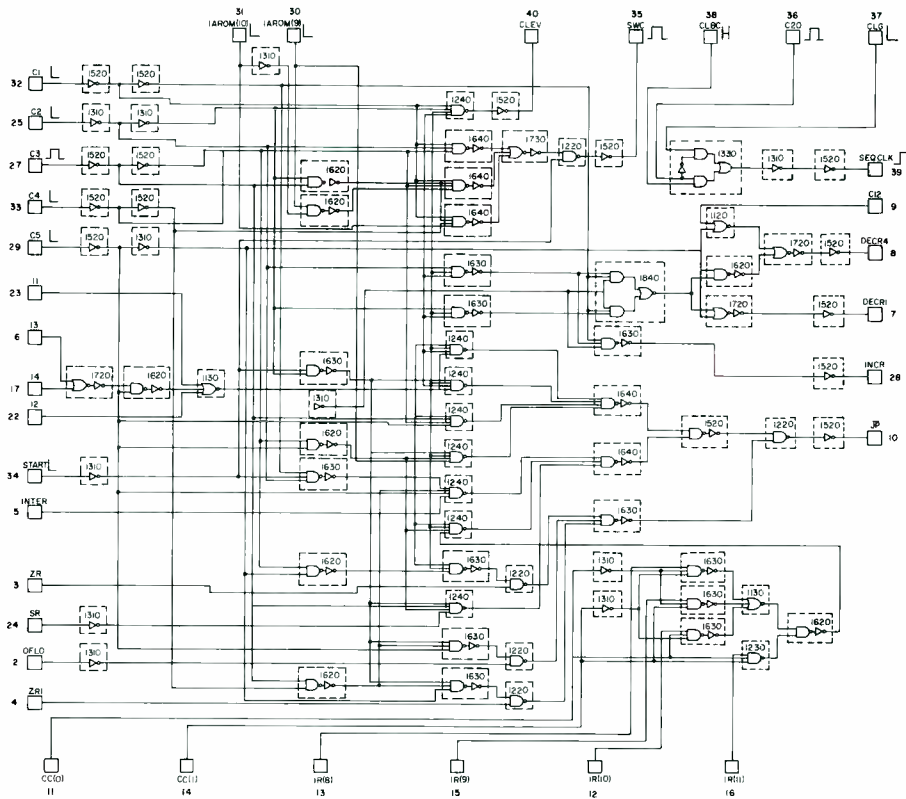


Fig. 6—Sequence counter control.

its use is encouraged as opposed to more sophisticated testing algorithms.

- **Functional testing of wafers and packaged chips**—This phase of the testing was performed by the semiconductor manufacturer with test sequences supplied by ATL. It is used as the basic for chip acceptance.

Table I—001A static leakage currents.

Batch No.	Chip No.	Leakage current (μA)	
		Inputs at ground	Inputs at 10V
7123F	9	4000	5700
7123F	12	2100	1650
7123F	17		<
7128C	1	420	0.8
7128C	2	2.3	110
7128C	3	0.4	1.0
7128C	4	0.7	0.6
7128C	6	3.0	46
7128C	7	0.4	0.4
7128C	8	1600	83
7128D	2	0.3	0.3
7128D	4	0.4	0.4
7128D	5	0.3	1.7
7135E	3	6000	1
7135E	4	1	1
7135E	5	180	1
7135E	8	1	6.5
7135E	10	1	1
7135F	1	0.4	0.4
7135F	2	0.4	0.4
7135F	5	1	1
7135F	7	1	1
7135F	8	1	1
7135F	10	1	1
7135F	12	1	1
7135F	14	1	1
7135F	15	1	1
7135F	16	1	1
7135F	19	1	1
7135F	20	1	1
7135F	22	1	1
7135F	23	1	1
7135F	26	1	1
7135F	28	1	1
7135F	29	1	1
7135F	30	85	1
7135F	31	1	80
7135F	32	1	1
7135F	33	1	1
7135F	35	1	1

- **Functional testing**—All chips were completely functionally tested by ATL with a low-cost flexible array tester built in-house for that specific purpose. The test sequence used to implement these tests was the same as that supplied to the process chip.

- **Other tests**—In addition to complete functional testing, all chips were subjected to static and dynamic testing; a few chip types were also tested at elevated temperatures and life tested. The static and dynamic tests included:

- **Leakage and dissipation measurements**—Table I shows the static leakage measurements on the PRR chip (ATL001A). This data is taken from chips delivered as part of contractual obligations. The measured dissipation for the same chip type as a function of frequency is shown in Fig. 4. These measured results approximate very closely the theoretical relationship between dissipation and frequency of operation. Table II shows the measured leakage current on ATL001A chips over the temperature range from 25°C to 100°C.

- **Dynamic (propagation delay) measurements**—Fig. 5 shows a portion of the logic and data path of the PRR chip and some propagation delay measurements taken between the various points as shown in the comparison table. For example, Test 2 in the table (Fig. 5) shows the time required to clock data stored in the master flip-flop (between nodes 7 and 8) into the slave (nodes 9 and 10) and to the output node 11. The total delay, as shown in the table, is 80 ns. Conservatively, there are five levels of logic—from node 12 to 13, 13 to 14, 14 to 15 (which

involve switching the inverter, turning off the transmission gate, turning on the transmission gate) through 9 to 10 and finally 10 to 11. This yields an average measured propagation delay of 16 ns. Average stage delays as measured on the chips varied from 13 to 35 ns. Propagation times in the SUMC/DV system were longer because of the large capacitance associated with the package and the interconnection system.

Another example of some of the measured propagation delay is shown in Table III, which lists the total and average propagation delays for various logic paths of the Sequence Counter Control chip, ATL010, shown in Fig. 6. Table III contains data for seventeen ATL010 chips. The numbers on the top row of the table designate the input and output nodes, while the associated waveforms indicate the polarities of the input and output signals.

Table II—001A static leakage life test at elevated temperatures.

Date	Temperature (°C)	Leakage Test Chip 1 (μA)	Leakage Test Chip 2 (μA)
7/8/71	25	25	0.014
7/9/71	60	33	0.055
7/13/71	60	41	0.16
7/19/71	60	41	0.15
7/30/71	60	41.5	0.16
8/6/71	60	42	0.19
8/12/71	60	42	0.20
8/18/71	60	42	0.18
8/30/71	60	42	0.20
9/10/71	85	43.5	0.40
9/13/71	85	43.5	0.21
9/21/71	85	43.5	0.22
9/28/71	85	44.5	0.21
10/5/71	85	44	0.21
10/12/71	85	43.5	0.21
10/18/71	85	43.5	0.19
10/25/71	100	46	0.23

Table III—Propagation delay of sequence counter control array (ATL010).

Batch No.	Chip No.	Delay time (ns)		C_L (pF)	Delay time (ns)		C_L (pF)	Delay time (ns)		C_L (pF)
		27	35		27	35		9	8	
EVAL	1	98	118		43		48		40	
EVAL	2	100	114	10.4	45		47	12.1	39	10.6
EVAL	3	108	122		49		47		42	
7148A	1	106	120	10.8	44		48	12.7	41	10.9
7148A	2	112	130		48		54		44	
7148A	3	95	112	10.7	44		48	12.3	41	10.8
7148A	4	106	124		45		50		42	
7148A	5	110	126	10.9	48		52	12.6	44	11.0
7148A	6	116	130		49		54		46	
7148A	8	115	130	10.6	48		54	12.3	44	10.9
7148A	9	104	122		47		50		42	
7148A	11	106	122	10.8	48		52	12.5	43	11.0
7148A	12	114	129		48		53		45	
7148A	13	102	120	10.8	47		51	12.5	42	10.9
7148A	14	108	123		47		51		43	
7184A	15	105	122		46		51		42	
7148A	17	114	131	11.0	51		53	12.5	43	11.0
Average delay (ns)		107.0	123.2		47.0		50.8		42.5	42.7
Average stage delay (ns)		13	15		12		12.5		10.5	10.5

The measurements were taken with a 10-V supply source.

Principal components

CPU (central processor unit)

The CPU essentially defines the basic computer structure and contains the hardware logic and decoders, the arithmetic functions, the wired control, and the data path. It is the portion of the system mechanized with the 54 standard-cell LSI arrays containing more than 18,000 transistors performing more than 6800 gate functions. There are ten different chip types; therefore each chip type is used an average of 5.4 times. Contained within these chips are four 16-bit, two 6-bit, and 7- and 8-bit registers. They are divided between master-slave and storage types. All but one of the 16-bit registers can be monitored directly on the special-purpose test set by way of the flat ribbon-cable connections. Although the CPU power dissipation is extremely difficult to measure accurately because of its low relative level, it appears to be operating at a 700-mW static level.

Main memory

The main memory is a 2048×16-bit purchased, self-contained TTL memory system comprised of four boards, each one containing 1024×8 bits.

The memory operates from a +5-V and -5-V supply source, operates at TTL levels, and consumes a measured 26 W. It is planned to add an additional 2048×16-bit beam-lead CMOS memory to the SUMC/DV before the end of the year. This memory, which will dissipate 1 watt of power at a 1-μs cycle time, is being developed by Solid State Technology Center.^{4,5}

Microprogramed read-only memory and instruction-address read-only memory

The microprogramed ROM containing 256 words with a 70-bit field and the IAROM containing 256 words with a 21-bit field is implemented with an electronically programed MOS memory that can be reprogramed. Each of the ROM chips contains 2048 bits organized in a 256×8-bit structure. Twelve such memory chips are used operating at a 15-V level and dissipating approximately 6.1 W.

Timing generation and distribution

The basic SUMC/DV timing is derived from a local adjustable oscillator driving a two-phase synchronous system utilizing two static shift registers. The SUMC clock pulses are derived by gating the various parallel outputs of the shift register. The basic operating speed of the SUMC is geared to the length of the elementary operation (EO) time, which is determined by the shift registers and the associated feedback circuitry. All of the clock generation and distribution utilizes standard COS/MOS circuitry.

A second oscillator, using the same basic configuration as the main oscillator but designed to operate with wider clock pulses, is available for use during the debugging or maintenance phase when the test set is connected.

The clock circuitry, including the buffer drivers, is contained on the IR board. The fanout requirements for the various clocks vary from 1 to 17. The fanout reaches out to all boards except the main memory and the IR board.

The power supply is a commercially available self-contained unit containing

three regulated supplies in one separate housing. The three supply voltages are +10, +5 and -5 V. Each of the supplies contains overvoltage protection and current limiting circuitry.

In addition to the self-contained protective devices in the power supply, additional protection is included in the SUMC/DV assembly. This includes separate fuses, zener diode overvoltage protection, and interconnecting supply diodes to eliminate the need for power-supply sequencing.

With the exception of some printed wiring along the edge of the cards, all power distribution is through conventional wiring.

The measured dissipation in the SUMC/DV is 38.8 W. Of this, 0.4 W is computed to be dynamic power. Table IV gives the SUMC/DV dissipation in terms of its three supplies. Dissipation associated with the two 5 V power supplies is in the memories and interface circuitry.

Table IV—SUMC/DV dissipation.

Supply (V)	Dissipation (W)
10	7.80
5	28.25
-5	3.7
Total	39.80

An approximate distribution of the dissipation in SUMC/DV is shown in Table V. The dissipation measurements of the main, MROM, IAROM, and scratchpad memories and the top panel are reasonably accurate. The dissipation associated with the various level shifters, terminating resistors and other discrete components is defined by the spread of 2.9 W to 5.2 W, representing estimated values of the average to the maximum dissipation. The total measured dissipation is 39.8 W. As shown in Table V, the difference between this measured total and the sum of the other components is 0 to 2.1 W, depending on the actual value used for the level shifter and discrete components. The bottom row in the table shows the dissipation (under normal dynamic operating conditions) obtained by a different approach, using both measured and computed information. There is fair correlation between the bottom two rows, indicating that a 1.1-W dissipation for the CPU (all CMOS circuits except memory and level shifters) is a reasonable one.

Table V—SUMC/DV power dissipation distribution.

SUMC/DV component	Measured dissipation (W)
Main memory	26.00
MROM and IAROM	5.64
Scratchpad	1.66
Top panel	1.50
Level shifter and discrete components	2.9 Average to 5.2 Maximum
SUMC/DV less CPU	37.7 to 40.1
SUMC/DV total (measured)	39.8
CPU	39.8 - 27.7 = 2.1
CPU (combined direct measurement and computed)	1.1

Preparation for program debug and performance verification

One obvious byproduct of implementing the system in CMOS LSI arrays is the dramatic reduction in total parts. Not including the main memory, scratchpad memory, mechanical items and lamps, there are 175 components, including the 54 LSI arrays, the commercially available COS/MOS and TTL IC's, resistors, capacitors and diodes. This reduction in total parts, combined with the physical compactness that resulted, greatly simplified and facilitated the initial debugging phase of the SUMC/DV program. A brief description of the important parts of that phase follows.

The steps involved in testing the LSI arrays have already been described. Testing of the LSI arrays serves as a functional check of most of the logic circuitry in the SUMC/DV since more than 90% of its logic is contained on the LSI arrays. Wirelists were generated by computer programs that sorted the signal wirelist in several ways: checked for opens, for missing and incorrectly programmed wires, and provided the basis for ohmic connectivity measurements.

Beyond the checking of the arrays and the wiring, three of the seven SUMC/DV cards received no additional checking before the program and performance debug phase. These three boards contained a large portion of the multiplexed data path, one of the two SUMC/DV 20-bit adder units, and the microprogrammed ROM and data registers. A fourth board, containing the other full 20-bit adder unit, was partially checked on the RCA Camden computer test facility. For this testing, a series of 15 test sequences, 72 bits wide, was generated by a joint

effort of CSD and ATL. The remaining tests were implemented in the SUMC/DV itself simply because of the early availability of the computer. The board containing the clock generator circuitry was debugged off-line in a conventional breadboard fashion since it consists of conventional COS/MOS circuits. The same applies to the CMOS scratchpad board. This board contains a complete 32×16-bit CMOS scratchpad with COS/MOS addressing and decode logic and uses RCA CA3054 bipolar sense amplifiers. The last board, containing input/output buffers and interfacing circuitry for communicating with a local teletype, was debugged on-line after the teletype connection was made.

Each of the main memory boards, containing a commercially-purchased fully-decoded beam-lead 1024×8 TTL memory with sense amplifier was checked out in at least two ways. Initially, the memory was tested on a special-purpose memory exerciser which tested the memory boards with worst-case patterns over the stipulated voltage range. The memory boards were checked again in the SUMC/DV, under normal operation conditions, with special purpose test programs that again exercised the memory in various operating modes.

For the reprogrammable MOS memory, extensive testing was done on several of the 256×8-bit chips to determine the input/output interfacing capabilities and requirements, the driving capability, the supply voltage requirements, and the access times. The ROM is used in such a way that an additional level shifting interfacing circuit is not needed between the TTL (0 to 5 V) main memory and the CMOS MROM registers.

To load the MROM memories, the desired bit sequences are programmed onto paper tape which is forwarded to the semiconductor manufacturer. Upon receipt of the programmed chips, each one is functionally checked to verify that the ROM fields have been loaded with the correct sequences.

The procedure for checking the ROM's uses the ATL array tester in exactly the same way as for the CMOS LSI arrays. An operational check of all controls plus final changes of the power supply adjustment and distribution completed the checkout.

Conclusions

A CMOS LSI general purpose computer,

using ten LSI array types, was designed, assembled, and checked out in less than one year. The LSI arrays were generated by the standard-cell design automation approach developed by ATL. The computer consists of more than 20,000 transistors, 18,522 of which are contained on 54 LSI arrays. The 18,522 transistors provide 6,856 gate functions, resulting in an average of more than 125 gates per chip. Weighing less than 17 lbs and occupying a volume of less than $\frac{2}{3}$ ft³, the total system, including a 2048 × 16-bit TTL memory, a 32×16-bit fully-decoded scratchpad memory with bipolar sense amplifiers, and eleven 256×8 MOS ROM chips, dissipates 39.8 W. The three memories alone dissipate 33.3 W of this total, with the main memory operating at a 26.0 W level.

Not including the main memory, the computer is contained on seven commercially available plug-in cards. The cards represent a low-cost packaging approach since no ground planes are required and all wiring is point to point.

Aided by computer programs developed by ATL and CSD, all of the arrays were tested functionally and dynamically on a low-cost array tester constructed in ATL. The computer programs used to check the arrays and to design and generate them are available in most RCA locations.

With most of the SUMC/DV system contained on the LSI arrays and the various memories, the number of total parts is minimized. This minimization of total parts, combined with the resulting compact system, greatly facilitated and simplified the checkout and debugging phase of the SUMC/DV program. This proved to be an outstanding additional benefit of using LSI arrays to implement complex systems.

Acknowledgment

R. Geshner provided the mask sets for this program; I. Kalish, W. Lewis, and C. Mulford, Jr. processed the wafers quickly and efficiently; and H. Borkan and T. Mayhew packaged and did the initial testing of the CMOS LSI arrays.

References

- Merriam, A., and Zieper, H. S., "Simulation: methodology for LSI computer design," *this issue*.
- Clapp, W. A., "LSI computer design—SUMC/DV," *this issue*.
- Feller, A., et al., "Computer-generated low-cost custom CMOS arrays," RCA Reprint, *Solid State Technology*, PE-552; *RCA Engineer*, Vol. 17, No. 3 (Oct/Nov 1971) pp. 10-15.
- Murray, L. A., and Richards, B. W., "Beam lead COS/MOS integrated circuits," *ibid.*, p. 50.
- Greig, W. J., Murray, L. A., Oberman, J. R., et al., "Manufacturing Methods for COS/MOS Memory," Tech. Rpt. AFML-1R516-0(11) (Sept. 1971).

LSI computer design— SUMC/DV

W. A. Clapp

Advanced Technology Laboratories has designed, built, and tested the first CMOS general-purpose computer. The computer executes 32 instructions that are operation-code compatible with the IBM 360 and RCA Spectra 70 series of computers. The computer is supported by 2k words of main-memory LSI storage and a TTY peripheral for input and output operations. Additionally, a simulator, an assembler, and a loader have been constructed to provide software support to the hardware. This paper and its companion in this issue¹ provide an overall picture of this computer project. The project proceeded from block diagram to a debugged, operational computer in 12 months.

W. A. Clapp, Ldr.
Machine Organizations
Advanced Technology Laboratories
Camden, N.J.

received the BA in Physics from Kalamazoo College in 1963. He received the BSEE and MSEE from the University of Michigan in 1964 and 1965, respectively. Since joining RCA in 1965, he has participated in the design and development of several digital equipments. These include solid-state display systems, high-speed magnetic-tape controllers, a real-time high-speed computer interface, and an interactive graphic display system. For the past four years, he has been directly involved with the application of large-scale integration to high-speed computing systems and real-time processing. This work includes the design of integrated arrays, the logic design of computers, and overall system definition for both general-purpose and special-purpose computer systems for military applications. Mr. Clapp has also been instrumental in RCA digital simulation efforts. Recently, Mr. Clapp has worked on tradeoff evaluation studies leading to the definition and specification of unique computer systems made feasible through the application of large-scale integration techniques. Mr. Clapp currently leads a group that has major programs in the design of associative processors, the design and application of LSI computers, digital system simulation studies, and the definition and application of digital system organizations. He is a member of the IEEE, Tau Beta Pi, and Eta Kappa Nu. He has taught seminars in digital simulation techniques, general electronics, and digital computers.



SPACE ULTRARELIABLE MODULAR COMPUTER DEMONSTRATION VEHICLE (SUMC/DV) is the first operational member of a series of LSI computers of the SUMC family. Preliminary work in computer systems and technology development has already begun on other members of the family. The specific goals of the SUMC/DV computer program are threefold:

- 1) To demonstrate the advantages in both time and cost of LSI design automation techniques;
- 2) To investigate and characterize the CMOS technology in an actual system environment; and
- 3) To fabricate a 16-bit demonstration-vehicle LSI computer ignoring packaging considerations and the speed of instruction execution.

By ignoring packaging considerations, the overall cost of the program was substantially reduced while simultaneously verifying the usefulness of the SUMC computer concept. Program costs were also minimized by not striving for ultra-high-speed instruction execution speeds because money was saved in the type and speed of memory units used in SUMC/DV.

System design

The SUMC/DV is a microprogrammed, real-time, general-purpose computer which combines several system components proven in previous computer designs. The data path and control philosophy are based on the SUMC computer developed at the NASA Marshall Space Flight Center. The instruction set and simultaneous input-output capability are based on the RCA Spectra 70 and IBM 360 computers, while the real-time multilevel interrupt structure

is based on the RCA 4100-series computers.

The data path is structured to provide a basic fixed-point set of instructions, with the ability to add a floating-point module that complements the hardware already present for fixed-point instructions. The data path is also designed to provide fast execution of the multiply, divide, and square-root instructions.

The control philosophy is based on a two-level hierarchy of microprogram control. The first level of control provides a set of control lines unique to a given step of the algorithm execution. This is the basic elementary operation (EO) level. The second level provides control levels unique to a particular instruction. This second level of microprogram provides control by instruction class or instruction type and therefore eliminates numerous decoding gates and flip-flops in the control logic.

Instruction formats

The addressing philosophy and instruction formats of SUMC/DV are identical with those of IBM 360, RCA Spectra 70, and RCA 215. The programmer is provided with a set of general-purpose registers, which are available to be used at the discretion of the programmer for base registers, index registers and fixed-point accumulators. Instructions then are provided to operate on data in memory, in a general register, or any combination of the two locations. The SUMC/DV departs from the IBM 360, RCA Spectra 70, and 215 computers in three ways:

- 1) It provides only single-length operands.
- 2) It provides a reduced number of general registers available, and
- 3) It provides a subset of the complete instruction repertoire.

All operands in SUMC/DV are 16 bits, and all Spectra 70 instruction types, when employed on the SUMC/DV, refer to 16-bit operands. The general register set available to programmers is eight halfword (16-bit) registers used as accumulators and index registers instead of the 16 fullword (32-bit) registers provided in Spectra 70. In addition, only four of the five instruction formats of Spectra 70 are provided in SUMC/DV. These formats are:

RR—register to register
RX—register to indexed main memory
RS—register to main memory

SI—main memory and immediate operand operation

The instruction subfields described below are defined as follows:

- R₁, R₂, R₃—four-bit general register designation used for an operand.
- X₂—four-bit general register designation used for indexing.
- B₁, B₂—four-bit general register designation used for base addressing.
- D₁, D₂—twelve-bit displacement.
- I₂—eight-bit immediate operand.
- M—four-bit mask.

For the RR format, the contents of the general register specified by R₁ is the first operand. The contents of the general register specified by R₂ is the second operand. The first and second operands can be the same, designated by identical R₁ and R₂ addresses:

OpCode	R ₁	R ₂
0	7 8 11	12 15

For the RX format, the contents of the general register specified by R₁ are the first operand. To obtain the address of the second operand, the contents of the general registers specified by X₂ and B₂ are added to the D₂ field.

OpCode	R ₁	X ₂	B ₂	D ₂
0	7 8 11	12 15	16 19	20 31

The RS format is used by shift instructions. The contents of the general register specified by R₁ are the first operand. The contents of the general register specified by B₂ are added to the D₂ field. The sum specifies the number of bits shifted over by the shift operation. The R₃ field is ignored.

OpCode	R ₁	R ₃	B ₂	D ₂
0	7 8 11	12 15	16 19	20 31

In the SI format, the contents of the general register specified by B₁ are added to the contents of the D₁ field to obtain the address of the first operand. The second operand is the immediate eight-bit byte in the I₂ field of instruction.

OpCode	I ₂	B ₁	D ₁
1	7 8 15	16 19	20 31

Interrupt structure

A significant feature of the SUMC/DV computer is the availability of three

priority-interrupt levels which allow the system to meet real-time control applications. The primary purpose of the priority-interrupt system is to eliminate the need for program-controlled scheduling and status testing of input/output transfers and to provide for servicing a multiplicity of programs on a priority basis. Each interrupt level has associated with it a number of input/output devices and a completely separate set of general registers. Each level has an assigned priority, and operates only if that level is the highest requiring service.

The interrupt structure is designed such that the highest priority level demanding service is in control of the system. Before execution of each instruction, the interrupt requests are examined to determine which of the levels demanding service has the highest priority.

This examination occurs during the instruction fetch and operand fetch activities, but ends before any registers have been altered. If the currently active program has the highest priority, the program proceeds without interruption; otherwise the system automatically transfers to the demanding level which has the highest priority.

When all the higher priority demands are satisfied, control returns to the interrupted program, which proceeds oblivious of the interruption. In this way, the priority-interrupt feature enables the data processor to interleave a number of different programs.

As mentioned above, each priority level may have associated with it a number of input/output devices. Whenever a device generates an interrupt, it is directed to the priority level associated with that device. However, a program currently running in a given priority level can address any device on any level.

An interrupt level may become "active" by either of two methods. The first method is by a peripheral device generating an interrupt. This will force the computer to the priority level associated with the particular input/output device when this priority level is the highest one requesting service. The second method is through the use of the program-control instruction. This instruction allows the programmer to alter bits of the interrupt register to control level changes. The flowchart of the

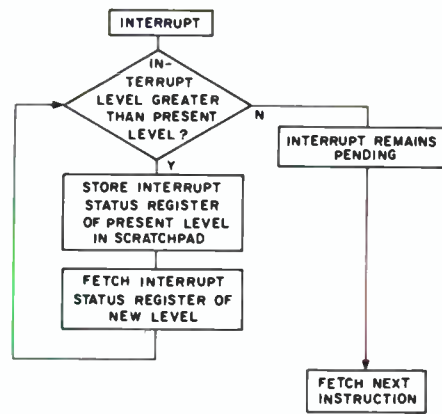


Fig. 1—Interrupt response.

interrupt action is shown in Fig. 1.

Program status register

Each program (interrupt) level has associated with it two halfword status registers which are located in scratchpad and which store the status of a program. The first one, the program register, contains the program counter which is the address of the next instruction to be executed at any given program level. The format of this register is shown below:

Not used	Next instruction address
0 3	4 15

The second one, the interrupt status register, stores the status of the program. A six-bit hardware register stores this information during actual program execution. When a program level is changed, the contents of the hardware register are stored in a standard scratchpad location dedicated to the level being changed. The new content appropriate to the new processing level is brought out of its standard location in scratchpad and inserted.

The register contains four fields as indicated below:

ILC	CC	ILI	Future expansion
0	1 2	3 5	6 15

- ILC—instruction length code, indicates whether the current instruction is word or halfword.
- CC—condition code, indicates the progress or result of the current instruction.
- ILI—interrupt level indicator, indicates the priority level of the previous program.

Input/output

The SUMC/DV provides two types of I/O

instructions: programmed I/O and simultaneous I/O. The programmed I/O provides the capability of transferring a halfword (16 bits) each time the instruction is executed. The simultaneous I/O provides the capability of initiating a device and then allowing it to transfer data to, or from, the main memory without further programmer intervention. Upon completion of the transfer, the device will generate an interrupt at the level assigned to the device. This operates like a direct memory access channel on current computers.

The simultaneous input-output operations are performed with the central processor unit (CPU) processing on a cycle-steal basis to main memory. Channel command words are set up by the program prior to executing an I/O instruction. For each halfword data transfer between the main memory and the peripheral device, the control words stored in scratchpad memory are accessed and updated. When the total amount of data requested by the program has been transferred, the peripheral device generates an interrupt, indicating that the desired transfer has been completed.

The complete I/O transfer is performed under read-only-memory (ROM) control using two halfword channel control registers. Channel control register I

(CCRI) contains the I/O command and the main memory address of the next data to be transferred. Channel control register II (CCRII) contains the physical address of the peripheral device (obtained from the I/O instruction) and the remaining count of halfword data yet to be transferred. The format of the two registers is shown below:

CCRI	Command		Main memory data address	
	0	3	4	15

CCRII	Device address		Remaining halfword count	
	0	3	4	15

The SUMC/DV provides for 16 I/O device addresses, and up to 4096 halfwords of data to be transferred in one operation.

Once the two control registers are set up in scratchpad memory, the input-output operation is initiated with a start device (SDV) instruction. After being started up, the peripheral device generates a service request when it is ready to transfer data. The CPU checks for the presence of a service request upon the completion of an instruction execution. If a service request is present, the

ROM control jumps to an input-output service routine prior to executing the next instruction. The input-output operation can be halted at any time by the execution of a halt device (HDV) instruction.

A second type of input-output instruction provides programmed I/O capability. By use of the read direct (RDD) and write direct (WRD) instructions, one halfword of data is transferred between the main memory address and peripheral device address specified in the instruction.

All peripheral devices are connected to SUMC/DV via a custom input-output interface. The SUMC/DV processor allows for direct functional addressing of 16 I/O devices, each of which is associated with one of three priority levels in the computer. Thus, when interrupts are generated by input/output devices, they are serviced on a priority basis. Devices can be initiated from any priority level; but, if an interrupt is required, it will be generated by a device at the priority level with which it is associated.

Emulation

Since the SUMC/DV is a microprogramed computer, it is capable of emulating other computer structures. It has

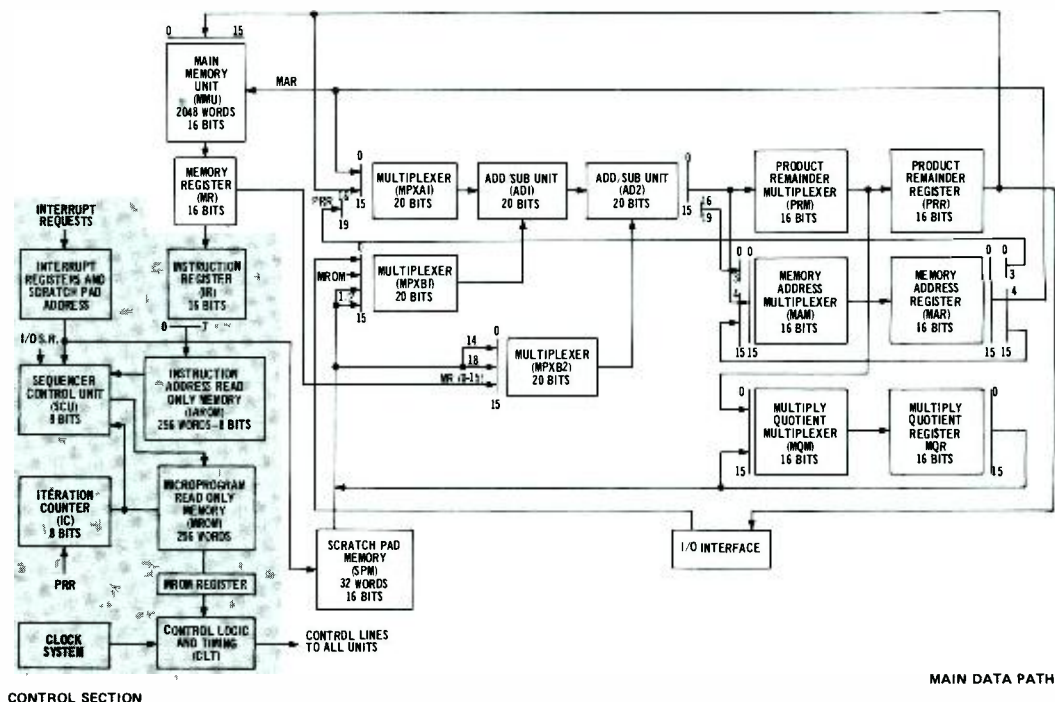


Fig. 2—SUMC/DV block diagram.

already demonstrated this flexibility. An entirely different computer system (instruction format, word size, addressing philosophy, interrupt structure, and input/output scheme) has already been built and delivered. Using the emulation capability of SUMC/DV, a completely new, custom tailored, LSI computer was designed, built, and delivered in three months.

Logic design process

The block diagram of the SUMC/DV computer is shown in Fig. 2. The main data path consists of an input multiplexer section (MPXA1, MPXB1, and MPXB2), tandem adders (AD1 and AD2), and output multiplexer section (PRM, MAM, and MQM), and three output registers (PRR, MAR and MQR). Data can be selected from the product remainder register (PRR), the memory address register (MAR), the memory address register (MR) or the scratchpad memory (SPM) by the input multiplex section and gated into the adders (AD1 and AD2). The output multiplexer section performs straight transfers, left or right shifts, and data-fill operations on the data from the second adder (AD2) prior to storage in one or more of the three output registers. The input multiplex section and the tandem adders are 20 bits wide, even though the data length is 16 bits. The extra 4 bits in the adder allow the multiply-and-divide algorithms to be accomplished 4 bits at a time.

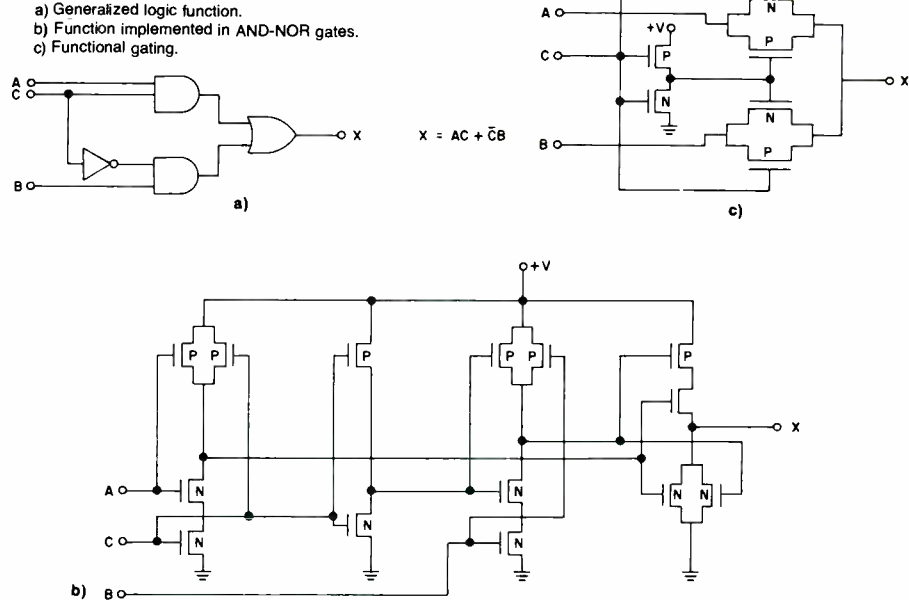
The scratchpad stores three independent sets of general registers and program status registers, one set for each of the three interrupt-level programs. Additionally, the two control registers for the simultaneous I/O are stored here. A memory map for the scratchpad memory is shown in Table I.

The control section of the SUMC/DV, as

Table I—SUMC/DV scratchpad memory map.

Physical Address	Contents	Physical address	Contents
0 GR1	Level 1	16 GR1	Level 3
1 GR2	Level 1	17 GR2	Level 3
2 GR3	Level 1	18 GR3	Level 3
3 GR4	Level 1	19 GR4	Level 3
4 GR5	Level 1	20 GR5	Level 3
5 GR6	Level 1	21 GR6	Level 3
6 GR7	Level 1	22 GR7	Level 3
7 GR8	Level 1	23 GR8	Level 3
8 GR1	Level 2	24 PGM CNTR	Level 1
9 GR2	Level 2	25 ISR	Level 1
10 GR3	Level 2	26 PGM CNTR	Level 2
11 GR4	Level 2	27 ISR	Level 2
12 GR5	Level 2	28 PGM CNTR	Level 3
13 GR6	Level 2	29 ISR	Level 3
14 GR7	Level 2	30 CCR1	Level 3
15 GR8	Level 2	31 CCR2	Level 3

Fig. 3—CMOS logic implementation of multiplex function.



shown in Fig. 2, consists of the instruction register (IR) which holds the instruction currently being executed, the IAROM which performs the translation of instruction operation code into an address for the microprogram ROM (MROM) and contains the control levels unique to an instruction, the MROM which contains all of the first level control words, the sequencer control unit (SCU) which is the address register for the MROM, the iteration counter (IC) which counts loops on iterations, and the interrupt registers which perform the hardware priority interrupt and scratchpad addressing.

Logic design

All of the logic was designed by using the C-MOS technology. This technology provides a very flexible and powerful logic implementation capability. The designer has his choice of straight gate implementation using AND, OR, NAND, NOR gates (the designer is not restricted to special gate types, as in some technologies) or a functional gating that was developed and used with relays several years ago. The choice of implementation for any one function depends on desired speed, transistor count, and boundary conditions of the possible set of input functions. An illustration of this choice is shown in Fig. 3. Fig. 3a shows the generalized logic function, Fig. 3b shows the function implemented in AND-NOR gates, and Fig. 3c shows the function implemented using functional gating. In this case, the functional gating shown in Fig. 3c can

be used only if one of the inputs is always present. If such is the case, eight transistors out of fourteen can be saved in the implementation of this logic function.

From the viewpoint of the logic designer, the only drawback to using CMOS is that there is a limitation with the "wired OR" capability. In CMOS, this function can be implemented only with transmission gates and hence does not have the driving power of a standard transistor gate. This drawback is offset, however, by the many system benefits of using CMOS, most of which are discussed in Ref. 1.

As stated earlier, one of the goals of this program was to utilize custom-designed LSI arrays. With a design automation system to support the chip design and fabrication process, logic designers are no longer constrained to design and use standard parts. The general guidelines provided to the designers for SUMC/DV were the following:

- 1) If a modular design is desirable, aim for a 4-bit module;
- 2) All arrays must have 40 pins or less, including power leads; and
- 3) The arrays should not contain more than 150 gates.

These guidelines were used to partition the SUMC/DV logic into ten array types. Table II shows the ten array types, along with their statistics. The array types are identified by their three-digit ATL-number (ATL000 through ATL010, less ATL003).² The main memory, the scratchpad memory, and

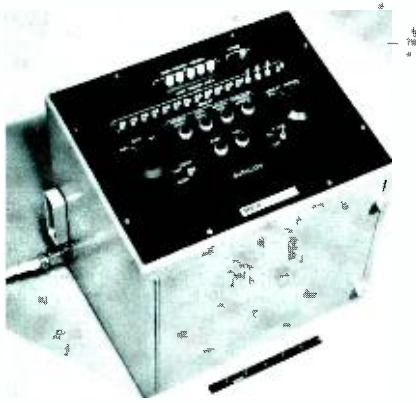


Fig. 8—SUMC/DV computer.

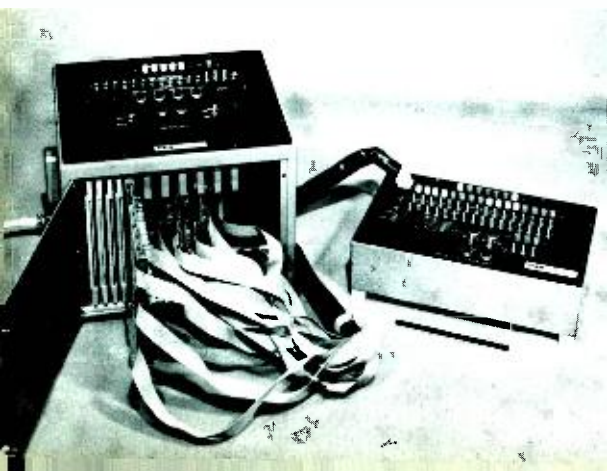
nal registers, read-only-memory, scratchpad memory, and main memory. Control of the computer by single EO at a time or even single instruction at a time is also provided by the test set. Fig. 9 shows the SUMC/DV computer and separable Test Set.

Computer debugging

Due to the heavy use of simulation and computer-aided design, the overall debugging philosophy was to look for a wiring error once a malfunction is discovered. This position is arrived at by testing most of the SUMC/DV components as individual units. Each LSI chip is completely checked with computer-generated test sequences. This accounts for about 90% of the total logic. Details of the component testing prior to computer debugging appear in Ref. 1.

After the tested parts were assembled, debugging of the SUMC/DV computer began. Using the test set described above, both the main memory and the scratchpad memory were loaded and verified to be operational. From this point the initial program load (IPL) se-

Fig. 9—SUMC/DV with test set.



quence was verified. The IPL sequence is an EO sequence which initializes the program counter to a value loaded into main memory as part of the manual bootstrap. The instruction residing at the main memory location indicated by the program counter is brought into the instruction register for execution. The RR instructions were then verified one by one, using the test set to load various data patterns into the main memory and scratchpad memory and then verifying the correct operation of the instruction by comparing the result with the result of the algorithm simulations performed during the design phase. This was performed by stepping through an instruction, one EO at a time, with the use of the test set. After several instructions were verified operational, program loops were set up to automatically process all possible data combinations for operations. After the RR instructions were operational, the RX, RS, and SI type instructions followed the same method of debugging. After all instructions were operational, the interrupt structure operation was verified. Finally, the programmed and simultaneous I/O instructions were validated.

The real benefits of simulation and design automation are demonstrated in this program. The entire debugging procedure required less than two man-weeks to verify complete operation of the SUMC/DV computer, which contains more than 7000 logic gates.

Teletype

A teletype has been interfaced to SUMC/DV to provide both input and output capability. A special controller has been built which interfaces the TTY to the standard I/O interface provided by SUMC/DV. This controller provides for programmed and simultaneous input-output operations.

Software support

In support of the SUMC/DV hardware, two major software programs are provided: an assembler and a simulator. Each program is written in Fortran and is operational on the RCA Spectra 70/45.

The assembler accepts SUMC/DV instructions and pseudo-operations on punched cards. The input data is syntax checked and assembled. The assembler produces error flags, symbol tables, source-card images, and hexadecimal

contents of the main memory locations. Additionally, a paper tape is generated in bootstrap format for loading into SUMC/DV. The assembler also provides a macro capability.

The simulator accepts as input either the paper tape output of the assembler or a magnetic tape created from previous simulation. Any input program is executed in a fashion identical to that used in the actual SUMC/DV computer. Here also the input data is syntax checked and error flags produced. The simulator provides for actual time records, many memory traces, and listings as aids to the user.

Summary

The SUMC/DV, the world's first CMOS LSI computer has been designed, fabricated, and debugged within one year by personnel at the Advanced Technology Laboratories. The success of this program can be attributed to two major factors: 1) the reliance on simulation and design automation techniques, and 2) a small closely knit, interdisciplinary, design team dedicated to the task.

The program has demonstrated the time and cost advantages of LSI design automation techniques—a complete 16-bit computer was conceived, designed, fabricated, and checked out within one year. The program has also led to the characterization of the CMOS technology in a system environment. The power of the logic functions have been illustrated here and the circuit operation characterization is discussed by A. Feller.¹ The third program goal has also been met—the computer is operational.

The SUMC/DV computer is completely supported with a test set, a TTY peripheral, an assembler, and a simulator. It is a microprogramed 16-bit, parallel computer with an instruction set of 32 general purpose instructions compatible with IBM 360/370, RCA Spectra 70, and RCA 215 computers.

References

1. Feller, A., "LSI Computer Fabrication—SUMC/DV," *this issue*.
2. Feller, A. et al., "Computer-Generated Low-Cost Custom CMOS Arrays," RCA Reprint, *Solid-State Technology*, PE-552, p. 12; *RCA Engineer* Vol. 17, No. 3 (Oct/Nov 1971) pp. 10-15.
3. Merrian, A. and Zieper, H. S., "Simulation: methodology for LSI computer design," *this issue*.

Holographic digital memories

R. H. Norwalt | P. L. Nelson

A feasibility-model holographic read-only memory (ROM) has been designed, built, and tested by Advanced Technology Laboratories—West. The ROM utilizes optical storage techniques to provide high-speed, high-density storage on rugged, low-cost, easily changeable media. The system is based on a 72-bit, 1024-word format that can be changed to provide 4096 words of 18 bits each at the data interface. This ROM interfaces with an address register, control logic, and a data register which utilize T²L logic levels (+0.2 V to +5.0 V nominal voltage swings).

DIGITAL DATA storage and retrieval techniques must be evaluated on the basis of data packing density, speed of access, cost, volatility, and environmental sensitivity. The interdependency of these parameters produces a number of conflicting requirements that create significant problems for the system designer. Possible solutions to a number of these problems for small, high-speed, card-changeable read-only memories and large, random-access, mass memories may reside in the disciplines of modern optics.

Modern optics, of which holography is a sub-set, can be defined as the study and application of coherent light. This technology offers the ability to store and retrieve, at optical wavelengths, the amplitude and phase information associated with the desired data. Storage at optical wavelengths also provides packing densities which are a function of the diffraction limit of the wavelength used for storage and retrieval. Recordings, which contain both amplitude and phase information, provide two advantages: First, individual

bits of data are recorded over the entire area of a multi-bit data block. Therefore, obscuring a portion of the recording does not destroy specific bits; it simply reduces the intensity of all the bits in that block by a small amount. Second, the existence of phase information allows the data image to be reconstructed in such fashion that it remains stable at a pre-determined position in space regardless of linear translation of the material upon which it is recorded. This feature greatly simplifies those problems that have been associated with alignment of the storage media in previous optical memory systems.

Holographic read-only memory

The holographic read-only memory (ROM), which is discussed in this article, is an optical memory using holographic media for data storage. The storage element of the ROM, shown in schematic form in Fig. 1, consists of modular subsections which provide for address decoding, word selection, storage, readout, and internal timing.

Authors Nelson (left) and Norwalt. On the table is the mechanical model of the read-only memory described in this paper.

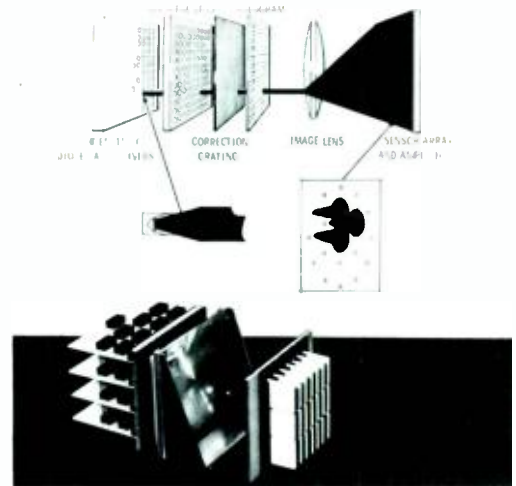


Fig. 1—Card-changeable read-only memory.

In operation, the address data is transferred into decoder-matrix driver electronics which select and drive one of an array of 1024 light emitting diodes. The light from the selected diode is collimated by one lens of a 32×32 lens array and passed through a hologram. There are 1024 holograms in the storage media, each containing 18 to 72 bits of

Perry L. Nelson
Design and Development Engineering
Advanced Technology Laboratories
Van Nuys, California

received the BS in physics and mathematics from St. Olaf College, Minnesota, and did graduate work in physics at Montana State University. While at RCA, Mr. Nelson has been actively engaged in research and first-stage design of new projects. He has been engaged in programs such as a near-surface burst capacitive fuze for bombs, an optical fuze employing GaAs laser diodes, and optical portions of a signaling system for submarines. Following this, Mr. Nelson studied possible uses of piezoelectric ceramics in the Ordnance area. He developed and tested a unique piezoceramic sensor and has done work on a solid-state piezoelectric transformer and a piezoelectric S&A device. In 1970, he became active in the area of voice-response techniques. This project includes a holographic storage and he has specifically been responsible for the holographic facility and research leading to a random access non-movable store of audio and video information.

Robert H. Norwalt, Ldr.
LSI Storage and Display Techniques
Advanced Technology Laboratories
Van Nuys, California

joined RCA after receiving his undergraduate degree from the University of Southern California in 1961. Before 1961, Mr. Norwalt was actively involved in the design and development of magnetic drum memory systems and associated solid-state control circuitry for Litton Industries and Magnavox Research Laboratories. From 1962 through 1964, he was responsible for the design and development of several memory systems. During 1965 and 1966 he was responsible for specialized military displays and the EASD display research and development programs. From 1966 through 1969, as Leader of the Military and Advanced Displays group, he was responsible for a number of special Military video display systems as well as for the development of a low-cost Military alphanumeric/graphic video display system. He is presently responsible for the development of advanced techniques for optical memories and large-scale solid-state integrated circuitry. Mr. Norwalt holds a patent on a semiconductor-controlled pulse shaper and has a number of disclosures pending. He is a member of the Society for Information Display and American Management Association.

Reprint RE-18-2-6
Final manuscript received

information. A portion of the light beam is diffracted by the hologram and projected by the imaging lens system onto a sensor array. This array, which contains one sensor for each bit position recorded in the hologram, transforms the optical energy contained in a bit representing a logical "one" into an electrical signal. This signal is then amplified and gated into an output register.

Address decoding

A single word location in the memory is selected by a 10-line address input. Ten binary bits are used to select a single light-emitting-diode (LED) location out of a 1024-LED array. Five address bits are used as a row address to select one out of 32 source drivers, while the other five address bits are used as a column address to select one out of 32 sink drivers. The chosen source and sink drivers define the LED that is to be activated.

LED drivers

The LED driver, shown in Fig. 2, uses an integrated circuit power gate to drive an isolation transformer which, in turn, drives the output transistor. Although this configuration requires more components than an equivalent integrated circuit driver, the standby power requirements are reduced by a ratio of 10 to 1. Since a relatively large number of circuits are required (64), the power dissipation requirements of the storage element structure are significantly reduced.

LED source array

The source array consists of 1024 light-

emitting diodes, organized in an X-Y matrix. Each diode is individually addressable through the unique selection of the appropriate row and column to which it is attached.

System considerations (such as, word length, optical efficiency, and memory cycle times) dictate that each source exhibit a small emitting area, about 0.04 mm^2 , a total power in excess of $100 \mu\text{W}$, and a response time less than 50 ns. RCA GaAlAs laser diodes, operated below lasing threshold, meet all these requirements. The intensity distribution for one axis of this diode is shown in Fig. 3. When driven by sub-threshold current pulses, these diodes can be operated for extended periods of time with duty cycles as high as 30%. An example of the change in power output, with respect to time, is shown in Fig. 4 for a representative diode driven by a 200-mA pulse with a 30% duty cycle. With this power output characteristic, a single diode in an array of 1024 diodes would exhibit a time between failures, at the 75% power point, in excess of 12,000 hours. The array structure is modular to allow individual diode testing at each step of the assembly process. This type of construction also provides for rework, should one of the emitters prove faulty during, or subsequent to, array fabrication.

Collimation and beam-forming optics

The collimation lens array is composed of 1024 lens elements in an X-Y format, identical to the LED matrix. The optical axis of each lens matches that of its associated LED. The beam-directing

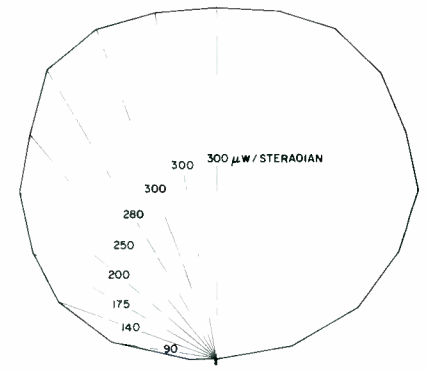


Fig. 3—Intensity distribution for one axis of a light-emitting diode.

optics which follow the lens array consist of a Fresnel prism placed coaxially with the lens matrix. The combination lens array and beam-directing prism is placed between the LED array and the hologram matrix, such that the emission from the selected diode is collimated and directed through the appropriate hologram.

The address beam that reconstructs a holographic image must closely approximate the reference beam which was used during construction of the hologram. This beam can be parallel, diverging, or converging. A parallel beam, however, provides minimum distortion and is most readily approximated for playout. The construction reference beam, besides being parallel, also forms a particular angle with the normal axis of the hologram. An equivalent angle, normalized for the difference in wavelength between the recording light and the reconstruction light, must be used during playout to maximize efficiency and minimize distortion.

To satisfy these requirements, the output of each LED (which resembles the emission from a Lambertian source) is collected by a lens located one focal length away from the junction. The light emerging from this lens is then passed through a prism which redirects the beam at the appropriate angle through the hologram. The inclusion of the prism satisfies the address-angle requirements and permits the hologram, lens, and LED arrays to be mounted coaxially. This provides an effective configuration for system packaging.

Since the emission from the LED is approximately Lambertian, a lens with a small f -number is required to collect a significant portion of the light. It can

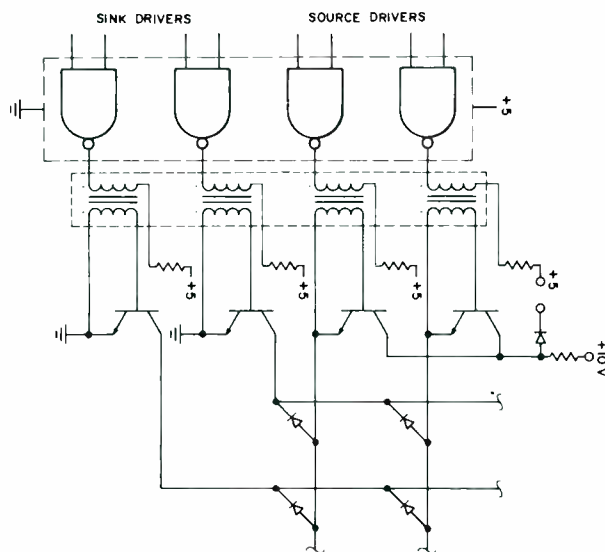


Fig. 2—Driver and switch arrangement for a 2×2 section of the light-emitting-diode address matrix.

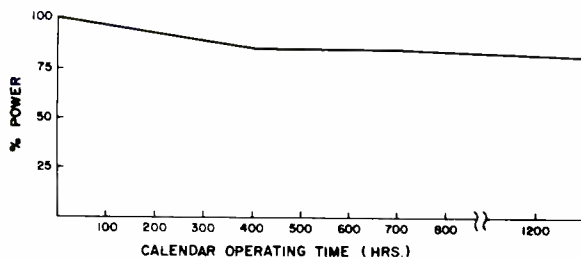
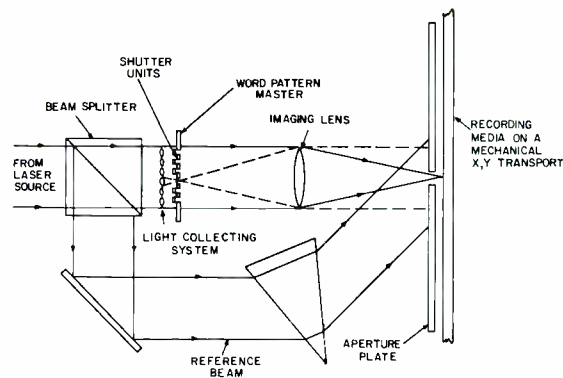


Fig. 4—Life-test data for a light-emitting diode driven by a 200-mA pulse with a 30% duty factor.

Fig. 5—Geometry and components used to construct a Fraunhofer hologram.



be shown that a $f/1.0$ lens will collect about 20% of the total emitted energy from a Lambertian source radiating in one direction. Fabrication of an array of 1024, $f/1.0$ glass lenses would be both difficult and expensive to produce. However, cylindrical lenses of the required size and speed can be ruled accurately on a master plate. Arrays of these lenses are fabricated by stamping or pressing from optical plastics. The beam-directing prism, which can also be fabricated by a ruling technique, is combined with the lens array to form a compact, low-cost, lightweight assembly.

Hologram matrix

Information in the form of digital words is stored in a matrix of holograms. This matrix is situated such that each collimated and directed beam from the associated LED and lens arrays passes through an associated hologram. Each hologram contains up to 72 bits of information. When a selected beam passes through its associated hologram, the information stored in that hologram is reconstructed at a plane in space.

The matrix of holograms consists of 1024 holograms arranged in a 32×32 array. The physical dimensions of the hologram array are the same as those of the previous LED and lens-prism arrays. The diameter of each hologram is slightly smaller than the center-to-center LED spacing. These relatively large holograms intersect the entire address beam, thus utilizing the total power in each beam. A small guard space is left between holograms to insure that the addressed hologram is the only one illuminated.

The choice of hologram type and recording material is determined by the requirements of the specific application. The ROM requires high diffraction efficiency, durability, image immobility, redundancy, and ease of replication. Diffraction efficiency is defined as

the percentage of address power that is projected into the readout image. Durability of the hologram matrix is important because the recorded information must not degrade when subjected to extremes of environmental conditions such as moisture and temperature.

Image immobility assures that the readout image remains stable on the sensor plane under all operating conditions. Redundancy of information assures that information will not be lost when a hologram is partially obliterated by dirt and scratches. Ease of replication is important for making multiple low-cost copies of hologram matrices.

Fraunhofer or far-field phase holograms (when recorded on the surface of an appropriate material as a relief pattern) satisfy the requirements for high diffraction efficiency, high redundancy, image stability, and simple low-cost reproduction.

The hologram recording material must meet the requirement for environmental durability. Photoresist is a photosensitive material that remains stable over a wide range of environmental conditions and is acceptably non-nutrient to biological growth. This material has well-defined procedures for preparation and coating, can be readily characterized, and is easily obtained. An important characteristic of photoresist is that it requires a single-step development process, which greatly reduces the construction time.

Matrix recording

The basic method for constructing Fraunhofer holograms is well defined. Fig. 5 is a diagram of the geometry and components used in Fraunhofer construction. As with all holograms, a reference portion of a laser beam is caused to interfere with an object portion of the same beam. The recording media, placed in the intersection of

these two beams, records the phase and amplitude of the interference pattern. The position of the object to be recorded is very important for a Fraunhofer hologram; it must be located in the front focal plane of the construction lens, and it must be illuminated with parallel light. The photosensitive plane, in the back focal plane of the same lens, records the object information which now (because of this lens) appears to originate at infinity. This relationship provides the immobility of the readout image.

A single Fraunhofer hologram is recorded by exposing the photosensitive storage media to the object and reference beams for a given length of time. The exposure time depends on the amount of power available and the sensitivity of the recording media. A matrix of Fraunhofer holograms is recorded by stepping the recording plane in an X - Y format and recording a hologram at each location.

Imaging optics

The reconstructed image from each of the holograms must be focused onto a sensor plane by a large imaging lens situated directly behind the hologram matrix. The lens brings each reconstructed image into focus in its back focal plane. A sensor matrix, arranged in the format of the object bit pattern, is located in the back focal plane. A test breadboard which shows the relative positions of each of the key elements is shown in Fig. 6.

The imaging lens is required in the system because of the constraints of Fraunhofer (far-field) type holograms. These holograms are recorded such that the object appears at infinity and, therefore, the reconstructed image from a Fraunhofer hologram appears stable and in focus only at infinity. A lens, placed in the path of a playout image from a Fraunhofer hologram, sees this data pattern arriving from infinity and

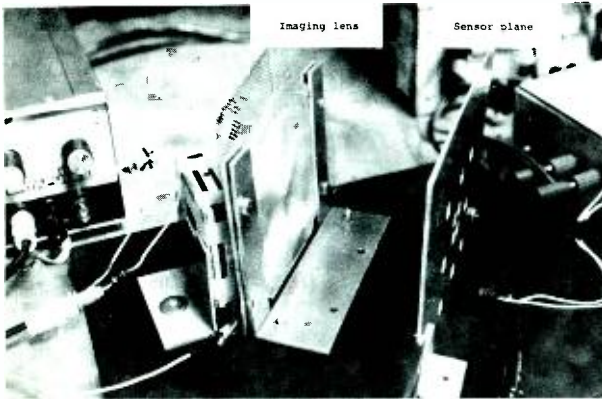


Fig. 6—Test breadboard showing the relative locations of key elements in the holographic read-only memory.

produces a real focused image in its back focal plane. This image still retains the image immobility which is characteristic of Fraunhofer holograms.

The imaging lens is large enough to receive the payout images from all holograms in the matrix. Because of the manner in which the matrix was recorded, all of the holograms play out along parallel center lines. The imaging lens is thus able to form each of the real focused images at a common position in space. A single sensor array, located at this position, detects the information from all of the holograms, irrespective of their position in the matrix.

There are two key requirements which the imaging lens must meet: it must be large enough to accept the payout from all holograms in the matrix and it must have a focal length sufficiently short to produce an image within the system dimensions. These requirements dictate a fast, low f -number lens.

There are two possible types of lenses which could satisfy the imaging requirements: classic lenses and Fresnel lenses. Fast ($f/1.0$ or less) classic lenses are physically thick and expensive. Fresnel lenses have an advantage over these in size, weight, and cost. Very fast $f/0.5$ Fresnel lenses can be ruled accurately and inexpensively on light-weight plastic sheets.

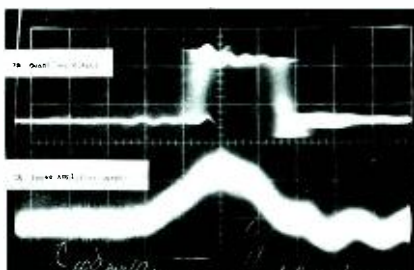


Fig. 7—Sense-amplifier waveforms.
a) Sense-amplifier output.
b) Quantizer output.

Sensor array and sense amplifiers

The information contained within the first order-beam from the hologram is imaged onto a sensor array. This array, which contains one sensor for each data bit of the stored word, must exhibit a response time less than 50 ns and a sensitivity of $0.4 \mu\text{A}/\mu\text{W}$ at 9050 \AA .

The sensor array transforms the light energy projected from the hologram into an electrical signal. This signal is then amplified and quantized by the sense amplifier. The sensors selected are similar to Solid State Radiations Model 100-PIN-RM. These units exhibit a transfer ratio of $0.35 \mu\text{A}/\mu\text{W}$ at 9000 \AA and a leakage of $1 \mu\text{A}$ at 75°C and 50 V. Their junction capacity is about 75 pF at 50 V, with a current risetime of 25 to 50 ns.

The output of each sensor in the array is fed into an amplifier/detector circuit. This circuit transforms the small signal at the diode output to the quantized levels of T^2L logic.

Effective utilization of the low-noise, high-speed characteristics of the PIN photodiode depends upon proper design of the preamplifier. Since the photodiode is a current source and the detector will be amplifier-noise limited, a high photodiode load impedance and a restricted bandwidth are required to produce an adequate signal-to-noise ratio. To meet these requirements, the amplifier/detector circuit uses a low-capacitance, low-noise FET input stage coupled to a bandwidth-limited amplifier. The load impedance for the PIN diode is determined by the input capacity of the FET and the stray wiring capacitance. It can be shown that the maximum signal-to-noise bandwidth product is obtained when the amplifier bandwidth is 1.5 times the center-band frequency. For a light pulse width of 100 ns, the PIN response signal has a center-band frequency of approximately 4 MHz. Based on this frequency, the amplifier is designed for a 6-MHz bandwidth with lower cutoff at 2 MHz and the upper cutoff of 8 MHz. The signal at the output of the preamplifier shown in Fig. 7 is passed through a DC restoring circuit into the quantizing amplifier. This amplifier accepts the 0.2 V to 1.2 V signal from the preamplifier and generates the logic level (0V to +5V) signal shown in Fig. 7. This quantized signal is then strobed by a time-

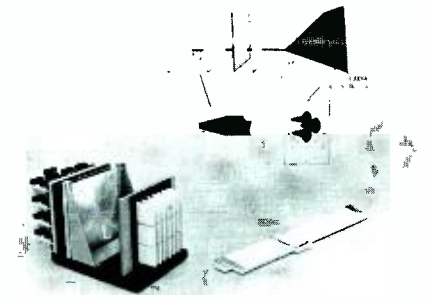


Fig. 8—Mechanical model of the holographic read-only memory.

discriminated signal into the output data buffer.

Summary

Fabrication, test, and evaluation of a feasibility model demonstrated that each of the elements required to construct a high speed, holographically recorded digital read-only memory are presently available utilizing state-of-the-art techniques. Small size, low quiescent power decoding and LED driving circuitry was built and tested. Infrared LED's with adequate power and sufficiently small junction areas are available for a reasonable cost. Optics for light-collimation beam direction and data imaging are possible through the use of low-cost molding and pressing techniques. Surface phase holograms with 14% efficiency at a signal-to-noise ratio greater than 50:1 have been constructed utilizing off-the-shelf equipment. Sensors have been identified and tested which, when properly terminated, provide adequate speeds and signal-to-noise rates. An amplifier technique has been identified which provides sufficient gain and signal-to-noise characteristics to achieve false alarm rates which are acceptable for tactical missions.

Fig. 8 shows a mechanical model of a holographic read only memory which would be capable of storing 1024 words of 21 bits each. The address selection electronics are contained on the four printed-circuit boards on the rear of the unit. The LED array, collimation array, beamforming optics, and holographic data matrix precede the imaging lens which is visible at the center of the unit. The 21 sense amplifiers can be seen mounted on the back of the sensor array on the right end.

The next phase of this effort will be the fabrication, test, and evaluation of a fully populated advanced development model for use in a modular computer system evaluation.

Holographic storage of multicolor information

G. T. Burton | B. R. Clay

The holographic storage documentation-type information is currently receiving particular attention in light of the increasing tendency to generate, store, and retrieve alphanumeric, graphic, continuous tone, color, and black-and-white data. Holography offers a method of storing this type of data in a compact, easily duplicated, inexpensive and readily retrievable manner.

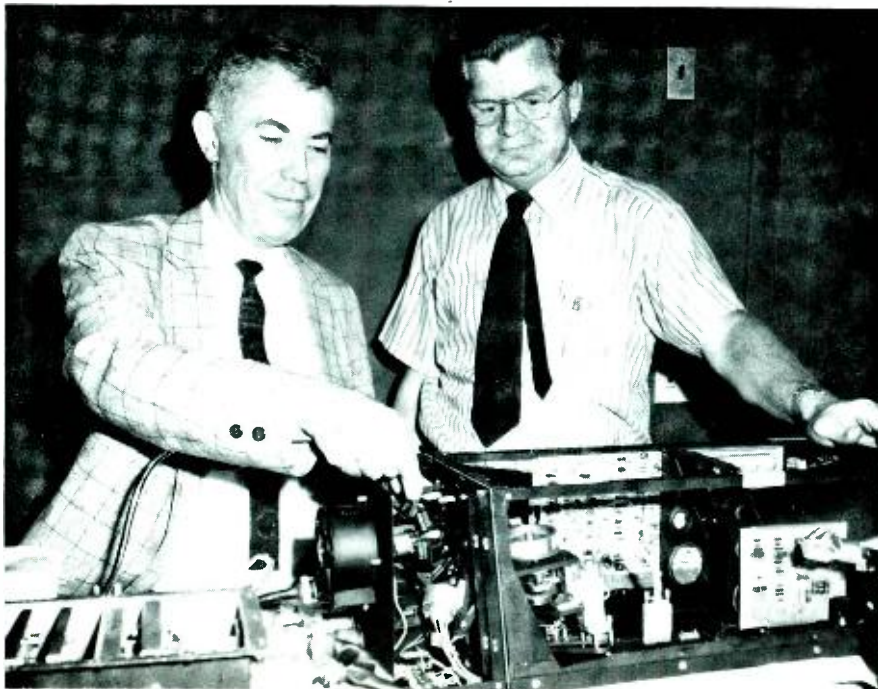
OVER the last four to five years, RCA has been actively engaged in the development of holography as an information storage and retrieval technique. Programs have been pursued for storing both digital and analog information at RCA Laboratories in Princeton,

New Jersey, at RCA's Zurich Laboratories, and at the Advanced Technology Laboratories (ATL) of the Government and Commercial Systems Division. A number of programs are being pursued in this area. Currently, display systems using the holographic technique are

G. T. Burton, Ldr., Pattern Recognition, Advanced Technology Laboratories, Burlington, Mass., received the BSEE from Drexel Institute of Technology in 1957 under the cooperative engineering program. He holds the MSEE from the University of Pennsylvania. Since joining Advanced Technology Laboratories in 1957, he has been engaged in the development of transistor circuitry for digital logic operations, IF and video signal-processing in noisy environments, and FM modulation systems. He has studied methods for synchronizing binary data transmission systems in noisy environments, modulation methods for transmitting pictorial information at high data rates, and techniques for reading printed documents automatically. He has extensive experience in the application of aperture response techniques to the analysis and design of electro-optic systems. Mr. Burton was responsible for development of the electronics and for the overall systems integration of the RCA ideographic composing machine used for the composition of Chinese text on photographic film. He developed an automatic exposure control system for night aerial cameras using image-amplifier tubes. He was responsible for the development of the broadband electronics and the wideband optical modulators for use in a high resolution Laser Beam Image Recorder and a Laser Beam Video Recorder. In 1967, he was promoted to Leader, Electro-Optic Techniques, and during the early part of 1969, he transferred to the Burlington Satellite of Advanced Technology Laboratories in his present capacity, where he is responsible for the direction of effort in technology areas related to the holographic storage and display of information, and to pattern recognition systems. He is a member of the IEEE and SMPTE.

B. R. Clay, Pattern Recognition, Advanced Technology Laboratories, Burlington, Mass., received the BS in Physics from Indiana University in 1949. He has had 20 years of professional experience at RCA which include nine years of electrical and magnetic circuit design and optical instrument development in color television; two years of computer systems and fiber-optics development; and six years of laser electro-optical and optical systems design. Since joining the ATL-Burlington, Mr. Clay has worked on laser electro-optical and optical design problems. He has been involved in the design of laser equipments and systems of advanced and neodymium lasers, micromachining laser systems and laser range-finders. He has been project engineer for development of several laser equipments including ground rangefinders and the RCA Huey Cobra laser rangefinder. Mr. Clay is currently working in the field of holography. His current activities include wavefront correction for optical systems, full color holography with incoherent reconstruction sources, and stereo displays. He recently received an RCA Technical Excellence Award for performance on the laser obstacle detection system for the Department of Transportation. He is a senior member of the IEEE, a member of OSA, SMPTE, and the Scientific Research Society of America, and holds thirteen U.S. Patents. He is listed in *Who's Who in the East*.

Authors Clay (left) and Burton.



being constructed for both the Navy and NASA. The Navy requirement is for the display of multicolor aerial chart information in an aircraft cockpit. NASA has an application in which volatile, computer-generated alphanumeric and graphical information and archival holographically stored information are viewed in superposition. Typical archival information includes maps, forms, flowcharts, block diagrams, and coordinate systems.

Holographic concept

Holography was chosen as the storage technique for the Navy and NASA document storage applications because it offers a number of advantages over more conventional image storage systems. These advantages result from two basic features associated with holographic recording. First, holography is a technique for recording and at a later time reconstructing optical wavefronts, and secondly, the nature of the wavefront recording is such that the recording can be accomplished on either phase or absorptive storage materials.

The parameters necessary to store an optical wavefront are recorded in the form of an interference pattern produced between a reference wavefront whose characteristics are known and which can be reproduced for readout and an information-bearing object wavefront. The two wavefronts must be derived from a common coherent source—most commonly a laser. The phase and amplitude information preserved in the recorded interference pattern is sufficient to allow reconstruction of the object wavefront when the interference pattern is interrogated by a readout beam similar to the reference beam used in recording. *The recorded interference pattern is a hologram.*

The reconstruction of a replica of the original optical wavefront by using the recorded hologram is accomplished by a diffraction effect (see Fig. 1a). In this diagram, two optical wavefronts derived from a common coherent source are caused to interfere with each other on a photosensitive recording medium. If two plane waves are recorded as shown the developed interference pattern consists of a sinusoidal grating having a pitch that depends on the angle between the two wavefronts and the wavelength of the optical source. The interference pattern is

Reprint RE-18-2-11
Final manuscript received June 26, 1972

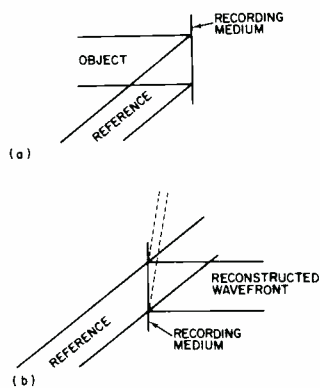


Fig. 1—Plane wave interference effect.

recorded on a photosensitive storage medium such as a silver halide film. When the film is developed and replaced in the reference beam as indicated in Fig. 1b, a portion of the energy passes directly through the film; a significant portion of the energy, however, is diffracted by the grating structure into a reproduction of the original object beam used in the construction of the grating. (Energy is also diffracted into a wavefront which rises almost vertically, shown by the dotted lines in the illustration.) This interference pattern which is used upon reconstruction as a diffraction grating is an elementary hologram. It is the recording of a plane wavefront. As the wavefront to be recorded becomes more complex, the recorded interference pattern or hologram takes on a more intricate nature, but the principle of recording an interference between two coherent wavefronts and using the interference pattern as a diffraction pattern to reconstruct the stored wavefront when the grating is interrogated by a reference wavefront remains the same.

The ability to record wavefronts in this fashion allows one the opportunity, at least in theory, to enter at any plane in an optical system and record the wavefront passing through that plane. The name assigned to a type of hologram is generally associated with the recording location within the optical system. Thus as indicated in Fig. 2, a Fresnel hologram is one recorded in the near field of an optical system, a Fraunhofer hologram is recorded in the far field, a Fourier transform hologram is a special case of the Fraunhofer hologram and is recorded in the Fourier plane of a lens system while a focused-image hologram is recorded in the image plane of an optical system.

Advantages of holography

Some advantages of holographic recording over more conventional image recording techniques are:

- Precise registration of stored images independent of the position of the storage medium,
- Highly redundant recording,
- Nonabsorptive recording medium,
- High density storage,
- Multiple image recording,
- Rapid and inexpensive duplication, and
- Archival storage.

A major advantage of a holographic system is the ability to reconstruct images that are stationary and precisely registered. The location of the recording plane largely determines the extent to which a holographic form possesses this property. The Fresnel and focused-image holograms upon restoration produce images that move in direct proportion to the motion of the storage medium, while the wavefront reconstructed from a Fraunhofer hologram produces an image that is stationary and precisely positioned in space even though the storage medium may be moving or displaced.

Most holographic recording systems employ redundant storage techniques so that a point contained in the object is recorded over a finite area on the storage medium. Thus, scratching or abrading the storage medium does not destroy the information, as is the case in a conventional storage system, (e.g., turning "1" to a "0" or a "0" to a "1" in a digital system) but rather tends to raise the background noise level. There are several exceptions to this case: one is the focused image case where the recording is accomplished in the image plane and is subject to the same type of degradation as is a conventional microfilm system. However, it is used in both the Navy and NASA applications because it allows the stored information to be retrieved using a white light source. A different type of effect is produced for Fourier-transform recording, where an inopportunistically located scratch will eliminate the background or low frequency information from the reconstructed image.

The remaining advantages associated with holographic document storage and display systems result from the medium used to store the information. In Fig. 1, the holographic reconstruction process was shown to result from a diffraction phenomenon resulting when a recorded

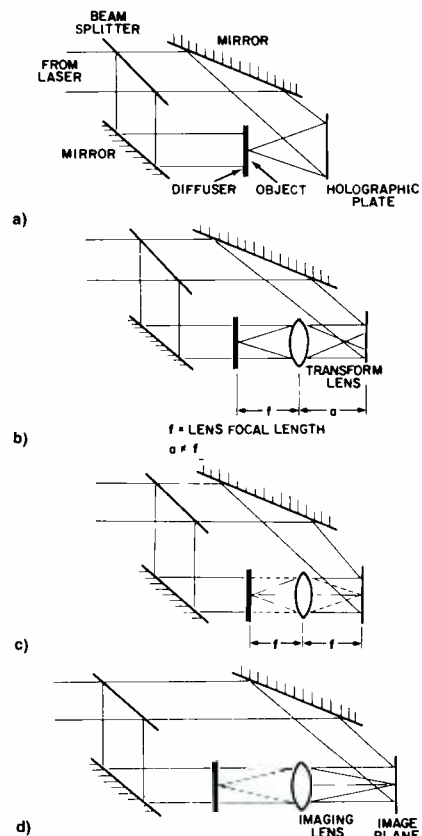


Fig. 2—Holographic forms. a) Fresnel; b) Fraunhofer; c) Fourier transform; d) Focused image.

interference pattern was interrogated by a readout beam. To this point in the discussion it has been assumed that the recording was produced on an absorptive medium similar to conventional photographic film. The same kind of effect is produced if, instead of absorbing energy from the optical wavefront to produce the diffracted wavefront, the phase characteristics of the wavefront are changed by the recorded interference pattern. This phase change is accomplished without absorbing energy from the wavefront. Consequently, the storage medium can be used to store energies at high densities without experiencing the difficulties encountered with conventional microfilm systems which occur when large amounts of optical power are passed through small areas of the storage medium in an attempt to produce a bright display. The absorptive nature of the display causes the medium to heat up to the extent that it pops in and out of focus or, in more severe cases, burns up. A holographic system using phase recording can be used to gate large amounts of optical power to produce bright displays.

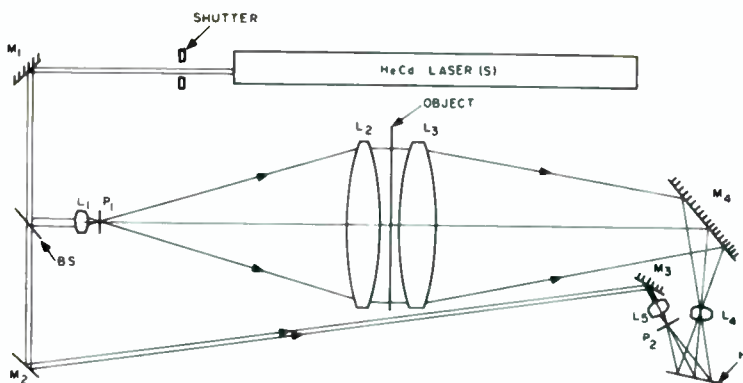
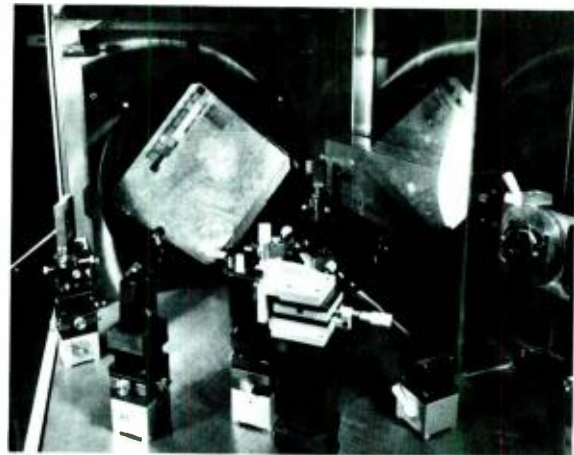


Fig. 3—Focused-image recording system.
Fig. 4—Laboratory recording system. →



In displays developed for the Navy and NASA, photoresist has been used extensively as the recording medium. A modified version of Shipley AZ-1350 deposited on glass or on a Kronar-tape base is used to produce the original hologram. Photoresist is used for several reasons, resulting in further advantages of holographic recording over more conventional photographic methods.

First, the photoresist material is a grainless recording material and as such its resolving capability is extremely high. We typically record gratings having resolutions of the order of 1000 to 1500 lp/mm (line pairs/millimeter) and use these gratings to store information at densities of the order of 250 to 350 lp/mm. In addition, as will be seen later, it is possible, as in any carrier system, to record multiple images in a common space. To do so, however, the dynamic range available in each image must be reduced. Since the available dynamic range in a holographic system is large when recording is accomplished on phase material, the reduction in dynamic range will not in most systems produce a loss of information if only two or three images are stored in a given area.

An additional advantage results from the use of photoresist. Original holograms on photoresist can be inexpensively and rapidly duplicated using a process similar to that developed in Princeton for the SelectaVision HoloTape program. Duplication of holograms is accomplished in the following manner. The hologram is first formed in the conventional manner by constructing an interference pattern between the reference beam and the object beam derived from a single coherent source—a helium-cadmium laser. The interference pattern is formed on the surface of the photo-

resist, a material that has the property that its solubility in a developing solution depends on its history of exposure to light.

For the case where the interference between the two wavefronts is constructive, the intensity of the exposure is high, resulting in an increase in the solubility of the photoresist; on the other hand where the two wavefronts interfere with each other to produce a low intensity exposure, the solubility of the material remains low. Thus, the interference pattern produced between the two wavefronts is stored as a latent image contained in the variation of solubility of the exposed photoresist material. The image is developed by washing the surface of the material with a basic solution, such as sodium hydroxide. This procedure washes the photoresist away slowly where the solubility is low and rapidly where it is high, resulting in a relief image on the surface of the photoresist which is a representation of the interference pattern formed between the two wavefronts. The recorded wavefront may be restored directly from the photoresist hologram by passing a reconstruction wavefront through the stored pattern or by reflecting the reconstruction wavefront from the photoresist surface. In either case, the reconstruction is accomplished by changing the wavefront characteristics of the restoration wavefront to produce the desired diffraction wavefront.

Due to the fact that the hologram is stored on the surface of the photoresist material as a surface relief image it is possible to produce metallic masters by depositing nickel on this surface to a depth of several thousandths of an inch and stripping the deposited metal from the photoresist. The result is that an original hologram is translated to the metallic master and can be used in a heat-embossing process to transfer the

hologram to an inexpensive and durable storage material such as a clear vinyl. The embossing process can be used to create literally hundreds of thousands of copies from a single master without degradation of the hologram quality (resolution, uniformity, etc.) from that of the original photoresist hologram. Techniques have also been developed for creating, from the original metallic master, second-generation metallic masters that can in turn be used to emboss on vinyl.

It is then for the advantages described above that holography appears as an attractive storage medium for the increasing mountains of documentation to which man must have rapid access.

Multicolor information recording

In the system developed by ATL for the storage and display of full-color information, the three elements of a color-separation set are stored as three superimposed holograms in a common recording area. Continuous tone red, blue, and green color separations of the information to be recorded are derived at 1:1 from the material to be stored and displayed by copying the original material through three separation filters (Wratten PM25A, PM61, and PM47B). Color highlight masking may be added at this stage to overcome nonlinearities in the holographic recording system if it is desired to produce colors of high fidelity. For most applications, such as the reproduction of maps, charts, block diagrams, etc., the color fidelity achieved without masking is adequate.

The color separations are used in three successive exposure operations to produce overlaid focused-image holograms. A schematic representation of a focused-image recording system is presented in Fig. 3. A laboratory embodiment of this system is shown in Fig. 4. As shown in Fig. 3, light from a *HeCd*

laser is split into reference and object beams by the beam splitter *BS*. The object beam is enlarged, collimated and cleaned up by lenses *L*₁ and *L*₂ and pinhole *P*₁. The collimated beam at the output of *L*₂ is passed through the object, collected by a condenser lens and imaged by imaging lens *L*₄ to plane *H*. The reference beam, shaped to a spherical wavefront by lens *L*₅ and pinhole *P*₂, is made to interfere with the object beam on the holographic recording plate located in the image plane of *L*₄. Recording in this plane produces a focused-image hologram; recording at a plane located closer or farther away from the imaging lens results in a quasifocused image hologram. Lens *L*₄ and pinhole *P*₂ are located such that the DC terms in the image (large areas of a solid color) result in a linear grating, *i.e.*, a grating whose elements are parallel.

(For the angular separation between the reference and object beams used in the moving-map-display system developed for the Navy, a grating is formed having a fundamental frequency of approximately 1100 lp/mm. For the map information recorded at a reduction of 25:1, this condition allows the recording of high frequency information by using this grating as a carrier at densities of 250 lp/mm, resulting in a display having a resolution of 10 lp/mm. [Resolution figures throughout this paper are presented at the 20% response point unless stated to the contrary.]

The linear grating effect is the property which allows the recording of multiple holograms in a common area. Superimposed recording of the elements of a three-element color-separation set is accomplished one after the other, but with the reference beam falling on the recording plate at a different angle so as to form a primary grating structure as indicated in Fig. 5. Separation of the image information is accomplished by the orientation of these three gratings. High frequency information is contained in each grating structure as fringe

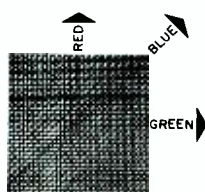


Fig. 5—Multiple grating orientation.

patterns which deviate from the indicated primary grating arrangement. But, for information recorded at the densities indicated above, the deviation is not sufficient, so that upon readout, the information associated with one grating structure is read out by a reference beam designed to interrogate other holograms oriented at a different angle.

The system in Figs. 3 and 4 is used to record the three-image holograms. The recording process is as follows. A holographic plate is placed in the film holder located in or near the image plane of lens *L*₄. The holographic plate consists of photoresist deposited on glass or, if a sequence of holograms is to be recorded, photoresist deposited on a Kronar tape and reeled in a spool. The first element of the color-separation set is entered in the object plane with its north axis vertical and an exposure is made by shuttering the laser beam to form the interference pattern between the reference beam and the object beam passing through the separation transparency. The second element of the separation set is inserted in the object plane, but with its north axis oriented at 40° to that of the original object. The holographic plate is rotated by the same amount and a second recording made such that the second image is recorded in registration with the first, but with the information associated with different primary colors recorded in holograms having different grating orientations with respect to the north axis of the information. The third element of the separation set is next placed in the object plane, this time with the north axis oriented at 90° to the original axis and a corresponding amount of rotation introduced to the holographic plate holder.

When the exposure is complete, duplicate holograms are produced by the process described in the previous section. In the present recording setup used to produce holograms for developmental display systems, an exposure time of approximately 5 s is employed to expose each element of the separation set. A 12.5×12.5-in. object is recorded on a hologram 12×12 mm, using a 15 mW *HeCd* laser as the coherent source. A large percentage of the energy at the output of the laser is lost in the recording system during processing of the beams to ensure that both the reference and object beams are uniform so that uniform color fields

appear in the reproduced images.

Indexing and registration recording

In addition to the three holograms containing the color information, two other holograms are recorded in registration with the image holograms when the information is stored in successive frames on a tape for use in a rapid-access system. These holograms, which are modified versions of the standard Fraunhofer and Fresnel holograms, are used respectively to store indexing and registration information. The display systems currently under development are designed to store hundreds or thousands of frames on a holographic tape strip reeled in a cassette. Access to a given frame is accomplished by inserting a digital number designating the desired frame into the system and searching for the designated frame, using as an indicator a frame designation recorded over the stored image information. This is the same system that is employed in a rapid retrieval system used in conjunction with microfilm tape strips. There is a significant difference, however. The microfilm systems, in general, employ a binary-coded edge track to store the indexing information. This track has several limitations which are eliminated by the use of holographic indexing systems. The binary track is subject to scratches and abrasions; there is no redundancy in the stored information. If the film is scratched in the coded area and a "1" transposed to a "0", or a "0" to a "1", the particular frame associated with that index is lost forever to the retrieval system. Also, the digital data can be read out only when the film is located in the position where the encoded bits are aligned with the sensing detectors. This restriction means that if the film is moving, the retrieval information is available to the retrieval system for only a small percentage of the retrieval time; *i.e.*, the reading duty cycle is low and extreme care must be taken to register the film so that it is read out properly. Recording the indexing information as a Fraunhofer hologram relieves these two constraints. The Fraunhofer recording technique is a redundant technique. If binary-encoded information is recorded, information related to a binary bit is recorded over the total frame area; consequently scratching or abrading the film does not cause loss

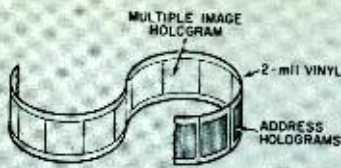


Fig. 6—Storage tape configuration.

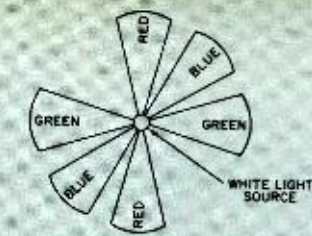


Fig. 8—Reconstruction system end view.

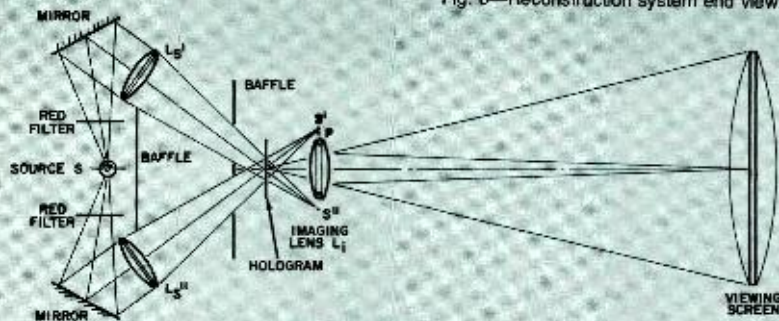


Fig. 7—Multicolor restoration.

of information. In addition, since the Fraunhofer hologram is a far-field hologram, moving the storage medium does not cause motion of the restored binary image. Consequently, as long as the reference beam is passed through the hologram, the information is read out in registration on the detector. If the reference beam is small with respect to the indexing hologram size, the information is available for a large percentage of the time taken to move a given frame through the viewing area and can consequently be used in a retrieval system in which the storage tape is moved at a much higher rate than is possible when using an edge-track registration system.

For indexing systems containing 9 to 12 bits, the registration information is recorded over a major portion of the storage frame and is read out by means of a *GaAs* source and a silicon photodiode detector array. (As many as 500 bits can be stored and read out in this manner over a 12×12 mm format if desired.)

Registration information, recorded as a fifth hologram, is used to properly position the holographic frame after the designated frame has been selected. Positioning information is recorded as a Fresnel hologram, which is a redundant recording form in that information about a point in the object is recorded over a large area in the recording plane. The Fresnel hologram also has the property that a restored image derived from a Fresnel hologram moves in direct proportion to the motion of the storage medium. Thus, it is an ideal form for recording registration information. The hologram of a single point is

recorded if it is only desired to position the film to the center of the frame. This point is reconstructed by using the same *GaAs* source as is used to read the indexing information. A diode quad cell is used as the pickup device. It supplies signals to the transport system used to position the holographic tape so that the reconstructed spot is driven to the center of the quad cell, thus causing the hologram to be centered in the viewing area with the result that the reconstructed image is centered in the display. If it is desired to position the information at a number of locations within the viewing area, a number of points are recorded and a series of detectors employed.

When generating a storage tape as indicated in Fig. 6, the image information is embossed on one side of the tape while the registration and indexing information are embossed on the reverse side but in registration with the image information. Techniques have been devised for performing the embossing process in precise registration.

Reconstruction

Reconstruction of the multicolor image from three superimposed focused-image holograms is accomplished by using a white-light source. In a display system delivered to the Navy, a 350-W tungsten-halogen source is used to produce a display having a brightness sufficient to maintain a display of high contrast (12:1) in a 2000 fL ambient environment. The basic reconstruction system is indicated in Fig. 6. As illustrated, a single color (red) reconstruction is shown only. Similar optical

paths are established for the other two primary colors. These paths are rotated out of the plane of the paper, one by 40°, the second by 90°, so that the beams strike the holograms at the proper angle to interrogate the holograms with a reference beam of the correct color. Fig. 8 shows an end view of the optical source, indicating the orientation of the blue and green reconstruction beams with respect to the red beams.

Considering only the red reconstruction, two cones of light radiating from the optical source are deflected by two mirrors and imaged by lenses L_3 to the points S' and S'' . The points S' and S'' are formed at a location which corresponds to the location of the pinhole of Fig. 3, used to form the reference beam in the hologram recording operation. The angle at which the reconstruction beam passes through the hologram is different than that used in construction to account for a shift in optical wavelengths; consequently, the point S is displaced from the pinhole recording location to accommodate this shift. The recording was accomplished with the 0.4416- μm line of the helium-cadmium laser, or in the deep blue, while the reconstruction is accomplished for the particular beam shown with an optical signal whose nominal wavelength is centered in the red. The offset of the reconstruction beam angle is required because the reconstruction process is a diffraction process resulting in a dependence of the angle on reconstruction of the object beam on the wavelength of the reconstruction signal.

A filter is inserted in the reconstruction path to produce a beam of the proper color to restore the red image. The filter is broadband red filter approximately 0.0800- μm wide, occupying about one-third of the visible spectrum.

In the diagram, the red hologram is oriented so that its fundamental grating structure consists of lines oriented orthogonally to the plane of the paper. The characteristics of the recorded information is such that it may be read out either by a reconstruction beam directed toward S' or toward S'' , although the hologram was constructed with a reference beam having its point of origin in the vicinity of S' . The reconstructed red wavefront is directed down the optical axis of imaging lens L_i in Fig. 7. For a 1:1 image reconstruction, this lens has the same parameters as

recording lens L_4 in Fig. 3. The action of lens L_i on the reconstructed wavefront forms a real image of the red information in the plane of the viewing screen.

Simultaneous readout of the red, blue, and green holograms with three pairs of reference beams derived from the same source produces a full-color image in the viewing area.

The screen may be a normal diffuse viewing screen for use in normal room ambients. For viewing in high light ambient environments, a specially designed high-gain, low-reflectivity viewing screen has been developed. This screen, which consists of a pair of condenser lenses and a lenticular dispersion element, concentrates the energy passing through the viewing aperture into a small eye-relief area. Typically, a 350-W source used to fill a 6-in. display using the above technique produces a display which can be easily viewed in a 2000-fL environment when the energy is concentrated in a 1-ft circular eye-relief area.

Display applications

The techniques described in preceding sections were developed under a series of internal programs and programs carried out under contract to the Navy and NASA. The techniques have been implemented in a display system delivered to the Navy for the display of multicolor moving map information and in a system under construction for NASA for the simultaneous display of computer-generated alphanumeric and graphical data and archival color information. In addition, systems have been proposed for the storage of operator instruction manual information in conjunction with machine language digital test programs for use with automatic test equipments. Currently under investigation is the possibility of using the same technique for the storage of high resolution information such as black-and-white aerial photographs.

Multicolor moving-map display

A demonstration model of a moving-map display (Fig. 9) has been constructed and delivered to the Navy. This display has the characteristics listed in column A of Table I. The system is packaged in two units. One contains the display composed of an optical source, reconstruction optics, a film transport,

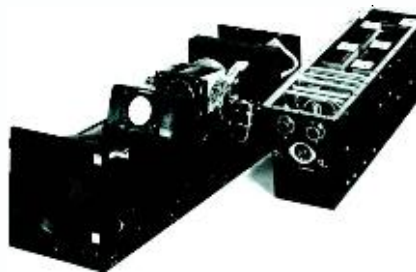


Fig. 9—Moving-map display model.

and registration and indexing readout optics and control logic. The second unit contains power supplies and the transport drive electronics. In this display 12×12-mm holograms are used to store 12½×12½-in. map segments. The display is designed as a moving-map display with a 6-in. viewing aperture. The restored 12½×12½-in. map segments are translated and rotated in the viewing area in accordance with external control signals. In later models an interface will be designed to allow a direct connection of the display with the navigational equipment of the aircraft. The display will then be used to indicate the aircraft's position. When used in a tracking mode, the map will move as the airplane moves to keep the position of the aircraft as indicated on the map centered in the display. In addition to translation of the map image, the image may also be rotated about the display center so that the display may be used in the track-up or north-up mode.

A transport system is incorporated in the delivered display which allows rapid access to any frame on a holographic tape strip containing 500 frames in under 6 s and any frame within ±30 frames of the frame being viewed in under 300 ms. Operation in this manner allows the display to be used as an area-coverage tracking map display system.

The demonstration model is provided with front panel controls to rotate and translate the displayed image, to select and retrieve a particular frame from 500 storage locations, and to dim the display for viewing at low light levels. Additional inputs are provided on the side of the display to simulate computer-generated control signals.

Work is continuing on the development of this technique into a qualified system.

NASA multifunction display

A display is currently being assembled for NASA which employs a holographic storage technique of the type used on the moving-map display for the storage and display of archival information. In addition, this display super-

imposes computer- and keyboard-generated alphanumeric and graphical information on the archival information. An artist's concept of the display is presented in Fig. 10. The characteristics of the archival holographic display portion of the system are presented in column B of Table I.

The alphanumeric and graphical data are displayed on a transparent, 512×512-element, neon-plasma panel. The panel, supplied by Owens-Illinois, is constructed as illustrated in Fig. 11. Gold electrodes spaced at 60 elements per inch are deposited on two pieces of plate glass. A dielectric coating is applied over the electrodes. The two glass plates are then sandwiched together, with the electrodes facing each other and aligned so that the line structures are perpendicular to each other, forming a crossbar addressing system. The plates are spaced apart and the space filled with a neon-rich gas. A 120-V, 50-kHz sustaining square wave applied across the electrodes is not sufficient to break the gas down. If, however, a 50-V pulse is applied on top of the 120-V signal at one or a number of junctions, the gas breaks down forming a plasma, resulting in a neon glow discharge. A wall charge builds up on the dielectric, creating a potential which opposes the applied potential. If no further action were taken, the arc would extinguish and the glow would cease. However, as this condition is reached, the sustaining voltage which is reversed at a 50-kHz rate is reversed; the wall charge now adds to the applied voltage and breaks the gas down in the opposite direction. The cycle repeats itself, sustaining the discharge. It does not have to be refreshed. Erasure of a cell is accomplished by applying an out-of-phase pulse as indicated in Fig. 11.

The unit used in the display has an 8½×8½-in. active area with 512×512 active elements. The holographic image is rear-projected through the plasma panel and fills the 8½×8½-in. viewing area. A transport system is used to retrieve the desired holographic frame. The frame is restored by using an optical system identical in concept to that described earlier.

A keyboard which can be used to select holographic frames and to write on the plasma panel is supplied for use as an input to the system. Alphanumeric information entered from the keyboard

is written on the plasma panel in a 10×16 -element character block, 16 elements at a time. Information may be entered directly from the keyboard or from a computer (an interface is provided for use with an IBM 360 computer). Sixteen bits can be written on the display every $20 \mu\text{s}$, allowing a full page dump to the display in 300 ms.

Graphical information may be entered from the keyboard on a point-by-point basis or from the computer as short vectors, the start and stop location of a vector being sufficient to draw the vector on the display.

A two-page local memory is provided so that the display may be used on-line or off-line. A light pen is also provided for item selection. A laboratory model of this display was scheduled for delivery to NASA in August of 1972.

Automatic-test-equipment information storage

Automatic test equipment such as the LCSS and VAST systems require the storage of a machine language digital test program of 5×10^5 bits and a hundred $8\frac{1}{2} \times 11$ in. pages for each type of unit to be tested. A system has been evaluated by using the techniques described above for storing the text information and a modified Fraunhofer technique for storing the digital information, thus allowing the storage of the one hundred text pages and 5×10^5 bits on a plastic card slightly larger than a credit card.

Conclusion

The advantages associated with the holographic storage of information are real. Holography offers the promise of utilizing some of these advantages to reduce the problems produced by man's increasing propensity to create and requirement to access large amounts of data. The technology and programs described above are but one facet of the holographic work being done within ATL and RCA to reduce these problems.

Acknowledgment

The authors wish to acknowledge the support given the development of the technology described here by Mr. J. Wolin of NASC and Messrs. J. Weldon and K. Warnick of NASA, as well as many people within RCA who have and are contributing to these programs.

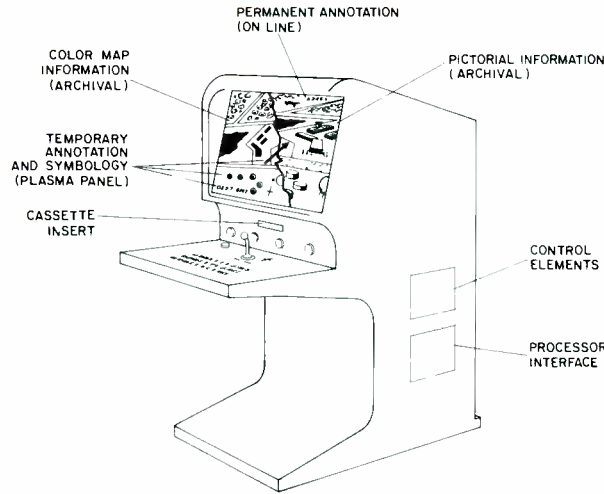


Fig. 10—Multifunction display.

Table I—Moving-map and multifunction display characteristics.

	A. Moving-map display	B. Multifunction display
<i>Resolution</i>	7 to 8 lp/mm, 65% response	7 to 8 lp/mm, 65% response
<i>Viewing area</i>	Circular, 6-in. diameter	$8\frac{1}{2} \times 8\frac{1}{2}$ -in.
<i>Color fidelity</i>	Equivalent to existing aerial charts	High performance in saturated colors
<i>Brightness</i>	Acceptable for viewing (12:1 contrast) in a 2000-fL environment	Acceptable for viewing in a 300-fL environment
<i>Configuration</i>	Two units: power supply and display unit	Floor-mounted console
<i>Display size</i>	$8\frac{1}{4} \times 8\frac{1}{4} \times 26$ -in.	$22 \times 30 \times 48$ -in.
<i>Display weight</i>	18 lb	
<i>Power supply size</i>	$19 \times 7\frac{1}{2} \times 4\frac{7}{8}$ -in.	N/A
<i>Power supply weight</i>	28 lb, 9 oz	
<i>Storage technique</i>		
<i>Map information</i>	Focused-image hologram	Focused-image hologram
<i>Indexing information</i>	Modified Fraunhofer hologram	Modified Fraunhofer hologram
<i>Registration information</i>	Fresnel hologram	Fresnel hologram
<i>Storage density</i>	12.5×12.5 -in. chart segment on 12×12 -mm hologram, 500 holograms per cassette.	$8\frac{1}{2} \times 8\frac{1}{2}$ -in. page stored as 12×12 -mm holograms, 500 per cassette.
<i>Access time</i>	Any one of 500 frames in under 6 s; ± 30 frames in under 300 ms.	Same
<i>Image motion</i>	X-Y translation over ± 3 -in., 360° rotation	
<i>Power requirement</i>	600 W, 115 V, 60 Hz	Not determined
<i>Projection source power</i>	370 W	Not determined
<i>Intended use</i>	Laboratory demonstration	Interface with plasma panel display for on-line use with IBM-360

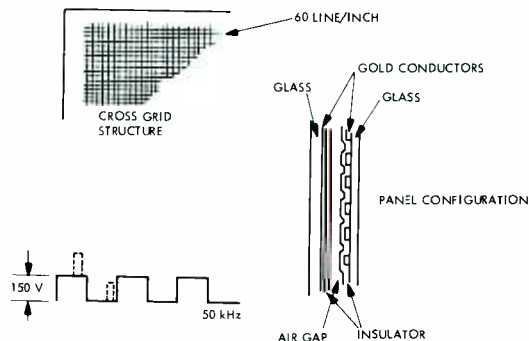


Fig. 11—Plasma-panel configuration.

Millimeter-wave imaging

B. J. Levin | B. R. Feingold | D. J. Miller

Millimeter-wave images of complicated, three-dimensional targets have been obtained for the first time by utilizing diffuse reflections. An aluminum-foil-wrapped letter R has been imaged with 94-GHz radiation, at a range of 3 meters, with a ½-meter-diameter lens. In real situations, the reflected radiation will contain both diffuse and specular components; strong reflections can mask the image. A novel application of spatial filtering has successfully removed these specular returns and allowed shape recognition of randomly oriented complex targets. An overall description of millimeter-wave imaging techniques is presented which includes an analysis of range, resolution, and field-of-view capabilities of practical systems.

Dr. B. J. Levin

Applied Physics Laboratory
Advanced Technology Laboratories
Camden, New Jersey

received the BSEE from Drexel University in 1964, the MSEE from MIT in 1965, and the PhD in Electrical Engineering from the University of Pennsylvania in 1969. He worked on the design of digital circuits on the Early Bird Satellite program at Bell Telephone Laboratories in 1964. In the summer of 1966, he worked on the development of GaAs microwave diode avalanche oscillators as a member of the technical staff of the RCA Laboratories. In the summer of 1967, he worked on frequency locking of microwave diode avalanche oscillators at American Electronics Laboratories. In July 1969 Dr. Levin joined the Applied Physics Laboratory of RCA's Advanced Technology Laboratories in Camden, N.J. At ATL he has continued his investigation of millimeter wave imaging techniques. Since July 1970, he has also made a major contribution to the development of an electronically controlled low-loss phase shifter operating in the 100-GHz region. This work will make possible the development of compact, moderate-range reconnaissance and surveillance systems capable of penetrating inclement weather and providing high resolution. Dr. Levin has published numerous papers and letters on various aspects of millimeter wave image conversion. He is a member of the IEEE, Sigma Xi, Tau Beta Pi, Eta Kappa Nu, and Phi Kappa Phi.

Coauthor B. J. Levin is shown below. Photos of Messrs. Miller and Feingold were not available.



THE MILLIMETER-WAVE PORTION OF the electromagnetic spectrum is a transition region linking two highly developed and very different frequency domains—the optical and the microwave. Millimeter-wave imaging attempts to take advantage of properties of both regions: imaging is done at a wavelength that is short enough to provide sufficient resolution to identify obstacles or targets visually, yet long enough to be able to penetrate optically opaque substances (such as fog or cloth) in a manner similar to microwaves.

Millimeter-wave imaging systems could provide moderate resolution in all types of weather at ranges up to a few hundred meters. The resolution improves as the target gets closer and relatively high-resolution images can be made at ranges of a few meters, even though the target may be behind a cloth or wood screen.

D. J. Miller, Ldr.

Masers and Millimeter Wave Devices
Advanced Technology Laboratories
Camden, N.J.

graduated from the University of Pennsylvania, receiving the BA in Physics in 1959 and the MS in Physics in 1963. He worked on the design of microwave components for airborne radars and ground-based phased arrays in the Microwave and Antenna group of the Philco Corporation from 1959 to 1961. In 1961, he joined the Advanced Technology Laboratories, where he has been primarily concerned with the development of traveling wave masers from S to Ka band. Mr. Miller was Project Engineer in the development of the first wide bandwidth maser, currently being used in the Applications Technology Satellite ground station at Mojave. In 1967 he was promoted to Engineering Leader. Since then he has been responsible for the development of several advanced masers, including the first three-channel C-band maser for radar installation capable of simultaneous "skin" and "beacon" tracking. In January of 1969, Mr. Miller's group activity broadened to include millimeter wave devices and millimeter wave imaging and detection. Mr. Miller has published numerous papers and letters on antennas and traveling wave masers. He is an active member of the IEEE and is a past chairman of the Philadelphia chapter of the PTGTTT-AP.

There are two main problems with the implementation of such a system. The first is the means of converting the millimeter-wave image into a visible display. Two approaches to the image conversion process have been suggested:

- 1) *Direct conversion* by an array of millimeter-wave receivers and
- 2) *Image dissection* by a semiconductor panel with a spatially controllable transmission characteristic.

The dissector requires only one receiver and is more economical; imaging systems based on the semiconductor panel dissector were studied at Ft. Monmouth^{1,3}, at the University of Pennsylvania^{4,5} and at RCA.^{6,7} The receiver array, however, is capable of longer ranges than the dissector and is currently being examined at RCA.

The second difficulty in the attainment of a practical millimeter-wave imaging system stems from the nature of the reflection process at millimeter-wave frequencies. Since at optical wavelengths most objects are rough compared to a wavelength, incident radiation is reflected diffusely. However, the same surfaces are smooth and flat when compared to a wavelength at millimeter-wave frequencies; consequently, incident millimeter-wave radiation is reflected specularly.

Initial millimeter-wave imaging work (images of separate disks and flat plates) used these specular reflections, which are affected by the target's orientation. If the target is not aligned properly, the reflected energy will miss the imaging

Reprint RE-18-2-21

Final manuscript received June 27, 1972.

B. R. Feingold*

Advanced Technology Laboratories
Camden, New Jersey

received the BS in Engineering-Physics from Columbia University in 1965, where he specialized in quantum electronics. He received the MS in Physics from the University of Pennsylvania in May 1967, and is now well into his course work for the PhD degree. In 1965, Mr. Feingold joined the Maser Group of Advanced Technology Laboratories. He has participated in, or was responsible for, programs concerning the development of high frequency traveling wave masers (35 GHz); the development of a three-channel maser for radar applications; EPR studies of Fe³⁺ in rutile to broaden its bandwidth; the investigation of an optically pumped maser utilizing rare earth ions (Tm²⁺, Dy²⁺) in CaF₂, and a study of spin echoes of paramagnetic ions to attain measurements of relaxation times.

*Since this article was written, Mr. Feingold has left RCA to pursue an advanced degree at Harvard University.

system completely. Furthermore, although specular reflections are intense, they provide little information about the overall shape of the target. In fact, the shape of the target can be masked by a specular reflection in the same way as a car can be obscured by the reflection of the sun from its windshield.

The work reported here was concerned mainly with imaging the nonspecular reflections from objects to achieve shape recognition of randomly oriented targets. These weaker, diffuse reflections from the edges of the object were used for the first time. This technique required more sensitivity, and led to reevaluation of image conversion using a receiver array.

In real situations, the reflected radiation contains both specular and diffuse components; therefore, a method was sought to filter out the shape-masking, specular components. A novel application of spatial filtering successfully accomplished this, and may be the key to imaging in a real environment.

Image recognition

Resolution

A millimeter-wave imaging system acts like a camera with a floodlight (see Fig. 1). The millimeter-wave source illuminates the entire object region, and reflected power is collected by the system optics. The optics focus the power at an image plane where it is converted into a visible display.

The resolution of the system is determined by the diameter of the optics and the wavelength of millimeter-wave radiation. The order of magnitude of the resolution can be found from the Rayleigh resolution criterion:

$$\theta_r = 1.22 \lambda/D$$

For a system operating at a wavelength, λ , of 3.75 mm (80 GHz) with lens diameter, D , of 1/2 meter, angular resolution

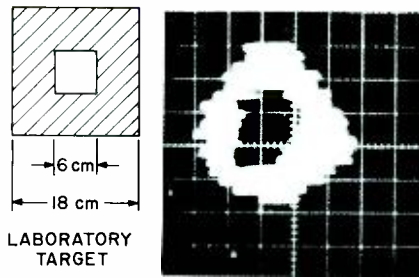


Fig. 2—Millimeter-wave image of square plate with square hole taken by dissector converter using a video detector receiver. Image was formed by specular reflections.

θ_r is about 9 milliradians. This is a linear resolution of 3.6 centimeters at a range of 4 meters.

An image of a flat plate with a square hole is shown in Fig. 2. The image was converted into a visual display by a dissector image converter which is discussed later. The system operated at 80 GHz, at a range of 4 meters, with a 1/2-meter diameter lens. The hole is clearly resolvable—its squareness is apparent in the image—indicating that the system is performing near the resolution limit. Rounding of the outside corners is due to the limited field of view of the system; a limited field of view is one of the disadvantages of the dissector converter.

The image was made using specular reflections from the plate. This made the alignment of the target very critical, as its orientation had to be such that reflections from all four flat regions were collected by the lens.

However, a plate is not a realistic target. Real targets will be three-dimensional, not flat. It is unlikely that all the surfaces from different parts of the object would be correctly oriented to reflect specularly into the lens. In addition, curved surfaces may not reflect specularly at all. Therefore, the resulting image would be missing some features. Thus, to achieve imaging capability for complicated shapes in random orientations, it is necessary to

use diffusely reflected radiation.

Imaging using diffuse reflections

Diffuse reflections scatter radiation in many directions, unlike specular reflections which occur in one direction only. Although it is possible for specular reflection to miss the collecting lens, some portion of diffuse reflections will always be collected.

At millimeter wavelengths, most objects appear flat and reflect specularly, but the object's edges and other surface irregularities in the order of a wavelength will reflect diffusely. Therefore, the diffuse reflections will contain much shape information. However, they will be much weaker than the specular reflections because they will emanate from only a small fraction of the object's surface area and because the energy in the reflected beam will be reduced when it gets to the lens by $1/R^2$.

To image diffusely reflected radiation, the imaging-system's sensitivity must be increased significantly. A special image converter was constructed to determine the image-recognition capability of the system. This converter was a superheterodyne receiver which could be mechanically scanned over the image plane. The output voltage was used to modulate the z-axis of a cathode-ray tube, with the x-y position on the tube corresponding to the position of the receiver in the image plane (Figs. 3 and 4). This image converter is, of course, not a practical device; the actual converter must operate in nearly real time. Its function was strictly to determine the quality of information in the reflected radiation.

The added sensitivity of the mechanical scanner was more than sufficient to produce images from diffuse reflections. A non-flat target (an aluminum-foil-wrapped letter R) was imaged. A photograph of the target is shown in Fig. 5, and two images are shown in Fig. 6. The foil was wrinkled, but not severely on a wavelength scale; the target had to be oriented to avoid strong specular reflections. Fig. 6 shows that the images have a lot of shape information; the curved portion and the straight portions are recognizable in both images. However, the images are partly specular. The images of the R in two positions look different. In Fig.

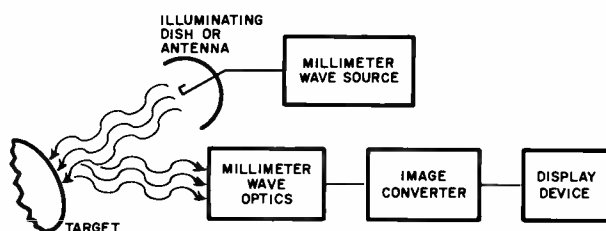


Fig. 1—Block diagram of millimeter-wave imaging system.

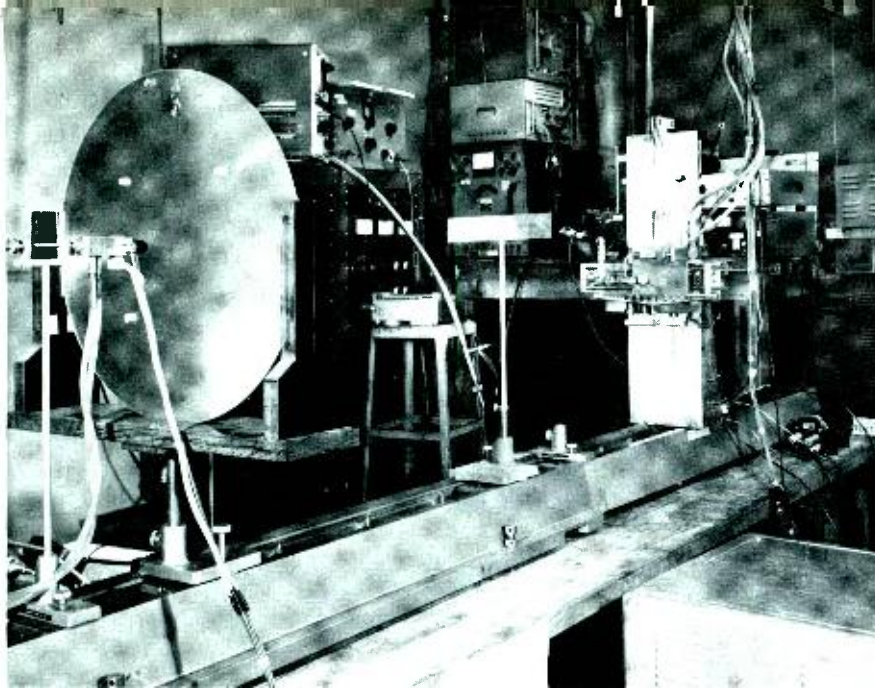


Fig. 3—System incorporating mechanical scanner.

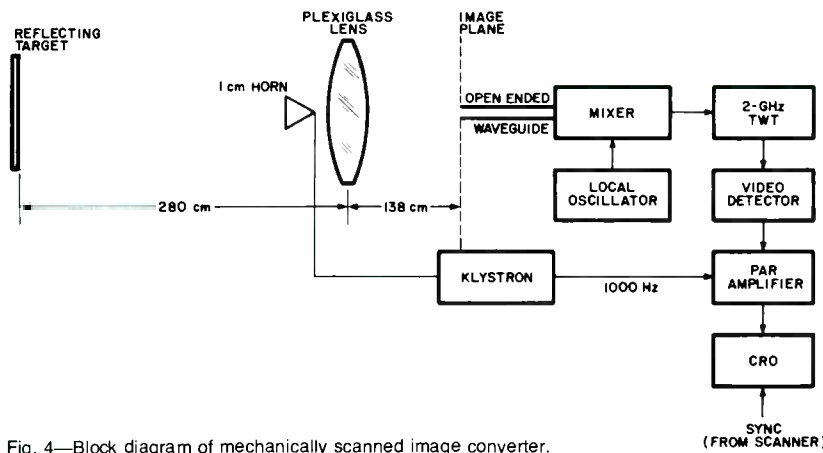
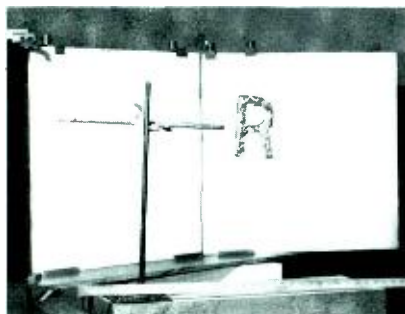


Fig. 4—Block diagram of mechanically scanned image converter.

6a the hole in the R is obscured; the appearance of signal where there shouldn't be is due to specular reflection (although in this case the specular reflection is weak). To obtain a useful imaging system, a means of filtering out the specular reflection is necessary so that target orientation is not required and so that true target shape is revealed. These goals have been accomplished with spatial filtering.



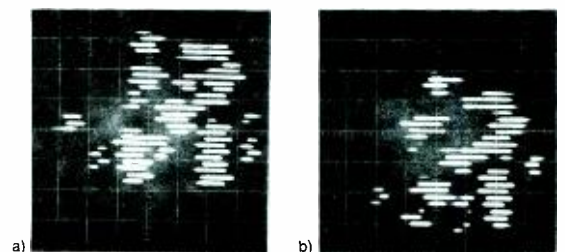
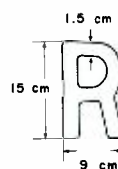
Spatial filtering

Spatial frequency

Fourier-transform techniques have provided a powerful tool in the analysis of linear systems in electronics. The concept of spatial frequency has enabled the introduction of Fourier-transform techniques to the analysis of imaging systems. In electronic networks, Fourier analysis expresses arbitrary waveform in terms of temporal

Fig. 5 (far left)—Aluminum-foil-covered letter R.

Fig. 6 (below)—Images of aluminum-foil-covered letter R taken using diffuse reflections by mechanical scanner. Range was 3 meters, frequency was 94 GHz, and lens diameter was 1/2 meter.



frequencies. In optical systems, an arbitrary wavefront is analyzed into spatial frequencies.

If the complex field distribution across any plane in an imaging system is analyzed, the various spatial Fourier components can be identified as plane waves traveling in different directions. To see this, consider $U(x, y, 0)$, a complex field traveling in the Z direction which is specified at some plane $z=0$ across the x - y plane. The function U has a two-dimensional Fourier transform defined as

$$A_0(f_x, f_y) = \iint_{-\infty}^{\infty} U(x, y, 0) \exp[-j2\pi(f_x x + f_y y)] dx dy. \quad (1)$$

Taking the inverse transform

$$U(x, y, 0) = \iint_{-\infty}^{\infty} A_0(f_x, f_y) \exp[j2\pi(f_x x + f_y y)] df_x df_y. \quad (2)$$

(f_x and f_y , the "spatial frequencies," have the units of inverse length.)

The equation for a unit-amplitude plane wave propagating in a direction given by direction cosines α , β and γ is

$$B(x, y, z) = \exp[j(2\pi/\lambda)(\alpha x + \beta y + \gamma z)] \quad (3)$$

where $\gamma = \sqrt{1 - \alpha^2 - \beta^2}$.

Therefore, at the $z=0$ plane, the complex exponential function, $\exp[j2\pi(f_x x + f_y y)]$, may be regarded as a plane wave propagating with direction cosines $\alpha = \lambda f_x$, $\beta = \lambda f_y$, and $\gamma = \sqrt{1 - (\lambda f_x)^2 - (\lambda f_y)^2}$.

The complex amplitude of that particular plane wave component is simply $A_0(f_x, f_y) df_x df_y$ evaluated at $(f_x = \alpha/\lambda, f_y = \beta/\lambda)$. Now the dimension of inverse length is explicit.

Thus, an arbitrary complex wave can be considered as a summation of plane waves propagating in different directions; this is referred to as the angular spectrum of the wave. Plane waves propagating at large angles with respect to the optic axis represent high spatial frequencies.



Fig. 7—Fourier transform of millimeter-wave source taken by mechanical scanner placed at the focal plane. Signal was limited to increase dynamic range in image.

In electronic networks, the display of the Fourier spectrum requires elaborate circuitry—a spectrum analyzer. Optically, things are much simpler—a simple lens can perform a two-dimensional Fourier transformation. The spectrum (Fourier transform) of a uniformly illuminated object placed in front of a lens is produced in the back focal plane of the lens.⁸

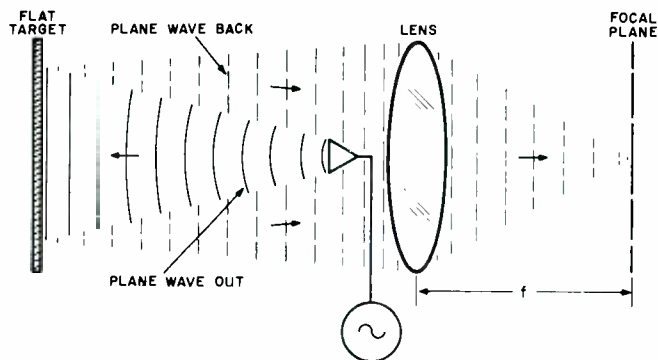
At the focal plane, low spatial frequencies appear near the optic axis and high spatial frequencies appear away from the optic axis.

The mechanical image plane scanner was used to demonstrate the Fourier transforming property of lenses at millimeter wave frequencies. Fig. 7 shows

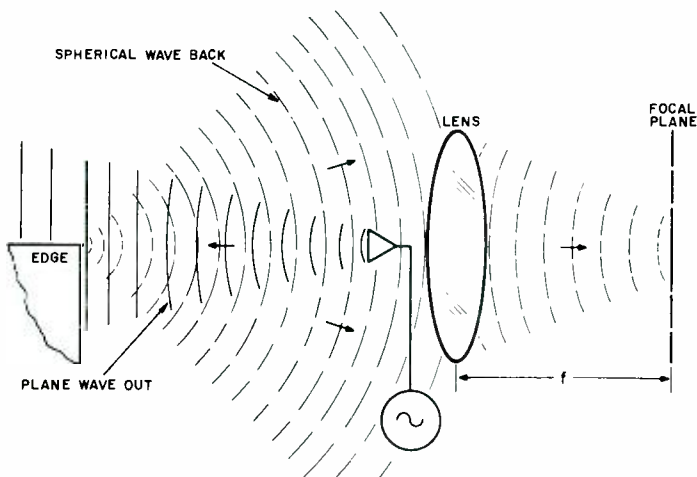
the focal plane image for a point source object (spatial pulse) at 94 GHz. The familiar ring pattern corresponding to the Fourier transform of a finite point can be seen in the image. Distortion in the ring pattern is due to the finite size of the lens aperture.

Removal of specular reflections by spatial filtering

Consider a target illuminated with a plane wave. Reflections from a flat surface (specular reflections) preserve the planar nature of the beam: the reflection will also be a plane wave (see Fig. 8). We have indicated that a plane wave



a) Specular reflection (single low spatial frequency).



b) Diffuse reflection (all spatial frequencies).

Fig. 8—Diagrams showing difference between specular and diffuse reflections.

contains a single spatial frequency; in the case illustrated in Fig. 8, the frequency is zero since the wave's direction of propagation is along the optic axis. Since the lens acts as a spatial Fourier analyzer, the energy from the reflection will be located at the optic axis in the focal plane.

Reflections from a surface with a small radius of curvature (an edge, for example) will be diffuse; energy will be reflected into a broad range of angles. The diffuse reflections can be analyzed into a sum of plane waves traveling at different angles with respect to the optic axis. Therefore, a broad range of spatial frequencies will be included in the reflected radiation, and the energy from the reflection will be spread out in the focal plane of the lens (see Fig. 8b).

Placing a stop at the focal plane, near the optic axis, blocks the specular reflections while letting most of the diffuse reflections pass. Thus, the strong, image masking, specular reflections are filtered out, and the object's shape will appear at the image plane (where before there was only a blob). Because of spatial filtering, the target need no longer be carefully oriented to avoid specular reflections.

The effectiveness of spatial filtering in removing specular reflections is illustrated in Fig. 9. Fig. 9a shows the shapeless, unrecognizable image of the letter *R* which had been placed in a random orientation. Fig. 9b shows the result of filtering out the specular returns; the *R* has appeared and is easily recognizable.

This result is dramatic and encouraging, but it is only a first step. The filter was "matched" for that particularly oriented letter. Since specular reflections will contain only one spatial frequency, they can be filtered. But that frequency will vary for different target orientations because the spatial frequency will depend on the angle

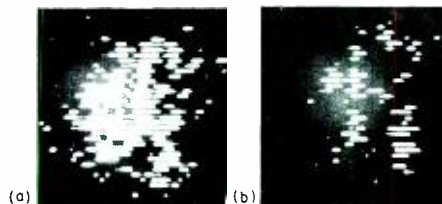


Fig. 9—Effectiveness of spatial filtering in removing specular reflections.

a) Image of letter *R*, randomly oriented.
b) Repeat of millimeter-wave image, but with 2x10 in. horizontal spatial filter placed at focal plane.

between the reflected wave and the optic axis. Furthermore, for complicated targets, there may be more than one specular reflection captured by the lens.

These problems are illustrated by the images of the filtered and unfiltered Fourier spectrum of the *R* (Fig. 10).

It is apparent that this image is not as easy to understand as was the transform of a point source (Fig. 7). The location of zero spatial frequency is not clear from Fig. 10; in fact, it looks as though the specular reflection has a non-zero spatial frequency. Furthermore, there were two specular reflections, which made it necessary to use a focal-plane stop in the shape of a horizontal bar (see Fig. 3) to block both frequencies.

The concept of spatial filtering must be studied further to determine ways of ensuring either that the specular reflections occur at known frequencies only (so permanent focal-plane stops can be incorporated in the imaging system), or providing a filter which can be moved. Such a movable filter could be implemented by incorporating an electronically controlled semiconductor panel (similar to the dissector discussed later) at the focal plane to act as a position-controllable stop.

Apodization

Another technique for image recognition enhancement that has been experimentally investigated is apodization (placing a stop at the plane of the lens.) In terms of the spatial-frequency ideas presented above, the lens has a transfer function associated with it. The object radiation is acted upon by this transfer function to produce the resultant image. Apodizing a lens modifies its transfer function. This has the effect of changing the relative amplitudes and phases of the Fourier components from which the image is synthesized. By removing the proper components (generally the low spatial frequencies), shape information in the image can be enhanced.

The focal-plane image of a point source (Fig. 7) was repeated with an 8-inch central stop placed on the lens. This apodization removes a band of low spatial frequencies (see Fig. 11). Apodization may be a second means of removing the specular components from the reflected radiation; application of apodization to specular reflection filtering is being investigated.

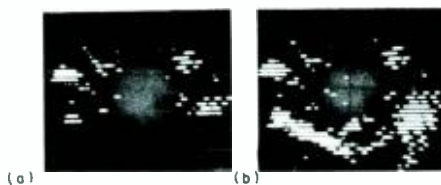


Fig. 10—Images of Fourier transform of letter *R* shown in Fig. 9.

- a) Spatial frequency spectrum of randomly oriented letter *R* taken by mechanical scanner placed in focal plane.
- b) Spatial frequency spectrum after filter that was used to extract image was employed.

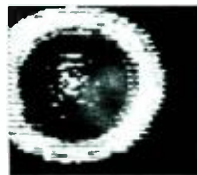


Fig. 11—Spectrum of millimeter-wave point source taken by apodized lens. Note removal of some low spatial frequencies.

Systems considerations

Dissector image converter

Conversion of the millimeter-wave image into a visible image was initially accomplished by dissection; the transmission mode of dissection is illustrated in Fig. 12. Millimeter-wave radiation impinging on the lens from a reflecting target is imaged onto a germanium panel. The panel is made up of slabs of single-crystal, high-resistivity germanium. Because of the low conductivity of the material, millimeter-wave radiation can pass through with very small losses. The entire panel is flooded with light which produces photoelectrons in the germanium. These carriers raise the conductivity of the material, and the increase in conductivity increases the attenuation of millimeter waves in the panel. By increasing the intensity of the light, the panel can be made opaque so that no radiation reaches the detector horn behind the panel.

A small portion of the light is then blocked, forming a shadow spot on the panel. Underneath that spot, the source of excess carriers is removed and the germanium returns to its normal low-attenuation condition. The millimeter-wave energy in that portion of the image under the shadow spot is then free to pass through the panel and be collected by the receiver horn. By moving the shadow across the panel in a raster pattern, the entire image is dissected. The output voltage from the receiver is used to modulate the *z* axis of an oscilloscope, with the *x* and *y* axes synchronized to the shadow-spot raster.

Single-crystal germanium is used because it is an efficient producer of photo-electrons. A light flux of 100 mW/cm² on a 2-mm-thick panel was experimentally determined to be sufficient to increase the attenuation of 80-GHz radiation by 40 dB.

The response time of the panel depends on the recombination time for electrons in the semiconductor. This recombination time can be adjusted to be ~0.33 ms for germanium, indicating that a 100-resolution-element dissector would be capable of operation at 30 frames/second.

The image of the plate with a hole (Fig. 2) was taken at a frame period of 8 seconds. There were two reasons for this. First, the shadow spot scanner was mechanical and not capable of scanning too much faster. Secondly, the receiver used was a simple crystal detector with a VSWR amplifier; sensitivity requirements dictated a longer frame time. In a practical dissector modulation of conductivity in the panel will be accomplished by direct injection of carriers [7], and a superheterodyne receiver would be used, so that real time operation would be achievable.

Range and resolution

The two most important system parameters are range and resolution. These parameters are related, in that resolution can be increased at the expense of range. However, the relationship between the two for the dissector converter is not obvious and is worth examining.

The angular resolution depends only on the wavelength and the lens diameter, but the number of resolution elements also depends on the field of view. The number of resolution elements needed to achieve target recognition is the important parameter. It is assumed that the wavelength and lens diameter will be adjusted to provide a sufficient number of resolution elements.

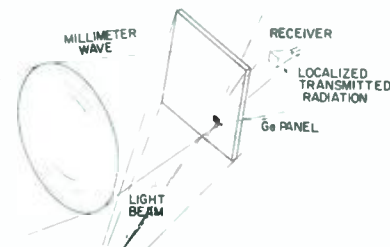


Fig. 12—Transmission mode of dissection.

Assume that the transmitting antenna uniformly illuminates the field of view and nothing more. Then each resolution element in the object field receives a power equal to the transmitter power divided by the number of resolution elements. A certain fraction of this power is reflected diffusely, in perhaps a lambertian distribution. The power collected by the lens, per resolution element, is then

$$P_{lens} = (P_t/N)\rho A/(1/\pi R^2) \quad (4)$$

where P_t is the transmitter power; N is the number of resolution elements; ρ is the reflectivity of the target element; A is the lens area; and $1/\pi R^2$ approximates lambertian scattering.

For the dissector converter, the power per element collected by the receiver is reduced by a factor of $1/N^2$ in passage through the system. This term comes from two factors: time sharing the receiver and fundamental collector antenna loss as expressed in terms of the reciprocity theorem. The effect of time sharing is straightforward; the receiver looks at each resolution element $1/N$ th of the time.

The receiver antenna collection inefficiency adds a second factor of $1/N$. This is due to the fact that the receiver antenna must be able to receive signal from all parts of the dissector panel (since the window can be anywhere), and therefore it must have a wide pattern. However, at any point in time signal emanates from only one window, from an area $1/N$ th of the field of view of the collector. Thus the collector operates inefficiently.

This loss is a fundamental minimum. In practice, of course, the loss is greater: losses such as attenuation in the lens have been ignored.

The power reaching the receiver is

$$P_r = (P_t/N^3)\rho(A/\pi R^2) \quad (5)$$

To get a feel for the numbers, the signal-to-noise ratio will be calculated for a lossless system at a 10-meter range.

For the purpose of calculation, the following, typical, state-of-the-art system was considered:

- 1) Klystron transmitter power=0.5 W
- 2) Receiver noise figure=16.2 dB
- 3) 1/2-meter-diameter (lossless) lens
- 4) 100-resolution-element system.

The value for reflectivity for diffuse reflections is at best a guess: $\rho=0.01$

(1%) will be assumed.

Thus, at 10-meter range

$$P_r = (0.5/10^6) \times 10^{-2} \times (0.2/3.14 \times 10^2) \\ = 3 \times 10^{-13} \text{ watt.}$$

To achieve a 100-element frame in 1/30 second, the receiver must have a bandwidth of 3000 Hz. Therefore, noise power P_n is

$$P_n = NF(kTB) = 5 \times 10^{-16} \text{ watt} \quad (6)$$

where NF is the noise figure; B is the bandwidth (3000 Hz); T is the temperature (300°K); and k is Boltzmann's constant.

The signal-to-noise ratio is 600, which is sufficient for a good dynamic range.

The range is highly dependent on the number of resolution elements. The image of the letter R shown in Fig. 9 contained 75 resolution elements in the field of view; the R itself had approximately 25 elements. To achieve the same resolution and field of view at a range of 10 meters (which can be done by making the lens diameter ~ 1 m and raising the frequency to 140 GHz), 750 resolution elements are required.

To obtain an image with this resolution at 10 meters, but with a more practical field of view (say 10°), would require ~ 7500 resolution elements.

As the required number of resolution elements increases, the receiver-array converter may become a better choice since it does not suffer the $1/N^2$ collection loss.

Receiver array converter

A receiver-array converter will not suffer the $1/N^2$ degradation associated with dissection. An array with one receiver for each resolution element, placed at the image plane, will have perfect collection efficiency; and each resolution element will be viewed continuously throughout the frame time. The disadvantage of this type of converter is the cost of having so many receivers.

Because the response time of each receiver need only be as fast as one frame time, a bandwidth of only 30 Hz is all that is required. Therefore, it may be possible to use pyroelectric elements as millimeter-wave detectors in the array.

The development of a pyroelectric array is still in its early stages. Each

element in the array will consist of a small horn to concentrate the millimeter-wave radiation, a thin-film pyroelectric, and an inexpensive amplifier. Each receiver element will be hard wired to an element in a suitable display, perhaps an electroluminescent diode array. Sensitivities comparable with that obtainable from video detectors are anticipated.⁹ Mass-fabricated pyroelectric detector elements would provide a relatively low-cost receiver array.

The receiver array has the advantage of being modular. To obtain a larger field of view, all that need be done is to add more elements, making the image plane larger.

Conclusions

It has been demonstrated that recognizable images of complex shapes can be obtained using millimeter waves. Images can be recognized even if the target is randomly oriented by filtering out specular reflections which often mask the image. Spatial filtering is being investigated further to make it applicable in all situations, and a more realistic (nearly real-time) system is being constructed for continued evaluation.

Applications for millimeter-wave imaging fall into two classes. The first is close-range, high-resolution pictures which may be taken through concealment. A system to detect weapons is under investigation; it has been found that the placement of a cloth screen between the target and the lens does not affect image quality. The second class of applications is longer-range (100 to 200 meters) lower-resolution imaging to provide all-weather reconnaissance.

References

1. Jacobs, H., Hofer, R., Morris, G., and Horn, E., "Conversion of millimeter waves into visible displays," *J. Opt. Soc. Am.*, Vol. 58 (Feb. 1968) pp. 246-253.
2. Jacobs, H., Morris, G., and Hofer, R. C., "Interferometric effect with semiconductors in the millimeter wave region," *J. Opt. Soc. Am.*, Vol. 57 (Aug. 1967) pp. 993-999.
3. Schumacher, J. D., Hofer, R. C., and Jacobs, H., "Performance of a single-collector millimeter-wave imaging device," *Proc. IEEE (Letters)*, Vol. 58, (Sept. 1970) pp. 1390-1391.
4. Levin, B. J., *Millimeter Wave Image Conversion* (Philadelphia: University of Pennsylvania; PhD dissertation; 1969).
5. Farhat, N. H. and Levin, B. J., "Image dissection and conversion at nonvisible wavelengths," *Applied Optics*, Vol. 9 (March 1970) pp. 765-769.
6. Feingold, B. R. and Levin, B. J., "Millimeter wave imaging," *1970 G-MTT Symposium Digest* (May 1970) pp. 126-130.
7. Levin, B. J. and Feingold, B. R., "All weather eye opens up with millimeter wave imaging," *Electronics*, vol. 43 (Aug. 1970) pp. 82-87.
8. Goodman, J. W., *Introduction to Fourier Optics* (New York: McGraw-Hill; 1968) p. 83.
9. Alday, J. R., "Millimeter wave detectors using the pyroelectric effect," *IEEE Trans. ED*, Vol. 16 (June 1969) pp. 598-601.

Advanced Technology Laboratories — a profile

M. Pietz

One all-important resource—people; one consistent characteristic—the capacity for dynamic evolution: those have been the key impellents in Advanced Technology Laboratories and its predecessors. They were there when a small group came to RCA in 1930 to work on sound recording techniques. They remained the key factors as the group expanded into magnetic recording and projection optics by 1938, into sound powered and infrared communications during World War II, into color television and transistor circuits in 1947, and by the mid 1950's into a span of efforts extending from mathematical analysis and specialized mechanical developments, to visual displays, digital circuitry and wideband recording.

As pointed out by James Vollmer¹, the role of industrial R&D groups has changed during the last decade. The mission of Advanced Technology Laboratories has changed also, if not in statement then in implementation concept. The regard for people as the

singular main resource and the capacity of those people for the initiation of effective technology evolution have not changed.

The basic and lasting product lines of ATL are imagination, creativity, technical excellence, dedication to accomplishment and responsiveness. Responsiveness to the technological needs of G&CS and other divisions of RCA is the mission of ATL and, as stated by Paul Wright², it is the key to ATL's success. An explicit statement of the primary mission of ATL is "the identification, development, and transfer of technologies critical to the success of G&CS business"

Identification of the right technical areas in which to concentrate response and commit resources is complex and absolutely essential. Identification true to present and future need requires constant and effective communication with all G&CS Divisions, and a penetrating insight into the direction of the Government market. Translation of the

Microsonics

Expandable Jammers—EASD

Broad Technology Base

Correlators for Advanced Radar—M & SR

Sensors

Target Designation Receivers

Pave Penny—ASD

Thermal Management

Broad Technology Base

LCRU (Lunar Communications Relay Unit)—GCS

CSAR (Coherent Synthesized Aperture Radar)—GCS

Computer Technology

Standard Cell Technology

MARC (MOS Array Computer)—AED

Advanced Technology Laboratories

- APPLIED COMPUTER SYSTEMS LABORATORY
- APPLIED PHYSICS LABORATORY
- ELECTRO OPTIC LABORATORY
- SIGNAL PROCESSING LABORATORY
- ATL BURLINGTON
- ATL WEST

acquired knowledge of need into program selection is a process described in Andrew Hospodor's article.³

Today there is a ten-unit framework of technologies over which ATL programs are concentrated. A view of the work being accomplished in these programs is given by the articles in this issue of the RCA Engineer. ATL is organized in such a way that the technology framework can be changed readily. The more than 100 members of the professional technical staff are assigned to four broadbased groups in the Central Laboratories, and to two flexible Satellite Laboratories. Physicists and Mathematicians work closely with Electrical and Mechanical Engineers in the same Laboratory. Two or more Laboratory groups often share responsibility for the same project, and special project teams may be composed of members from several groups. The organization chart below shows that the Laboratories are designated by broad scientific disciplines rather than by

product line or specific technology.

The effective transfer of needed technology to the product divisions is indeed the truly successful culmination of all ATL effort. Transfers accomplished in 1971 are pictorially represented on these pages. Continued transfer at an increasing rate of effectiveness is a target receiving intense ATL management concentration. Satellite laboratories in distant G&CS divisions represent a new organizational approach to immediate and continuous technology transfer. The value of this approach has been proven. It will be continued and perhaps expanded in the future.

ATL expects and is prepared for continuing change in the future. There will be organizational changes, market changes, and changes in its technology framework. ATL will be able to reorganize periodically to meet RCA's evolving needs. The future marketplace will be different; emphasis will be on social and environmental problems. Faster

reaction and more efficient performance will be required. ATL will contribute to RCA's competitive strength in this challenging market. New technologies will be required for success in the future—some are beginning to emerge now; charge-coupled devices, COS/MOS-SOS microcircuits, associative processors, holography, microsionics—others are as yet unknown. ATL will continue to derive product knowledge from new technologies, and to transfer this knowledge to product divisions.

Advanced Technology Laboratories has made valuable contributions to Government and Commercial Systems. An even more significant role awaits ATL in the future of G&CS, and in the future of RCA.

References

1. Vollmer, J., "The Role of Laboratories", *this issue*.
2. Wright, P., "A Unique Organization", *cover message—this issue*.
3. Hospodor, A., "Role of Advanced Technology Marketing", *this issue*.

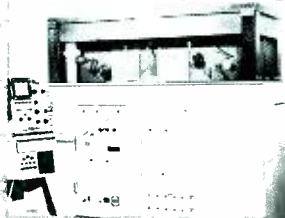
Laser Recording



Basic Techniques



PAR-5 (Precision Airborne Recorder)—GCS



LBIR (Laser Beam Image Reproducer)—AED

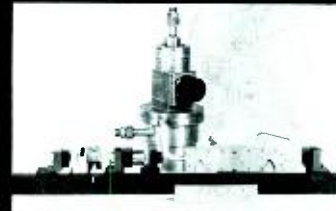
Laser Applications



Optical Monopulse Tracker



AN/FPS 16 Radar—M & SR (Future Optical Painting and Tracking)



Breadboard Target Designator

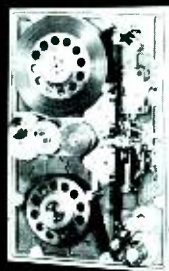


Nd Designator—ASD

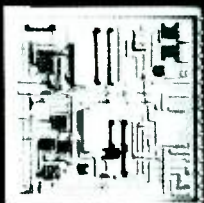
LSI & Hybrids



Phase-Locked Loop & Multiplexer Design



ERTS Recorder—GCS



Continuously Variable Slope Delta Module



ICMS (Integrated Circuit Message Switching System)—GCS



Merle G. Pietz, Ldr., Information Processing Advanced Technology Laboratories, Government and Government Systems, Camden, N.J. received B.S. in Physics 1960. He has completed 60 quarter hours toward the MBA at Drexel Institute of Technology. He joined RCA with the Advanced Technology Department as a Pub-

lications Engineer in 1960, and was promoted to Leader of the Technical Publications group in 1963. In 1967, Mr. Pietz was appointed Technical Publications Administrator for Defense Engineering. In May of 1968, he assumed responsibility for the Advanced Technology Computation Center, in addition to the information Communications group. The Advanced Technology Computation Center, which comprises a Spectra 70/45 computing system, specializes in the processing of Scientific and Engineering problems. The center serves the Camden engineering community. The Information Communications group specializes in the written communication of technical information, serving the engineering groups in Defense Engineering. Mr. Pietz is a member of Sigma Pi Sigma, the American Management Association, and the American Ordnance Association.

The Engineer and the Corporation

Role of Advanced Technology Marketing

A. T. Hospodor

The preceding articles clearly indicate the technical depth and expanse of coverage of the Advanced Technology Laboratories. They also may have generated two key questions in the minds of the readers: How does ATL management select the correct programs? How can RCA afford the expense of such extensive, long-range programs under current economic conditions? These questions and answers to them are not mutually independent. In discussing them, it is necessary to explain the role of Advanced Technology Marketing; to describe some management strategies and policies; and, finally, to say a few words about the future.

THE MOST SIGNIFICANT INPUTS TO ATL program selection are the long-range plans of Government and Commercial Systems. These detailed, comprehensive plans are the result of intensive effort by G&CS management. The plans, which are formulated annually and updated to meet changing environments, contain explicit statements of business objectives for both G&CS as a whole, and for each of its operating divisions. They provide the framework for investment, charter development, and technology direction, in addition to stating planned areas of new business.

Advanced Technology Marketing performs the critical task of integrating the G&CS 5-year plans into the ATL program selection process. This task requires review of the divisional plans, placing special emphasis on the Business Development and Target Capture portions. This one data set provides direction for future business, and the strategies and tactics to be used in the marketplace. ATL Marketing management works with Advanced Technology Laboratories management to convert these broad plans into specific requirements for technological support. Selected technology programs are subsequently reviewed with the G&CS Divisions, and firm ATL programs evolve. It is the broad scope, but specific focus of the Division plans, that affords ATL the opportunity to provide significant technical efforts toward their success.

Andrew T. Hospodor, Mgr., Marketing, Advanced Technology, Camden, New Jersey received the BSME from Cornell University in 1960 and the MSME from Lehigh University in 1963. Lehigh also awarded Mr. Hospodor the MBA in 1967. Mr. Hospodor is responsible for the direction of, and planning for the sale of Advanced Technology programs to the U.S. Government. Mr. Hospodor joined RCA in 1966 as a sales representative in Advanced Technology Marketing. In 1969 he was promoted to sales manager of this organization, and was promoted to his present position in April of 1972.



Reprint RE-18-2-2
Final manuscript received June 8, 1972.

Financial support

The financial support to carry out these efforts comes from three principal sources: Independent Research & Development, G&CS profit, and contract support provided by the Federal Government. Either internal R&D or profit funds might be employed exclusively in those rare cases where G&CS finds itself behind the state-of-the-art, or where a policy of industrial secrecy might provide a market advantage. However, the use of these RCA funds to finance a majority of ATL's efforts would result in a forced reduction in the level of ATL's activity and a subsequent denial of the broad-base technology support required for the healthy future of G&CS.

Key policy

It is now necessary to make a key point regarding the business philosophy of the Advanced Technology Laboratories. They do not stress the normal profit center motivations; nor is their function the forced spawning of new businesses. Rather, their function is technology support in those areas where there is a coincidence of Government need, G&CS need, and ATL skills. This business philosophy has led to the evolution of a key ATL policy: the U.S. Government is much more than a source of funds, it is a co-investor in G&CS's future. Aware of the Government's and Divisions' long-range plans, ATL Marketing and Engineering agree to initiate a program in a given technology area, in many cases prior to identification of an exact source of Government funds. If the planning has been done correctly, the funds for R&D will become available. When they are available, ATL should already have a demonstrable skill in a key technology area, providing G&CS with market leverage and the Government with an excellent co-investment opportunity.

How is the customer convinced that investment in RCA provides him with a viable solution to his technical problem? As a first step, he is made an integral part of the planning process. From the initiation of the G&CS yearly planning cycle, the customer is briefed at the planning, management and technical level. The Government knows what ATL is going to do before the fact. In many cases a customer offers informal direction to internal ATL programs to better fit his requirements.

Selling

Without the successful implementation of another major marketing responsibility—selling—the best plans in the world are of little value. Where planning tends to be a top-down process within both G&CS and the Government, selling advanced technology is a process that requires substantial effort at all levels. The major selling roles of Advanced Technology Marketing are the identification of those Government agencies likely to be technical monitors in areas of ATL technical skill, and the initiation of a professional relationship between RCA engineers and Government technical personnel. Once the needed relationship has been established, the remainder of the process is very straightforward.

Establishing mutual professional respect and interest between RCA and Government technologists places a unique burden on the ATL Marketing men. They must possess substantial technical knowledge; for, on the basis of this knowledge, they are required to generate customer confidence. They must be planners, salesmen, and engineers; similarly, ATL Engineers bear a heavy burden of selling and planning responsibility.

This method of marketing is complementary to that being performed by the Divisions. ATL contracts are generally less than \$100K, and are sold to a single individual or a small group of individuals within a single customer organization. The Divisions, on the other hand, operate in a marketplace which has the added complexity of multiple customers (both organizationally and geographically) with multiple decision points. The normal time from a decision to initiate a new ATL program to contract execution is probably eighteen months, while a Division may pursue a major system program for four or five years before a contract is signed. This long-range characteristic, in combination with the broad scope of G&CS plans, is precisely the reason that ATL can provide long-range technology support for major system targets.

Technology transfer

The results of these planning and marketing efforts have been quite gratifying. For the last five years, Advanced Technology Marketing has met or exceeded all of its goals in the marketplace. Meeting these goals has provided the financial basis for a more critical goal—technology transfer within RCA. In 1971, significant technology transfer occurred in seven of the ten technologies currently being undertaken by ATL. Earlier in this paper, two questions were raised, and a statement was made regarding the interdependent nature of the questions and their answers. In 1971, and previous years, the ways in which these questions were answered produced satisfactory results. What about 1972 and future years?

Technology transfer is the focus of attention for ATL Marketing and Laboratories in 1972. Programs in the infant stage which did not provide transfer in 1971 are being nurtured and culled to provide healthy, lively candidates for future transfer. In all cases, transfer is occurring as a result of proposals, customer briefings, symposia, and contracts, in which the Advanced Technology Laboratories and the Divisions of G&CS are participating as partners in the future of RCA.

Ion implantation

Dr. C. W. Mueller | Dr. E. C. Douglas

Ion implantation has become a new and advanced scientific tool in the highly sophisticated silicon technology. RCA Laboratories has assembled a dual-line ion implanter which is capable of performing both production and experimental work.

Dr. Charles W. Mueller, Fellow
Process and Materials Applied Research Laboratory
RCA Laboratories
Princeton, New Jersey

received the BSc (*magna cum laude*) from Notre Dame University in 1934, an MSEE and ScD in physics from Massachusetts Institute of Technology in 1936 and 1942, respectively. Between 1936 and 1938, he worked on electron tubes at the Raytheon Production Corporation, and at M.I.T. he worked on tubes for computing purposes. He joined RCA Laboratories in 1942 and presently supervises ion implantation research and development in the Process and Materials Applied Research Laboratory. Dr. Mueller developed the first alloy junction transistor for higher-frequency operation and developed the thyristor-type switching transistor. He supervised the work leading to a parametric diode and the development of a low inductance ceramic enclosure for diodes. He participated in the development of tunnel diodes for which he was one of the recipients of the David Sarnoff Team Achievement Award in Science in 1962. More recently, he has been working on the growth of single-crystal silicon films on sapphire and the use of these films for electron devices and integrated circuits. Dr. Mueller has contributed to the recent developments of silicon vidicons and storage tubes, and holds many patents in the fields of electron tube and solid state devices. In 1961-62 Dr. Mueller held the RCA European Study Fellowship and spent the year on special studies in the field of solid state physics at the Swiss Federal Institute of Technology in Zurich, Switzerland. Dr. Mueller was awarded the David Sarnoff Outstanding Achievement Award in Science in 1966 with the citation "for outstanding contributions to semiconductor devices and circuits." He is a Fellow of the IEEE and a member of the American Physical Society and Sigma Xi.

Authors Douglas (left) and Mueller.



AN ION IMPLANTER¹ is a machine that produces the desired ion species, accelerates them, sorts them according to mass, and then implants them uniformly over the surface of a solid. The ion implantation process has been used for several years by the physicist for solid state experiments. In the last two years, rapid progress has been made in the complex instrumentation of these machines and in understanding the annealing and channeling technology so that ion implantation has now become a tool of the engineer for making semiconductor devices.

The physicist built up his machine by purchasing the individual parts, assembling them into systems, and then gradually bringing the individual systems into a properly functioning unit. This process frequently took from one to two years. Now, fortunately, an advanced ion implantation machine can be purchased and put into operation rapidly. The machine to be described, which is much more complex than production types, was assembled and put into operation at RCA Laboratories in

Reprint RE-18-2-22
Final manuscript received May 17, 1972

Dr. Edward C. Douglas,
Process and Materials Applied Research Laboratory
RCA Laboratories
Princeton, New Jersey

performed his undergraduate work at the College of Wooster, Wooster, Ohio where in 1962 he was granted the BA degree with honors in physics. His graduate work was performed in the Electrical Engineering Department at New York University where he worked also as a graduate assistant, taught undergraduate courses, and was awarded an NSF graduate fellowship. In 1964, he received the MEE degree and was granted the PhD in 1969. Dr. Douglas became a Member of the Technical Staff at RCA Laboratories in 1969. He has worked in the area of lensless, high-resolution projection techniques and has studied the high-light-level overload characteristics of RCA's silicon vidicon. He is presently studying the physics of implanted ions and is working on the application of ion implantation techniques to integrated circuit devices. Dr. Douglas is a member of Eta Kappa Nu, Sigma Xi, IEEE, and the American Physical Society.

about two weeks with the assistance of the manufacturer, Accelerators, Inc.

The necessary parts of an ion implanter are: an ion source, accelerating column, mass separator, and target chamber. Fig. 1 shows how these parts were integrated in the construction of the machine at RCA Laboratories. This implanter is essentially two machines in one: a research and development (R&D) line and a production beam line with a common ion source, accelerating column, and mass separator. Ions can be implanted using one line while work is being setup in the other.

Ion source

The photograph of Fig. 2, taken inside the lead-shielded room, shows the ion source with its controls and the accelerating column. An ion source must provide an intense source of the desired ion, be readily controlled, and remain stable when set. Two ion sources are available that can be attached to the machine. One utilizes a 100-MHz oscillator which ionizes a gas of the desired material in a Pyrex tube with exterior electrodes. The gas from a large bottle is continuously fed into the system through a thermomechanical leak. The ionized gas is pulled from the discharge by a DC voltage and focussed magnetically through a small hole into the accelerating column. This form of ion source is easy to use for any material that can be obtained as a gas or vaporized by RF discharge. For non-gaseous materials, the material is placed in a heated chamber, and the vapor is ionized by an electron stream. By proper choice of either of these two sources, ions of most elements can be produced. All the source controls are at +300kV with respect to ground and are cantilevered from the grounded support at the wall of the lead-shielded room (Fig. 2). Thus, all the equipment outside of the lead-shielded room is at ground potential. The controls of the ion source are driven by servo motors at ground potential through 2-1/2 foot-long plastic rods passing along the accelerating column. Controls for the servo motors are at the main control panel.

Accelerating column

The accelerating column consists of two rows of accelerating rings—one to accelerate the ions and the other row,

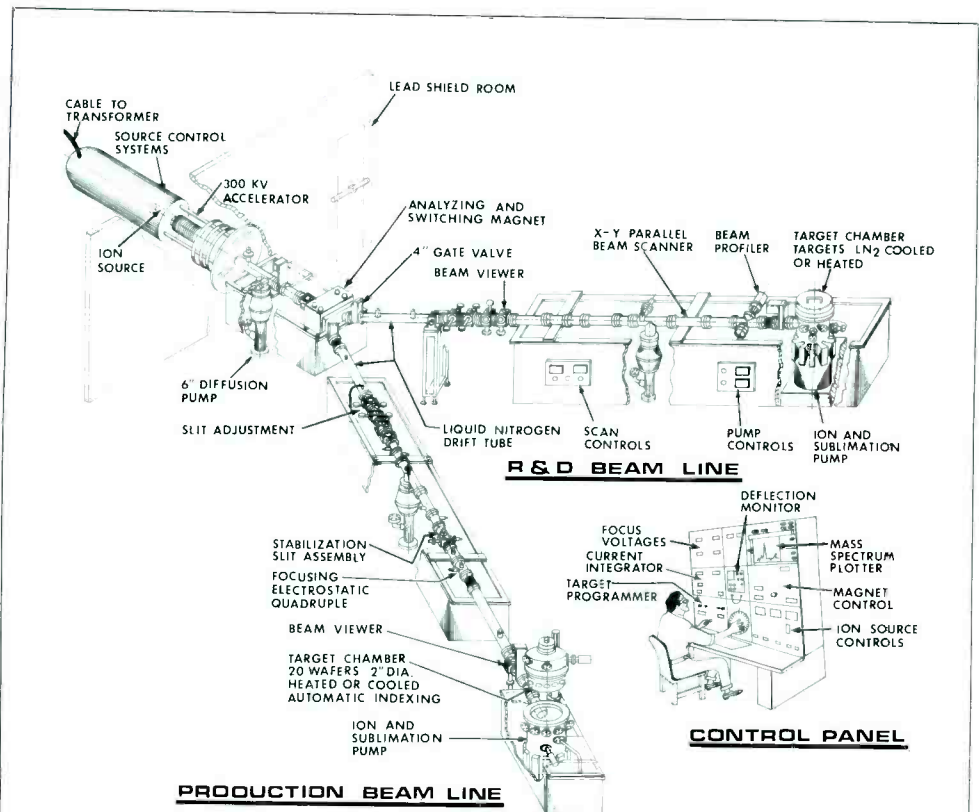


Fig. 1—Ion implanter.

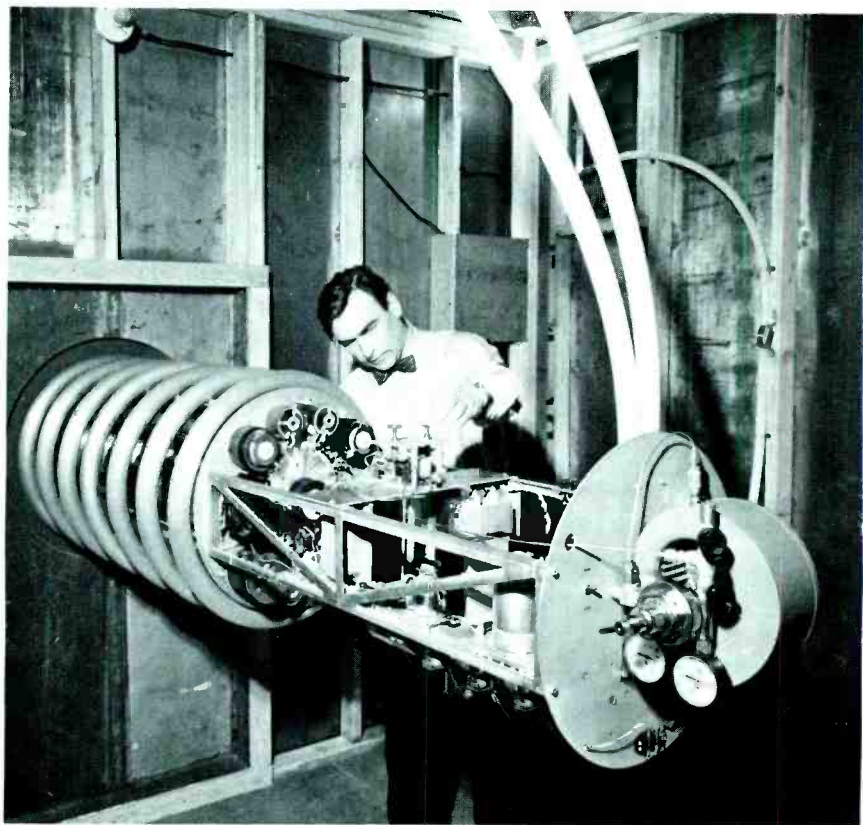


Fig. 2—View of ion source and accelerating column taken inside lead-shielded room (F. Kolondra adjusts gas flow).

which surrounds the first, to help distribute the voltage more uniformly and decrease corona (Fig. 2). The voltage is provided by a well-regulated transformer housed in a steel tank and insulated with SF_6 gas.

Electrons that are produced at the grounded end of the accelerating column travel in the opposite direction to the positive ions and can create 300 keV X-rays when they strike the end of the tube. Also, with gas pressurizing around the accelerating column, the range of the machine can be extended to 450 keV. To prepare for this future increase in voltage, the lead shielding was chosen to be ¼-inch thick. An interesting feature of the room is that it was constructed of plywood with a ¼-inch lead sheet laminated to one side. Lead sheet and plywood were cut at the same time with circular power saws during assembly.

An additional Einzel lens is used at the end of the accelerating column to help focus the ions when low-voltage (25 kV) operation is desired.

Mass separation

Immediately outside of the lead-shielded room is a 6-inch diffusion pump that pumps out both the neutral gas escaping from the ion source into the accelerating column and the line going through the magnet. All the diffusion pumps on the system have anti-creep liquid nitrogen traps. Gate valves isolate various sections of the vacuum lines and are automatically closed if the pressure rises too high.

The magnet provides the dual function of mass separation and of switching the beam into either the R&D beam line or the production beam line. The magnet provides a $M \times E$ product of 72 at 15°. A gauss meter is used to set the value of the magnet field so that the desired ion mass is directed down the tube. A mass spectrum plotter on the control panel traces out the amount of ion current as a function of magnet field. From the shape and magnitude of the plotted spectrum, the desired mass peak can usually be recognized.

Beam lines

The beam is about ¼-inch in diameter after it passes through the magnet and enters either drift tube. The drift tubes can be set at $\pm 30^\circ$ or $\pm 15^\circ$. Normally

the production beam line is set at 30° to get the best resolution and the R&D line is set at 15° to handle higher mass ions. Both lines have adjustable slits which are set to cut out unwanted ions which may be close to the desired ion. The slits are connected to a feedback system which automatically keeps the ion beam in the center of the beam line.

To obtain uniformity of ion dose over a 2-inch target, the beam is scanned in raster fashion. The R&D beam scan has a double deflection so that the beam always enters the material in a constant direction with respect to the crystal lattice. This allows channeling experiments to be performed where the exact vector relations between the beam and the crystal axis are important. The R&D beam line also has a beam profiler which is a rotating wire that samples the current of the ion beam at various points across the beam and displays the current on an oscillograph.

The production beam line has a carousel chamber which holds 20 silicon wafers, each 2 inches in diameter. The structure of the carousel is depicted in the photograph of the machine (and the authors) at the beginning of this article. The number of ions entering the target is counted by a current integrator and after a preset dose is reached, the carousel is automatically indexed to the next wafer. Experiments can be performed quickly because many wafers can be implanted to the same dose of each wafer can have a different dose and/or a different implant energy. The uniformity of the implant over the 2-inch wafers is better than 2% and is usually better than the bulk silicon slices. The silicon wafers in both chambers can be cooled to liquid nitrogen temperature or heated to any desired temperature up to 600°C. Each chamber has an ion and a titanium sublimation pump.

Uses of ion implantation

One of the major and most successful uses of ion implantation, to date has been the application of the technique to silicon devices² and circuits. However, ion implantation is not a new way to make devices but a way to perform certain steps in the ever increasingly sophisticated silicon technology. Ion implantation is not a replacement

for diffusion or epitaxial growth. In fact, it would not be economically advisable to replace any of the present methods where the older and well-developed ways are adequate. Some of the distinguishing characteristics and particular applications where ion implantation has unique advantages are listed below:

- High uniformity and reproducibility
 - High-value resistors
 - Matched devices
 - P wells for CMOS
- Low-temperature Processing
 - Closed-spaced bipolar and MOS transistors
- Precise control of dopant concentration and depth
 - Impatt high-frequency diodes
 - Varactors
 - Buried layers
- Implantation through an oxide
 - MOS threshold adjustment
 - Guard bands
- Self-aligned structures
 - MOS transistors
- No cross contamination
 - Combine n- and p-type devices

Ion implantation has inherent advantages where precise control of low doping concentrations and uniformity over the wafer are necessary. Exactness and uniformity are made possible by actual counting of the ions deposited and by sweeping the beam over the target surface. In low-concentration doping production, freedom from contamination introduced by the furnace walls and the impurities in doping gases are important. The magnetic mass separation avoids the cross contamination of n- and p-type impurities. The same chamber is used for low n- and p-type doping and one operation can immediately follow the other.

Another feature of ion implantation is that unique profiles in the material can be accurately designed. The diffusion technique is limited to the shape set by the driving force (which is the impurity gradient) and the laws of diffusion. With ion implantation, very thin and very abrupt profiles can be obtained and the profile can be changed by adjusting the bombardment voltage. This possibility has been exploited in the hyper-abrupt junction, which has had its maximum use in very-high-frequency Impatt diodes or in varactor diodes where a rapid change of capacitance with voltage is desired.

Another interesting application is to implant into silicon through an oxide. The oxide protects the surface during

handling. This type of implantation can be used to accurately adjust the threshold voltage of MOS transistors or to make guard bands or channel stoppers that prevent surface inversion leakage paths.

Annealing and channeling

When 100-kV ions smash into a crystal of silicon, each ion on the average displaces 10,000 atoms of silicon. This is excessive damage for most device applications. With proper treatment, fortunately, the crystal can be annealed to produce very useful properties very close to that of the original single crystal. Also, by the proper choice of annealing temperature some defects can be left in the crystal that are useful. For example, the temperature coefficient of implanted resistors can be controlled in this manner.

The symmetry of a crystal allows certain paths or channels to exist in the solid through which ions can travel 3 to 4 times the distance they would travel in amorphous material of the same density. One must, therefore, carefully consider the effect desired and then decide what the angle between the beam and the crystal axis should be. To get sharper profiles in silicon, channeling is minimized by bombarding the crystal in a direction that is about 7° off the <111> or <100> direction.

Implantation depth, profile, and dose

The depth at which an implanted ion comes to rest depends on the ion mass, the mass of the atoms in the bombarded crystal, and other factors such as temperature, crystal structure, etc. If the angle of beam incidence on the crystal is set so that no channeling occurs, the shape of the distribution inside the crystal is to a good approximation a Gaussian. Formulas have been derived^{3,4} for calculating the depth of penetration or range, R_p , and the spread of the Gaussian ΔR_p , given the energy and mass of the incident ion and the mass of the atoms in the substrate. Fig. 3 shows a plot of a typical profile that results when boron or phosphorus is implanted in a silicon wafer using 150 keV.

The value of the impurity concentration, N_{max} , at the peak of the Gaussian distribution is controlled by measuring

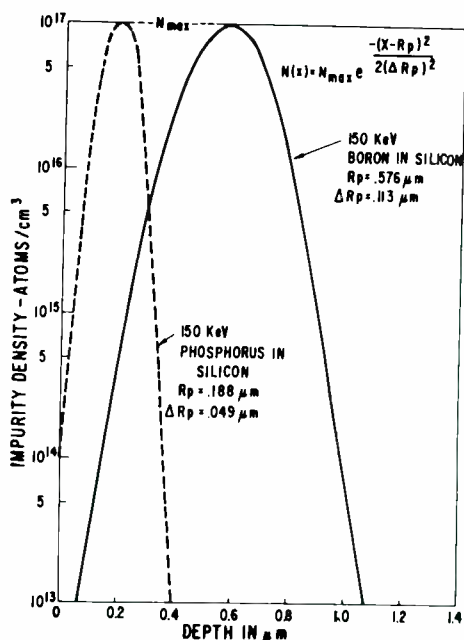


Fig. 3—A plot of the Gaussian-shaped profiles that result from the implant of boron or phosphorus in silicon using 150 keV. The value of the Gaussian profile at the peak is chosen as a representative value.

the ion dose, N_{Dose} , i.e., the total number of atoms/cm² incident on the wafer surface. N_{max} and N_{Dose} are related by the following expression:

$$N_{Dose} = \sqrt{\frac{\pi}{2}} N_{max} \Delta R_p \left(1 + \operatorname{erf} \left[\frac{R_p}{\sqrt{2} \Delta R_p} \right] \right)$$

If the target chamber is provided with

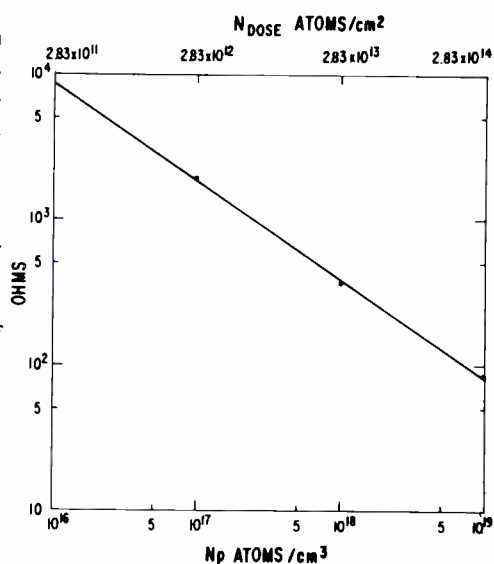


Fig. 4—A plot of the results of the making resistors using 150 keV boron atoms implanted in a 50 Ω-cm n-type substrate. Any value of resistance in the range shown can be obtained within a few percent by selecting and controlling the value of the dose N_D .

a suppressor electrode which prevents secondary emission electrons from escaping from the target, the dose, N_D , can be measured to a high degree of accuracy by integrating the current flowing in the target as a result of the incident ions.

Fig. 4 shows the results of an experiment in making resistors using ion implantation. Boron atoms were implanted in a 50Ω-cm n-type silicon substrate using an energy of 150 keV. Any desired value of resistance in the range shown can be obtained within a few percent by selecting and controlling the proper ion dose.

Conclusion

The applications that have been discussed have been with silicon, mainly because this is where most of the work has been done. There will, of course, be many uses developed for ion implantation in other materials as the demand for accurate ion placement or synthesis increases and this, in turn, will lead to the development of the accompanying knowledge applicable to the specific material. Physical and chemical reactions inside a material, especially a compound material, are quite complex, however, and we cannot simply assume that in ion implantation one has a "Maxwell demon" who puts the implanted ion exactly where it is wanted without producing side effects.

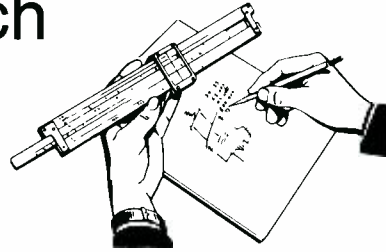
Ion implantation is a new tool now available to the solid-state engineer for building devices. With it some old tasks can be done with much higher precision, and a number of new tasks can be accomplished which otherwise would be difficult or impossible. In the near future, every large semiconductor factory will be equipped with some form of ion implanter that will be used routinely where necessary and economically feasible for the production of particular semiconductor devices.

References

1. Mayer, J. W., Eriksson, and L., Davies, J. A., "Ion Implantation in Semiconductors," Academic Press, New York, 1970; Gibbons, J. F., "Ion Implantation in Semiconductors—Part I: Range Distribution Theory and Experiments," *Proceedings of the IEEE*, Vol. 56, pp. 295-319; European Conference on Ion Implantation Petergrinus Ltd., England (1970).
2. Many different silicon device applications are discussed in the abstracts of the ion implantation sessions in the International Electron Devices Meeting, 1971.
3. Johnson, W. S. and Gibbons, J. F., "Projected Range Statistics in Semiconductors," distributed by Stanford University Book Store (1969).
4. Lindhard, J., Scharff, M., and Schiott, H. E., "Range Concepts and Heavy Ion Ranges," *Dan. Vid. Selsk., Mat. Fys. Medd.*, Vol. 33 (1963) pp. 1-39.

Engineering and Research Notes

Brief Technical Papers of Current Interest



Logic-level-to-pulse converter

Michael Lipka
Missile and Surface Radar Division
Moorestown, New Jersey



The converter circuit (shown in Fig. 1) serves as an interface between low-level logic timing circuits and the triggering input of a high-power transmitter modulator. It converts the 4.5-V logic levels usually associated with *DTL* (diode transistor logic) or *TTL* (transistor transistor logic) to the relatively higher pulse levels that are generally required to trigger transmitter modulators. The circuit output is applied to a line driver which can drive up to 500 ft of 75-ohm line. The potential separation between source and load and the low output impedance of the circuit provide a high degree of noise isolation between the strong electromagnetic fields generated in the vicinity of the modulator and the sensitive gated logic circuits at the source.

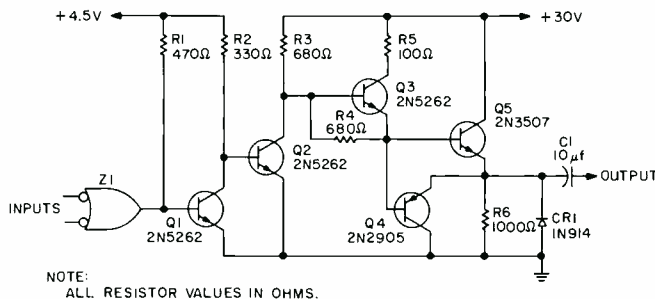


Fig. 1—Typical circuit for logic-level-to-pulse converter.

The converter is activated by a power OR gate Z1, capable of "sinking" (handling) up to 20 mA of current. The inputs to the gate are normally high, and the following transistor stage Q1 is turned off by the low output from the gate. With Q1 in the off state, Q2 conducts, resulting in a low output at the bases of Q3 and Q5, which are therefore nonconducting. If any one of the inputs to the gate Z1 is made to go low, Q2 will be turned off and Q3 and Q5 on, resulting in an output to the load for the duration that an input to Z1 is low.

Transistor Q4 serves to speed-up the fall time of the lagging edge of the pulse. Diode CR1 serves to clip the undershoot portions of the pulse. Such functions are sometimes referred to in the transmitter art as "backswing clipping" (diode CR1) and "tail biting" (transistor Q4). C1 is included for loads which are transformer coupled to protect Q3 from burnout if a logical latch-up should occur ahead of the input to Z1.

The converter will operate effectively at a duty cycle of 10% and pulse widths up to 30 μ s. Pulse rise and fall times into a 75-ohm load are less than 50 ns and transmission delay is less than 150 ns. Pulse amplitudes can range from 10 to 30 V and minimum pulse widths less than 200 ns are possible.

In a usual installation, the design can be made to fit on a module board to complement a family of modules in a pulse-timing subsystem. The converter was operated in a transmitter test-bed installation for driving two hard-tube modulators requiring 30-V triggers for jitter-free operation.

In sum, a converter circuit typically illustrated by Fig. 1 provides voltage level conversion and noise isolation between logic-type circuits and transmitter pulse modulators. It is used to convert *DTL* or *TTL* logic levels to pulse levels suitable for modulator triggering of the type useful in radar systems in which the timing signals are derived from gated logic.

Reprint RE-18-2-72 | Final manuscript received March 7, 1972.

Integrating sphere for use with a spectroradiometer

Dr. L. J. Nicastro
A. L. Lea
Advanced
Technology
Laboratories
Camden, New Jersey



Nicastro



Lea

In many optical systems, it is of great importance to know the spectral distribution of light at remote or practically inaccessible locations in the optical path of the system. A spectroradiometer used for measuring the spectral distribution at such locations is illustrated in Fig. 1. The purpose of the diffuser in Fig. 1 is twofold: A constant fraction of the light incident on the diffuser passes through the entrance slit of the monochromator and impinges on the monochromator grating. The diffuse light at the entrance slit of the

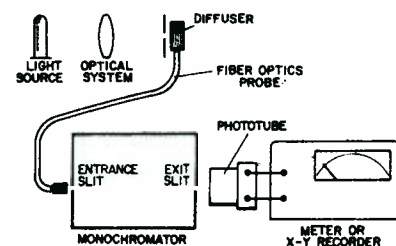


Fig. 1—Experimental setup for measuring spectral distributions.

monochromator ensures that the entire surface of the monochromator grating is illuminated. To obtain absolute measurements of spectral distributions, it is necessary that both of the above conditions be met. The first condition is required because in general the geometry of the calibration source differs from that of the source to be measured. In our work, for example, the standard source used to calibrate the spectroradiometer is a point source of known spectral irradiance, while the distribution to be measured is at the focal plane of a low-*f*-number optical

system. The second condition is required so that errors due to any irregularities in the grating may be minimized.

In commercially available spectroradiometers, the diffuser of Fig. 1 consists of a plastic button or a piece of opal glass, and accurate spectral measurements can be obtained as long as the intensity of the incident light is relatively high. At lower intensities (of the order of 10 nW/cm²/nm), the dark current of the phototube becomes an important factor in the accuracy of the measurements. This lower limit on the intensity that can be measured is determined in large part by the fact that most of the light incident on the diffuser is scattered out of it, and consequently does not pass down the fiber-optics probe to the entrance slit of the monochromator.

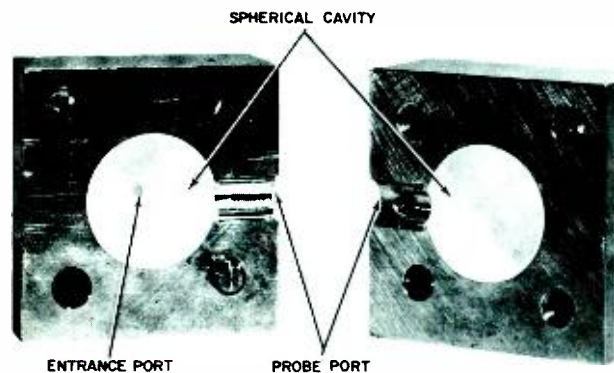
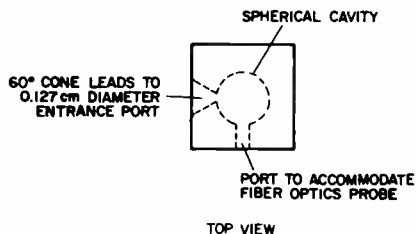


Fig. 2—Configuration of the integrating sphere.

To increase the amount of light incident on the entrance slit of the monochromator, a small integrating sphere was designed for use with the fiber-optics probe. The small integrating sphere, shown

in Fig. 2, was fabricated by cutting a spherical cavity, ½ inch in diameter, out of the two halves of a 1-in. cube of aluminum. A 60° cone was cut out of one face of the cube so as to obtain a 0.050-in.-diameter entrance port at the surface of the spherical cavity. At right angles to the entrance port, a hole of ⅛-in. diameter was drilled to accommodate the fiber optics probe. The surface of the spherical cavity was painted with Eastman No. 6080 white reflectance paint, then the sphere was held together by means of two screws properly placed in the outer cube.

Two sets of spectral measurements were carried out with a setup equivalent to that illustrated in Fig. 1. In the first set of observations the diffuser was a plastic button (the measurements are recorded in Fig. 3); in the second set of observations the diffuser was the integrating sphere, (see Fig. 4). The apparatus that was used for both sets of measurements included: an X-Y recorder, a multiplier phototube with extended S-4 photosurface, a monochromator for dispersing the visible part of the spectrum, a fiber-optics probe, and a 200-W standard tungsten source placed at a distance of 40 cm from the 0.050-in.-diameter entrance port. (The entrance port of the plastic button was obtained by means of a 0.050-in.-diameter hole drilled in a piece of 5-mil-thick copper, which was placed directly against the plastic button.)

Advantages

The advantage of the integrating sphere is that it not only diffuses the light incident at the entrance port, but it also has the capability of collecting it. This capability is clearly demonstrated by a comparison of the spectral measurements of Figs. 3 and 4. For these measurements, the output current of the phototube was adjusted so that it was approximately the same for both sets of observations. This was accomplished by setting the phototube high voltage at 585 V for the plastic-button measurements, and at 450-V for the integrating-sphere measurements. Calibration of the equipment showed that this difference in phototube high voltage represents a factor of 8 increase in the intensity at the entrance slit of the monochromator when the integrating sphere was used as compared to when the plastic button was used. The significance of this result is that spectral measurements can be made at intensities almost an order of magnitude lower when using the integrating sphere. It also may be noted, from Figs. 3 and 4, that there is an improvement in the signal-to-noise ratio (by about a factor of 3) for the integrating-sphere measurements. This is extremely important for obtaining accurate measurements at low light intensities. It is expected that additional improvements can be made with the integrating sphere since the painting of the sphere with white reflectance paint was not done under optimum conditions, and because no attempt was made to optimize the ratio of sphere diameter to exit port diameter (the diameter of the fiber-optics probe).

Reprint RE-18-2-17 | Final manuscript received June 14, 1972.

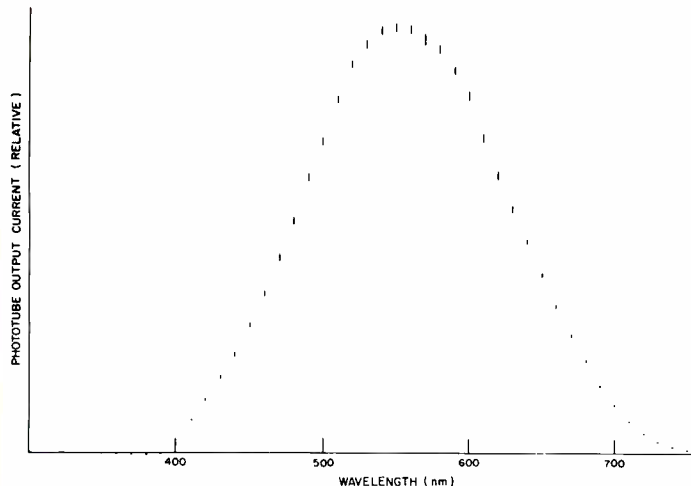


Fig. 3—Spectral distribution measurements carried out with a plastic button diffuser.

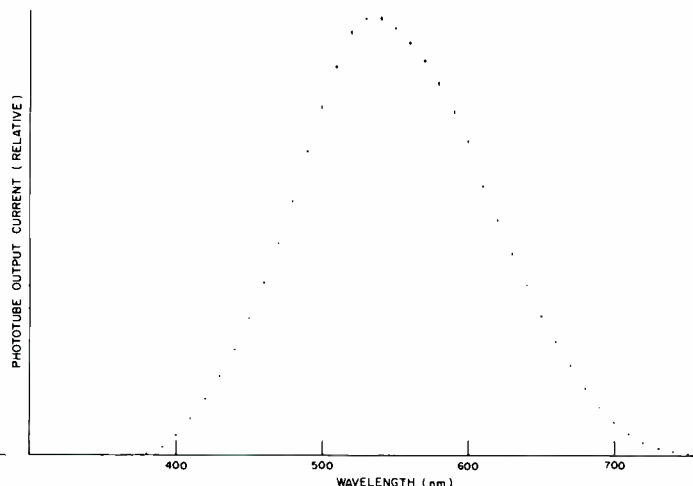


Fig. 4—Spectral distribution measurements carried out with an integrating sphere.



Pen and Podium

Recent RCA technical papers and presentations

Both published papers and verbal presentations are indexed. To obtain a published paper, borrow the journal in which it appears from your library, or write or call the author for a reprint. For information on unpublished verbal presentations, write or call the author. (The author's RCA Division appears parenthetically after his name in the subject-index entry.) For additional assistance in locating RCA technical literature contact, RCA Staff Technical Publications, Bldg. 2-8, RCA, Camden, N.J. (Ext. PC-4018).

This index is prepared from listings provided bimonthly by RCA Division Technical Publications Administrators and Editorial Representatives—who should be contacted concerning errors or omissions (see inside back cover).

Subject index categories are based upon standard announcement categories used by Technical Information Systems, Corporate Engineering Services, Bldg. 2-8, Camden, N.J.

Subject Index

Titles of papers are permuted where necessary to bring significant keyword(s) to the left for easier scanning. Authors' division appears parenthetically after his name.

SERIES 100 BASIC THEORY & METHODOLOGY

105 Chemistry

... organic, inorganic, & physical.

BLOCKED ISOCYANATES, The Chemistry of I, Kinetics and Mechanism of the Reaction of Macromolecular Benzophenone Oxime Carbamates with Dibutylamine—A. W. Levine, J. Fech, Jr., (Labs, Pr) *J. of Organic Chemistry*, Vol. 37, No. 10, pp. 1500-1503; 5/19/72

125 Physics

... electromagnet field theory, quantum mechanics, basic particles, plasmas, solid state, optics, thermodynamics, solid mechanics, fluid mechanics, acoustics.

ANISOTROPIC PLASMAS, Pulse Distortion by—M. P. Bachynski, B. W. Gibbs (RCA Ltd., Mont) *Canadian J. of Physics*, Vol. 50, No. 6; 6/72

ELECTROPHOTOGRAPHY—A Review—R. B. Comizzoli, G. S. Lozier, D. A. Ross (Labs, Pr) *Proc. of the IEEE*, Vol. 60, No. 4, pp. 348-369; 4/72

LIGHT SCATTERING by Second Sound, Theory of—R. K. Wehner, R. Klein (Labs, Pr) Colloquium on Physics of Very High Frequency Phonons, Saint-Maxime, France; 6/72

130 Mathematics

... basic & applied mathematical methods.

GRAPHS Yield Circuit Q for Gyrotors and Other Reactive Elements—H. A. Wittlinger (SSD, Som) *IEEE/EDN Magazine*; 6/1/72

160 Laboratory Techniques & Equipment

... experimental methods & equipment, lab facilities, testing, data measurement, spectroscopy, electron microscopy, dosimeters.

DIELECTRIC FILMS, Recent Trends in Determining Composition and Imperfections of—W. Kern (Labs, Pr) Callinan Award Address Lecture, Electrochemical Society Mtg., Houston, Texas; 5/7-12/72

INSTRUMENTATION—a Review, Selected Topics in—R. E. Honig (Labs, Pr) *Advances in Mass Spectroscopy*, Vol. 5, pp. 249-268; 1972

REFLECTIVITY MEASUREMENTS at 0.6328 and 10.6 μ , Comparative Study of—D. Bennett, A. Waksburg (RCA Ltd., Mont) Aerospace Electronics Symp. Quebec; 3/72

TIN SENSITIZING SOLUTIONS, Contact Angle Measurements of—N. Feldstein, J. A. Weiner (Labs, Pr) *J. of the Electrochemical Society*, Vol. 119, No. 6, pp. 668-671; 6/72

VAPOR-PHASE CRYSTAL GROWTH II, GaN, Mass Spectrometric Studies of—V. S. Ban (Labs, Pr) *J. of the Electrochemical Soc.*, Vol. 119, No. 6, pp. 761-765; 6/72

X-RAY SECONDARY-EMISSION, (Fluorescence) Spectrometry, Practical Aspects of Chemical Analysis by—E. P. Bertin (Labs, Pr) Annual Summer Short Course on Fundamentals and Applications of X-ray Emission Spectrometry, State Univ. of N.Y., Albany, N.Y.; 6/5-9/72

170 Manufacturing & Fabrication

... production techniques for materials, devices & equipment.

EPITAXIAL GROWTH, Dislocations as Related to—M. S. Abrahams (Labs, Pr) Colloquium, Central Research Laboratories, Texas Instruments, Dallas, Texas; 5/11/72

EXPITAXIAL GROWTH, Dislocations as Related to—M. S. Abrahams (Labs, Pr) Electrochemical Soc. Mtg., Houston, Texas; 5/7-11/72

HYDROGEN CHLORIDE AND CHLORINE GETTERING: An Effective Technique for Improving Performance of Silicon Devices—R. S. Ronen, P. H. Robinson (Labs, Pr) *J. of the Electrochemical Soc.*, Vol. 119, No. 6, pp. 747-765; 6/72

MICROWAVE IC's, Production Techniques for—C. Karnitsis, R. Minton, (SSD, Som) Electronic Components Conf., Washington, D.C.; 4/72; Conf. Proc.

PRODUCIBILITY—The Critical Engineering/Manufacturing Interface—A. Levy (EASD, Van Nuys) 1972 WESCON Professional Program, Los Angeles

RF-SPUTTERING TECHNIQUES, Control of Film Properties by—J. L. Vossen (Labs, Pr) Seminar, Laboratories RCA Ltd., Zurich, Switzerland; 5/23/72

SEALING, Hermetic Package—S. Goldfarb (Labs, Pr) Int'l Soc. for Hybrid Microelectronics Joint Metropolitan—Keystone Mtg., RCA David Sarnoff Research Center, Princeton, N.J.; 5/10/72

SILICON ON SPINEL, Substrate Effects in the Heteroepitaxial Growth of—G. W. Cullen (Labs, Pr) 2nd Int'l Conf. on Vapor Growth and Epitaxy, Jerusalem, Israel; 5/21-25/72

TIPPING TECHNIQUE for LPE Film Growth, A New—I. Gordon (Labs, Pr) 2nd Int'l Conf. on Vapor Growth and Epitaxy, Jerusalem, Israel; 5/21-25/72

VAPOR GROWTH SYSTEMS, Effects of Natural and Forced Convection in—J. P. Dismukes (Labs, Pr) Electrochemical Soc. Mtg., Houston, Texas; 5/7-11/72

VAPOR PHASE GROWTH SYSTEMS, Effects of Natural and Forced Convection in—B. J. Curtis, J. P. Dismukes (Labs, Pr) 2nd Int'l Conf. on Vapor Growth and Epitaxy, Jerusalem, Israel; 5/21-25/72

175 Reliability, Quality Control & Standardization
... value analysis, reliability analysis, standards for design & production.

COS/MOS BEAM LEAD DEVICES, Reliability of—W. J. Greig, I. H. Kalish (Labs, Pr) Electronic Components Conf., Washington, D.C.; 5/15-17/72

MNOS MEMORY TRANSISTOR Characteristics and Failure Mechanism Model, Degradation of—M. H. Woods, J. W. Tuska (Labs, Pr) 5th Annual Failure Analysis Seminar, Philadelphia, Pa.; 5/18/72

MOS INTEGRATED CIRCUIT RELIABILITY Considerations—G. L. Schnable (Labs, Pr) 5th Annual Failure Analysis Seminar, Univ. of Penna., Philadelphia, Pa.; 5/18/72

QUALITY PROGRAM For Technical Data—D. Wright, D. Lesser (M&SR, Mrstin) ASQC Annual Technical Conf. Washington, D.C.; 5/8/72

PRODUCTION CYCLE, Reliability in the—W. C. Hiltner (SSD, Som) Advisory Board Panel, 1972 Symp. on Reliability, San Francisco; 1/72

180 Management & Business Operations
... organization, scheduling, marketing, personnel.

INDUSTRY TECHNOLOGY and Methods to Obtain It, Sources of—T. O. Stanley (Labs, Pr) 8th National Symp. on Technology Transfer, Washington, D.C.; 6/13/72

NETWORK PLANNING AND SCHEDULING Models, Decision Making and Decision Models Using—M. Buckley (M&SR, Mrstin) AMA Seminar, New York City; 6/20/72

SERIES 200 MATERIALS, DEVICES, & COMPONENTS

205 Materials (electronic)
... preparation & properties of conductors, semiconductors, dielectrics, magnetic, electro-optical, recording, & electro-magnetic materials.

Al₂O₃ FILMS In Integrated Circuits, The Use of—K. H. Zaininger (Labs, Pr) 2nd Int'l Conf. on Vapor Growth and Epitaxy, Jerusalem, Israel; 5/21-25/72

Al₂O₃ FILMS Prepared by Electron Beam Evaporation, Effect of Substrate Potential on—D. Hoffman, D. Leibowitz (Labs, Pr) *J. of Vacuum Science and Technology*, Vol. 9, No. 1, pp. 326-329; 1-2/72

BISMUTH-TITANATE FE-PC Optical Storage Medium - Further Developments—S. A. Keneman, A. Miller, G. W. Taylor (Labs, Pr) *Ferroelectrics*, Vol. 3, NOS. 2/3/4, pp. 131-137; 2/72

CALCIUM VANADIUM IRON GARNETS, Magneto-optical Effects in Certain—A. Akseirad (Labs, Pr) *Proc. of the Conf. on Magnetism and Magnetic Materials* (Chicago, Illinois, Nov. 1971) pp. 249-253-1972

CARBON-DOPED GALLIUM PHOSPHIDE, Electrical Properties of—D. P. Bortfeld, B. J. Curtis, L. Meier (Labs, Pr) *J. of Applied Physics*, Vol. 43, No. 3, pp. 1293-1294; 3/72

COMPOUNDS K_xFe_{1-x} and K_{0.2}Fe_{2.8}O_{6.2}, Magnetic and Crystallographic Properties of the—L. Darcy, P. J. Wojtowicz, M. Rayl, D. Gutman (Labs, Pr) *Materials Research Bulletin*, Vol. 7, No. 5, pp. 381-384; 5/72

COSPUTTERED FILMS, Calculation of Deposition Profiles and Compositional Analysis of—J. J. Hanak, H. W. Lehmann, R. K. Wehner (Labs, Pr) *J. of Applied Physics*, Vol. 43, No. 4, pp. 1666-1673; 4/72

CO-SPUTTERED DILUTE MULTI-COMPONENT ALLOYS, Compositional Determination of—J. J. Hanak, B. Bolker (Labs, Pr) Int'l. Conf. on Thin Films, Venice, Italy; 5/15-19/72

Sc and O on Si (100): Negative Electron Affinity, Thermal Desorption, Surface Plasmas, LEED-Auger, Studies of—B. Goldstein (Labs, Pr) The Solid-Vacuum Interface, The Netherlands; 6/22/72

ELECTROPHOTOGRAPHIC MATERIALS, Especially in ZnO-Layers, On the Discharge Mechanisms in—H. Kiess (Labs, Pr) *Chimia*, Vol. 26, No. 4; 1972

FERROELECTRIC SbSi, Soft-Mode Coupling and Critical Rayleigh Scattering in—E. F. Steigmeier, G. Harbeck, R. K. Wehner (Labs, Pr) *Proc. of Conf. on Light Scattering in Solids*, (Flammarion-Medecine, Paris, 1971) pp. 369-400; 1972

FERROMAGNETIC SEMICONDUCTORS, Electric-Field-Dependent Magneto-Resistance In—I. Balberg, H. L. Pinch (Labs, Pr) *Physical Review Letters*, Vol. 21, No. 14, pp. 909-913; 4/72

GbAs-(AlGa) As COLD-CATHODE STRUCTURE and Factors Affecting Extended Operations, A Novel—H. Schade, H. Nelson, H. Kressel (Labs, Pr) *Applied Physics Letters*, Vol. 20, No. 10 pp. 385-387; 5/15/72

GRANULAR NICKEL FILMS, Magnetic Properties of—J. I. Gittleman, B. Goldstein, S. Bozowski (Labs, Pr) *Physical Review*, Vol. 5, No. 9, pp. 3609-3621; 5/71

III-V HETERO-EPITAXIAL FILMS Grown on Sapphire and Spinel, Lang Topographic Studies of—S. H. McFarlane, C. C. Wang (Labs, Pr) *J. of Applied Physics*, Vol. 43, No. 4, pp. 1724-1732; 3/72

HETEROJUNCTION and Variable Composition Devices and Materials—M. S. Abrahams (Labs, Pr) Electrochemical Soc. Mtg., Houston, Texas; 5/7-12/72

In_{1-x}Ga_xP for p-n Junction Electroluminescence, Vapor Growth of—A. G. Sigai, C. J. Nuese, M. S. Abrahams, R. E. Enstrom (Labs, Pr) Electrochemical Soc. Mtg., Houston, Texas; 5/7-12/72

LIQUID HELIUM, Properties of Electron Surface States on—R. S. Crandall, R. Williams (Labs, Pr) *Physical Review A*, Vol. 5, No. 5, pp. 2183-2190; 5/72

LITHIUM NIOBATE, Optical Properties and Holographic Storage in Transition-Metal-Doped—W. Phillips, J. J. Amodei, D. L. Staebler (Labs, Pr) Int'l Quantum Electronics Conf., Montreal, Canada; 5/8-11/72

LIQUID SURFACES, Non-Ohmic Electron Transport on—R. S. Crandall (Labs, Pr) *Physics Letters*, Vol. 37A No. 5, pp. 389-390; 12/20/71

LONG EPITAXIAL GaAs n-Layer, Electric-Field Profile and Current Control of a—G. A. Swartz, A. Gonzalez, A. Dreeben (Labs, Pr) *Electronics Letters*, Vol. 8, No. 4, pp. 93-94; 2/24/72

METAL CdCr₂Se₄ JUNCTION, Magneto-capacitance Effect in a—M. Toda, S. Tosima (Labs, Pr) *J. of Applied Physics*, Vol. 43, No. 4, pp. 1751-1756; 4/1/72

Mo³⁺ in SrTiO₃, Electro-Paramagnetic-Resonance Spectrum of—An Example of the Dynamic Jahn-Teller Effect—B. W. Faughnan (Labs, Pr) *Physical Review B*, Vol. 5, No. 12, pp. 4925, 4931; 6/15/72

Nb₃Sn DOPED with Group-III, -IV, and -VI Elements, Preparation, Microstructure, and High-Field Superconducting Properties of—R. E. Enstrom J. R. Appert (Labs, Pr) *J. of Applied Physics*, Vol. 43, No. 4, pp. 1915-1923; 4/72

NEMATIC LIQUID CRYSTALS In Low-Frequency Fields, The Electrohydrodynamic Instabilities in—D. Meyerhofer, A. Sussman (Labs, Pr) *Applied Physics Letters*, Vol. 20, No. 9, pp. 337-339; 5/1/72

n-GaAs, Role of Ionization Inhomogeneities in the S-Type Characteristic of Moderately Heavily Doped—P. D. Southgate (Labs, Pr) *J. of Applied Physics*, Vol. 43, No. 3, pp. 1038-1041; 3/72

NICKEL, Critical Size for Ferromagnetism in—M. Rayl, P. J. Wojtowicz, M. S. Abrahams, R. L. Harvey, C. J. Buicchi (Labs, Pr) *Proc. of the Conf. on Magnetism and Magnetic Materials* (Chicago, Illinois, Nov. 1971) pp. 472-476; 1972

p-TYPE SILICON ON SAPPHIRE Using Dual Rate Technique, The Preparation and Properties of—G. E. Gottlieb (Labs, Pr) 2nd Int'l Conf. on Vapor Growth and Epitaxy, Jerusalem, Israel; 5/21-25/72

p-TYPE SILICON ON SPINEL USING a Dual-Rate Deposition Technique, The Epitaxial Growth and Properties of—G. E. Gottlieb (Labs, Pr) *J. of Crystal Growth*, Vol. 12, pp. 327-333; 1972

PHOTORESISTS III. Adhesion of the Work of Adhesion of Photoresist Films on SiO₂—E. B. Davidson, G. Lei (Labs, Pr) *Electrochemical Soc. Mtg.*, Houston, Texas; 5/7-12/72

ScN, Electron Effective Mass in—G. Harbecke, E. Meier, J. P. Dismukes (Labs, Pr) *Optics Communications*, Vol. 4, No. 5, pp. 335-338; 1/72

SILICON FILMS ON SAPPHIRE Using the MOS Hall Technique, Variations in Electrical Properties of—A. C. Iprì (Labs, Pr) *Applied Physics Letters*, Vol. 20, No. 1, pp. 1-2; 1/1/72

SILICON ON SPINEL: The Interaction Between Deposition Constituents and the Substrate Surface—G. W. Cullen, F. C. Dougherty (Labs, Pr) 2nd Int'l Conf. on Vapor Growth and Epitaxy, Jerusalem, Israel; 5/21-25/72

SnO₂:Sb and In₂O₃:Sn, The Properties of Very Thin RF-Sputtered Transparent, Conducting Films of—J. L. Vossen, E. S. Poliniak (Labs, Pr) Int'l Conf. on Thin Films, Venice, Italy; 5/15-19/72

SUPERCONDUCTING THIN FILMS AND FOILS. III, Pb, Sn, and In, Magnetic Transitions of—G. D. Cody, R. E. Miller (Labs, Pr) *Physical Review B*, Vol. 5, No. 5, pp. 1834-1843; 3/1/72

STRONTIUM TITANATE at the 105°K Transition, Ultrasonic Properties of—W. Rehwald (Labs, Pr) *Physik der kondensierten Materie*, Vol. 14, pp. 21-36; 1971

THIN DIELECTRIC FILMS in MOS Technology, The Role of—K. H. Zaininger (Labs, Pr) Int'l Conf. on Thin Films, Venice, Italy; 5/15-19/72

VAPOR-DEPOSITED Nb₃Sn Effect of Impurity Gas Additions on the Superconducting Critical Current of—R. E. Enstrom, J. J. Hanak, J. R. Appert, K. Strater (Labs, Pr) *J. of the Electrochemical Soc.*, Vol. 119, No. 6, pp. 743-747; 6/72

Y₂O₃:Yb:Er—New Red-Emitting Infrared-Excited Phosphor—J. P. Wittke, I. Ladany, P. N. Yocom (Labs, Pr) *J. of Applied Physics*, Vol. 43, No. 2, pp. 595-600; 2/72

210 Circuit Devices & Microcircuits

... electron tubes & solid-state devices (active & passive), integrated, array, & hybrid microcircuits, field-effect devices, resistors & capacitors, modular & printed circuits, circuit interconnection, waveguides & transmission lines.

CHARGE-COUPLED DEVICES, Fast Interface State Losses in—J. E. Carnes, W. F. Kosonocky (Labs, Pr) *Applied Physics Letters*, Vol. 20, No. 7, pp. 261-263; 4/1/72

CMOS MEMORY MODULE, A Multilayer, Hybrid, Thin-Film 10024 × 3—F. Gargione, G. Noel, W. Keyser (AED, Pr) 1972 Electronic Components Conf., Washington, D.C.; 5/15/72

DIGITAL DEVICES Utilizing Trapped-Plasma Phenomena—H. Kawamoto (Labs, Pr) 1972 Device Research Conf., The Univ. of Alberta, Edmonton, Canada; 6/21-24/72

ELECTRON EMITTERS Based on Negative Electron Affinity—H. Schade (Labs, Pr) Solid State Seminar, Swiss Federal Institute of Technology, Zurich, Switzerland; 6/22/72

FILTERS, Acoustic Surface Wave—C. L. Grasse, D. A. Gandolfo (EASD, Van Nuys) IEEE/EIA Components Conf., Washington, D.C.; 5/72

HEISENBERG FERRIMAGNETS, High-Temperature Susceptibility and Critical-Point Behavior of—S. Freeman, P. J. Wojtowicz (Labs, Pr) *Physical Review B*, Vol. 6, No. 1, pp. 304-307; 7/72

HYBRID CIRCUITS, Cost Effective Military—J. Bauer (M&SR, Mrstn) IEEE Computer Soc. "Microcircuit Packaging Workshop"; 5/17/72

INTEGRATED CIRCUIT DRIVERS, Monolithic High Power—R. N. Guadagnolo (EASD, Van Nuys) IEEE/EIA Components Conf., Washington, D.C.; 5/72

INTEGRATED CIRCUITS for UHF and L-Band Applications, Lumped Element—H. S. Veloric, S. Lazar, R. Monton, H. Meisel, P. Schnitzer, C. Kamnitsis (SSD, Som) First Regional Seminar on High Frequency Applications of Hybrid Microelectronic Technology - Applications and Possibilities, Cambridge, Mass.; 6/72

ITR - A New Reverse Conducting Thyristor Having Unique Properties for Horizontal Deflection—L. S. Greenberg, E. F. McKeon (SSD, Som) Electronic Components Conf.; 4/72; Washington, D.C.; Conf. Proc.

LINEAR IC's. . . And Some of Their Applications, A Cornucopia of—M. V. Hoover (SSD, Som) IC Update Seminars - *Electronic Products Magazine* - Wash. DC and Boston 6/6-7/72; Proc. of IC Update Seminar

LINEAR INTEGRATED CIRCUIT Building-Blocks for Appliance Control Applications—G. J. Granieri (SSD, Som) Appliance Suppliers Exhibit and Conf., 6/72; Chicago, Ill.

MICROWAVE HYBRID CIRCUITS, Parallel Gap Dual Beam Lead Bonding for—R. Schelhorn (M&SR, Mrstn) NEPCON '72 EAST; 6/12-13/72

OPERATIONAL AMPLIFIER Applications—H. A. Wittlinger (SSD, Som) Trenton State College, Trenton, N.J.; 5/72

OPERATIONAL TRANSCONDUCTANCE AMPLIFIER (OTA) With Power Capability, An IC—L. Kaplan, H. Wittlinger (SSD, Som) IEEE Chicago Spring Conf. on Broadcast and TV Receivers; 6/72; *IEEE Trans. on Broadcast and TV Receivers*.

POWER HYBRID TECHNOLOGY and Applications—S. Letcourt, J. Pilecki (SSD, Som) IEEE Conv. New York, NY; 3/72; *Convention Digest*

SHOCKLEY DIODES and Semiconductor-Controlled Rectifiers, GaAs Vapor-Grown—C. R. Wronski, C. J. Nuese, H. F. Gossensberger (Labs, Pr) *IEEE Trans. on Electron Devices*, Vol. ED-19, No. 5, pp. 691-692; 5/72

TUBE SYSTEM for Portable TV Receivers, New RCA Color Picture Tube—R. L. Barbin, R. H. Hughes (EC, Har) IEEE Spring Conf.; 6/12-13/72; Published by IEEE

UHF TRANSISTORS and Hybrid Modules for Mobile Applications, Recent Developments in—B. Maximon, M. F. O'Molesky, C. Kamnitsis (SSD, Som) SEMINEX, London, England; 4/72

UNIFORMLY MULTIPLYING AVALANCHE PHOTODIODES: The Distribution of Gain in Theory—R. I. McIntyre (RCA Ltd., Mont) *IEEE Trans. on Electron Devices*, Vol. 19, No. 6; 6/72

215 Circuit & Network Designs

... analog & digital functions in electronic equipment: amplifiers, filters, modulators, microwave circuits, A-D converters, encoders, oscillators, switches, masers, logic networks, timing & control functions, fluidic circuits.

CMOS MEMORIES Using Silicon-on-Sapphire Technology, High-Performance, Low-Power—E. J. Boleky, J. E. Meyer (Labs, Pr) *IEEE J. of Solid-State Circuits*, Vol. SC-7, No. 2, pp. 135-145; 4/72

COMPLEMENTARY MOS MEMORY, Beam Lead—J. R. Oberman, A. G. Dingwall (Labs, Pr) Lehigh Valley Semiconductor Symp. 5/5/72

GaAs MILLIMETER WAVE AVALANCHE OSCILLATOR and Amplifier Noise, Investigation of—K. P. Weller (Labs, Pr) 1972 Microwave Symp., Chicago, Illinois; 5/22/72

MHW CONVERTER Sublimation/Compatibility—G. Silverman (EC, Har) IECEC Conf., San Diego, Calif.; 9/72

OSCILLATORS, Improved Coupled-Line Microstrip Circuit for L and S Band—A. Rosen, J. R. Reynolds, J. J. Thomas (Labs, Pr) *Electronics Letters*, Vol. 8, No. 5, pp. 136-137; 3/9/72

PHASE LOCKED LOOP, A Micro-Power—G. W. Steudel (SSD, Som) *IEEE Conv. Digest*, IEEE Conv., New York, NY; 3/72

TAPPED DELAY LINE for Digital Signals, Optimum—A. A. Guida (Labs, Pr) ICC 1972 Mtg., Philadelphia, Pa.; 6/19-21/72

220 Energy & Power Sources

... batteries, solar cells, generators, reactors, power supplies.

MICROWAVE POWER SOURCES, Avalanche Diode—A. S. Clorfeine (Labs, Pr) Seminar, Drexel Univ., Philadelphia, Pa.; 5/3/72

225 Antennas & Propagation

... antenna design & performance, feeds & couplers, phased arrays, radomes & antenna structures, electromagnetic wave propagation, scatter, effects of noise & interference.

PHASED ARRAY for AN/SPY-1, Compact, Constrained Feed—W. Patton, R. Scudder, N. Landry, H. Goodrich (M&SR, Mrstn) Tri-Service Symp. Monterey, Calif.; 6/6-7-8/72; Symp. Record

PHASED ARRAYS for ECM Applications, Solid State—J. H. Budansky (ASD, Burl) NAECON, Dayton, Ohio; 5/15-17/72; Proc.

240 Lasers, Electro-optical & Optical Devices

... design & characteristics of lasers, components used with lasers, electro-optical systems, lenses, etc. (excludes: masers).

(AlGa)As-GaAs HETEROJUNCTION LASER DIODES: Threshold and Efficiency, Large-Optical-Cavity—H. Kressel, H. F. Lockwood, F. Z. Hawrylo (Labs, Pr) *J. of Applied Physics*, Vol. 43, No. 2, pp. 561-567; 2/72

HETEROJUNCTION COLD CATHODES, (AlGa)As-GaAs—H. Kressel (Labs, Pr) *Electrochemical Soc. Mtg.*, Houston, Texas; 5/7-12/72

HETEROJUNCTION LASERS, Lasing Transitions in p+n-n (AlGa) As-GaAs—H. Kressel, H. F. Lockwood (Labs, Pr) *Applied Physics Letters*, Vol. 20, No. 4, pp. 175-177; 2/15/72

HOLOGRAMS Recorded in Photoresist, Improved Development for—R. A. Bartolini (Labs, Pr) *Applied Optics*, Vol. 11, No. 5, pp. 1275-1276; 5/72

HOLOGRAPHIC OPTICAL MEMORY Techniques—W. C. Stewart (Labs, Pr) Joint Mtg. of the Boston Chapters of the Soc. for Information Display and the Soc. of Photographic Scientists and Engineers, Boston, MA.; 5/17/72

HOLOGRAPHIC STORAGE in Electro-Optic Crystals—J. J. Amodei (Labs, Pr) Symp. on Optical Information Storage, American Physical Soc., Columbus, Ohio; 5/13/72

HOLOGRAPHIC STORAGE IN LiNbO₃, Coupled-Wave Analysis of—D. L. Staebler J. J. Amodei (Labs, Pr) *J. of Applied Physics*, Vol. 43, No. 3, pp. 1042-1049; 3/72

IMAGE SENSOR ARRAYS, Solid State—F. V. Shallcross (Labs, Pr) Seminar, Westinghouse Research Laboratory, Pittsburgh, Pa.; 6/26/72

INFRARED PHOTOCATHODE, Possible Field-Assisted—V. L. Dalal (Labs, Pr) *J. of Applied Physics*, Vol. 43, No. 3, pp. 1160-1164; 3/72

INJECTION LASERS, Optical Saturation and the Internal Dynamics of—H. S. Sommers, Jr., D. O. North (Labs, Pr) Int'l Quantum Electronics Conf., Montreal, Canada; 5/8-11/72

LASER DIODES, Recent Trends in the Room-Temperature—H. Kressel (Labs, Pr) Int'l Quantum Electronics Conf., Montreal, Canada; 5/8-11/72

LED'S, The Future for—C. J. Nuese, H. Kressel, I. Ladany (Labs, Pr) *IEEE Spectrum*, Vol. 9, No. 5, pp. 28-38; 5/72

LIGHT-EMITTING DIODES, GaN Blue—J. I. Pankove, E. A. Miller, J. E. Berkeyheiser (Labs, Pr) *J. of Luminescence*, Vol. 5, No. 1, pp. 84-86; 3/72

LIGHT-VALVE ARRAYS for Optical Memories, Ferroelectric—G. W. Taylor, W. F. Kosonocky (Labs, Pr) *Ferroelectrics*, Vol. 3, Nos. 2/3/4, pp. 81-99; 2/72

OPTICAL WAVEGUIDES, Dispersion and Loss in New Thin Film—D. J. Channin, J. M. Hammer, J. P. Wittke (Labs, Pr) Int'l Quantum Electronics Conf., Montreal, Canada; 5/8-11/72

PHOTOCATHODES, Near Infrared and Low-Light-Level Imaging Using Negative Electron Affinity—B. F. Williams (EC, Har) First European Electro-Optics Markets & Technology Conf. & Exhibition, Geneva, Switzerland; 9/12-14/72

PHOTOCONDUCTIVITY-CONTROLLED DEVICES, The Role of Space-Charge-Limited Currents in—A. Rose (Labs, Pr) *IEEE Trans. on Electron Devices*, Vol. ED-19, No. 4, pp. 430-433; 4/72

SILICON TARGET CAMERA TUBE Technology, Non-Blooming and Other Advances—R. L. Rodgers, W. N. Henry (EC, Har) The Electro-Optical Systems Design Conf., New York Coliseum; 9/12-14/72

SINGLE HETEROJUNCTION (AlGa) As-GaAs LASER DIODES, Dependence of Threshold Current Density and Efficiency on Fabry-Perot Cavity Parameters—M. Ettenberg, H. Kressel (Labs, Pr) *J. of Applied Physics*, Vol. 43, No. 3, pp. 1204-1210; 3/72

STORAGE-DISPLAY TUBE with High Resolution Capability, Improved High Contrast, Cathodochromic Sodalite—B. W. Faughnan, I. Gorog, P. Keyman, I. Shidlovsky (Labs, Pr) 1972 Solid State Device Research Conf., Edmonton, Canada; 6/21-24/72

THERMALLY FIXED HOLOGRAMS in LiNbO₃, —D. L. Staebler, J. J. Amodi (Labs, Pr) *Ferroelectrics*, Vol. 3, Nos. 2/3/4, pp. 107-113; 2/72

THICK PHASE HOLOGRAMS in LiNbO₃, Multiple Storage of—D. L. Staebler, J. J. Amodi (Labs, Pr) Int'l Quantum Electronics Conf., Montreal, Canada; 5/8-11/72

THIN FILM OPTICAL WAVEGUIDES, Dispersion and Loss in New—D. J. Channin, J. M. Hammer, J. P. Wittke (Labs, Pr) Int'l Quantum Electronics Conf., Montreal, Canada; 5/8-11/72

245 Displays
... equipment for the display of graphic, alphanumeric, & other data in communications, computer, military, & other systems, CRT devices, solid state displays, holographic displays, etc.

HOLOCARD ID System, The RCA—D. L. Greenaway (Labs, Pr) SPIE Conf. on: Photo-Optical Applications in Security, Surveillance and Law Enforcement, Chicago, Illinois; 5/24-26/72

HOLOGRAPHIC MOVIES, Holotape-Embossed—W. J. Hannan (Labs, F, 25th Annual Conf. of the Soc. of Photographic Scientists and Engineers, San Francisco, Calif.; 5/7-12/72

IMAGE STORAGE in Display Terminals, Introductory Commentary—B. J. Lechner (Labs, Pr) 1972 SID Int'l Symp., San Francisco, Calif.; 6/6/72

SERIES 300 SYSTEMS, EQUIPMENT, & APPLICATIONS

315 Military Weapons & Logistics

... missiles, command & control.

COMMAND & CONTROL, Multiple Vehicle—D. Shore (M&SR, Mrstn) Symp. on Remotely Piloted at IDA Arlington, VA.; 5/30-31/72; 6/1/72

CONTROL SYSTEM - Walt Disney World, Automatic Monitoring and—W. B. Locke (ASD, Burl) Soc. of Women Engineers 22nd Annual Conv., Cambridge, Mass.; 6/21-25/72

CONTROL SYSTEM for Disney World, An Automatic Monitoring and—A. Orenberg (ASD, Burl) Int'l District Heating Assoc., Chicago, Illinois; 6/14/72

CONTROL SYSTEM, Cobra Night Fire—R. E. Rooney (ASD, Burl) NAECON, Dayton, Ohio; 5/15-17/72; Proc.

CONTROL SYSTEMS, Synthesis of a Control Law of Variable - Increment, multisampler, discrete-continuous—J. J. Mandas (M&SR, Mrstn) *Dissertation - 1970, Univ. of Penn.*

320 Radar, Sonar, & Tracking Systems

... microwave, optical, & other systems for detection, acquisition, tracking, & position indication.

AEGIS System - Engineering For the Future—W. Goodwin (M&SR, Mrstn) AIAA Regional Student Conf., Drexel Univ., 5/6/72

AUTOMOBILE Harmonic Radar System—H. Staras (Labs, Pr) Symp. Workshop on Automotive Radars, Univ. of Michigan, Ann Arbor; Michigan; 6/26/72

CONTROL Architecture, AEGIS Radar—R. Baugh, R. Ottinger, E. Prettyman (M&SR, Mrstn) Tri-Service Symp. Monterey, Calif.; 6/6-7-8/72; Symp. Record

DISCRIMINATION, Plus/Minus Mode—S. McCammon, D. Oseroff, R. Roop (M&SR, Mrstn) *OHD Symp. Proc.*

DOPPLER RADAR Using High-Efficiency Transferred Electron Devices—H. C. Johnson, Y. S. Marayan (Labs, Pr) Symp. Workshop on Automotive Radars, Univ. of Michigan, Ann Arbor, Michigan; 6/26/72

HF RECEIVER, The AN/FPS-95 High Instantaneous Dynamic Range—R. St. John, F. Palmer (M&SR, Mrstn) *OHD Symp. Proc.*

RADAR, Description of the AN/FPS-95 OTH-B—A. Leder, C. Wright (M&SR, Mrstn) OHD Technical Review, Monterey, Calif.; 5/3-4/72

RADAR Moving Target Indication, Direction Sensitive—H. Urkowitz (M&SR, Mrstn) *Dissertation, Univ. of Penn.*; 6/72

TRANSMITTER Design Considerations, AN/SPY-1—I. Schottenfeld, W. Zinger (M&SR, Mrstn) Tri-Service Symp. Monterey, Calif.; 6/6-7-8/72

VEHICULAR HEADWAY CONTROL AND COLLISION AVOIDANCE, Harmonic Radar for—J. Shefer, R. J. Klensch (Labs, Pr) Int'l Conf. on Communications, Philadelphia, Pa.; 6/72

WEAPON SIGHT, Development of a New Electronic—R. Van Olst, L. Lenz (M&SR, Mrstn) Tri-Service Symp., Monterey, Calif.; 6/6-7-8/72

325 Checkout, Maintenance, & User Support

... automatic test equipment, maintenance & repair methods, installation & user support.

RF TEST SYSTEM, A Computer Controlled—F. Pflifferling, D. Williamson (M&SR, Mrstn) *IEEE Trans. on Manufacturing Technology*; 6/72

340 Communications Equipment & Systems

... industrial, military, commercial systems, telephony, telegraphy, & telemetry, (excludes: television and broadcast radio).

COMMUNICATIONS for President Nixon's Visit to Peking, Setting up—P. Schneider (GLOBCOM, NY) *Computers in Communications*, 6/14/72

OPTICAL COMMUNICATIONS—A. Waksberg (RCA LTD., Mont) Princeton, N.J.; 3/72

RECEIVER, An ELF Wideband Noise—J. O. Sinniger (Labs, Pr) *IEEE Trans. on Geoscience Electronics*, Vol. GE-10, No. 2, pp. 113-118; 4/72

TELEMETRY from GARP Balloons to a TIROS Weather Satellite—E. Austein (AED, Pr) Inst. of Navigation 28th Annual Mtg., West Point, N.Y.; 6/27-29/72

360 Computer Equipment

... processors, memories, & peripherals.

COMPUTER, The Inventive Spirit and the—J. A. Rajchman (Labs, Pr) Keynote Address, 5th Australian Conf., Brisbane, Australia.; 5/22-26/72

COS/MOS MEMORIES, Applications for—J. Oberman (SSD, Som) IEEE Conv., New York, N.Y.; 3/72 *IEEE Conv. Digest*

MEMORIES, Holographic Optical—R. D. Lohman (Labs, Pr) Mtg. on Optical Memories, Rocoquecourt, France; 5/3/72

TIME SHARING TERMINAL Using a Cathodochromic Storage Tube, An Alphanumeric/Graphic—F. Marlowe, P. Keyman (Labs, Pr) 1972 SID Int'l Symp., San Francisco, Calif.; 5/23-25/72

365 Computer Programming & Applications

... languages, software systems, & general applications (excluding specific programs for scientific use).

SOFTWARE—R. Turkington (ASD, Burl) IEEE Boston Section Seminar on Computer Controlled Test and Monitoring Systems, RCA, ASD, Burlington, Mass.; 5/2/72

380 Graphic Arts & Documentation

... printing, photography, & typesetting; writing, editing, & publishing; information storage, retrieval, & library science; reprography & microforms.

ENGINEERING DOCUMENTATION for Spacecraft in a "Skunk-Works" Environment—H. P. Howard (AED, Pr) American Ordnance Ass'n, King of Prussia, Penna.; 5/4/72

GRAPHICS in Relation to College Training—A. T. Farrell (ASD, Burl) American Ordnance Assoc. Mtg., Prussia, Pa.; 5/3-4/72

INTERACTIVE GRAPHICS, Picture Generation for—L. J. French (Labs, Pr) 9th Annual Design Automation Workshop, Dallas, Texas; 6/26-28/72

Author Index

Subject listed opposite each author's name indicates where complete citation to his paper may be found in the subject index. An author may have more than one paper for each subject category.

Aerospace Systems Division

Budiansky, J.H., 225
Farrell, A.T., 380
Locke, W.B., 315
Orenberg, A., 315
Rooney, R.E., 315
Turkington, R., 365

Astro-Electronics Division

Austein, E., 340
Gargione, F., 210
Howard, H.P., 380
Keyser, W., 210
Noel, G., 210

Electromagnetic And Aviation Systems Division

Gandolfo, D.A., 210
Grasse, C.L., 210
Guadagnolo, R.N., 210
Levy, A., 170

Electronic Components

Barbin, R.L., 210
Henry, W.N., 240
Hughes, R.H., 210
Rodgers, R.L., 240
Silverman, G., 215
Williams, B.F., 240

RCA Global Communications, Inc.

Schneider, P., 340

Missile and Surface Radar Division

Bauer, J., 210
Baugh, R., 320
Buckley, M., 180
Goodrich, H., 225
Goodwin, W., 320
Landry, N., 225
Leder, A., 320
Lenz, L., 320
Lesser, D., 175
Mandas, J.J., 315
McCammon, S., 320
Oseroff, D., 320
Ottinger, R., 320
Palmer, F., 320
Patton, W., 225
Pflifferling, F., 325
Prettyman, E., 320
Roop, R., 320
Schelhom, R., 210
Schottenfeld, I., 320
Scudder, R., 225
Shore, D., 315
St. John, R., 320
Urkowitz, H., 320
Van Olst, R., 320
Williamson, D., 325
Wright, C., 320
Wright, D., 175
Zinger, W., 320

RCA Limited

Bachynski, M.P., 125

Bennett, D., 160
Gibbs, B.W., 125
McIntyre, R.I., 210
Waksberg, A., 160, 340

Solid State Division

Granieri, G.J., 210
Greenberg, L.S., 210
Hittinger, W.C., 175
Hoover, M.V., 210
Kamnitsis, C., 170, 210
Kaplan, L., 210
Lazar, S., 210
Lefcourt, S., 210
Maximov, B., 210
McKeon, E.F., 210
Meisel, H., 210
Minton, R., 170, 210
Oberman, J., 360
O'Molesky, M.F., 210
Pilecki, J., 210
Schnitzer, P., 210
Stuedel, G.W., 215
Veloricik, H.S., 210
Wittlinger, H., 130, 210

RCA Laboratories

Abrahams, M.S., 170, 205
Akseirad, A., 205
Amodi, J.J., 205, 240
Appert, J.R., 205
Baiberg, I., 205
Ban, V.S., 160
Bartolini, R.A., 240
Berkeyhelsler, J.E., 240
Berlin, E.P., 160
Bolesky, E.J., 215
Bolker, B., 205
Bortfeld, D.P., 205
Bozowski, S., 205
Buiocchi, C.J., 205
Carnes, J.E., 210
Channin, D.J., 240
Clorfaine, A.S., 220
Cody, G.D., 205
Comizzoli, R.B., 125
Crandall, R.S., 205
Cullen, G.W., 170, 205
Curtis, B.J., 110, 205
Dalal, V.L., 240
Darcy, L., 205
Davidson, E.B., 205
Dingwall, A.G., 215
Dismukes, J.P., 170, 205
Dougherty, F.C., 205
Dreeben, A., 205
Enstrom R.E., 205
Ettenberg, M., 240
Faughnan, B.W., 205, 240
Fech, J., Jr., 105
Feldstein, N., 160
Freeman, S., 210
French, L.J., 380
Gannon J.J., 205
Gittleman, J.J., 205
Goldfarb, S., 170
Goldstein, B., 205
Gonzalez, A., 205
Gordon, I., 170
Gorog, I., 240
Gossenberger, H.F., 210
Gottlieb, G.E., 205
Greenaway, D.L., 245
Grelg, W. J., 175
Guida, A.A., 215
Gutman, D., 205
Hammer, J.M., 240
Hanak, J.J., 205
Hannan W.J., 245
Harbeke, G., 205
Harvey, R.L., 205

Hawrylo, F.Z., 240
Heyman, P., 240, 360
Hoffman, D., 205
Honig, R.E., 160
Ipri, A.C., 205
Johnson, H.C., 320
Kalish, I.H., 175
Kawamoto, H., 210
Keneman, S.A., 205
Kern, W., 160
Kless, H., 205
Klein, R., 125
Klensch, R.J., 320
Kosonocky, W.J., 210, 240
Kressel, H., 210, 240
Ladany, I., 205, 240
Lechner, B.J., 245
Lehmann, H.W., 205
Lei, G., 205
Leibowitz, D., 205
Levine, A.W., 105
Lockwood, H.F., 240
Lohman, R.D., 360
Lozier, G.S., 125
Marlowe, F., 360
McFarlane, S.H., 205
Meier, E., 205
Meier, H., 205
Meyer, J.E., 215
Meyerhofer, D., 205
Miller, A., 205
Miller, E.A., 240
Miller, R.E., 205
Neison, H., 210
Nuese, C.J., 205, 210, 240
Oberman, J.R., 215
Pankove, J.J., 240
Phillips, W., 205
Pinch, H.L., 205
Polinak, E.S., 205
Rajchman, J.A., 360

Rehwal, W., 205
 Reynolds, J.R., 215
 Robinson, P.H., 170
 Ronen, R.S., 170
 Rose, A., 240
 Rosen, A., 215
 Ross, D.A., 125
 Schade, H., 210

Schnable, G.L., 175
 Shallock, F.V., 240
 Shidlovsky, I., 240
 Shefer, J., 320
 Sigal, A.G., 205
 Sinniger, J.O., 340
 Sommers, Jr., H.S., 240
 Southgate, P.D., 205

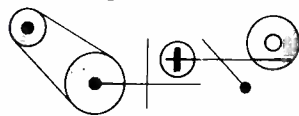
Staebler, D.L., 205, 240
 Stanley, T.O., 180
 Staras, H., 320
 Stelgmeier, E.F., 205
 Stewart, W.C., 240
 Sussman, A., 205
 Swartz, G.A., 205
 Taylor, G.W., 205, 240

Thomas, J.J., 215
 Toda, M., 205
 Tosima, S., 205
 Tuska, J.W., 175
 Wang, C.C., 205
 Wehner, R.K., 125, 205
 Weiner, J.A., 160
 Weller, K.P., 215

Williams, R., 205
 Wittke, J.P., 205, 240
 Wojtowicz, P.J., 205, 210
 Woods, M.H., 175
 Wronski, C.J., 210
 Vossen, J.L., 170, 205
 Yocom, P.N., 205
 Zaininger, K.H., 205

Patents Granted

to RCA Engineers



Aerospace Systems Division

Clamp Circuit for Preventing Saturation of Operational Amplifier—G. J. Thibodeau (ASD, Burl.) U. S. Pat. No. 3679989, July 25, 1972

Astro-Electronics Division

Radio Facsimile Postal System for Multiple Addressees—D. S. Bond (AED, Pr.) U. S. Pat. No. 3678180, July 18, 1972

Missile & Surface Radar Division

Electronic Editing Apparatus—T. Bolger (M&SR, Mrstn.) U. S. Pat. No. 3646260, May, 1972

Printed Circuit Balun—O. M. Woodward (M&SR, Mrstn.) U. S. Pat. 3678418, July 18, 1972

Target Acquisition Antenna—J. Grabowski/W. E. Powell (M&SR, Mrstn.) U. S. Pat. 3623094, November 23, 1971

Continuous Rapid Access Film Processor—A. Blatz (M&SR, Mrstn.) U. S. Pat. 3621769, November 23, 1971

Gated Oscillator—J. Krupa (M&SR, Mrstn.) U. S. Pat. 3662286, May 9, 1972

Field Effect Transistor Modulator Circuit—J. Krupa/M. Paglee (M&SR, Mrstn.) U. S. Pat. 3668561, June 6, 1972

Advanced Technology Laboratories

Electrostatic Printing Apparatus—M. L. Levene/M. Yamamoto (ATL, Cam.) U. S. Pat. No. 3672763, June 27, 1972

Method of Making Matching Photoprinting Masters—J. A. Dodd, Jr. (ATL, Cam.)/G. H. Lines (PBD, Cam.) U. S. Pat. No. 3674488, July 4, 1972

Comparator Circuit—E. P. McGrogan, Jr. (ATL, Cam.) U. S. Pat. No. 3676702, July 11, 1972

Communications Systems Division

Multi-Function Logic Gate Circuits—D. Hampel (CSD, Som.) U. S. Pat. No. 3678292, July 18, 1972

Palm Beach Division

Method of Making Matching Photoprinting Masters—J. A. Dodd, Jr. (ATL, Cam.)/G. H. Lines (PBD, Palm Bch. Gardens) U. S. Pat. No. 3674488, July 4, 1972

Laboratories

Recording of a Continuous Tone Focused Image on a Diffraction Grating—C. C. Ih/M. J. Lurie (Labs., Pr.) U. S. Pat. No. 3669673, June 13, 1972

Method of Making Abrasion-Resistant Metal-Coated Glass Photomasks—N. Feldstein (Labs., Pr.) U. S. Pat. No. 3669770, June 13, 1972

Low Temperature Silicon Etch—J. P. Dismukes (Labs., Pr.) U. S. Pat. No. 3669774, June 13, 1972

Electrical Circuit—W. S. Pike (Labs., Pr.) U. S. Pat. No. 3670179, June 13, 1972

Digital Light Deflector Using Optical Resonators—A. Miller (Labs., Pr.) U. S. Pat. No. 3672746, June 27, 1972

Method of Preparing a Substrate for Depositing a Metal on Selected Portions Thereof—N. Feldstein (Labs., Pr.) U. S. Pat. No. 3672925, June 27, 1972

Television Apparatus Responsive to a Transmitted Color Reference Signal—P. S. Cam/G. Schiess (Labs., Zurich, Switz.) U. S. Pat. No. 3673320, June 27, 1972

Bubble Domain Sonic Propagation Device—R. B. Clover, Jr. (Labs., Pr.) U. S. Pat. 3673582, June 27, 1972

Liquid Crystal Display Device Including Side-By-Side Electrodes on a Common Substrate—J. A. Castellano, R. N. Friel (Labs., Pr.) U. S. Pat. No. 3674342, July 4, 1972

Non Air-Polluting Corona Discharge Devices—H. G. Kiess (Labs., Zurich, Switz.) U. S. Pat. No. 3675096, July 4, 1972

Method of Operating an Information Storage Tube—E. Luedicke/R. S. Silver (Labs., Pr.) U. S. Pat. No. 3675144, July 4, 1972

Magnetic Compositions—M. Robbins (Labs., Pr.) U. S. Pat. No. 3676082, July 11, 1972

Decoders and Coupling Circuits for Solid State Video Pickup—P. K. Welmer (Labs., Pr.) U. S. Pat. No. 3676590, July 11, 1972

Magnetic Head with Modified Grain Boundaries—H. I. Moss/E. F. Hockings (Labs., Pr.) U. S. Pat. No. 3676610, July 11, 1972

Logic Circuits Employing Switches such as Field-Effect Devices—J. F. Meyer, Jr. (Labs., Pr.) U. S. Pat. No. 3676711, July 11, 1972

Method and Material for Etching Semiconductor Bodies—A. I. Stoller/S. T. Opreko (Labs., Pr.) U. S. Pat. No. 3677848, July 18, 1972

Magnetic Compositions—F. Okamoto/Y. Wada/K. Miyantani (Res. Lab., Tokyo, Japan) U. S. Pat. No. 3679379, July 25, 1972

Electro-optical Memory Employing Ferroelectric Element—S. A. Keneman/A. Miller (Labs., Pr.) U. S. Pat. No. 3680060, July 25, 1972

Method for Activating a Semiconductor Electron Emitter—D. G. Fisher (EC, Pr.) U. S. Pat. No. 3669735

Machine Implemented Method for Positioning and Inspecting an Object—L. A. Rempert, E. P. Helpert (SST, Pr.) U. S. Pat. No. 3670153, June 13, 1972

Decoder Circuit—M. M. Kaufman (SSTC, Cam.) U. S. Pat. No. 3679911, July 25, 1972

Entertainment Tube Division

Method of Mounting a Mass in a Cathode Ray Tube Using Retractable Spacing Units—L. B. Kimbrough (EC, Lanc.) U. S. Pat. No. 3672014, June 27, 1972

Process for Screening Cathode Ray Tubes Including Salvaging of Excess Phosphor Slurry—F. T. D'Augustine (EC, Lanc.) U. S. Pat. No. 3672932, June 27, 1972

Method for Making a Light Intensity Correction Filter—F. R. Ragland, Jr. (EC, Lanc.) U. S. Pat. No. 3676129, July 11, 1972

Industrial Tube Division

Method of Making a Heat Pipe Having an Easily Contaminated Internal Wetting Surface—R. A. Freggens (EC, Lanc.) U. S. Pat. No. 3672020, June 27, 1972

Hybrid Thermoelectric Generator—L. J. Caprarola (EC, Hrsn.) U. S. Pat. No. 3674568, July 4, 1972

Support for Electrical Components and Method of Making the Same—J. R. Collard (EC, Hrsn.) U. S. Pat. No. 3678995, July 25, 1972

Solid State Division

Method of Connecting Semiconductor Device to Terminals of Package—S. Y. Husni (SSD, Som.) U. S. Pat. No. 3668770, June 13, 1972

Method of Fabrication of Photomasks—A. G. F. Dingwall (SSD, Som.) U. S. Pat. No. 3673018, June 27, 1972

Input Transient Protection for Complementary Insulated Gate Field Effect Transistor Integrated Circuit Device—T. G. Athanas (SSD, Som.) U. S. Pat. No. 3673428, June 27, 1972

Gain Controlled Cascode-connected Transistor Amplifier—J. R. Harford (SSD, Som.) U. S. Pat. No. 3673498, June 27, 1972

Combined Tuning and Signal Strength Indicator Circuit with Signal Strength Indication Derived from each IF Amplifying Stage—J. Avins/J. Craft (SSD, Som.) U. S. Pat. No. 3673499, June 27, 1972

Synchronous Demodulator Employing a Common-base transistor Amplifier Input—A. L. Limberg (SSD, Som.) U. S. Pat. No. 3673505, June 27, 1972

Filamentary Display Devices—R. A. Bonnette (SSD, Som.) U. S. Pat. No. 3673652, July 4, 1972

High Capacity Deposition Reactor—K. Strater/W. B. Hall/E. M. Mihalick (EC, Hrsn.)/W. C. Stever (SSD, Som.) U. S. Pat. No. 3673983, July 4, 1972

Formation of Openings in Insulating Layers in MOS Semiconductor Devices—T. G. Athanas (SSD, Som.) U. S. Pat. No. 3674551, July 4, 1972

Transmission Gate and Biasing Circuits—B. Zuk (SSD, Som.) U. S. Pat. No. 3675144, July 4, 1972

Method for Making Transistors Including Base Sheet Resistivity Determining Step—W. G. Einthoven/E. S. Jetter/C. F. Wheatley, Jr. (SSD, Som.) U. S. Pat. 3676229, July 11, 1972

Delay Line Using Integrated MOS Circuitry—R. W. Ahrens (SSD, Som.) U. S. Pat. No. 3676711, July 11, 1972

High Gain MOS Linear Integrated Circuit Amplifier—R. W. Ahrens (SSD, Som.) U. S. Pat. No. 3678407, July 18, 1972

Metal-Oxide-Metal, Thin-Film Capacitors and Method of Making Same—F. P. Daly (SSD, Som.) U. S. Pat. No. 3679942, July 25, 1972

Alarm Circuit—G. D. Hanchett (SSD, Som.) U. S. Pat. No. 3680068, July 25, 1972

Method for Filling an Evacuated Electron Tube with Gas to Atmospheric Pressure—E. S. Thall (SSD, Scranton) U. S. Pat. No. 3679284, July 25, 1972

Consumer Electronics

Method of Making a Thick-Film Hybrid Circuit—T. R. Allington (CE, Indpls.) U. S. Pat. No. 3669733, June 13, 1972

Method of Making Electrical Connections to a Glass-Encapsulated Semiconductor Device—C. J. Jacob, G. W. Lawton (CE, Indpls.) U. S. Pat. No. 3669734, June 13, 1972

Video Blanking and Sound Muting Circuit—P. C. Olson/P. C. Tang (CE, Indpls.) U. S. Pat. No. 3673318, June 27, 1972

Automatic Beam Current Limiter—D. F. Griepentrog (CE, Indpls.) U. S. Pat. No. 3674932, July 4, 1972

Capacitors of Constant Capacitance—W. L. Lehmann (CE, Indpls.) U. S. Pat. No. 3675095, July 4, 1972

Method of Electrically Mounting Components in Hybrid Circuits—T. R. Allington (CE, Indpls.) U. S. Pat. No. 3676252, July 11, 1972

Balanced Variable Gain Amplifier—J. Craft (CE, Som.) U. S. Pat. No. 3678403, July 18, 1972

Amplifier-Limiter Circuit with Reduced AM to PM Conversion—J. Avins (CE, Som.) U. S. Pat. No. 3678405, July 18, 1972

Variable Gain Amplifier—J. Avins (CE, Som.) U. S. Pat. No. 3678406, July 18, 1972

Control Apparatus for a Color Television Receiver—J. Avins, L. R. Kirkwood (CE, Som.) U. S. Pat. No. 3679816, July 25, 1972

Video Blanking and Sound Muting Circuit Employing Grounded Tuner Switches—P. C. Olson/P. C. Tang (CE, Indpls.) U. S. Pat. No. 3679819, July 25, 1972

Optical Apparatus for Continuous Television Film Projection System—C. D. Boltz, Jr. (CE, Indpls.) U. S. Pat. 3679827, July 25, 1972

Synchronous Demodulator Employing Common Base Transistor Amplifier Input and Base-Emitter Clamping Action—A. L. Limberg (CE, Som.) U. S. Pat. No. 3679981, July 25, 1972

Synchronous Demodulator Employing Transistor Base-Emitter Clamping—A. L. Limberg (CE, Som.) U. S. Pat. No. 3679982, July 25, 1972

RCA Records

Tape Winding Mechanism—G. V. Taylor (Rec. Div., Indpls.) U. S. Pat. No. 3677505, July 18, 1972

Computer Systems

Computer with Program Tracing Facility—R. D. Smith (ISD, Riverton) U. S. Pat. No. 3673573, June 27, 1972

Sampling Decoder for Delay Modulation Signals—G. J. Meslener (CSD, Marlboro) U. S. Pat. No. 3670249, June 13, 1972

Corporate Staff

Three-Dimensional Television System—A. N. Goldsmith (Staff, New York) U. S. Pat. No. 3674921, July 4, 1972

Dates and Deadlines



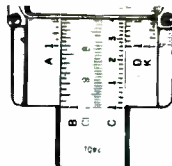
As an industry leader, RCA must be well represented in major professional conferences . . . to display its skills and abilities to both commercial and government interests.

How can you and your manager, leader, or chief-engineer do this for RCA?

Plan ahead! Watch these columns every issue for advance notices of upcoming meetings and "calls for papers". Formulate plans at staff meetings—and select pertinent topics to represent you and your group professionally. Every engineer and scientist is urged to scan these columns; call attention of important meetings to your Technical Publications Administrator (TPA) or your manager. Always work closely with your TPA who can help with scheduling and supplement contacts between engineers and professional societies. Inform your TPA whenever you present or publish a paper. These professional accomplishments will be cited in the "Pen and Podium" section of the *RCA Engineer*, as reported by your TPA.

Calls for papers—be sure deadlines are met

Date	Conference	Location	Sponsors	Deadline Date	Submit	To
FEB. 1-2, 1973	SPSE Symposia	New Orleans, La.	SPSE	10/25-27/72	ms	Papers Chairman: Albert Materazzi, Vice President Lith-Kem Corp. 5307 Westpath Way Washington, DC 20016
FEB. 14-16, 1973	IEEE International Solid-State Circuits Conference	Sheraton Hotel Philadelphia, Pa.	SSCC Univ. of Pa. Phila. Sect.	9/20/72 post-dead-line 1/5/73	abst sum abst (100 wd) sum (300-500 wd)	ISSCC 73 European or Asian secretaries: H. Riichardt, Siemens AG, HB-ISTL Balanstrasse 73 D-8 Munich 80, Germany or H. Mukai, Musachino Electrical Communication Laboratory 3-9-11, Midori-cho, Musashino-shi Tokyo, 180, Japan Chairman: S. Triebwasser, IBM T. J. Watson Research Center P. O. Box 218, Yorktown Heights, N.Y. 10598
MARCH 5-7, 1973	1973 Particle Accelerator Conference	San Francisco, Calif.	AEC NSF APS	11/15/72	abst	Chairman of the Program Committee: Richard B. Neal Stanford Linear Accelerator Center Stanford, California 94305
APR. 9, 10, 11, 1973	1973 IEEE International Symposium on Circuit Theory	Four Seasons Sheraton Hotel Toronto, Canada	IEEE	10/31/72	papers	Program Chairman: Professor M.N.S. Swamy Dept. of Electrical Engineering Sir George Williams University, Montreal 107, Quebec, Canada
APR. 16-18, 1973	AIAA Computer Network Conference	Huntsville, Ala.	AIAA Tech. Comm.	10/5/72	abst	Technical Program Chairman: W. S. Holmes, Vice President-Director Applied Technology Group Cornell Aeronautical Lab., Inc., P. O. Box 235, Buffalo, N.Y. 14221
APRIL 29-MAY 2, 1973	Offshore Technology Conference	Astrophall, Houston, Texas	TAB Oceanog- raphy Coor. Comm. et al	10/1/72	abst	IEEE Headquarters, 345 E. 47th St. New York, NY 10017
APRIL 30-MAY 2, 1973	Southeast-CON	Galt House, Louisville, KY	Region 3	10/1/72	abst	R. D. Shelton, Univ. of Louisville, EE Dept., Louisville, KY 40202
JUNE 20-22, 1973	1973 Joint Automatic Control Conference (JACC)	Ohio State Univ., Columbus, OH	AIAA, AIChE, ASME, IEEE, ISA, SIAM, TAPPI, ITE and SCI	1/19/73	papers	JACC Program Chairman: Dr. Robert E. Larson (1 Copy), Systems Control Inc., 260 Sheridan Ave., Palo Alto, Calif. 94306 and AIAA Program Committee Representative: Dr. Herman Redless (5 Copies), Chief, Flight Cont. Analysis, NASA Flight Research Center, P. O. Box 273, Edwards, Calif. 93523



Staff Announcements

Government and Commercial Systems

David Shore, Division Vice President, Government Plans and Systems Development has appointed **F. P. Henderson**, Manager, Requirements Planning, for Government and Commercial Systems, Moorestown, N.J.

Electronic Components

Gene W. Duckworth, Division Vice President, Equipment Marketing and Distribution, has appointed **Robert B. Means**, Division Vice President, Market Planning.

Marketing

Lee Adler, Director, Marketing Research, has appointed **Leo C. Melas**, Manager, International Marketing Research.

Government Communications Systems

James M. Osborne, Division Vice President has appointed **F. Donald Kell**, Manager, Recording Systems, for RCA's Government Communications Systems, Camden, N.J.

Advanced Technology Laboratories

Paul E. Wright, Director, RCA Advanced Technology Laboratories has appointed **Richard F. Kenville**, Manager, Electro-Optic Laboratory; **Dennis J. Woywood**, Manager, Applied Physics Laboratory.

Missile and Surface Radar Division

Howard G. Stewart, Division Vice President, Marketing has appointed **Victor W. Hammond**, Manager, Division Program, Range and Instrumentation Systems, Missile and Surface Radar Division.



Nesboda is new TPA for Aerospace Systems Division

Paul Nesboda has been appointed Technical Publications Administrator for the Aerospace Systems Division, Burlington, Mass. In this capacity, Dr. Nesboda is responsible for the review and approval of technical papers; for coordinating the technical reporting program; and for promoting the preparation of papers for the *RCA Engineer* and other journals, both internal and external.

Dr. Nesboda received the Doctorate Degree in Mathematical Science from the University of Pisa (Italy) in 1943 and the License in Mathematics from the *Scuole Superiori* of Pisa in 1944. From 1944 to 1946, he was assistant professor of Mathematical Analysis at the University of Trieste. In 1946 through 1947 he held a post-doctoral fellowship at the University of Paris (France). In 1947, he joined the staff of the Institute for Advanced Study in Princeton, N.J. From 1948 to 1952 he was a member of the faculty in the Mathematics Department of the Catholic University of America, Graduate School of Arts and Sciences, where he taught

Functional Analysis, Numerical Analysis and directed Master and PhD dissertations.

Dr. Nesboda joined RCA in 1952 in the Advanced Development section of the Engineering department. Since then, he has been engaged in statistical study related to communications, sensors optimizations and information processing.

His work at RCA has been in the fields of communications and radar detection. Currently, Dr. Nesboda is engaged in the administration and coordination of the Divisional IR&D.

Dr. Nesboda is a member of the American Mathematical Society, the Mathematical Association of America, Sigma Xi, the Scientific Research Society of America, and the Society of Industrial and Applied Mathematics and is the author of several technical papers. He is listed in "American Men of Science," in "Who's Who" in the East and in the International Register of "Who's Who." Dr. Nesboda is a registered professional engineer in the Commonwealth of Massachusetts.

Promotions

Advanced Technology Laboratories

Anne Merriam from Sr. Member Engrg. Staff to Ldr., Engrg. Staff, Applied Computer Systems Lab. (H. Zieper, Camden)

Electronic Components

R. A. McLaughlin from Sr. Engr. Prod. Development to Engrg. Ldr., Product Development (Gilbert Silverman, Harrison)

Licensed engineers

When you receive a professional license, send your name, PE number (and state in which registered), RCA division, location, and telephone number to: RCA Engineer, Bldg. 2-8, RCA, Camden, N.J. As new inputs are received they will be published.

Astro-Electronics Division

J. Bacher, AED, Princeton, N.J. PE-18719, New Jersey

W. Cable, AED, Princeton, N.J. PE-18814; New Jersey

A. W. D'Amanda, AED, Princeton, N.J. PE-18747; New Jersey

J. D'Arcy, AED, Princeton, N.J. PE-10696E; Pennsylvania

F. Yannotti, AED, Princeton, N.J. PE-19246; New Jersey

Consumer Electronics

D. M. Carrol, CE, Indianapolis, Ind. PE-14440; Indiana

R. D. Snyder, CE, Indianapolis, Ind. PE-14500; Indiana

Degrees granted

R. Blasewitz , M&SR, Mrstn.	MSEE, U. of Penna.,	5/72
M. Brazet , ASD, Burl.	MSEE, Northeastern U.,	6/72
R. Dashner , M&SR, Mrstn.	MS, Engineering Mgmt, Northeastern U.,	6/72
H. A. Edels , M&SR, Mrstn.	MSEE, U. of Penna.,	12/71
G. Gessler , ASD, Burl.	MSEE, Northeastern U.,	6/72
J. C. Heavner , M&SR, Mrstn.	BS, Business Adm., Lowell Technical Inst.,	6/72
R. Hertich , ASD, Burl.	AAS, ME, Lowell Technical Inst.,	6/72
J. Legay , ASD, Burl.	BS, Business Adm., U. of New Hampshire,	6/72
R. E. Main , M&SR, Mrstn.	BS, Electronic Physics, LaSalle,	5/72
W. Martin , ASD, Burl.	BS, Industrial Tech., Northeastern U.,	6/72
D. J. Olmstead , CE, Indpls.	MBA, Butler U.,	6/72
T. C. Robinson , M&SR, Mrstn.	BA, Finance & Business Adm., U. of Penna.,	5/72
R. Sharland , ASD, Burl.	AAS, EE, Northeastern U.,	6/72
W. H. Sheppard , M&SR, Mrstn.	MS, Engineering Mgmt, Drexel U.,	5/72
H. J. Seigel , M&SR, Mrstn.	BS, Engineering Mgmt, Drexel U.,	6/72
H. Urkowitz , M&SR, Mrstn.	Phd., EE, U. of Penna.,	5/72
A. Vallance , ASD, Burl.	MSEE, Northeastern U.,	6/72

New COS/MOS integrated circuits manual issued by RCA

A new edition of the *RCA COS/MOS Integrated Circuits Manual* is now available from Solid State Division, Somerville, N.J.

The new *RCA COS/MOS Integrated Circuits Manual*, Technical Series CMS-271, provides detailed information on the design, construction, and application of COS/MOS digital integrated circuits. The basic theory, design and layout techniques, processing and assembly operations, and packages for these devices are discussed. The basic building blocks for COS/MOS integrated circuit are described, features and characteristics of current RCA types are pointed out, and the basic design rules for COS/MOS logic systems are explained. This 224-page Manual, 40 percent larger than the preceding edition, has been updated to include descriptive data and logic diagrams for recently announced commercial types and broader, more extensive applications information on RCA COS/MOS integrated circuits. Design examples and performance data are given for use of COS/MOS devices in a wide variety of circuit applications, such as NOR and NAND gates, arithmetic units, multivibrators, sinusoidal oscillators, counters, registers, digital display systems, and digital frequency synthesizers.

The new Manual, like its preceding edition, is intended primarily as a guide to circuit and systems designers. It contains detailed tutorial information on the operation, design, construction, and application of COS/MOS integrated circuits that will be found useful by engineers, educators, students, technicians, hobbyists, and others that use or are interested in solid-state digital circuits and logic systems. This information is presented in twelve well-illustrated, easy-to-read text sections, as follows:

Fundamentals of COS/MOS Integrated Circuits—Basic principles of MOS field-effect transistors, fabrication of COS/MOS integrated circuits, COS/MOS design and layout.

Basic Building Blocks for COS/MOS Integrated Circuits—Inverter, transmission gates, transmission gate and inverter applications, input protection.

Features and Characteristics of RCA COS/MOS Integrated Circuits—Functional classifications and logic diagrams, performance characteristics.

COS/MOS Logic/System Design Rules—Maximum-rating considerations, short-circuit considerations, unused inputs, input signal swing, paralleling gate inputs, parallel inputs and outputs of gates and inverters, capacitive loading, wired "OR" function, common busing, positive/negative logic conversion, noise immunity, interfacing COS/MOS with other logic forms, clocking requirements, cascading considerations, power-source considerations.

Astable and Monostable Multivibrators—Astable circuits, monostable circuits.

Thirty-Two-Bit Adder—Functional description of arithmetic unit, arithmetic-unit operation, performance data.

Counters and Registers—Circuit design, practical counter circuits, practical register circuits.

Digital Display Systems—Circuit operation and performance characteristics, display drivers, interfacing counter/dividers with display devices, digital timer/clock/watch applications, digital meter applications.

Digital Frequency Synthesizers—Fundamentals of phase-locked loops, practical digital phase-locked loops, FM receiver synthesizers.

Linear Biasing of COS/MOS Inverters—Biasing methods, performance.

Crystal Oscillators—Basic circuit, crystal characteristics, feedback network, resonance and antiresonance, COS/MOS oscillator circuits.

Circuits—Logic diagrams and descriptive writeups for a selection of twenty-five circuits that illustrate practical design ideas for use of COS/MOS in a wide variety of applications.

Copies of the *RCA COS/MOS Integrated Circuits Manual* can be obtained at a special discount price to RCA Engineers by sending a check for \$1.50 to RCA Solid State Division, Box 3200, Somerville, N. J. 08876. The check should be made out to "RCA Corporation."

Changes on RCA Board of Directors

Election of Dr. Cecily Cannan Selby and John R. Petty as members of the RCA Board of Directors was announced by RCA Chairman Robert W. Sarnoff following a regular meeting of the Board.

Mrs. Selby, National Executive Director of the Girl Scouts of the U.S.A., is the third woman who has served on the RCA Board. She has directed the Girl Scouts national organization since last April, and has an extensive background in science, education, and administration. Mrs. Selby was also elected to the Board of Directors of the National Broadcasting Company.

Mr. Petty has been a Managing Director of Lehman Brothers, Inc., and head of the firm's Washington, D.C., branch office since March. Previously, he was Assistant Secretary of the Treasury for International Affairs. In that capacity, he was one of the architects of U.S. international monetary policy and a principal in the highly complex negotiations that led to devaluation of the dollar.

The resignation of Dr. George H. Brown as a member of the RCA Board was also accepted. Dr. Brown, who has served the corporation in a series of important engineering and scientific posts for almost 40 years, also has relinquished his position as RCA Executive Vice President, Patents and Licensing, but will continue with the company until his retirement next year.

Dr. Hershenov named Research Director of Japanese Laboratories

Appointment of Dr. Bernard Hershenov as Director of Research of RCA Research Laboratories, Inc. (Tokyo) has been announced by Dr. Jan A. Rajchman, Vice President of the RCA subsidiary.

Located on the outskirts of Tokyo, RCA Research Laboratories was established in 1961 to foster closer relations between the Japanese and American scientific communities. With the exception of the Director, all 35 employees of the Laboratories are Japanese, including 15 research scientists investigating physics, chemistry, communications theory, and other basic fields of electronics.

Dr. Hershenov is replacing Dr. Philip K. Baltzer, who is returning to the scientific staff of RCA Laboratories in Princeton, N.J., after being Director of the Japanese Laboratories since 1967.

Dr. Hershenov joined the Microwave Research Laboratory of RCA Laboratories in 1960, and in 1968 was named Head of the Microwave Integrated Circuits Group, the position he held prior to his present appointment.

221 graduate from RCA Institutes

Some 221 students, including individuals from 19 foreign countries, were graduated recently from RCA Institutes in New York City.

The degree of Associate in Occupational Studies (A.O.S.) was awarded to 54 students for completion of the school's Electronics Technology Program, a two-year college level engineering technology course which stresses communications and computer technology.

Credit for the Electronics Technology course is given at many colleges and universities—including Massachusetts Institute of Technology, Yale, and Columbia—to RCA graduates who elect to continue their education toward the baccalaureate degree.

Other graduates were awarded certificates in Electronics Circuits and Systems, Radio-Television and Electronics Servicing, and Electronic Circuits following courses of study ranging from nine months to 1½ years.

RCA Review, June 1972		
Volume 33, Number 2		
Contents		
Noise Sources in Charge-Coupled Devices	J. E. Carnes W. F. Kosonocky	
A Solid-State Transponder Source Using High-Efficiency Silicon Avalanche Oscillators	J. F. Reynolds J. Assour A. Rosen	
Negative Resistance in Cadmium Selenide Powder—Comparison of Experiment and Theory	L. J. Nicastro E. L. Offenbacher	
Luminescence from GaN MIS Diodes	J. T. Pankove P. E. Norris	
Infrared Transmission Microscopy Utilizing a High-Resolution Video Display	R. A. Sunshine N. Goldsmith	
Modulation Transfer Function Calculation of Electrostatic Lenses	I. P. Csorba	
A Simplified Method for the Determination of Particle Size Distributions of Fine Magnetic Powders	J. W. Robinson E. F. Hockings	
Electrophotography: A Review	R. B. Comizzoli G. S. Lozier D. A. Ross	
The <i>RCA Review</i> is published quarterly. Copies are available in all RCA libraries. Subscription rates are as follows (rates are discounted 20% for RCA employees)		
	DOMESTIC	FOREIGN
1-year	\$6 00	\$6 40
2-year	10 50	11 30
3-year	13 50	14 70

Editorial Representatives

Technical Publication Administrators listed above are responsible for review and approval of papers and presentations.

Government and Commercial Systems

Aerospace Systems Division

P. P. NESBECA Engineering, Burlington, Mass.
J. J. DUFFIN Industry Systems Burlington, Mass.

Electromagnetic and Aviation Systems Division Astro-Electronics Division

C. S. WELCH Engineering, Van Nuys, Calif.
J. McCONOUGH Engineering, Van Nuys, Calif.

Missile & Surface Radar Division Government Engineering

T. M. SEIDEN Engineering, Princeton, N.J.
S. WEISBLUM Advanced Development and Research, Princeton, N.J.
T. G. GREENE Engineering, Moorestown, N.J.

Government Plans and Systems Development

M. R. PHETZ Advanced Technology Laboratories, Camden, N.J.
J. E. FRIEDMAN Advanced Technology Laboratories, Camden, N.J.
J. L. SAUGER Central Engineering, Camden, N.J.

Communications Systems Division Commercial Systems

E. J. RODELL Engineering Information and Communications, Camden, N.J.

Government Communications Systems

Palm Beach Division

T. J. LIND Chairman, Editorial Board, Camden, N.J.
S. M. ZUCKERMAN Advanced Development, Meadow Lands, Pa.
J. R. HALL Studio, Recording, & Scientific Equip. Engineering, Camden, N.J.
K. E. HANN Broadcast Transmitter & Antenna Eng., Gibbsboro, N.J.

A. T. LUBRIN Engineering, Camden, N.J.

P. W. WOODLEY Palm Beach Product Laboratory, Palm Beach Gardens, Fla.

Research and Engineering

Laboratories

J. J. SAUNDERS Research, Princeton, N.J.
C. H. AUSTIN Solid State Technology Center, Somerville, N.J.
R. A. CRITMAN Solid State Technology Center, Somerville, N.J.

Electronic Components

Entertainment Tube Division

C. W. KEYS Chairman, Editorial Board, Harrison, N.J.

T. K. JEFF Receiving Tube Operations, Woodbridge, N.J.
J. W. HENNING Television Picture Tube Operations, Marion, Ind.
F. K. MADENFORD Television Picture Tube Operations, Lancaster, Pa.

Industrial Tube Division

J. W. FORMAN Industrial Tube Operations, Lancaster, Pa.
H. W. WOLSTEIN Microwave Tube Operations, Harrison, N.J.

Solid State Division

L. M. B. FLETCHER Chairman, Editorial Board, Somerville, N.J.
J. M. B. HALL Solid State Division, Mountaintop, Pa.
K. S. EBERHART Power Transistors, Somerville, N.J.
F. H. GUY Integrated Circuits, Somerville, N.J.
J. D. YOUNG Solid State Division, Findlay, Ohio

Consumer Electronics

F. H. COYNT Chairman, Editorial Board, Indianapolis, Ind.
R. L. THOMAS Engineering, Indianapolis, Ind.
R. W. RAY Radio Engineering, Indianapolis, Ind.
J. H. COLEMAN Advanced Development, Indianapolis, Ind.
E. W. ANSON Black and White TV Engineering, Indianapolis, Ind.
W. E. EDWARDS Ceramic Circuits Engineering, Rockville, Ind.
R. W. BARKER Color TV Engineering, Indianapolis, Ind.
R. H. JAMES Engineering, RCA Taiwan Ltd., Taipei, Taiwan

Services

RCA Service Company

M. J. BARKER Consumer Products Administration, Cherry Hill, N.J.
W. W. DOK Consumer Products Service Dept., Cherry Hill, N.J.
D. M. JAMES Technical Support, Cherry Hill, N.J.
R. P. LAMB Missile Test Project, Cape Kennedy, Fla.

Parts and Accessories

RCA Global Communications, Inc.

C. J. RANZ Product Development Engineering, Deptford, N.J.
W. J. LEE RCA Global Communications, Inc., New York, N.Y.
J. D. COLLIER RCA Alaska Communications, Inc., Anchorage, Alaska

National Broadcasting Company Inc.

W. A. HOWARD Staff Eng., New York, N.Y.
M. J. WHITEHORN Record Eng., Indianapolis, Ind.

RCA Records

RCA International Division

C. A. PASSEVANT New York, N.Y.

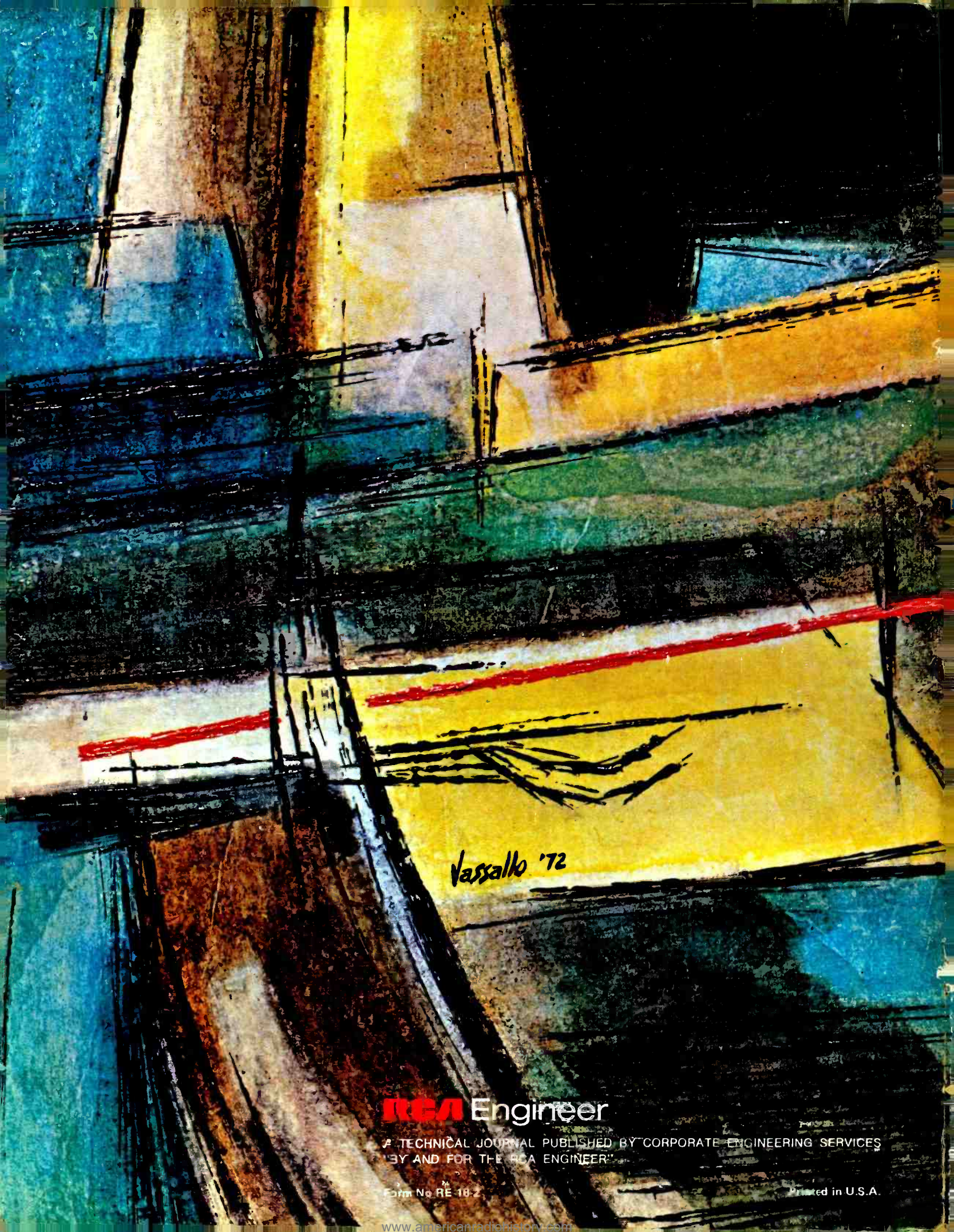
RCA Ltd.

W. A. THISHOLM Research & Eng., Montreal, Canada

Patents and Licensing

J. EPSTEIN Staff Services, Princeton, N.J.

*Technical Publication Administrators listed above are responsible for review and approval of papers and presentations.



Vassallo '72

RCA Engineer

A TECHNICAL JOURNAL PUBLISHED BY CORPORATE ENGINEERING SERVICES
"BY AND FOR THE RCA ENGINEER"

Form No. RE 18-2

Printed in U.S.A.

www.americanradiohistory.com